FATIGUE CHARACTERISTICS OF BONDED POST-TENSIONED CONCRETE I - BEAMS

by

K. M. PRICE
B.Sc.(Eng.),D.I.C.

A thesis submitted for the Degree of
Doctor of Philosophy
in the Faculty of Engineering of the
University of London

Imperial College of Science and Technology
London

May 1969

ABSTRACT

The investigation is concerned with the fatigue behaviour of post - tensioned prestressed concrete I - beams subjected to bending and to combined bending and shear.

A critical review of previous investigations was carried out to determine the shortcomings in the knowledge of fatigue. The most important conclusion to emerge from this was the fact that existing theories may, in a number of cases, give a considerable over - estimation of the fatigue life of flexural members.

An experimental investigation was carried out (on 29 beams) to determine the quantitative effects of repeated loading on flexural cracking, and to investigate the fatigue behaviour of the beams in a cracked state. Fatigue fracture of the prestressed reinforcement was found to be the most important criterion of failure, and associated fatigue tests in air were carried out on the prestressing strand.

A comprehensive theory for the prediction of flexural cracking and failure in fatigue is presented. The method is based on an analysis of stresses and deformations in prestressed concrete flexural members subjected to repeated loading. The theory has a statistical basis and takes into account reductions in the fatigue strength of steel when embedded in prestressed concrete beams.

An experimental investigation of shear strength in fatigue was conducted on 17 post - tensioned thin - webbed I - beams. The results provide information on diagonal tension cracking, both under static loading and in fatigue. The main part of the investigation was concerned with the overall behaviour, failure modes and criterion of failure under repeated loading, of beams having diagonal cracks. For the beams tested, stirrup fracture was found to be the criterion of fatigue failure in all cases.

ACKNOWLEDGEMENTS

The author is grateful to Professor A.L.L. Baker, D.Sc., F.I.C.E., M.I.Struct.E., under whose general supervision the investigation reported herein was conducted.

My sincere thanks are due to Dr. A.D. Edwards, Ph.D., D.I.C., B.Sc.(Eng)., M.I.C.E., for his advice and guidance throughout the duration of the investigation.

Thanks are also due to Dr. C.W.Yu, Ph.D., D.I.C., M.A.S.C.E., M.I.C.E., for his help and co-operation in organising the laboratory work.

The author is indebted to the Road Research Laboratory of the Ministry of Transport under whose sponsorship the research was carried out.

All the laboratory work was carried out with the untiring assistance of Mr. J. Baulch, to whom I am most grateful.

My thanks are due to Mr. R. Loveday for his technical advice, and Messrs. J. Turner, P. Jellers, C. Mortlock and other members of the technical staff for their help in the laboratory work.

I wish to thank Miss J. Gurr who took the photographs and prepared the plates, and also Miss S. Rumble who gave meticulous assistance in the preparation of the figures.

Grateful thanks are proffered to Miss V.A. Martyn who performed the unenviable task of typing the script with imperturbable stoicism.

Thanks are due to Messrs. S. Krishnamoorthy and D.N. Trikha for their useful suggestions and many hours of discussion, both academic and political !

Finally, I would like to express my gratitude to the Association of Commonwealth Universities, London, for the award of a scholarship, without which, the research reported here would not have been possible.

CONTENTS

2.4) .....

Page

Page

6.4) .....

Page

SIGN CONVENTION

Stresses, stress - resultants, cable - eccentricities, and material strengths have algebraic values. All other parameters, such as geometric section properties and strains, have numerical values only.

Distances measured in the direction of fibre 2 are considered to be positive, and in the direction of fibre 1 they are considered to be negative. The extreme fibres are denoted arbitrarily fibre 1 (bottom) and fibre 2 (top).

Compression stresses are considered to be positive, and tension stresses negative.

A positive moment produces a positive stress in fibre 2.

NOTATION

The notation employed in this thesis makes use of both subscript and superscript notation:-

a) SUPERSCRIPTS

m	=	General moment, M.
max	=	Maximum load (or stress) in a repeated load cycle.
min	=	Minimum load (or stress) in a repeated load cycle.
r	=	Range of load (or stress) in a repeated load cycle.
tr	=	Condition at which previously formed flexural cracks begin to open.

b) SUBSCRIPTS

c	=	Concrete in general.
s	=	Prestressing steel.
sm	=	Mild steel.
1	=	Concrete in extreme fibre 1 (bottom).
2	=	Concrete in extreme fibre 2 (top).
3	=	Concrete at the join of the top flange and the web.
g	=	Centroid of the section.
cs	=	Concrete at the level of the prestressing steel.
crf	=	Flexural cracking condition.
crws	=	Web cracking condition.
p	=	Effective prestress condition.
u	=	Ultimate load condition.

c) SECTION PROPERTIES

A	=	Gross concrete cross - sectional area.
A_s	=	Total area of prestressing steel.
A_v	=	Area of one member of web reinforcement, i.e. one stirrup.
D	=	Overall depth of the beam.
d	=	Effective depth of the beam, i.e. depth from the extreme fibre 2 to the centroid of the prestressing steel.

c) continued:

d_f = Depth of top flange.

b = Total breadth of the beam (or top flange of an I - beam).

b_o = Breadth of web.

e_1 = Distance of the extreme bottom fibre 1, from the centroid of the section.

e_2 = Distance of the extreme top fibre 2, from the centroid of the section.

e_s = Cable eccentricity, i.e. the distance from the centroid of the prestressing force, P, to the centroid of the section.

I = Second moment of area.

Z_1 = $^I/e_1$

Z_2 = $^I/e_2$

p = Percentage of prestressing steel in section, $\frac{A_s\ 100}{b\ d}$

r = Ratio of web reinforcement $= \frac{A_v}{b_o s}$

s = Spacing of web reinforcement.

a = Length of the shear span

d_n = Neutral axis depth.

d_c = Depth of centre of compression below top fibre $= k_2\ d_n$.

d) MATERIAL PROPERTIES

f_{cu} = 6" cube crushing strength of concrete.

f_c' = 6" x 12" cylinder crushing strength of concrete.

f_r = Modulus of rupture strength of concrete.

f_t = Cylinder splitting strength of concrete.

f_{crf} = Static flexural cracking strength of concrete.

f_{crws} = Static diagonal tension cracking strength of concrete.

f_{su} = Ultimate tensile strength of prestressing steel.

$\overline{f_{su}}$ = Mean ultimate tensile strength of prestressing steel.

f_{smy} = Yield stress of web reinforcement.

f_{smu} = Ultimate tensile strength of web reinforcement.

E_c = Modulus of elasticity of concrete.

E_s = Modulus of elasticity of steel.

e) STRESS - RESULTANTS

P = Prestressing force in general.

P_o = Initial effective prestressing force.

P_e = Final effective prestressing force at any particular time after losses have taken place.

P_{crf} = Effective prestressing force at the moment when flexural cracking takes place.

M = Bending moment in general.

M_p = Total absolute moment due to prestress.

M_{crf} = Moment of resistance of a section at flexural cracking.

M_{crws} = Moment of resistance of a section at diagonal tension (web) cracking.

M^{tr} = Moment in a load cycle at which previously formed flexural cracks begin to open.

M^{min} = Minimum moment level in a repeated load cycle.

M^{max} = Maximum moment level in a repeated load cycle.

M_u = Static ultimate moment of resistance of a section.

$\overline{M}_u$ = Mean static ultimate moment of resistance of a section.

V = External shear force in general.

V_{crws} = Shear force causing diagonal tension (web) cracking.

V^{min} = Minimum shear force in a repeated load cycle.

V^{max} = Maximum shear force in a repeated load cycle.

V_u = Ultimate static shear resistance of a beam.

$\overline{V}_u$ = Mean ultimate static shear resistance of a beam.

C = Total compressive force resisted by the concrete compression zone.

T = Total tensile force resisted by the prestressing steel.

f) STRESSES

σ_c = Concrete stress in general.

σ_{c1} = Stress in extreme fibre 1 (bottom).

σ_{c2} = Stress in extreme fibre 2 (top).

σ_s = Steel stress in general.

σ_{sp} = Effective prestress in steel.

σ_s^m = Steel stress under a moment, M.

σ_s^{min} = Steel stress under minimum load in a repeated load cycle.

σ_s^{max} = Steel stress under maximum load in a repeated load cycle.

σ_s^{r} = Steel stress range in a repeated load cycle $= \sigma_s^{max} - \sigma_s^{min}$.

g) STRAINS

ε = Strain in general.

ε_c = Concrete strain in general.

ε_{cspo} = Elastic strain in concrete at steel level due to P_o.

ε_{csp} = Elastic strain in concrete at steel level due to P_e.

ε_{c1} = Concrete strain in fibre 1 (bottom).

ε_{c2} = Concrete strain in fibre 2 (top).

ε_{cs}^{m} = Apparent tensile strain in concrete at steel level under a moment, M.

ε_{cu} = Maximum strain in concrete in compression at failure (static).

ε_s = Steel strain in general.

ε_{spo} = Steel strain corresponding to prestressing force P_o.

ε_{sp} = Steel strain corresponding to prestressing force P_e.

ε_s^{m} = Steel strain under a moment, M.

ε_s^{min} = Steel strain under M^{min}.

ε_s^{max} = Steel strain under M^{max}.

ε_s^{r} = Steel strain range in a repeated load cycle, $= \varepsilon_s^{max} - \varepsilon_s^{min}$.

h) DEFORMATIONS

ϕ = Curvature at a section.

w_{cr} = Crack width.

i) **RATIOS AND COEFFICIENTS**

F	=	Bond strain compatibility factor.
k_2	=	Factor relating depth of centre of compression in concrete, d_c, to neutral axis depth, d_n.
N	=	Number of load cycles in general.
$\bar{N}$	=	Mean fatigue life.
N_1	=	Number of cycles to the first fatigue fracture of a steel element.
N_f	=	Number of cycles of complete beam failure in fatigue.
$\log N$	=	$\log_{10} N$
$\overline{\log N}$	=	Mean of $\log_{10} N$.
x	=	$\log_{10} N$
$\bar{x}$	=	$\overline{\log_{10} N}$
S	=	Standard deviation of a sample of measurements.
C_v	=	Coefficient of variation of a sample of measurements.
PR	=	Probability of failure at or before N load cycles.
u	=	Number of steel elements in the beam at depth, d.
K	=	Factor relating the mean fatigue strength of steel in a beam to the mean fatigue strength of steel in air, for failure after the same number of load cycles.

DEFINITIONS.

Fatigue life, N.

The number of cycles of stress or strain of a specified character that a given specimen sustains before failure of a specified nature occurs.

Load cycle

The smallest algebraic portion of the load - time function which is repeated periodically.

Maximum load (or stress, σ^{max}).

The load (or stress) having the highest value in the load cycle.

Minimum load (or stress, σ^{min}).

The load (or stress) having the lowest value in the load cycle.

Range of load (or stress, σ^{r}).

The difference between the maximum and minimum load (or stress, $\sigma^{r} = \sigma^{max} - \sigma^{min}$) in the load cycle.

S - N diagram

A plot of load (or stress), S, against the number of cycles to failure, N. The load may be maximum load (or σ^{max}), or range of load (or σ^{r}). In all cases in this thesis, the diagram indicates the S - N relationship for a specified value of the minimum load (or σ^{min}), and a specified probability of failure (which is 0.5, if not stated). For N, a log scale is always used, and for S, a linear scale is employed.

Fatigue limit

The limiting value of the median fatigue strength as N becomes very large.

Fatigue strength at N cycles.

A hypothetical value of the load (or stress) for failure at exactly N cycles, as determined from an S - N diagram. The fatigue strength thus determined is subject to the same conditions as those which apply to the S - N diagram.

Fatigue life for a probability of failure, PR.

An estimate of the fatigue life that a proportion, PR, of the population would fail to attain or exceed between given stress levels, where:-

$$1 \geqslant PR \geqslant 0$$

The observed value of the median fatigue life estimates the fatigue life for a probability of failure of 0.5.

S - N curve for a probability of failure, PR.

A curve of the estimated fatigue life for a probability of failure, PR, at each of several stress levels. It is an estimate of the relationship between applied stresses and the number of cycles that a proportion, PR, of the population would fail to survive.

CHAPTER 1

INTRODUCTION

1.1) INTRODUCTION

Improvements in design methods in recent years have resulted in a reduction in the relative sizes of structural members, together with a decrease in the magnitude of effective safety factors. The effect of this is to increase the possibility of fatigue failures under working loads, and although, (to the author's knowledge) no fatigue failures have yet occurred in prestressed concrete structures in use, fatigue damage is a progressive and cumulative effect, and failure may yet occur in present day structures at some stage in the future. The importance of fatigue in bridge structures is further emphasized with the realization that the magnitude of wheel loads is continually increasing and bridges may now be expected to be subjected to a considerable number of loads which approach the magnitude of full working load. Fatigue is particularly important in structures in which the dead load forms a small proportion of the working load.

In practice, there are many prestressed concrete structures which are subjected to fatigue:-

i) Bridge structures - vehicle loads and temperature effects.
ii) Buildings - wind loads.
iii) Factories - wind and crane loads.
iv) Machine foundations.

The fatigue loading may take several different forms, the simplest being loading which varies continually with time between constant maximum and minimum values. In practice, however, the loading spectrum is generally far more complicated, consisting of repeated loads of different magnitude, which occur in a random sequence at varying intervals of time.

Fatigue failures are generally brittle in nature, and occur suddenly with no prior indication of failure. Thus, if a structure is dependent upon the strength of a single element in which fatigue fracture is possible, the failure will be immediate and catastrophic. In general, though, structures are dependent upon many elements and, therefore, fatigue failure of an element will not cause complete collapse, although progressive failure could occur in other elements, eventually leading to collapse.

1.2) BEHAVIOUR OF PRESTRESSED CONCRETE STRUCTURES SUBJECTED TO REPEATED LOADING.

1.2a) IN FLEXURE

Fatigue failures in flexure may occur in either steel or concrete depending on the section properties and amount of reinforcement, and on the magnitude of the repeated load. However, the criterion and mode of failure under static loading will not necessarily be the same under repeated loading, and will, in most cases, be different. Sections which give an under - reinforced concrete crushing failure under static loading will, in general, fail by steel fatigue at low levels of repeated loading, but concrete fatigue failures are also possible in the same section when failure takes place after a relatively small number of load cycles.
In over - reinforced sections, steel fatigue failures are still possible at low repeated load levels, but concrete fatigue failures are more likely to occur.

In pretensioned beams, bond failures are also possible in regions where there are steep gradients in the bending moment - i.e. where the shear forces are significant.

1.2b) IN SHEAR.

Little is known of the fatigue strength in shear of prestressed concrete structures, but it is possible that the failure modes may take several different forms : -

i) Shear compression failure of concrete, or fatigue fracture of steel at flexural - shear cracks.

ii) Diagonal tension (no shear reinforcement) - failure in concrete in tension.

iii) ......

iii) Diagonal tension (with shear reinforcement) - failure of shear reinforcement.

iv) Web crushing failure in thin - webbed I - beams.

In some cases, failure may even be possible by a combination of the above effects.

1.3) PREVIOUS INVESTIGATIONS

A survey of the literature shows the existence of many test results pertaining to the fatigue of flexural members, but a close scrutiny reveals that most results are extremely limited in application. All too often, the investigation only applies to the particular sections tested and the results are of little general use, being presented in terms of load, and not stresses. Much qualitative information is available, but precise design for fatigue is impossible with any degree of confidence. Considerable scatter is evident in all the results, but many investigators have ignored the important statistical aspect of fatigue.

With regard to shear, even the amount of qualitative information is negligible, and it is not possible to even predict the fatigue failure mode, let alone the fatigue life.

1.4) OBJECT AND SCOPE OF PRESENT INVESTIGATION

1.4a) FLEXURE

i) To carry out a detailed survey and study of all previous investigations and correlate the information in such a way that it is of maximum general value. This includes determination of the sections in which knowledge is lacking, or the available information is open to some doubt.

ii) To carry out experimental investigations to provide information on those subjects in which the knowledge is limited. Broadly speaking, these are :-

a) Quantitative investigation of flexural cracking in fatigue in prestressed concrete beams.

b) Comparison of the fatigue behaviour of prestressing steel when embedded in beams, with its behaviour when tested in air.

The tests were all fully instrumented so as to provide detailed information on stresses and deformations. The steel tests were designed on a statistical basis so that maximum confidence could be placed in the results.

iii) To produce a comprehensive theory for the prediction of the fatigue strength and life in flexure of prestressed concrete members. This applies to repeated loading between extremes which are of constant magnitude - it is not considered that the state of knowledge at the moment warrants extension to repeated loading of variable magnitude.

1.4b) SHEAR.

Since the previous information is so sparse, and even the static theories largely incomplete, it is not considered that, at the present time, even a tentative theory is feasible for the prediction of the fatigue strength in shear of prestressed concrete members.

The experimental investigations were, therefore, designed on a statistical basis to provide information on shear cracking, deformation, overall behaviour, failure modes, and criterion of failure under repeated loading.

CHAPTER 2

CRITICAL REVIEW OF PAST WORK

2.1) BEHAVIOUR OF PLAIN CONCRETE UNDER REPEATED LOADING

The literature on the fatigue behaviour of plain concrete has been reviewed periodically (1, 2) and it has not been found necessary to repeat those reviews here, but the main conclusions of the workers so listed have been summarised, and the findings of later investigators added. One subject which has not been dealt with very extensively in the previous reviews is the effect of repeated loading on the stress - strain characteristics of concrete - this has, therefore, been treated in more detail.

No results are available on the effect of repeated loading on concrete in axial tension, nor have any tests been reported of the effect of repeated loading on the cylinder splitting strength of concrete.

2.1a) FATIGUE OF PLAIN CONCRETE UNDER AXIAL COMPRESSION

The investigations completed by the author do not include the phenomenon of fatigue failure of concrete in compression, in either control specimens or test beams, but a brief review is included here for completeness.

Investigations were started as early as 1903 by Van Ornum (3), and contributions were added in later years by Probst (4), Antrim and McLaughlin (5), Bennet and Muir (6), and others. These were all concerned with the behaviour of prisms or cylinders under a uniform state of stress. In 1966, Ople and Huslbos (7, 8) published the results of tests conducted on prisms with various stress gradients; they showed that the effect of a stress gradient was to increase the fatigue strength by up to 17% above that of uniformly stressed specimens. A possible reason, from the statistical standpoint, being that the uniformly stressed specimen has all its fibres stressed at the maximum level, whereas the non - uniformly stressed specimen has only one fibre at the maximum stress level. The importance of this increase in strength is obvious when considering the extrapolation of the behaviour of plain concrete specimens to the concrete in the compression zone of beams, although the results can only be used as a guide until further tests have confirmed these findings.

The main conclusions on the fatigue of concrete under axial compression may be summarised as follows :-

a) The fatigue strength at 10×10^6 cycles of loading from zero stress to a maximum, is approximately 55% of the short - term static ultimate strength.

b) The fatigue strength for varying minimum stress levels may be expressed by a modified Goodman diagram as shown in fig. 2.1. The fatigue strength increases with increasing minimum stress but the qualitative results available are somewhat limited in number.

c) No fatigue limit exists for concrete up to 10×10^6 cycles of loading.

d) The fatigue properties, when expressed in terms of short - term static ultimate strength, are statistically independent of the nominal strength, air - entrainment, type of aggregate, and frequency of testing speed.

e) The fatigue strength is significantly affected by the presence of a stress gradient, and increases with increasing stress gradient, being a minimum under uniform stress.

f) The effect of rest periods on the fatigue strength is not known.

2.1b) STRESS - STRAIN CHARACTERISTICS OF CONCRETE UNDER REPEATED AXIAL LOADING.

Van Ornum (3) noted that the stress - strain curve, originally convex upwards, became linear at all load levels after a few repetitions of loading. Following this, if the maximum stress was above the level sufficient to cause fatigue failure, the curve became progressively concave upwards, with significantly reduced stiffness at lower stress levels, and only marginally decreased stiffness at levels approaching the maximum stress level as shown in fig. 5.3. If the maximum stress level was below that necessary to cause fatigue failure, the curve became simply linear and remained so, although the modulus of elasticity was reduced to about 70% of its initial tangent value, as shown in fig. 5.4.

Probst (4) reached similar conclusions to Van Ornum, but further stated that the immediatly recoverable elastic strains, and the residual strains, increased with the number of repetitions of load until a stable state was achieved after about 200,000 load cycles. Stability of the recoverable strains on unloading was always attained before the residual strains became constant. This stable state was not achieved if the maximum load level was above that required to cause fatigue failure. He also concluded that if a stable state was reached, the limit of linearity was increased over that of non - preloaded concrete but no significant effect was apparent in the ultimate load. 300,000 cycles of loading with a maximum stress of 37.5% of the static ultimate strength was found to create a linear modulus of elasticity of 12% less than its initial tangent value. In a subsequent test to failure, this linearity in E_c was found to exist up to 50% of the ultimate strength. Residual strains were found to recover during rest periods but the modulus of elasticity was unaffected.

Murdock (2) concluded that the stress - strain curve is cycle dependent, but tends to become independent of the number of repetitions of load when the maximum stress is too low to produce failure. He also found that older concrete exhibits better elastic properties with smaller permanent deformations which stabilize more quickly. Bennett (6) found that the stable state was reached after about 300,000 cycles with a decrease in the modulus of elasticity of 17%. He found considerable recovery (up to 50% in some cases) of residual strains in rest periods.

Warner and Hulsbos (38, 48) conducted tests on cylinders at maximum stress levels of 53% and 69% of the static ultimate strength with a view to relating the characteristics obtained to the stress distribution in the compression zone of prestressed concrete beams. However, the results must be open to some doubt since only two stress levels were investigated.

The conclusions drawn from the investigations are clear and generally confirm one another but, with the exception of Hulsbos and Probst, the main objective of the investigations was determination of the fatigue properties of the material and the stress - strain characteristics were secondary results. Consequently, in no case have the complete stress - strain characteristics been obtained to show the variation with the number of repetitions of loading, and intensity of loading.

2.1c) FATIGUE OF PLAIN CONCRETE UNDER FLEXURAL LOADING.

The fatigue of plain concrete under flexural loads is a more urgent problem than that of concrete in compression and, therefore, the results available are more detailed and comprehensive.

Clemmer (13) commenced the investigations into flexural fatigue in 1922 with tests on cantilever beams and obtained a value of 53% of the static ultimate strength for the fatigue limit from zero stress to a maximum. He also found that specimens (when tested at greater load intensities) which had a previous history of repeated loading, had an increased fatigue strength.

Crepps (14) and Hatt (15) conducted tests on beams subjected to completely reversed flexural loading, and found a fatigue limit of approximately 55% of the static ultimate strength, indicating that the fatigue resistance is dependent upon the tensile strength of the concrete. They also found that previous repeated loading below the fatigue limit increased the fatigue strength at higher intensities of load. Stabilization of strains was judged the criterion for the given stress level being below the fatigue limit.

Williams (16) concluded from tests on beams with lightweight aggregates that a fatigue limit did not exist. This is in contradiction to the conclusions of Clemmer, Hatt and Crepps.

In 1953, Kesler (17) reported the results of tests conducted to determine the effect of the speed of testing on the flexural fatigue strength of normal concrete. The results indicated that within the range of 70 to 440 cycles/min the speed of testing had no effect on the fatigue strength. He also concluded that no fatigue limit existed up to 10×10^6 cycles, and estimated that the fatigue strength at 10×10^6 cycles was about 55% of the static ultimate strength, and when expressed as a proportion of that strength, was independent of the nominal strength.

Kesler and Murdock (18) investigated the effect of the stress range on the flexural fatigue strength - their results are best shown in the modified Goodman diagram in fig. 2.2. Once again, there was no indication of a fatigue limit up to 10×10^6 cycles. The insertion of regular rest periods of 5 minutes duration was found to increase the fatigue strength at 10×10^6 cycles by about 8%. They found limited evidence indicating an increase in the fatigue strength with previous loading at a level too low to cause failure.

McCall (19) carried out tests on small specimens subject to reversed flexural loading and included an important new variable in his investigation - the probability of failure. No fatigue limit was found, but for a probability of failure of 0.5, the fatigue strength at 10×10^6 cycles was 50% of the static ultimate strength.

Hilsdorff and Kesler (20) investigated the effect of rest periods on the fatigue strength of flexural specimens and found that regular rest periods of duration greater than 5 minutes interspersed throughout a fatigue test, increased the fatigue strength at 10×10^6 cycles by about 8%.

The main conclusions about the behaviour of concrete under flexural loading may, therefore, be summarised as follows :-

a) The fatigue strength at 10×10^6 cycles of loading from zero stress to a maximum is approximately 50 - 55% of the short - term static ultimate strength.

b) .....

b) The fatigue strength for varying minimum stress levels may be expressed by a modified Goodman diagram as shown in fig. 2.2.

c) No fatigue limit exists up to 10 x 10^6 repetitions of loading.

d) The fatigue properties, when expressed in terms of the short - term static ultimate strength, are statistically independent of the nominal strength and the frequency of the testing speed.

e) Prior repeated loading at a level too low to cause failure increases the fatigue strength in subsequent tests at greater load intensities, over that of non pre - loaded specimens, by an undetermined amount.

f) Regular rest periods of duration greater than 5 minutes significantly increase the fatigue strength.

2.2) BEHAVIOUR OF STEEL UNDER REPEATED LOADING.

The number of published results on the fatigue behaviour of high tensile steel as used for prestressing is quite large, but the wide range of fatigue strengths found indicates that this value is not simply related to the static strength, but is dependent on a number of parameters, the effects of which are only qualitatively understood, and have not been widely investigated.

2.2a) HIGH TENSILE WIRE

Bennett and Boga (34) carried out tests on short specimens at 9000 cycles/min to determine the effect of indenting and crimping on the fatigue strength of 7 mm wires. Four types of wire were tested - plain round, "Swiss" indented (2.8 mm long elliptical indentations), "Belgium" indented (8.0 mm long elliptical indentations) and crimped. With a minimum stress level of 0.49 f_{su}, the plain round wire gave a fatigue limit stress range of 0.28 f_{su}. For the "Swiss" and "Belgium" indented wire, the fatigue limit stress range was reduced to 0.256 f_{su}, (a reduction of 8.5%), and for the crimped wire, the fatigue limit stress range was reduced to

0.137 f_{su}, (a reduction of 51%). The fatigue response under varying minimum stress levels was investigated for the plain round wire and is given in fig. 2.3. In subsequent static tests on specimens which did not fail after 5×10^6 load cycles, no significant change in the ultimate tensile strength was found.

Gorodnitsky and Konevsky (35) carried out tests on 5 mm wires to investigate the effect of the shape of indentations - these were all 0.3 mm deep, but varied from sharp angular (135°) to smooth cylindrical (10 mm radius). With a minimum stress level of 0.59 f_{su}, the smooth round wire gave a fatigue limit stress range of 0.14 f_{su}, that with the 10 mm radius cylindrical indentations gave an equivalent fatigue limit, but the fatigue limit was reduced progressively for the other wires as the stress concentration effect of the indentations was increased - for the sharp angular indentations, the fatigue limit stress range was 0.06 f_{su}, (a reduction of 57%).

They also carried out tests to determine the effect of stress - relieving (at temperatures of about 400°C) on the fatigue strength strength - it was found to increase the fatigue limit stress range by 6% with a minimum stress level of 0.5 f_{su}.

Baus and Brenneisen (36) have given the results of the Belgian tests carried out to investigate the effect of stress - relieving on the fatigue strength with varying minimum stress levels. The results show that stress - relieving increases the fatigue strength and that the increase is greater as the minimum stress is reduced. The static ultimate strengths of the stress - relieved and the non stress - relieved steel were the same. The results of several investigations are given in fig. 2.3 which shows the variation of fatigue limit stress range with varying minimum stress level.

Bo and Leporati (cited in (36)) carried out tests on a large number of 6 mm and 7 mm wire specimens to determine the effect of pre - stretching and ageing. Pre - stretching to give a residual strain of 0.4% was found to increase the fatigue limit stress range from 0.095 f_{su} to 0.111 f_{su}, (an increase of 17%) with a mean stress of 0.5 f_{su}. Specimens similarly pre - stretched, but aged at room temperature for 4 - 5 months, were found to have their static ultimate strength increased by 4.8%, while the fatigue limit stress range increased to 0.122 f_{su} with a mean stress of 0.5 f_{su}, (an increase of 29%). Pre - stretching was, however, found to increase the scatter of the test results since it tended to magnify the manufacturing flaws. They also investigated the distribution of test results for particular test conditions and found that the logarithm of the number of cycles to failure had a practically normal distribution.

Rehm and Russworm (cited in (36)) carried out a qualitative investigation of the effect of flaws on the scatter of test results. They divided the total scatter into two portions - that due to the fatigue characteristics of the fault - free material and that due to the presence of microscopic flaws, although, in practice, the two parts were found to be inseparable. A number of manufacturing flaws were found to have an effect on the fatigue strength, including : decarburation at grain boundaries causing embrittlement in the presence of corrosion; impurities in the form of inclusions, in particular those occurring at the surface; shape effects, causing cracks during the drawing process; flaws due to ribs or indentations involving notch effects. In addition, flaws arising after manufacture due to mechanical damage or corrosion also had a significant effect on the fatigue strength.

2.2b) HIGH TENSILE STRAND

Warner and Hulsbos (37, 38) investigated the fatigue behaviour of 7/16" diameter strand under constant magnitude load cycling and cumulative damage load cycling. An investigation was carried out on 20 specimens at one particular load level to determine the statistical distribution - the logarithm of the number of cycles to failure was found to be normally distributed with a goodness of fit well within the 0.05 significance level. The results were analysed statistically, and the probability, PR, was introduced into the derived equation connecting the stress levels with the number of cycles to failure. The results are included in fig. 2.4.

Gorodnitsky and Konevsky (35) carried out tests on strand with diameters varying between 4.5 mm and 15 mm. The individual wires of the strands were all cold - drawn, and the centre wire was 10% greater in diameter than the outer wires. The initiating fatigue cracks were found to occur at either the interface between the centre wire and outer wire, or between two other wires. The fatigue strength was found to decrease with increasing diameter, but this was only a general trend, and some results were irregular. The results are summarised in fig. 2.4. Specimens which did not fail in fatigue were subsequently tested to failure and showed an 8 - 12% increase in the 0.2% proof stress due to cold - hardening, but the elongation at failure was reduced by 40%, with no change in the value of the ultimate tensile strength.

In discussing the lower fatigue strength of strand as compared generally to that of wire, Baus and Brenneisen (36) state that it may be due to the low torsional strength of drawn steel, but note also the importance of stress concentrations caused by rubbing between individual wires. All the available results are summarised in fig. 2.4.

2.2c) EFFECTS OF FRETTING ON FATIGUE RESPONSE.

The only investigation to determine the effect on the fatigue strength of embedding steel in concrete was carried out by Wascheidt (39) on plain and ribbed bars for reinforced concrete. He tested the bars both free (in air) and embedded in concrete at various stress levels and determined the fatigue limits. He found that the difference between the fatigue limits was zero for well - bonded (ribbed) bars, but for poorly - bonded (smooth) bars there was a reduction of up to 20% in the fatigue limit stress range. This was explained by the fact that rubbing of the concrete on the steel near the cracks produced an abrasion phenomenon which made the bar surface chemically active and caused oxidation, which lowered the fatigue limits.

Several investigators have noted a reduction in the fatigue strength of steel in beam tests and these are discussed in section 2.4.

Fatigue failures due to fretting are well known in aircraft and mechanical engineering structures and the effects have been noted by many investigators, but the phenomenon is not yet quantitatively understood.

Harris (40) discussed the main parameters influencing fretting fatigue and described the phenomenon as the interaction of two surfaces held in contact and subjected to relative slip in an oscillatory manner, and in the case where chemical reaction with the environment was possible, fretting corrosion occurred, leading to "micro - welds" at surface junctions, which were subsequently subjected to plastic shearing causing high tensile stresses in the surface - this eventually led to the formation of fatigue cracks, which were able to propagate into the parent metal. The fretting effect was found to be dependent on the magnitude of the relative slip, the normal compressive pressure on the contact surface, and the coefficient of friction between the surfaces.

Cox and Fenner (to be published) found that the reduction in the fatigue strength was almost linear with increasing slip amplitude up to about 5×10^{-4} ins - above that value, the reduction was much greater and could in some cases, be as much as 90%.

Fenner and Field (41) tested aluminium specimens in tension with a bridge piece creating fretting under varying pressure - the fatigue strength was found to be increasingly reduced as the pressure was increased. The reduction also increased as the number of cycles to failure increased.

Heywood (29) states that the process of fretting takes some tens of thousands of load cycles to develop, but once the initiating cracks have been formed, it plays no further part in the progression of the crack leading to eventual failure, and removal of the cause of fretting after a certain minimum number of cycles will not increase the fatigue life of the specimen.

The main conclusions that may be arrived at from the results of previous investigations are as follows :-

1) The available fatigue data shows a great variation for similar test conditions, which indicates that the fatigue properties are dependent on many factors - the static ultimate tensile strength is only one of many parameters involved. The prediction of fatigue strengths must, therefore, be based on data determined from tests on the particular steel in question.

2) Statistical treatment of fatigue data is essential in any analysis. The logarithm of the number of cycles to failure for one particular set of test conditions may be assumed to be normally distributed.

3) An endurance (or fatigue) limit exists for steel.

4) In general, strand has a lower fatigue strength than wire. This is probably due to fretting between individual wires, and the presence of torsional stresses.

5) Fretting has a very significant effect on the fatigue behaviour of steel - the effects are only qualitatively understood.

6) The effect on the fatigue strength of embedding high tensile steel in concrete is not known.

7) Repeated loading below the fatigue limit increases the proof stress, but does not affect the ultimate strength.

8) Indenting and crimping have an adverse effect on the fatigue strength.

10) The fatigue strength of strand decreases with increasing nominal diameter.

11) Pre - stretching and ageing have a beneficial effect on the fatigue strength.

12) Flaws formed during and after manufacture have a very significant adverse effect on the fatigue properties.

2.3) EFFECT OF REPEATED LOADING ON THE BOND STRENGTH OF CONCRETE

The amount of useful information pertaining to the effect of repeated loading on the bond strength of concrete is extremely limited and no quantitative conclusions can be drawn at this stage. The majority of the investigations have consisted of pull - out tests on short embedment lengths in which either the fatigue strength for complete failure has been determined, or the effect of repeated loading on the subsequent static pull - out strength has been investigated. The results are of marginal value since the embedment length is of vital importance in determining the magnitude of bond strength reductions - this is well illustrated by Muhlenbruch's tests. Only Bresler and Bertero (45) have attempted to investigate the bond stress distribution, which is the most important factor involved.

Lea (43) carried out a few pull - out tests under repeated loading on ½" diameter plain mild steel bars embedded to a depth of 3". The bond fatigue limit was found to be about 50% of the static pull - out strength regardless of whether the bar was subjected to stresses from zero to a maximum tension or completely alternating stresses.

Le Camus (44) conducted push - out tests on 30 mm. diameter bars and concluded that the fatigue strength at 1×10^6 cycles was 69% of the static push - out strength - however, the choice of test conditions in this case was not altogether suitable, since the effect of Poisson's ratio on the steel in compression is to increase the bond strength, whereas the effect is the opposite when the bar is in tension.

Muhlenbruch (46) carried out a comprehensive series of tests on pull - out specimens, using 5/8" diameter deformed bars embedded in concrete prisms to a depth varying between 5" and 10". The specimens were not tested to failure in fatigue, but for varying numbers of cycles - the specimens were then tested statically to failure to determine the effect of repeated load on the subsequent static pull - out strength. The only instrumentation utilised was measurement of the slip at both loaded and unloaded ends. The results showed that the reduction in strength is highly dependent upon the embedment length. Curves were drawn to show the reduction in pull - out strength for various levels of repeated loading after varying numbers of cycles of load. The static pull - out strength was decreased in all cases when preceded by repeated loading, the reduction being greater, for a specified number of prior load cycles, as the level of repeated load was increased. The reduction was also found to increase as the number of cycles of prior loading was increased, and did not show a limiting value.

Hanson (47) carried out tests on six beams pretensioned with 0.2" diameter wires with a view to determining the effect of repeated loading on the bond strength. Three beams were constructed with clean wires and three with rusted wires, and one of each was tested statically to failure. The wires were instrumented with electrical resistance strain gauges to a limited extent to obtain some estimation of the bond stresses. The beam with the clean wires failed statically in bond, but that with the rusted wires failed by fracture of the reinforcement and, therefore, the maximum bond stresses were not attained. Under repeated loading the beams with clean wires failed in bond after 7,200 cycles with maximum bond stresses of 84% of those obtained in the static test, and after 654,000 cycles when the maximum bond stresses were 70% of the static values. No estimation of the ratio of maximum bond stresses could be made for the beams with rusted wires, but the reduction in bond strength due to fatigue was sufficient to change the failure from a wire fracture to a bond failure.

Bond breakdown, and even complete failure in bond in beam tests under repeated loading was noted by several investigators (Venuti (63), Warner and Hulsbos (38,48), Bate (60, 61, 62), Nordby and Venuti (76), Ozell and Ardaman (58), Ozell and Diniz (59)), but only Warner and Hulsbos (38, 48) attempted to measure the magnitude of the effect - they measured the bond by a factor relating the compatibility of strain between steel and concrete at a cracked section and found that this factor was reduced after about 100,000 cycles of loading to about 65% of its value in the first cycle, although the absolute magnitude of the factor was found to vary greatly between similar beams.

In 1968, Bresler and Bertero (45) reported the results of well - instrumented tests which were carried out on specimens consisting of 1⅛" deformed bars embedded through the length of 6" diameter x 16" long cylinders which were notched at the mid - point to ensure the formation of a crack there under load - tension was applied to both ends of the bar thus simulating the conditions existing in the tension region of a beam subjected to constant moment. The bars were hollowed out and instrumented with electrical resistance strain gauges at $1\frac{1}{2}$" spacing, to give an accurate estimation of the bond stress distribution, but unfortunately, the scope of the tests was somewhat limited. The results showed that even at low load levels, before repeated loading, high bond stresses existed at the ends of the specimens, but the stresses quickly dropped to zero nearer the centre. Under higher loads and after the concrete had cracked, bond was broken down at the ends, and the peak bond stresses moved towards the centre. Under repeated load, the bond was rapidly broken down, and after only 65 cycles the average bond stresses were reduced to less than 30% of the initial values, the maximum peak values being reduced even further. The effectiveness of the bond was found to be particularly sensitive to the maximum peak stress level and was reduced when the maximum stress level was increased beyond a certain value; at lower stress levels in subsequent load cycles, the effectiveness of the bond was greatly reduced. Each specimen was subjected to load cycles which were increased in intensity at intervals during the test, a total of 65 cycles being applied to each of 4 specimens.

Few informative conclusions can, therefore, be drawn from the previous investigations, except that the bond strength of concrete is adversely affected by repeated loading, even at low levels of stress.

2.4) BEHAVIOUR OF PRESTRESSED AND REINFORCED CONCRETE BEAMS UNDER REPEATED FLEXURAL LOADING.

Several papers summarising the results of tests on prestressed and reinforced concrete beams have been published (1, 49, 50) and it is not intended to repeat those summaries here, but relevant details which were not included in those papers are reported here together with more detailed information on papers published subsequent to Hawkins' review (50) in 1964.

A quick glance at the number of beams which have been tested under repeated loading tends to indicate that the amount of information available is extensive, but in fact, this is not so. There are three main reasons for this :-

1) Many testing programs have been quite unsuitable for providing information for the development of a comprehensive theory to predict fatigue life.

2) ....

2) Most investigations have employed little useful instrumentation in the tests.

3) Few investigators have carried out associated independent tests on the component materials in order that their basic fatigue properties may be related to the prediction of their behaviour when combined together in a beam.

The first fatigue tests on prestressed concrete were carried out by Freyssinet (51) in 1934. These were followed by tests by Lebelle (52) and Abeles (53, 54) and then Campus (55), all on pretensioned constructions. Magnel (56) carried out the first tests on post - tensioned beams, followed by Xercavins (57) in 1955.

Ozell and Ardaman (58) tested 8 rectangular beams pretensioned with 7/16" diameter strands at various levels of maximum load, and obtained failures by fatigue fracture of the strand in all cases. Estimated steel stresses in the beams indicated that the fatigue limit stress range was only about 30% of the value for the free strand, based on information supplied by the manufacturer. No assessment was made of bond quality or slip, and no strain measurements were taken.

Ozell and Diniz (59) reported the results of tests which continued from the series (58) above, this time using $\frac{1}{2}$" diameter strands. The beams appeared to show little change in stiffness during the tests until strand fracture took place. Estimated steel stresses indicated that the fatigue limit stress range was about 60% of the value for the free strand. The reduction in the fatigue strength is considerably different from that above, but no explanation is offered for the variation.

Bate (60) has reported the results of fatigue tests on composite T - beams pre - tensioned with various types of plain, indented and crimped wires. All fatigue failures occurred by wire fracture. No other strain measurements were taken, but estimation of the steel stresses indicated that the maximum fatigue limit stress range for the plain wires was about 25% of the static ultimate strength; the lowest strength was obtained for the crimped wire for which the corresponding value was only 15%. No comparison was made with the fatigue properties of the wires when tested free in air.

In a subsequent series (61), Bate carried out tests on rectangular beams post - tensioned with varying numbers of plain 0.276" diameter wires - no useful conclusions could be drawn from the tests.

In a further series (62), Bate tested T - beams pre-tensioned with specimens of $\frac{1}{2}$" diameter strand obtained from four different manufacturers. Calculated steel stresses indicated that the fatigue strength (stress range) at 1×10^6 cycles varied between 16% and 22% of the static ultimate strength with a minimum stress level of 52% of the static ultimate strength. These results must be open to some doubt since the fatigue strengths are much higher than those normally obtained for steel strand. In all three series of tests reported by Bate, the beams which did not fail in fatigue showed no significant change in the subsequent static ultimate strength from unfatigued specimens.

Leonhardt (32) reported that in tests carried out by Wittworth on beams post - tensioned with ribbed wires in corrugated, grouted, metal sheaths, the fatigue limit stress range was reduced to 11% below the corresponding value for the free wire. He also gives the results of tests carried out by Birkenmaier on beams post - tensioned with 6 mm. diameter indented wires - in this case the fatigue limit stress range was 18% less than the corresponding value for the free wire.

Raus and Breneisen (36) have reported that in tests conducted on beams pre - tensioned with 8 mm. diameter ribbed wires, the fatigue limit stress range was reduced by 16%, due to embedment in the beams.

Soret (42) and Wascheidt (39) have published the results of fatigue tests conducted on high strength steel for reinforced concrete in which they compared the behaviour of bars with different bonding properties when tested free in air and in reinforced concrete beams. The results show conclusively that, for well - bonded bars, the fatigue strength in air is equal to that when embedded in concrete but, as the bond efficiency is decreased, the fatigue strength is decreased proportionately. Wascheidt has plotted this change in strength by relating the properties to the surface area of the ribs on the bars. The maximum reduction found in the fatigue limit stress range was 35%, for a smooth round bar.

In 1965, Venuti (63, 64) published the results of an extensive series of tests carried out on rectangular beams pre - tensioned with $\frac{3}{8}$" strand. 106 similar beams were tested in all, 18 at each of five different maximum levels of repeated load, which varied from 50% to 90% of the static ultimate strength, and 16 statically to failure. In the static tests, 14 beams failed by concrete crushing, one in flexural-shear, and one in bond.

Under repeated loading at the lower levels of stress, the tendency was for failure to occur by strand fracture, and at the 50% level, only 2 beams failed by concrete compression, whereas at higher load levels this was reversed, and at the 80% level, only one beam failed by strand fracture. It was noted that in the beams which failed in tension, the flexural stiffness decreased with cycles, rapidly at first, but then levelled out and the decreases were small after 2,000,000 cycles; in those beams which failed in compression, the stiffness continued to decrease throughout the test. It was also noted that the specimens which failed in fatigue showed a greater decrease in stiffness than those specimens which did not fail after 5,000,000 cycles. In the subsequent static tests to failure, the run - out specimens showed no change in ultimate strength over un - fatigued specimens. Strand fractures always occurred at a flexural crack and in some cases spalling off of the concrete occurred at fracture points. The scatter of the data was considerable, and was much greater than that generally expected from the fatigue properties of the component materials. On average, for a specified load level, the beams which failed in compression showed a considerably lower life than those which failed by strand fracture. No information on cracking was reported. Unfortunately, no instrumentation, other than deflection readings, was employed.

The data was analysed statistically, and it was found that for a given load level, the logarithm of the fatigue life was approximately normally distributed, although the fit was better at lower stress levels than higher ones. The variability of the fatigue life increased with increasing stress level, and curves were plotted to show the relation between the probability of failure at any stress level and the fatigue life. The investigation is the only one to date which has examined statistically the variation of beam fatigue life, but the results are of limited value since no estimation of steel and concrete stresses was made, and consequently, no general theory for the prediction of beam fatigue life was put forward.

Sawko and Saha (65) published the results of tests which were carried out to determine the effect of repeated loading on the static ultimate strength of post - tensioned beams. The results are significant but cannot be regarded as conclusive since the tests were limited in number. They found that repeated loading at levels below 55% of the static ultimate strength increased the ultimate strength by a varying amount which was a maximum of about 15% when the repeated load level was 30% of the static ultimate strength; at a repeated load level of 55%, there was no increase in strength. This was explained as being caused by creep hardening at lower levels causing an increase in strength, whereas the onset of micro - cracking at higher load levels resulted in a decrease in strength.

Two analytical studies have been published of the fatigue behaviour of prestressed concrete in flexure. The first was by Ekberg, Walther and Slutter (66) in 1957 - the method has been reported in detail by several authors (32, 50, 67) and is not repeated here, but the limitations of the theory are pointed out. The method is based on a theoretical determination of the relation between stress (in steel and concrete) and moment, used in collaboration with experimentally obtained fatigue failure envelopes for the component materials of steel and concrete. The method ignores, however, the possibility of progressive bond breakdown around tension cracks with its consequent effect on the stress - moment relationship; it also assumes that the stress concentrations associated with the cracks have no detrimental effect on the fatigue strength of the steel, although this assumption has been shown to be incorrect (32, 42, 58, 59, 60, 68). Furthermore, it ignores the essentially statistical nature of fatigue data, since the parameter of probability is not included in the analysis.

In 1962, Warner and Hulsbos (38,48) published a theoretical study for predicting the fatigue life of flexural members based on tensile fracture of the reinforcement. A method was also suggested for determining a lower - bound to the beam fatigue life as limited by fatigue failure of the concrete compression zone. The theory predicts the response of the beam to load, i.e. the relation between the steel stress and the applied momen with the loading being considered in two stages : -

i) .....

i) From zero to the moment, M^{tr}, at which previously formed cracks begin to open.

ii) From M^{tr} to the static ultimate moment.

In stage (i), linear stress - strain relations are assumed for concrete and steel, and as cracks are closed by the prestress, sections behave elastically up to M^{tr}.

Analysis of behaviour in stage (ii) is based on the stress-strain relations for concrete and steel, equilibrium of internal forces, and assumed compatibility of deformations between concrete and steel. The relation between the steel stress and the applied moment, used in conjunction with statistically analysed fatigue properties of the steel, enables the beam fatigue life to be predicted with any probability.

Three pretensioned beams were tested under constant magnitude repeated loading, all at the same level, in order to verify the theory. The load level was high (80% of static ultimate strength), and although all the beams were similar, considerable variation was found in the bond efficiency between beams - the bond factor, F, which has a significant effect on the fatigue life, was found to vary by 50% - from theory, this variation caused a change in the fatigue life of 150%. The theory was found to agree fairly well with the experimental results, but tended to overestimate the fatigue life slightly - the amount of overestimation increased as the bond efficiency was reduced. The theory showed that the fatigue life was very sensitive to small changes in the load level, the bond factor, the prestress losses and the assumed centre of compression in the concrete. The conclusions to be drawn from the investigation are that the theory appears to be suitable for predicting the fatigue life of the type of beams tested, but it cannot be accepted universally since it assumed identical fatigue behaviour of steel when tested free in air and embedded in a beam, and this has been shown to be incorrect (32, 42, 58, 59, 60, 68) - it would, therefore, lead to unsafe results, and allowance must be made for this reduction in the fatigue strength of steel when embedded in a beam.

The state of knowledge of the fatigue behaviour of prestressed concrete flexural members may, therefore, be summarised as follows :-

1) The fatigue limit of prestressed concrete members, in flexure, varies between about 45% and 85% of the static ultimate strength, depending on the design of the section.

2) The existence of flexural cracks is essential for the occurence of fatigue failures and, in general, the fatigue limit is above the static cracking load, but may not be so in a badly proportioned beam, assuming an overload to cause cracking.

3) The most common type of fatigue failure is by fracture of the steel reinforcement. Concrete compression failures occur only at high levels of repeated load, or in over - reinforced beams.

4) Bond failures in pretensioned beams are possible if tested with short shear spans.

5) The information available on flexural cracking under repeated loading is extremely limited.

6) The fatigue strength of steel in beams may equal its strength in air or be reduced by as much as 70%, depending on the bond conditions existing in the beam.

7) Statistical treatment of fatigue data is essential in any analysis.

8) Repeated loading at levels below the fatigue limit will generally increase the ultimate strength of sections, but repeated loading at higher stress levels may reduce the ultimate strength.

9) A theory exists for prediction of the fatigue life of flexural members, but although it is applicable to all sections and reinforcements, it does not invoke all the important parameters, and will, in general, overestimate the fatigue life of members.

2.5) SHEAR STRENGTH OF PRESTRESSED CONCRETE BEAMS SUBJECTED TO REPEATED LOADING.

The available information pertaining to the fatigue strength in shear of prestressed concrete beams is extremely limited and only Hanson Hulsbos (84) have reported the results of tests which are related to those carried out by the author.

When static loading is considered, the picture is somewhat different since a considerable number of investigations have been carried out, with a variety of approaches to the problem. Unfortunately, the subject of shear strength under static loading is not yet understood from a fully rational point of view, and many design equations are based on empirical experimental results, particularly those relating to the ultimate strength. This makes it virtually impossible to extrapolate, with any confidence, the behaviour under static loading to that under repeated loading. Furthermore, it cannot be assumed that the criterion of failure is the same under both static and repeated loading.

Investigations of the static shear strength are normally concerned with the determination of the shear cracking load, as well as the ultimate load. In thin-webbed I - beams without web reinforcement, tested at $^{a}/d$ ratios greater than about 2.0, it has been found (85, 86, 87, 88) that the diagonal tension cracking load represented the ultimate strength of the beam; theoretical investigations showed that this load could be satisfactorily predicted by the usual methods of calculation of principal stresses assuming an uncracked, homogeneous, elastic section, with the limiting tensile strength of the concrete being determined from experimental results. It was also found (89, 90, 91, 92, 86, 88, 93) that the diagonal cracking load was unaffected by the presence of web reinforcement. It is, therefore, possible that, as the fatigue properties of plain concrete in tension are known, the diagonal tension cracking life may be predicted by calculating the principal tensile stresses as outlined above; however, no results are available to verify this.

Most equations for determining the ultimate strength in shear of prestressed concrete beams are of the form:-

$$V_u = V_{conc} + V_v + V_d$$

where: V_u = ultimate shear force.

V_{conc} = shear carried by concrete.

V_v = shear carried by web reinforcement.

V_d = shear carried by dowelling action of the longitudinal reinforcement.

Bruce (94) has indicated that the term V_d may be neglected in prestressed concrete sections and, therefore, the equation simplifies to:-

$$V_u = V_{conc} + V_v$$

Tests incorporating many variables have shown that the contribution of the concrete compression zone, V_{conc}, at failure to the shear strength, in beams with bonded stirrups, is numerically equal to the value of the inclined cracking shear, V_{crws}; this relation is purely empirical and is not based on any rational theory. Since this empirical relationship applies to the static failure condition, it cannot be used at lower load levels of repeated loading. Therefore, at the present time, it is not possible to perform an accurate analysis to determine the stresses in the concrete and web reinforcement in a beam containing inclined shear cracks.

Hanson and Hulsbos (84) have reported the results of fatigue tests on two prestressed concrete I - beams with inclined cracks. The beams contained different amounts of web reinforcement, and the maximum load level in the two tests was also different. In static control tests on similar beams, failure occurred in flexure, and, therefore, the ratio of maximum load level to static ultimate shear strength was unknown. In the repeated load tests, the beams were overloaded in the first cycle of loading to 78% of the ultimate flexural capacity, in order to create the inclined shear cracks. In the beam with the smaller amount of web reinforcement, fatigue fracture of a stirrup took place after 1,500,000 load cycles, and complete collapse occurred after 2,007,500 cycles. In the other beam, fatigue fracture of the prestressing steel took place in the constant moment zone after 4,527,000 cycles, at which stage, stirrup fracture had not occured. No estimate of stirrup stresses was made.

The state of knowledge relating to the fatigue strength in shear of prestressed concrete beams may thus be summarised as follows :-

1) It is possible that the theory used to predict the static diagonal tension cracking load may be extrapolated for use when repeated loading is being considered, but experimental results are not yet available to verify this.

2) It is not possible to carry out an accurate analysis of the stresses in the concrete and web reinforcement in a beam containing inclined shear cracks, at load levels below the ultimate strength.

3) In beams containing inclined shear cracks, one possible criterion of failure under repeated loading is by fatigue fracture of the web reinforcement.

4) The fatigue characteristics of steel, when used as web reinforcement in a prestressed concrete beam, are unknown.

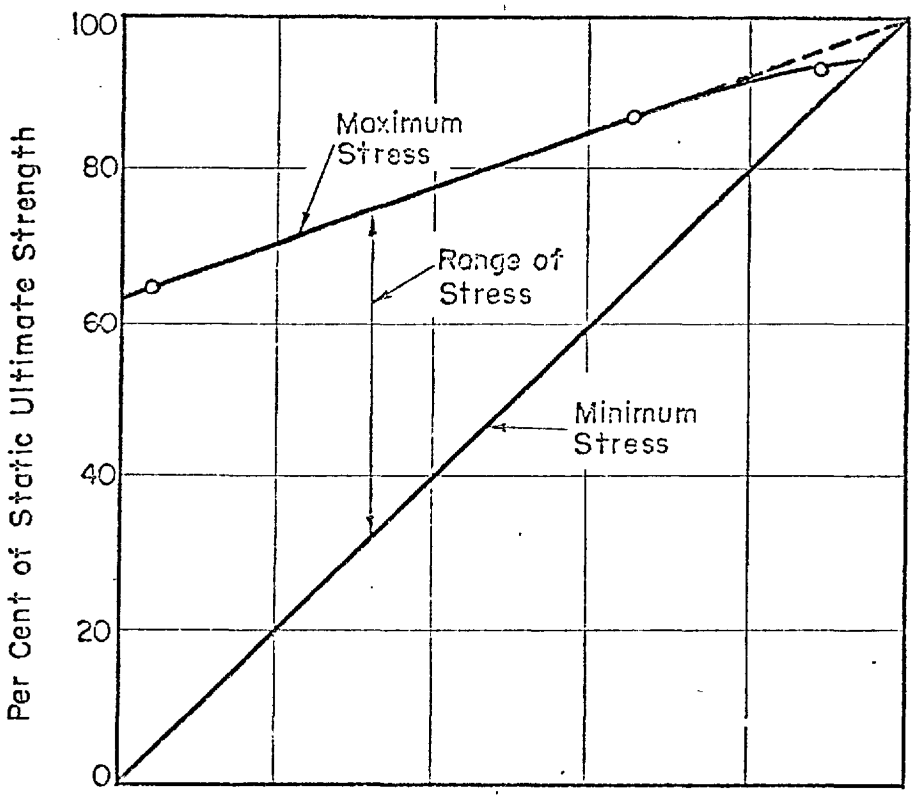

FIGURE 2.1 MODIFIED GOODMAN DIAGRAM FOR CONCRETE SUBJECTED TO REPEATED AXIAL LOADING. BASED ON GRAF AND BRENNER (cited in (2))

FATIGUE LIFE: TWO MILLION CYCLES

Fig 2.1

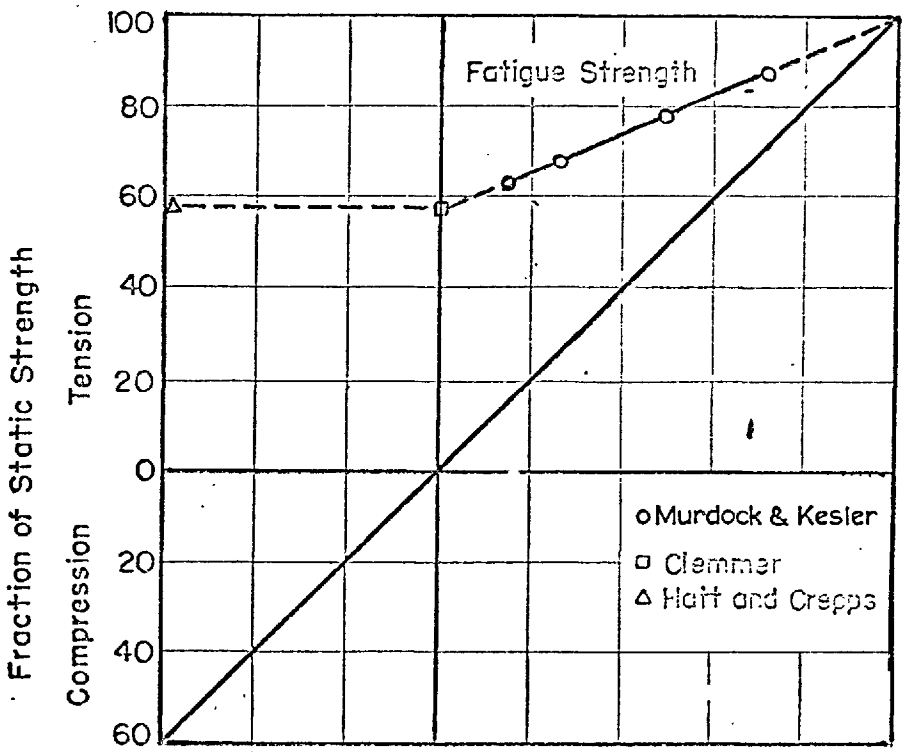

MODIFIED GOODMAN DIAGRAM SHOWING EFFECT OF RANGE OF LOADING ON THE FATIGUE LIMIT OF PLAIN CONCRETE UNDER REPEATED FLEXURAL LOADING. BASED ON MURDOCK AND KESSLER (18)

Fig. 2.2

HIGH TENSILE WIRE

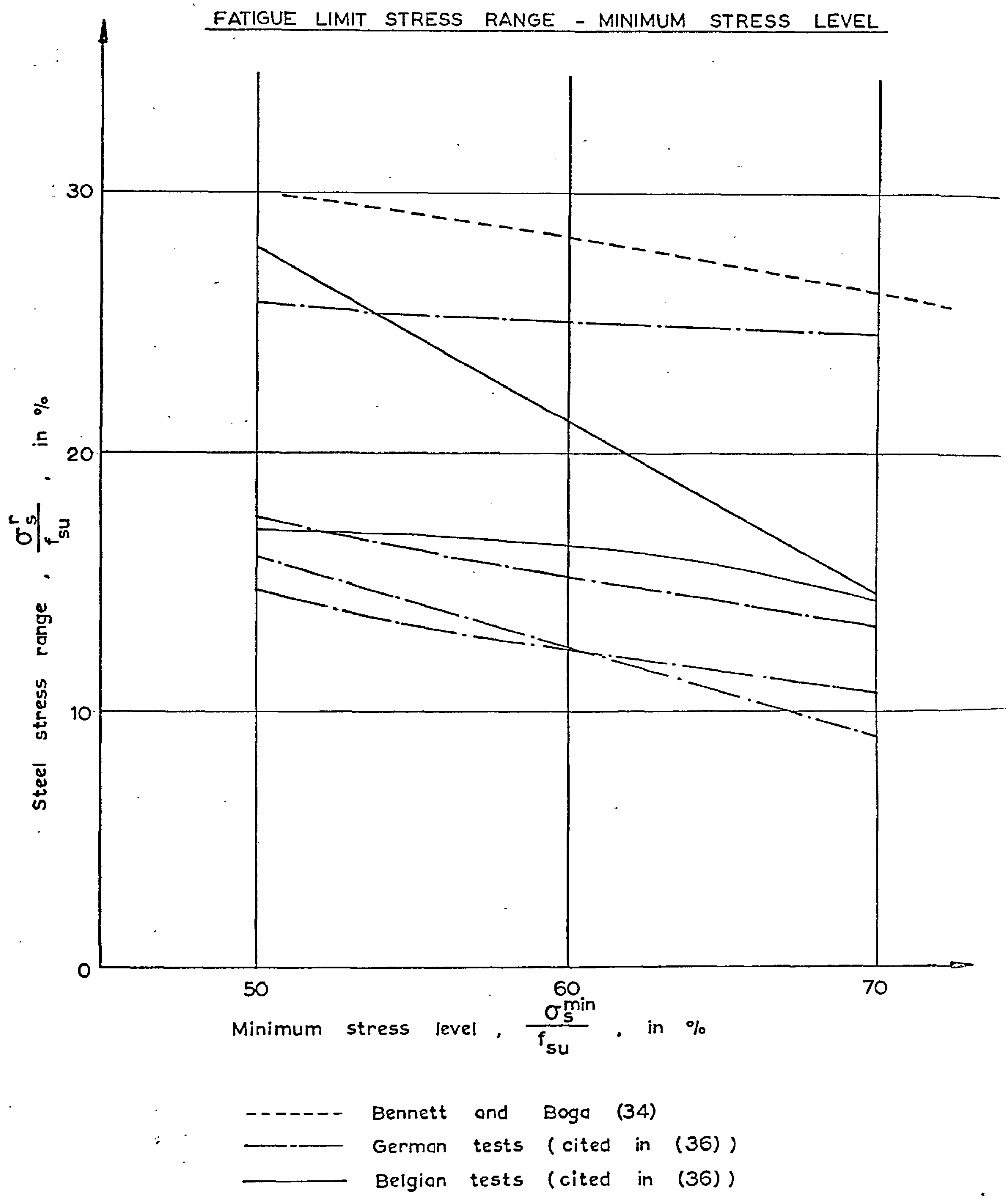

Fig. 2.3

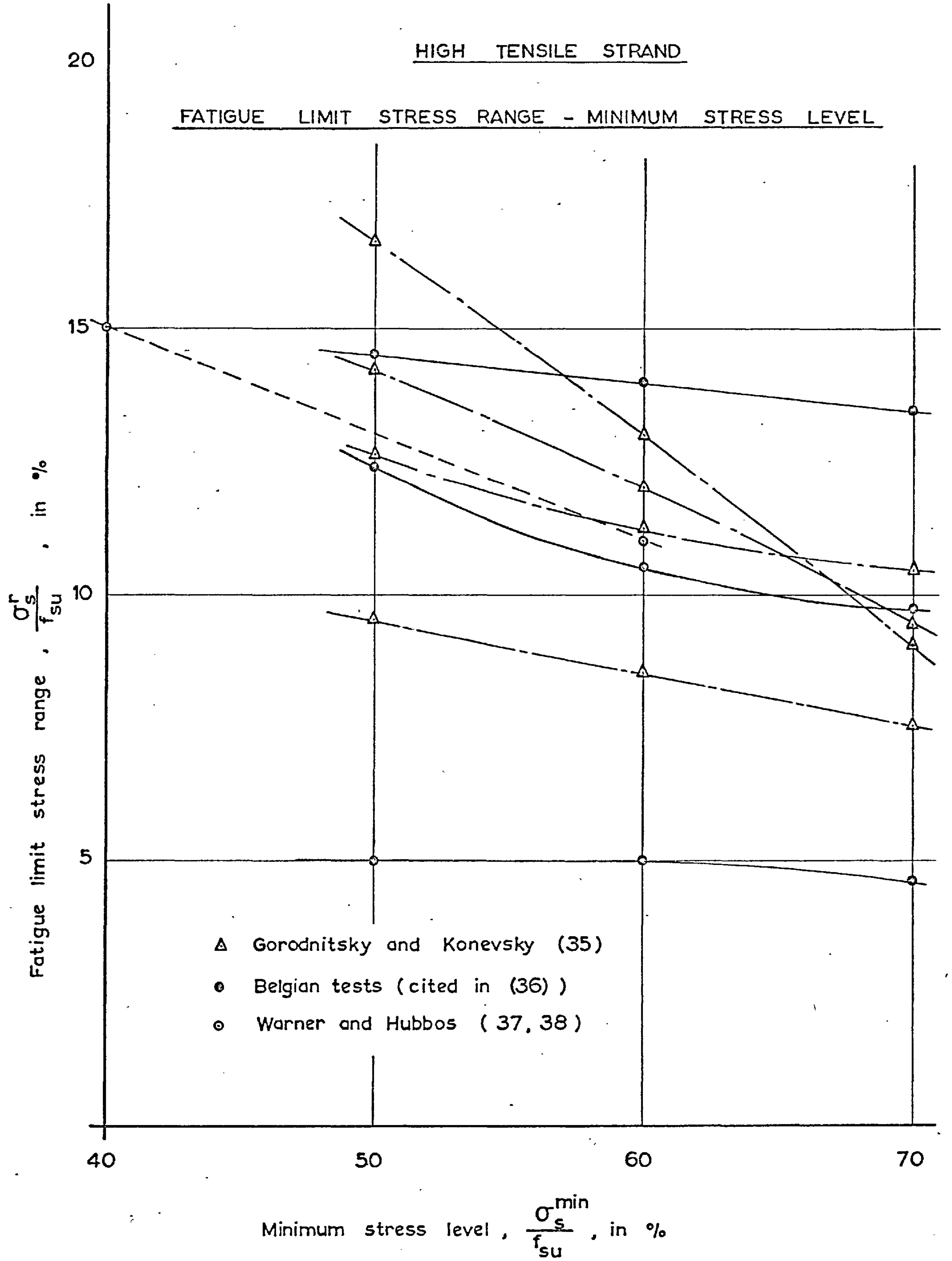
HIGH TENSILE STRAND
FATIGUE LIMIT STRESS RANGE - MINIMUM STRESS LEVEL
20
15
10
5
40
50
60
70
Fatigue limit stress range , $\frac{\sigma_s^r}{f_{su}}$, in %
Minimum stress level , $\frac{\sigma_s^{min}}{f_{su}}$, in %
Δ Gorodnitsky and Konevsky (35)
Belgian tests (cited in (36))
Warner and Hubbos (37, 38)

Fig. 2.4

CHAPTER 3

EXPERIMENTAL TECHNIQUES AND PROCEDURE.

3.1) INTRODUCTION

The testing of both materials and structures under the action of repeated loading requires the use of experimental techniques which cannot be simply extrapolated from experience and knowledge gained in static testing. Reports of past work generally gave little information on testing techniques, and many of those which did, appeared to be far from satisfactory and obviously there was much room for improvement. With this limited information in mind, preliminary tests under repeated loading were carried out and all the experimental techniques described here were subsequently developed and proven to be comprehensively satisfactory before being accepted as such. The subject is by no means complete, particularly in so far as instrumentation is concerned, but it must be realised that, for prestressed concrete, this is a relatively new field, and when it is considered that the Aeronautical and Mechanical Engineering industries have not yet fully overcome similar problems, this is understandable. Furthermore, the fact that it was necessary to modify the fatigue testing machine in the manner described later, tends to indicate that some manufacturers are possibly out of touch with the requirements of testing laboratories - a most unsatisfactory situation for the successful and efficient development of experimental techniques.

3.2) MATERIALS AND THEIR PROPERTIES

3.2a) CONCRETE

In order to be in accordance with the recommendations of the Ministry of Transport, the concrete was designed to have a 28 day cube strength of 7500 lbs/in^2 (51.7 N/mm^2). The casting and testing programme was designed so that the beams could be tested at a minimum age of 90 days for series F to obtain consistency in the concrete strengths and also to ensure that the strength did not change significantly during the period of the repeated loads tests which, in some cases, lasted for a period of 7 days. This had the further advantage of reducing the amount of creep and shrinkage which took place during the tests. After a series of trial mixes, the following mix proportions were chosen as most suitable, and used for all beams and specimens cast for the investigation:-

Actual Water/Cement ratio	=	0.50
Effective Water/Cement ratio	=	0.45
Total Aggregate/Cement ratio	=	3.40

Coarse Aggregate	:	total Sand ratio	=	52.5 : 47.5
Coarse sand	:	fine sand ratio	=	70 : 30

Ordinary portland cement and Thames valley river aggregates were used throughout.

Coarse aggregate	:	that passing $\frac{3}{8}$" B.S.S. but retained on 3/16 B.S.S.
Coarse sand	:	that passing 3/16" B.S.S. but retained on No. 25 B.S.S.
Fine sand	:	that passing No. 25 B.S.S. but retained on No. 100 B.S.S.

The properties of the fresh concrete were as follows :-

True slump value $\doteqdot$ 3"
Compacting factor = 0.98

The properties of the hardened concrete were as consistent as could be expected over the period in which the tests were carried out, and the summarised properties are given in tables 4.5 and 6.2. An example of the stress - strain curve for the concrete obtained from a compression test on a 12" x 6" diameter cylinder is given in fig. 3.1. The strains were the mean of the readings given by two 60 mm electrical resistance strain gauges placed diametrically opposite on the specimen, which was subjected to a constant rate of total strain.

3.2b) PRESTRESSED REINFORCEMENT

The $\frac{3}{8}$" diameter 7 - wire high tensile strand and the 0.128" diameter high tensile wire used in the tests was manufactured by Richard Johnson and Nephew Limited, and was tested in the laboratory to obtain the load - strain characteristics which are given in figs. 3.2 and 3.3. The properties obtained were identical to those provided by the manufacturer:-

$\frac{3}{8}$" diameter strand : Ultimate tensile strength = 22,570 lbs (100,370 Newtons)

Based on an area of 0.08 sq. ins., this is equivalent to a stress at ultimate of 282,070 lbs/in^2 (1,944.8 N/mm^2).

0.128" diameter wire : Ultimate tensile strength = 259,690 lbs/in^2 (1,790.5 N/mm^2).

The fatigue characteristics of the $\frac{3}{8}$" diameter strand are described in section 4.8.

3.2c) MILD STEEL SHEAR REINFORCEMENT

3/16" diameter mild steel, with a yield stress of 65,000 lbs/in^2 (448 N/mm^2), was used as the untensioned shear reinforcement in the webs of the beams of series S. The load - strain characteristics are given in fig. 3.4. The ultimate strength, f_{smu}, was 70,570 lbs/in^2 (486.6 N/mm^2).

3.3) BEAM DETAILS

3.3a) BEAMS OF SERIES F

The beams in this series were numbered F1 to F30, and all the beams had identical dimensions as shown in fig. 3.5. The reinforcement details are also shown in fig. 3.5.

The 9' - 9" long beams were cast in standard steel shutters, with wooden inserts over a length of 7' - 6" forming the web, thus leaving rectangular sections to form the end - blocks at either end - these sections were reinforced with a $\frac{3}{8}$" diameter mild steel helix.

The ducts in beams F1 to F28 were formed by inflateable rubber ductubes. A $\frac{3}{8}$" diameter bar, threaded at the ends, passed through the ductube so that it could be tensioned in position in the mould, which had been accurately drilled, to form a perfectly straight duct - the bar had a hole to a depth of 12" at one end so that the ductube could be inflated before casting, and then deflated and removed 24 hours after casting. The ductube was inflated until the outside diameter was $\frac{3}{4}$", thus leaving a straight smooth hole, $\frac{3}{4}$" in diameter, in the hardened concrete.

In beams F29 and F30, the ducts were formed by $\frac{3}{4}$" internal diameter corrugated metal ductube as supplied by C.C.L. - this ductube had negligible tensile strength. An 11/16" diameter bar, threaded at the ends, passed through the ductube and was tensioned accurately in position in the drilled mould.

The control specimens for beams F1 to F23 and F27 consisted of three 6" cubes, three 12" x 6" diameter cylinders, three 9" x 6" diameter cylinders and three 4" x 4" x 20" beams. After it was found that concrete fatigue was never the criterion of failure, no further 12" x 6" diameter cylinders were cast - i.e. for beams F24, F25, F26, F28, F29 and F30. Beam F27 was used for a static control test and 12" x 6" diameter cylinders were, therefore, cast with it.

3.3b) BEAMS OF SERIES S

The beams in this series were numbered S1 to S17, and all the beams had identical dimensions and reinforcement as shown in fig. 3.6. The 13' - 0" long beams were also cast in standard steel shutters with wooden inserts, and had similar end - blocks to those of series F. In all beams the ducts were formed by $\frac{3}{4}$" internal diameter C.C.L. corrugated ductube as in beams F29 and F30.

The control specimens for each beam consisted of three 6" cubes, three 9" x 6" diameter cylinders, and three 4" x 4" x 20" beams.

3.4) CASTING AND CURING.

For the beams of series F, only one mix was necessary per beam and all its control specimens.

For series S, two mixes per beam were necessary, the 4" x 4" x 20" beams and 9" x 6" cylinders being taken from the first batch and the 6" cubes from the second batch.

The concrete was vibrated by means of a single shutter vibrator bolted to the centre of the mould.

After the beam and control specimens had been cast, they were cured for 24 hours under wet hessian and polythene sheeting. The side shutters and ductube bars were then removed and the hessian and polythene replaced for a further six days. Thereafter, the beams and control specimens were air cured until testing.

3.5) PRESTRESSING

The beams of series F were stressed at slightly differing ages, those for the preliminary tests being stressed at about 70 days, and those for the main series of tests at about 100 days, but at this stage, the strength was almost constant and varied only slightly with age. The creep and shrinkage rate was a more important parameter, but had also decreased to a small value by this time and the maximum variation from the mean of final prestressing force for the beams of the main section of series F was only 3%.

The beams of Series S were stressed at ages of between 30 and 50 days, the maximum variation from the mean of the final prestressing force being 4%.

The end blocks for prestressing were constructed out of 1" mild steel plate - the blocks were drilled accurately to just take the prestressing steel, so that it was in the correct position in the beam irrespective of the position of the duct. Holes for grouting were also drilled in the blocks.

All the beams were stressed from one end only using a C.C.L. jack. The force was measured by means of a 5 Ton load cell, and was applied with an estimated sensitivity of $\pm$ 50 lbs ($\pm$ 0.5%). All the strands were first stressed to approximately the correct load and anchored off, then they were restressed finally using a special restressing bridge designed to fit the strand layout - the gap between the anchorage and the end - block was then filled with shims of varying thickness down to 0.004". This enabled the losses due to elastic shortening to be completely removed.

The creep and shrinkage losses were obtained directly from the mean of four 8" demec gauge readings on the concrete at the level of the centre of gravity of the prestressing steel.

Relaxation losses were neglected on the basis of information supplied by the manufacturer.

The details of the prestressing forces and losses are given in Table 4.4 for Series F, and Table 6.1 for series S.

3.6) GROUTING

The length of time between grouting and testing varied, but in no case was it less than 7 days. Grouting was carried out by means of a high pressure hand pump.

For beams F1 to F28, the grout consisted of high alumina cement, water and aluminium expanding agent in the following proportions :-

Water/Cement ratio = 0.35

Aluminium additive/Cement = 0.22%

On the basis of the recommendations given in reference (107), the grout was changed for Beams F29 and F30, and S1 to S17, and consisted of rapid hardening portland cement (Ferrocrete), water and aluminium additive in the following proportions :-

Water/Cement ratio	=	0.55
Aluminium additive/Cement	=	0.22%

3.7) PRELIMINARY TEST RIG.

The preliminary tests under repeated load were carried out in the 20 Ton planar internal reaction frame as shown in plate 3.1. The steel frame was stressed to the top flange of a prestressed concrete box girder which forms the base of the reaction frame. The box girder was approximately 70 ft in length, with external dimensions of 7'-6" deep x 5'- 0" wide, with 12" deep top flange and 6" walls and bottom flange. It was mounted at each corner on 2 banks of helical springs, each bank consisting of 2 springs. The two point loading was applied to the test beam by one 20 Ton/10 Ton Amsler jack through a spreader beam incorporating a pin and roller bearing. The beams were supported at each end on spring loaded roller bearings (see section 3.9) resting on concrete pedestals. This system had been used quite successfully for static tests, but it was expected that some difficulties might be encountered under repeated loading - however, experience of the problems involved was gained on the old rig before designing a new one. Under repeated load it was found that the rig was not sufficiently rigid in a plane parallel to the axis of the test beam - this was due to the longitudinal forces applied by the jack when it moved out of a vertical plane, a situation which always occurred due to the asymmetric support system and random cracking of the specimen - any movement thus created in the rig was amplified by the dynamic forces consequently set up by the heavy cross - beam of the rig. Furthermore, it was found that the natural frequency of vibration of the rig in this direction was about 400 cycles/min, which was within the range of testing frequencies of the Amsler pulsator.

3.8) FINAL TEST RIG

On the basis of the knowledge and experience gained in the preliminary tests, a new test rig was designed and installed. This took the form of a space frame utilising two jacks as shown in plates 3.2 and 3.3, and was designed to be five times as stiff in a longitudinal direction, as the previous frame. This also increased the natural frequency of the rig by a factor of 1.5. The frame was constructed of 10" x 10" x $\frac{1}{2}$" mild steel hollow sections stressed together and to the prestressed concrete box girder by means of 1" diameter Macalloy bars. It was designed for a total load of 80 Tons. With this system, the jacks applied the load directly to the test beam through 1" steel plates, thus obviating the use of a spreader beam with the necessary bearings. The two jacks were connected by rigid steel pipe to a distributor which was in turn connected by a single line to the pulsator, as shown in plate 3.3. The jacks were piped to the distributor in such a way that on loosening the joints and knuckles, the jacks could be freely placed in any position on the loading beam. The rig incorporated enlarged concrete pedestals which were also stressed to the box girder and were designed so as to have a height which was variable over 12". The test beams were supported on spring - loaded roller bearings as described in section 3.9. This rig was found to be completely rigid and quite satisfactory under all conditions to which it was subjected.

3.9) SUPPORT BEARINGS

Three different types of bearings were used to support the test beams in the preliminary tests under repeated load. Initially, symmetrical bearings were used, consisting of laminated rubber to take up longitudinal movement, and a fixed roller to allow rotation; under high loads, these did not give enough lateral stability and were rejected. These were then substituted for a system consisting of a fixed roller allowing rotation only at one end, and a free roller allowing longitudinal movement and rotation, at the other - all bearing surfaces were made up of p.t.f.e. impregnated bronze to reduce fretting corrosion. This was also unsatisfactory since the unsymmetrical longitudinal forces created, caused the beam to progressively move out of the test rig. This led to the use of symmetrical spring loaded roller bearings as shown in fig. 3.7 and plate 3.4, which combined the advantages of the two previously described systems. The springs, which acted to restrain the beam in position in the rig, were replaceable and could be exchanged for springs of stiffness to suit the test in question. Clamps on the top plate restrained the beam from movement in a lateral direction, and the rollers themselves were held in position by four involute - shaped pins which fitted the conical holes in such a way that they were just in tangential contact for all positions of the roller. The bearing material was high grade tool steel, and the components were designed in such a way that all wearing surfaces consisted of hardened on non - hardened material - this gave optimum resistance against fretting corrosion. After approximately 30×10^6 cycles of loading, the wear was found to be virtually negligible.

3.10) LOADING EQUIPMENT

3.10a) STATIC TESTS

For all static tests, the load was applied to the beams by means of an Amsler pendulum dynamometer and Amsler hydraulic jacks. During intervals in which readings were taken, the beams were subjected to conditions of constant load.

3.10b) MAIN REPEATED LOAD TESTS.

For these tests, the load was applied by means of Amsler pulsator equipment through Amsler jacks. This system applied a constant minimum load, which was independent of any change in the response of the beam specimen, and superimposed on top of this, the pulsator delivered a volume of oil to the system which varied approximately sinusoidally with time. The magnitude of the maximum volume delivered was constant and, therefore, the maximum load applied was dependent on the response of the beam. This necessitated adjustments to the machine from time to time as the stiffness of the beam altered. The loading rate was 300 cycles/min for Series F, and 400 cycles/min for Series S. The seismic cut - out supplied by the manufacturers was found to be entirely unsatisfactory for determining the point of fracture of a single strand wire or bar in a beam, and a new system was, therefore, devised which operated on the principle of a drop in the maximum load with fracture. This was subsequently installed by the manufacturers and employed a second maximum load gauge with an extremely sensitive limit switch which cut out the superimposed oscillating load only, when the maximum load dropped by more than 0.25% of the full - scale gauge reading - this sensitivity could be set to any value less than 0.25% if required. This enabled the tests to be continued again after the first fracture, without the minimum load being removed from the specimen, a situation which could vastly change its subsequent behaviour. The maximum and minimum loads were applied with a sensitivity of $\pm$ 0.1% of the full scale gauge reading, which for series F and S, was equivalent to $\pm$ 0.01 Tons, or $\pm$ 0.25% and $\pm$ 0.14% respectively of the static ultimate strengths.

3.10c) SLOW SPEED REPEATED LOAD TEST

One beam, F28, was tested under repeated load at a rate of 4 cycles/min using the slow - cycling device of an Amsler pendulum dynamometer. This applied conditions of constant magnitude maximum and minimum load to the beam throughout the test without adjustment.

3.11) INSTRUMENTATION

3.11a) ELECTRICAL RESISTANCE STRAIN GAUGES

It was originally intended to measure both steel and concrete strains under static and repeated load by means of electrical resistance strain gauges, and the instrumentation programme was arranged with this in mind. Furthermore, it was intended that, under repeated load, the test would not be stopped until failure to eradicate the effect of rest periods, and therefore, if possible, the strain readings were to be measured dynamically. This required the choice of a recording system from the following :-

i) Ultra - violet recorder.

ii) High - speed data logger.

iii) Peekel dynamic strain recorder coupled to an oscilliscope.

Method i) was rejected on the basis of insufficient sensitivity, and method ii) because of the excessive cost and limited number of channels which could be recorded. Method iii) was, therefore, chosen, although it also had disadvantages in that it was slow, and, therefore, the number of channels which could be recorded had a practical limitation. This method also made the dynamic measurement of deflections and rotations possible by means of induction type linear transducers. Strain readings on the concrete were, therefore, taken by this means in the preliminary tests under repeated load, but it was soon found that the electrical resistance strain gauges were themselves failing in fatigue well before the specimens - the fatigue fractures were always found to occur at either the join of the actual resistance wire, or at the join of the lead wire to the gauge. Encasing the leads in strain gauge cement was found to increase the life of the gauges, but is was still shorter than that required for the series of beam tests. Special high fatigue life strain gauges were known to be available, but a large number were required for the tests, and the cost of these gauges prohibited their use. Certain of the preliminary test beams in series F had electrical resistance strain gauges attached to the central prestressing wire, and beams S1 and S8 had electrical resistance strain gauges on the stirrups, but failure occurred very quickly under repeated load and, therefore, the results only gave an indication of strains involved during the early part of these tests - these gauges were protected by a layer of waterproofing, but it is probable that failure occurred due to slip between steel and concrete at the gauge, and not by fatigue failure of the gauge.

3.11b) DEMEC GAUGES

After careful consideration of the problems and results obtained with the methods described in sections 3.11a, it was decided that the only reliable means of determining strains and crack widths was by stopping the tests at intervals and taking measurements statically with demec gauges under the maximum and minimum loads which were being applied in each load cycle. The use was, therefore, limited to measurements on the concrete. This meant the introduction of intermittent rest periods into the tests, but it was found that under minimum load, the recovery which took place was quite negligible, and was only significant if the load was completely removed.

For the beams of series F, 4" demec gauges were used to measure the average strains in the compression flange at four levels over five sections in the constant moment zone on both sides of the beams, as shown in fig. 4.1.

In series S, 8" demec gauges were used to measure the average strains at four sections on the top surface in the shear spans, and 12" demec gauges were used to measure the crack widths between flanges at stirrup positions as shown in fig. 6.3.

The estimated sensitivity of the measurements was as follows :

4" demec gauge : $\pm 13 \times 10^{-6}$ strain.

8" demec gauge : $\pm 2.5 \times 10^{-6}$ strain.

12" demec gauge : $\pm 5 \times 10^{-5}$ inches.

3.11c) DEFLECTIONS AND ROTATIONS

The deflection of the beams was measured at the centre line and at the load points, in both series F and series S, by means of 0.001" dial gauges - the gauges had a clamp attached to the spindle so that they could be held away from the beam while the test was in motion, and released to take readings statically.

The rotation at each end of the beam was measured by means of bubble clinometers - the sensitivity of the clinometers was 0.000025 radian.

3.12) STATIC AND FATIGUE TESTS ON STEEL STRAND

3.12a) STATIC TESTS

Static tests to failure were conducted on ten specimens of $\frac{3}{8}$" diameter steel strand. The tests were carried out in an Amsler universal testing machine, the load being applied by a hydro - pacer unit - this unit applied load such that the overall strain in the specimen increased at a constant rate; for the tests described here, the strain was increased at a rate of 0.005 in/in/minute throughout the test to failure.

In order to obtain failure within the gauge length of the specimens, they were gripped by two $\frac{1}{8}$" thick soft aluminium angles as shown in plate 3.5. The surfaces of the angles which faced onto the strand were coated with fine carborundum powder to prevent slip. The angles were gripped in the testing machine jaws, and load was thus transferred to the steel strand through the aluminium without creating a notch effect in the surface of the strand. Plate 3.5 shows a polythene shim surrounding the lead - in length of the grip - this was used only in the fatigue tests and not in the static tests to failure as it was found to induce failure in the grips under static loading.

The test length of the specimens between gripping points was 18". The lay length of the strand was 5.25".

3.12b) FATIGUE TESTS

The original intention was to test the strand specimens in an Amsler high speed vibrophore testing machine - the testing speed of the machine, which operates on an electro - magnetic principle, is about 6,000 cycles/min - ten times as fast as the maximum speed possible with the Amsler pulsator. As a large number of test specimens were required to obtain reliable results from the fatigue tests, a high test speed was convenient for reducing the total testing time.

However, although many preliminary tests were carried out in the vibrophore, no success was achieved in obtaining failure of the specimens within the test length. Several methods of gripping the strand were used. Moulded cylinders were cast around the strand in the gripped length employing both epoxy and polyester resins with silica flour and glass fibre as fillers, and in some cases, the casting was made in white metal; all were unsuccessful as the small amount of slip which occurred prevented satisfactory operation of the machine which is very sensitive to changes in the response of the specimen. Surrounding the gripped length with aluminium as described in section 3.12a was also unsuccessful as the high testing speed appeared to accentuate the effect of fretting and failures always occurred at the grips.

On the basis of these results, it was finally concluded that the vibrophore was not suitable for testing steel strand, contrary to the claims of the manufacturers. Furthermore, the effect of such a high testing speed on the fatigue properties of strand is unknown, and may have a considerable effect due to heating and the interaction between individual wires.

The fatigue tests were, therefore, carried out in the Amsler universal testing machine with the load being applied by the pulsator at a rate of 600 cycles/min. The sensitivity of the maximum and minimum load pressure gauges was not considered to be suitable for the load range being used, and to improve this, the volume of pulsating oil delivered (as measured by the stroke of the reciprocating piston) was calibrated against the difference between the pressure gauges. This vastly increased the sensitivity of application of the pulsating load to $\pm$ 0.1% of the static ultimate strength of the strand, but the sensitivity was now dependent on:-

i) Constant losses within the oil system of the pulsator and testing machine.

ii) A constant value of the modulus of elasticity of the strand.

iii) A constant value of the length of the specimen between gripping points.

It was assumed that these values did not change significantly during the tests.

The corrections due to the dynamic forces set up in the moving parts were calculated as described in section 4.3a.

The test specimens were gripped in aluminium angles as shown in plate 3.5 and described in section 3.12a except that for the fatigue tests a polythene shim was placed between the strand and the aluminium angles over a length of $\frac{3}{4}$" at the entry of the strand into the grip - the shim consisted of a single layer of polythene sheet, 0.005" thick. The effect of this shim was to reduce fretting between the aluminium and the strand in the length in which the load was transferred from the strand to the grip, since some relative slip between the surfaces always occurred in this section. In the final series of tests, 88% of the specimens failed within the test length; the result of specimens which failed in the grips was ignored in analysis, and the test repeated.

The tests were terminated in each case when fracture of the first wire caused the seismic cut - out to stop the machine.

No instrumentation was employed in the tests.

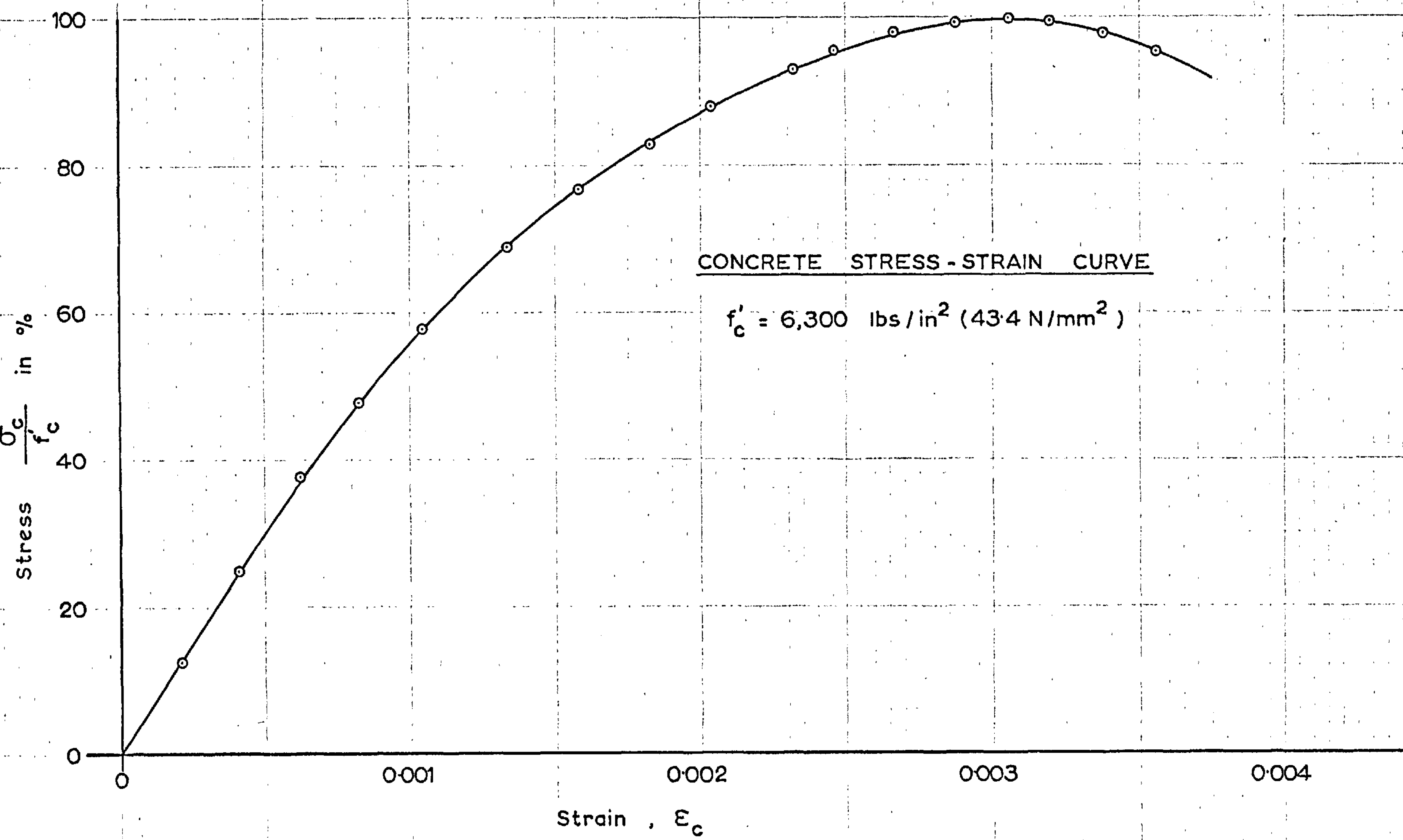
CONCRETE STRESS - STRAIN CURVE
f'_c = 6,300 lbs / in^2 (43·4 N/mm^2)
Stress $\frac{\sigma_c}{f'_c}$ in %
0
20
40
60
80
100
0
0·001
0·002
0·003
0·004
Strain , ε_c

Fig. 3.1

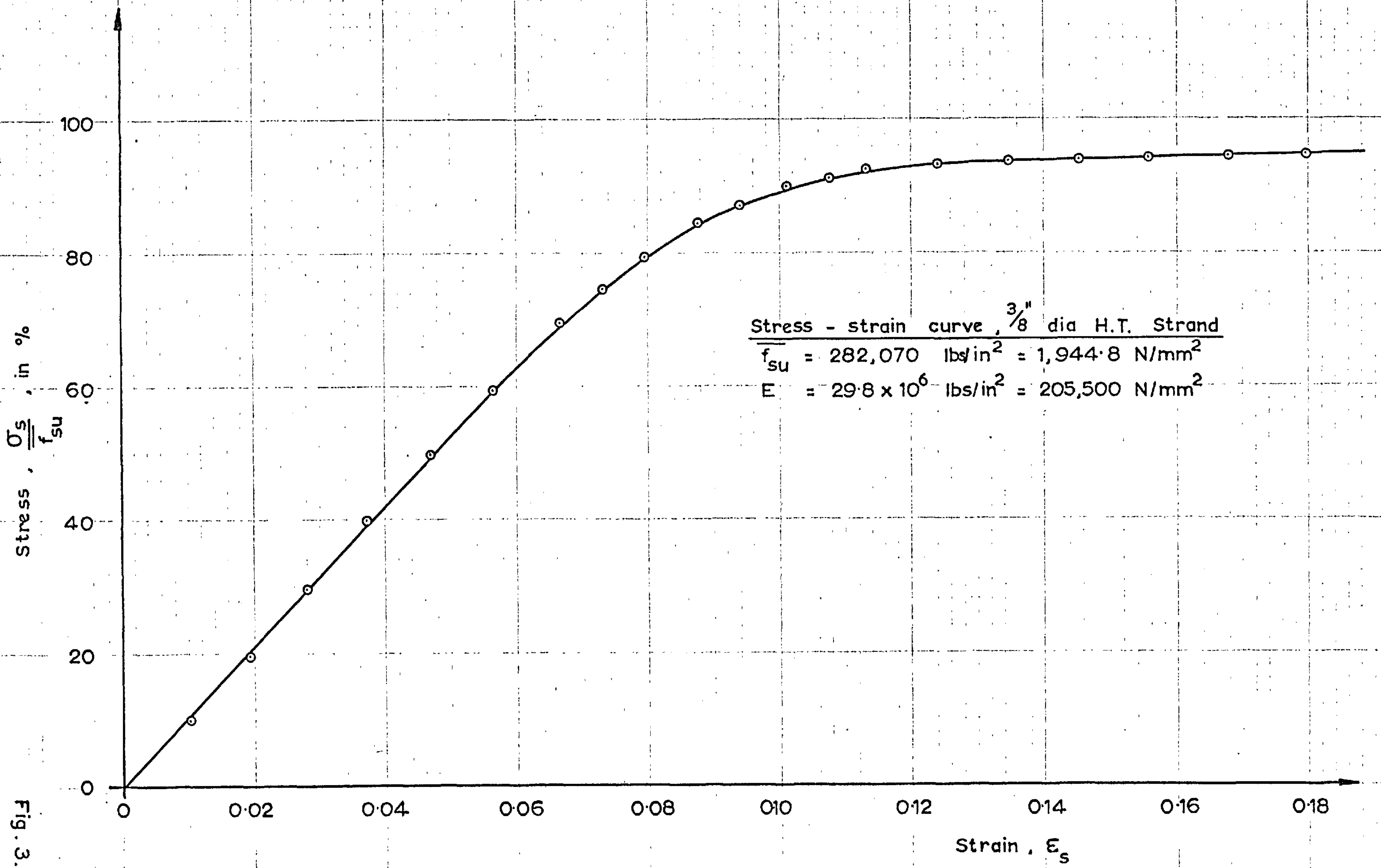
Stress - strain curve, 3/8" dia H.T. Strand
f_{su} = 282,070 lbs/in^2 = 1,944·8 N/mm^2
E = 29·8 x 10^6 lbs/in^2 = 205,500 N/mm^2
Stress, $\frac{\sigma_s}{f_{su}}$, in %
Strain, ε_s
0
20
40
60
80
100
0·02
0·04
0·06
0·08
0·10
0·12
0·14
0·16
0·18

Fig. 3.2

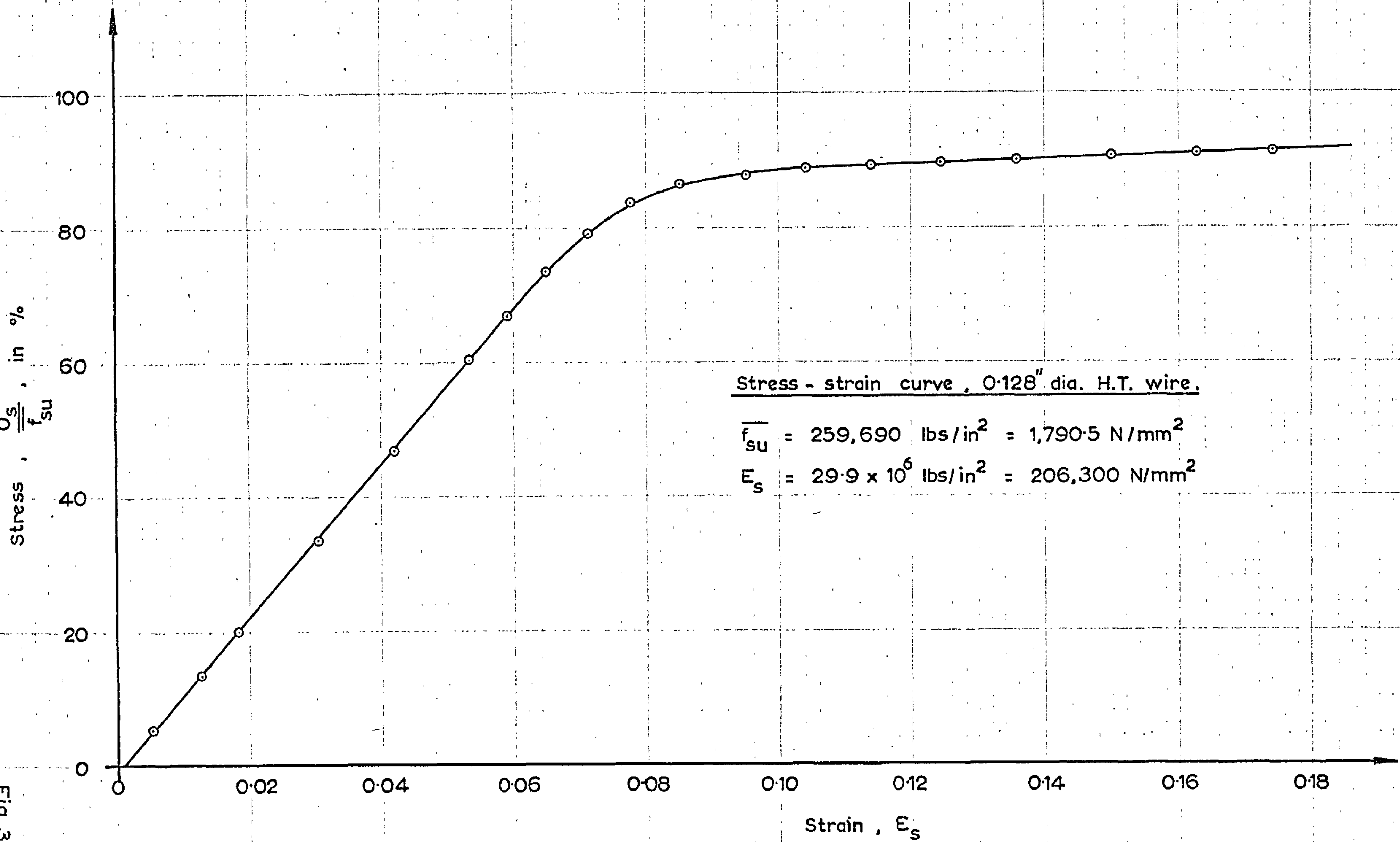
Stress , $\frac{\sigma_s}{\overline{f_{su}}}$, in %
0
20
40
60
80
100
0
0·02
0·04
0·06
0·08
0·10
0·12
0·14
0·16
0·18
Strain , ε_s
Stress - strain curve , 0·128" dia. H.T. wire.
$\overline{f_{su}}$ = 259,690 lbs/in^2 = 1,790·5 N/mm^2
E_s = 29·9 x 10^6 lbs/in^2 = 206,300 N/mm^2

Fig. 3.3

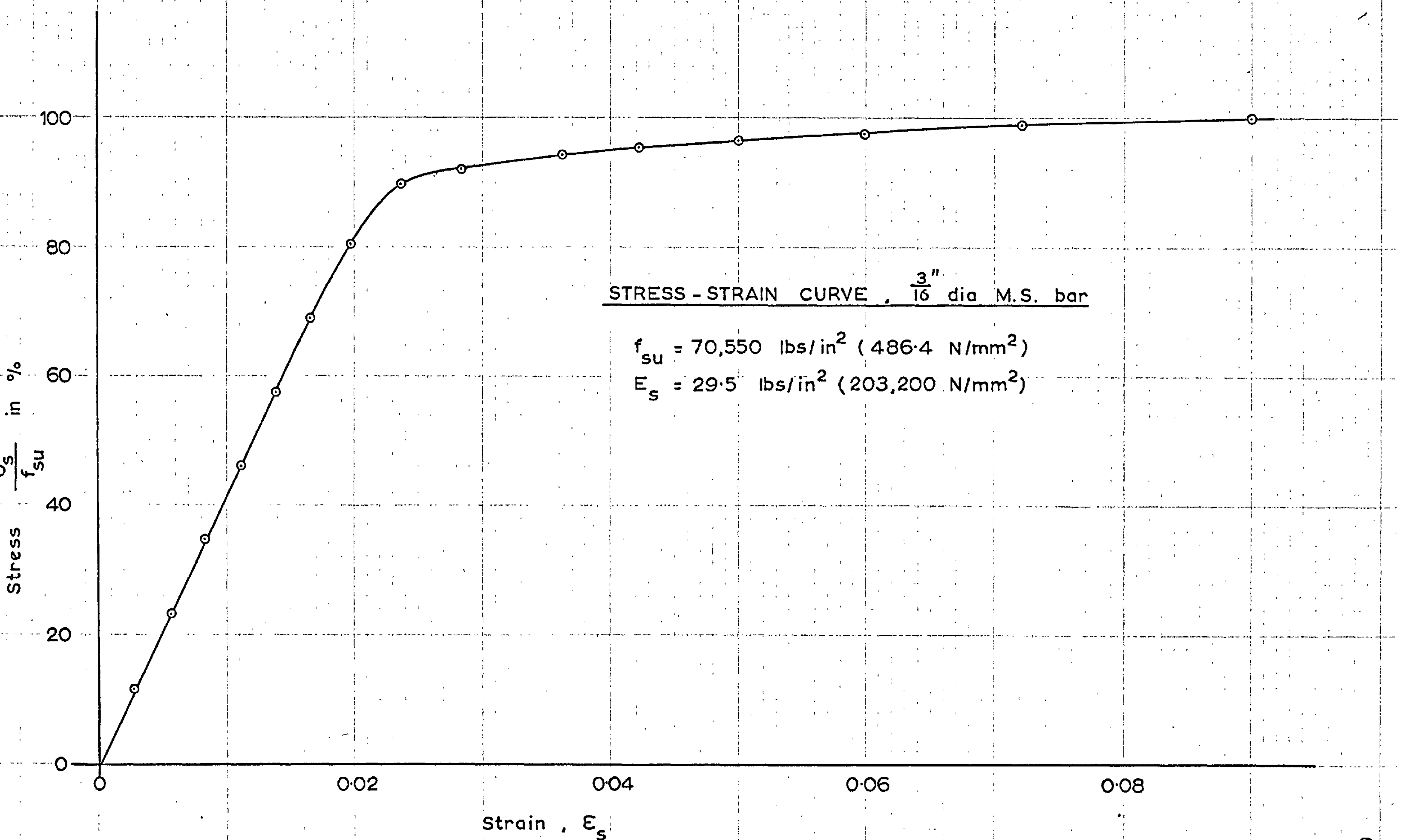
STRESS - STRAIN CURVE, 3/16" dia M.S. bar
f_{su} = 70,550 lbs/in^2 (486·4 N/mm^2)
E_s = 29·5 lbs/in^2 (203,200 N/mm^2)
Stress $\frac{\sigma_s}{f_{su}}$ in %
100
80
60
40
20
0
0
0·02
0·04
0·06
0·08
Strain, ε_s

Fig. 3.4

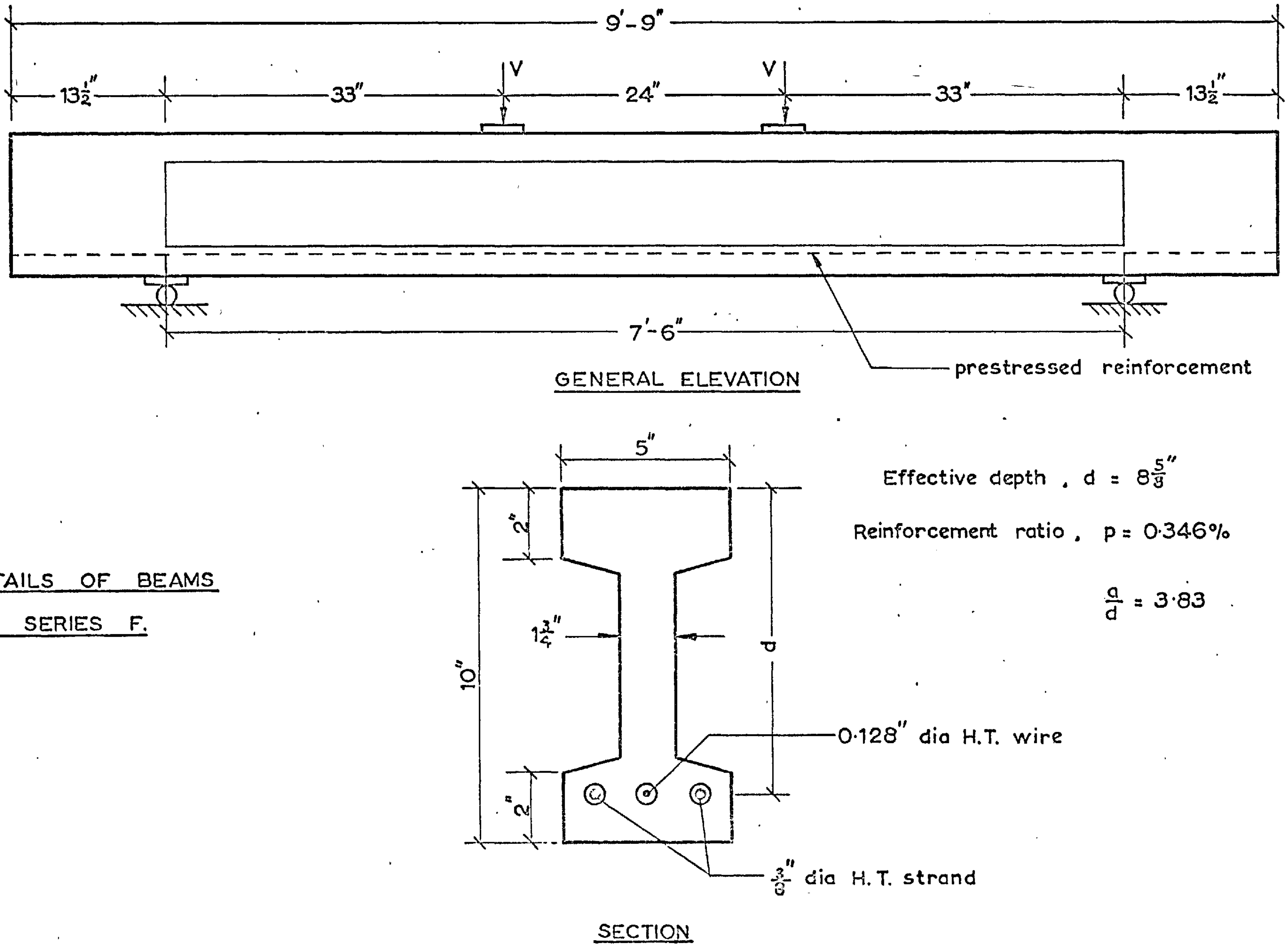

DETAILS OF BEAMS OF SERIES F.

Fig. 3.5

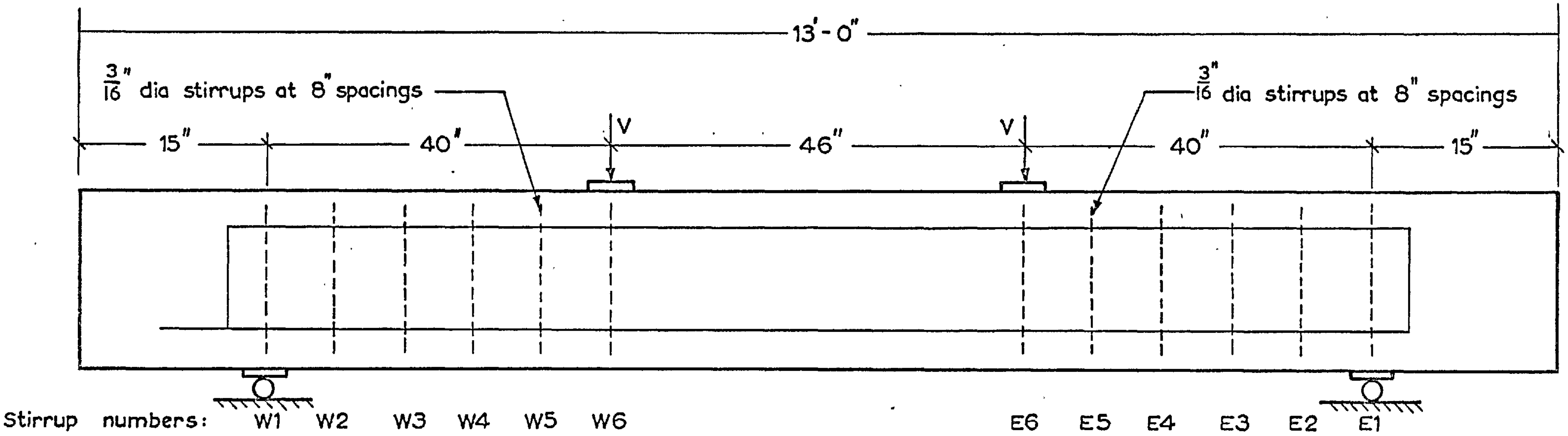

GENERAL ELEVATION

DETAILS OF BEAMS OF SERIES S.

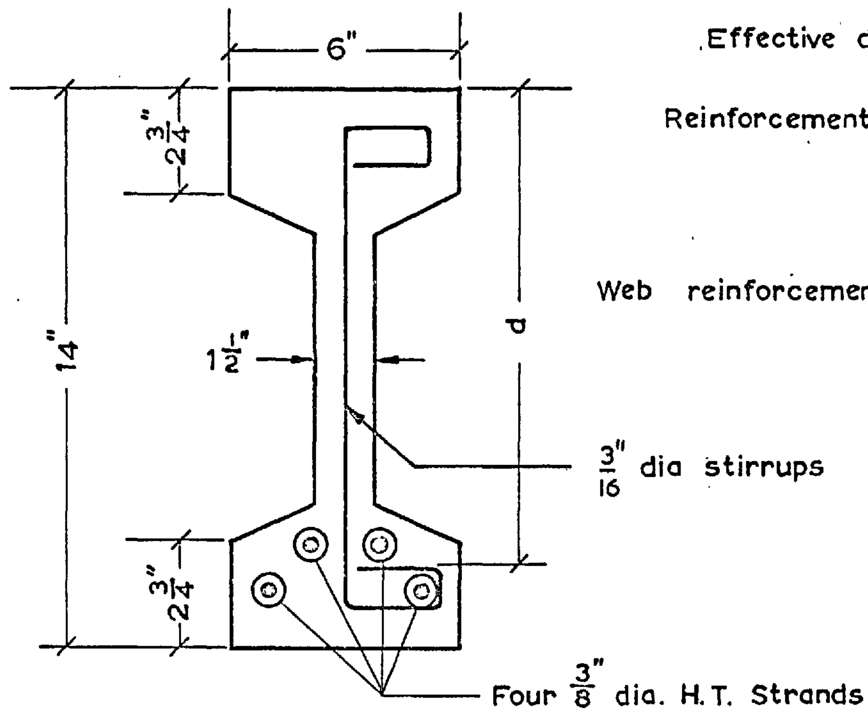

SECTION

Effective depth, d $= 11\frac{7}{8}$"

Reinforcement ratio, $p = 0{\cdot}76\%$

$\frac{a}{d} = 3{\cdot}40$

Web reinforcement ratio, $r = 0{\cdot}23\%$

$\frac{r.\, f_{smy}}{100} = 145$

Fig. 3.6

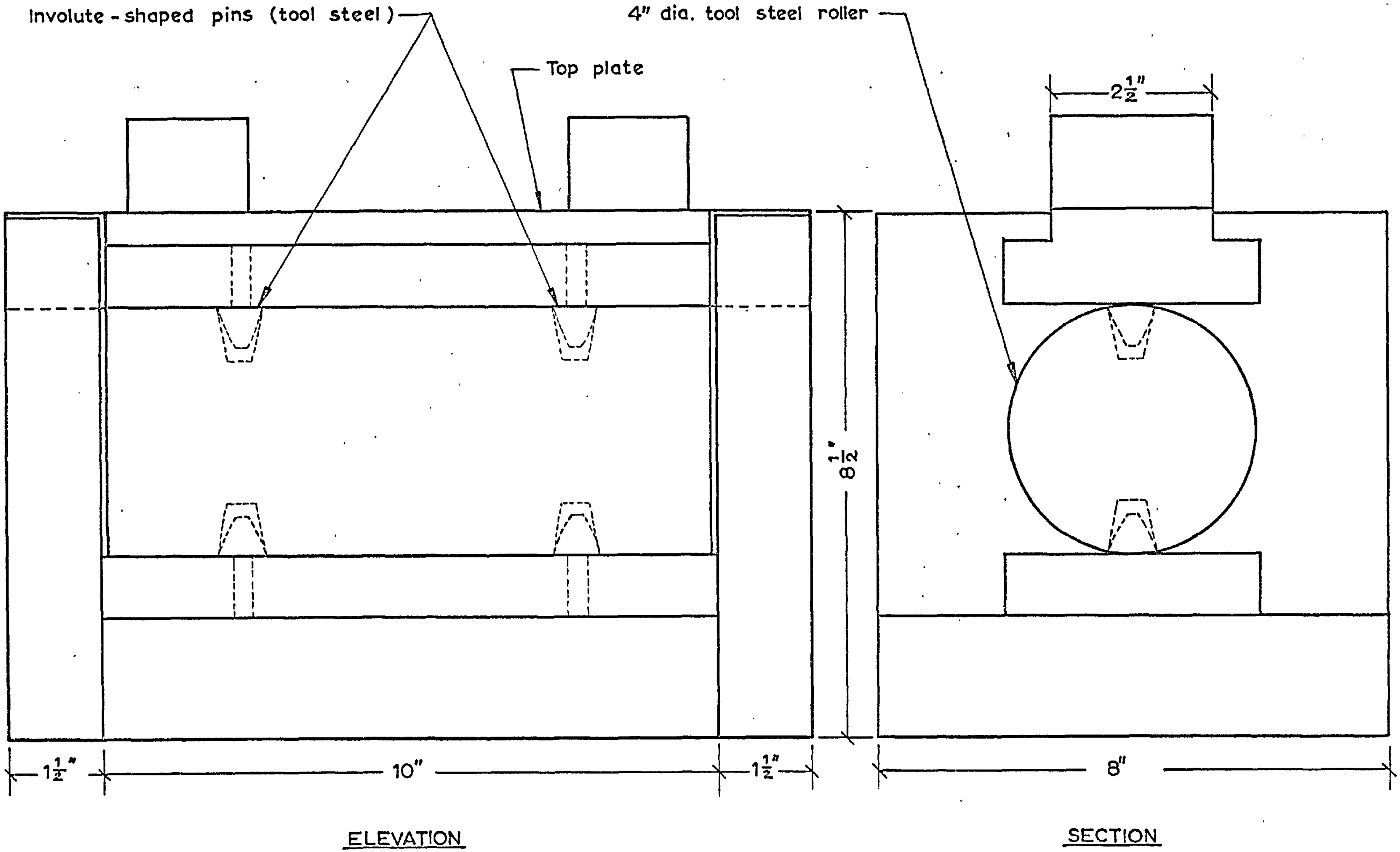

BEARING DETAILS

Fig. 3.7

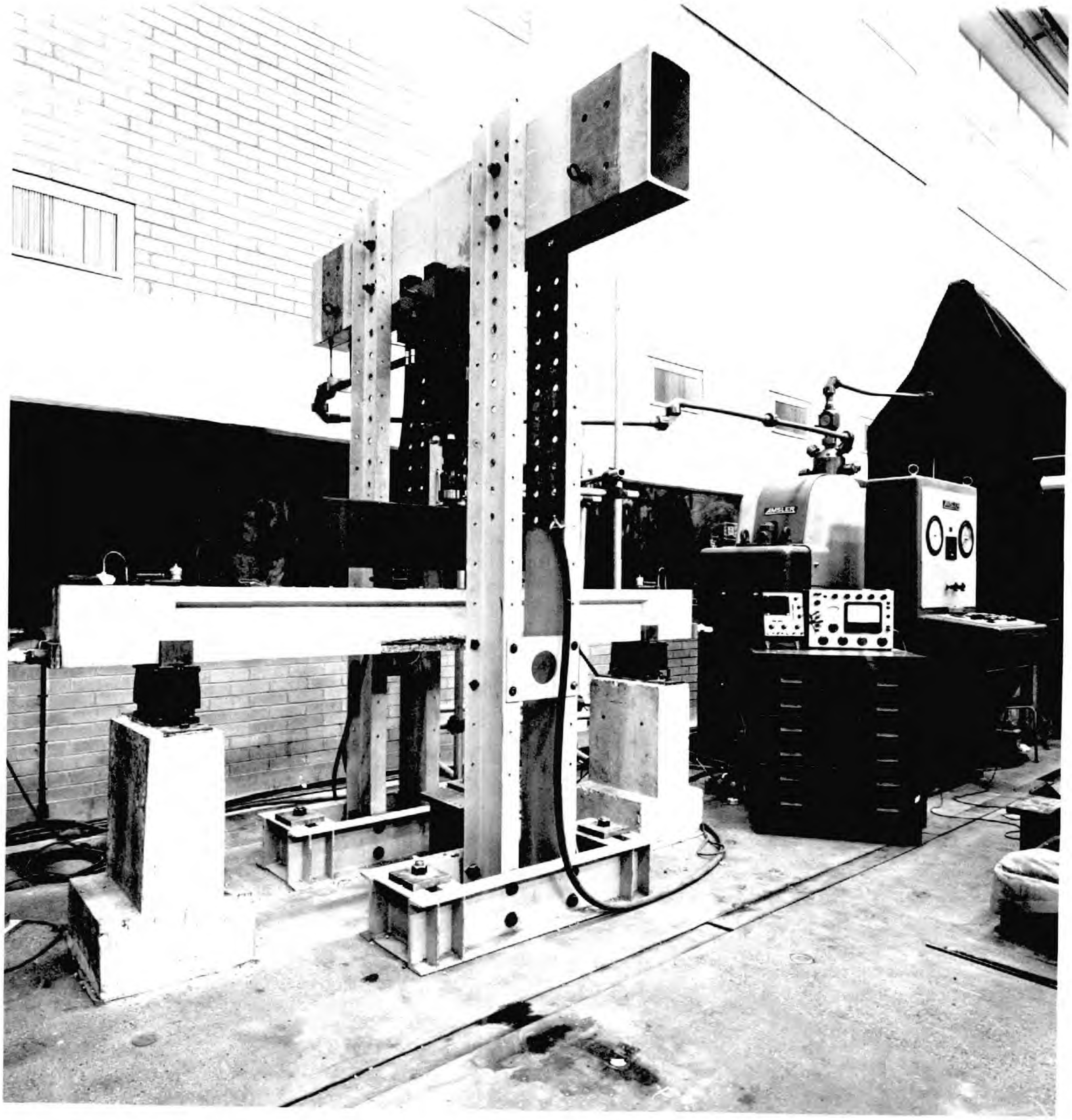

GENERAL VIEW OF PRELIMINARY TEST RIG

PLATE 3.1

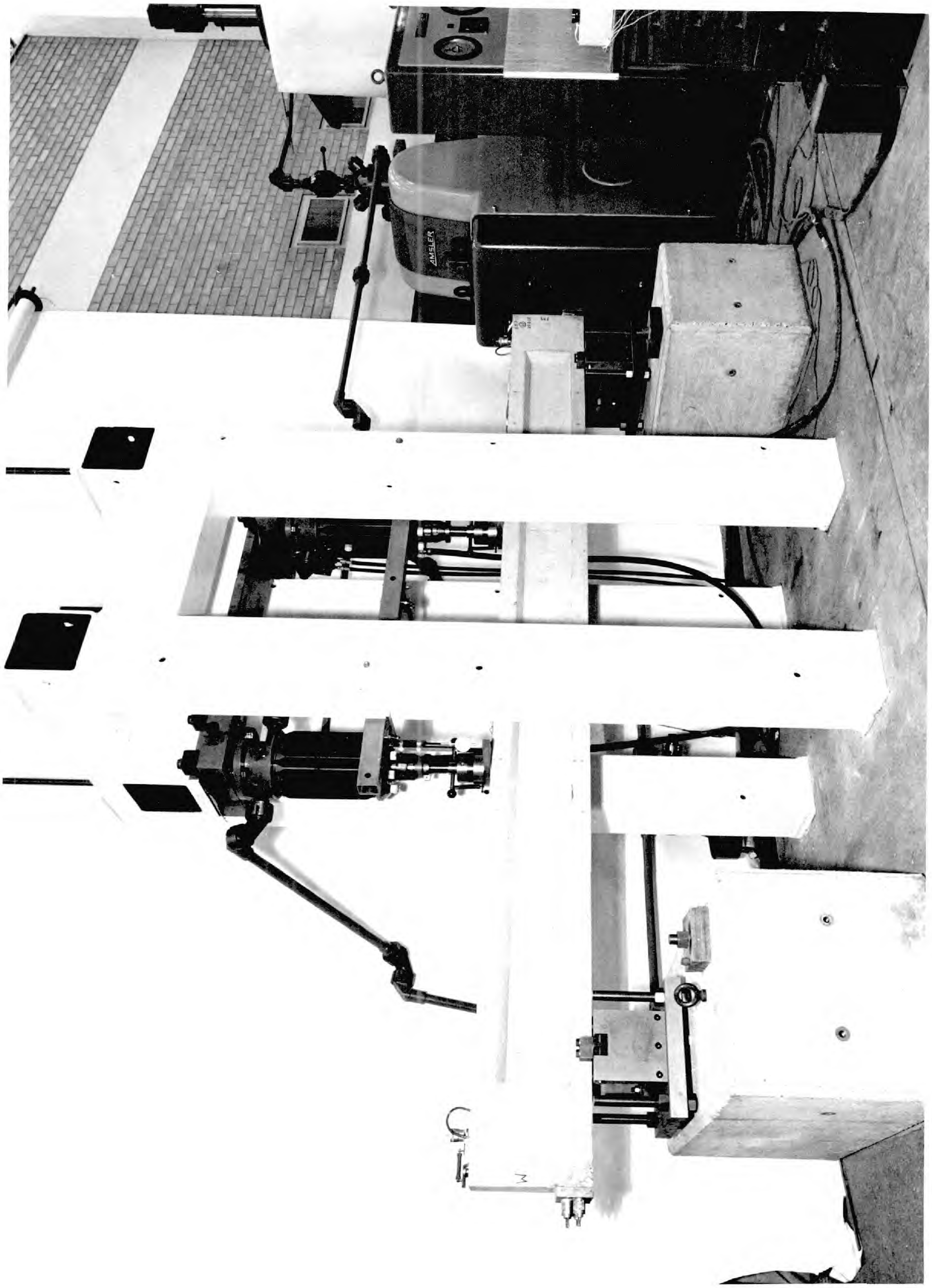

GENERAL VIEW OF FINAL TEST RIG

PLATE 3.2

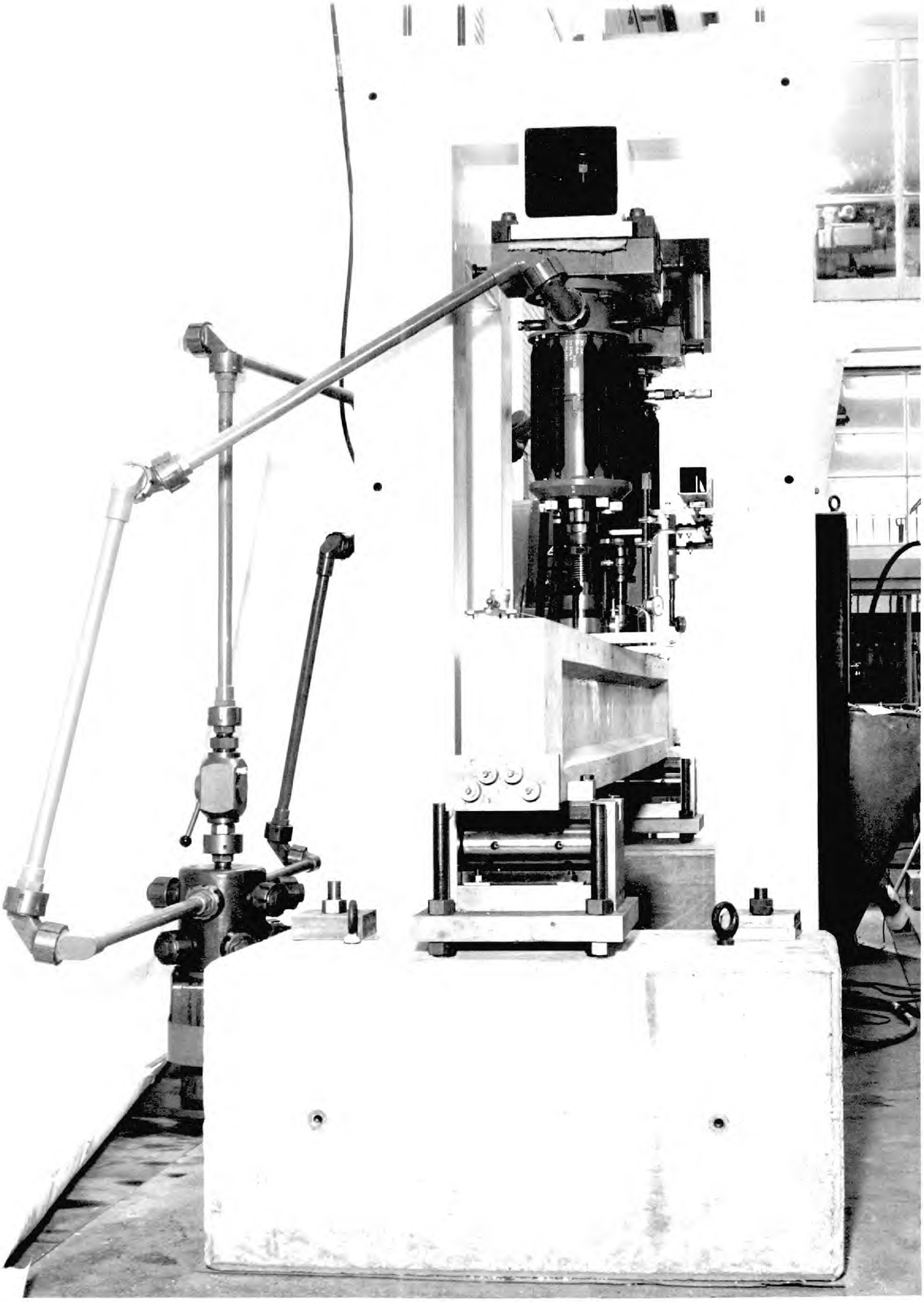

GENERAL VIEW OF FINAL TEST RIG

PLATE 3.3

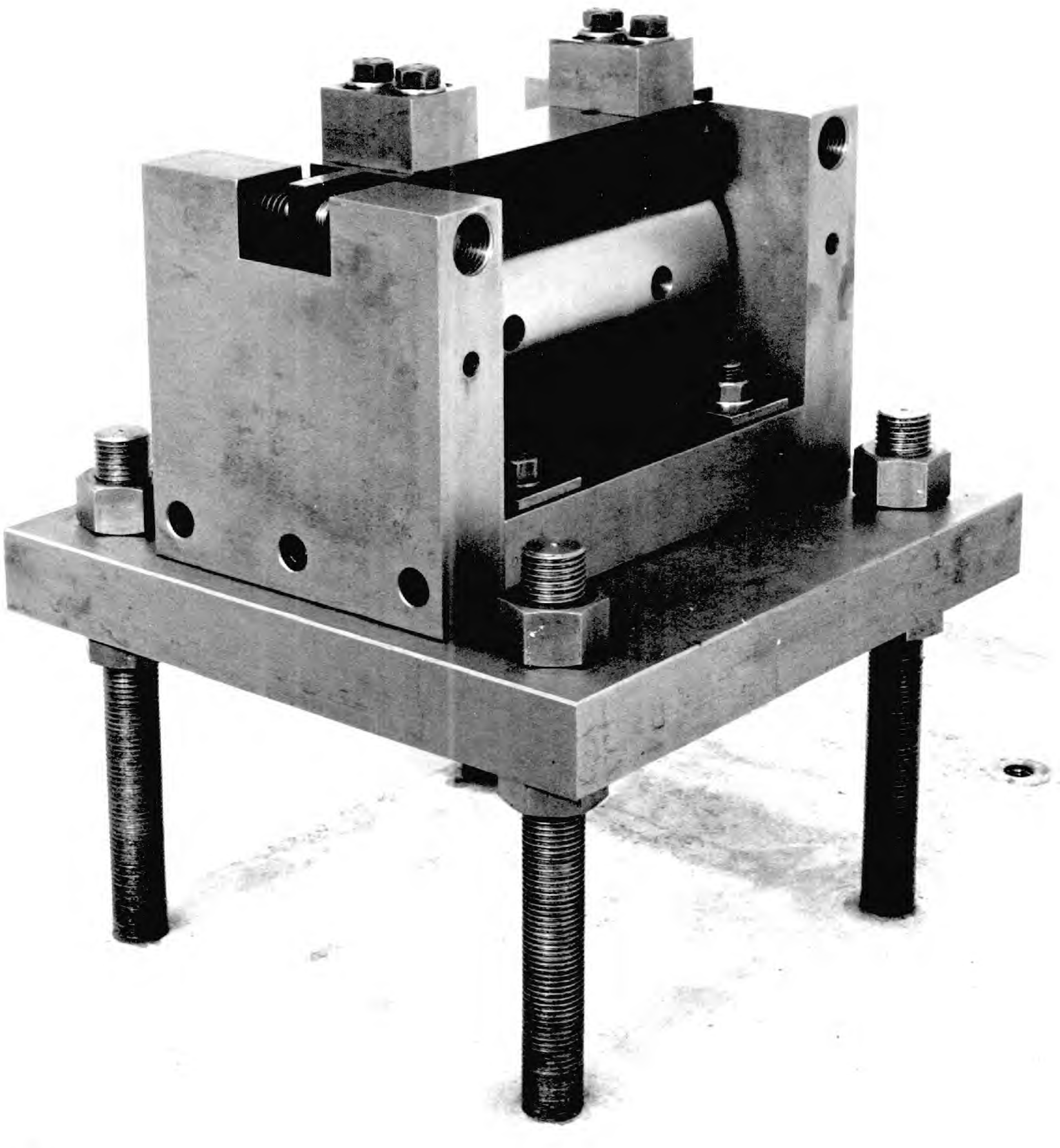

SPRING LOADED ROLLER SUPPORT BEARING

PLATE 3.4

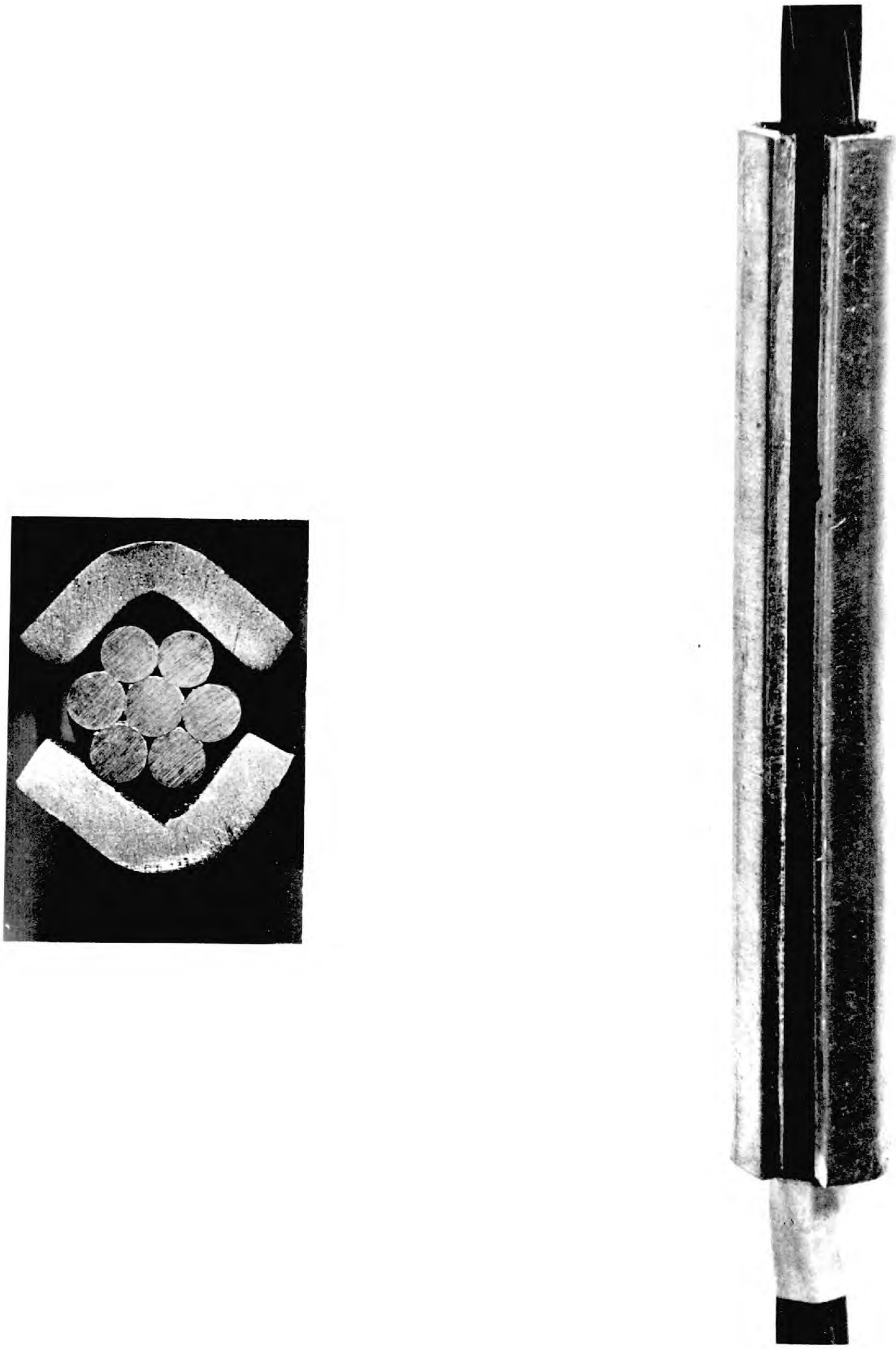

DEVICE FOR GRIPPING STEEL STRAND

PLATE 3.5

CHAPTER 4

EXPERIMENTAL INVESTIGATION OF THE FATIGUE BEHAVIOUR OF PRESTRESSED CONCRETE FLEXURAL MEMBERS

TEST SERIES F

4.1) OBJECT AND SCOPE

The test specimens were originally designed to investigate the effect of repeated loading on the behaviour of prestressed concrete beams in which static failure occurred in:-

a) Diagonal tension.

b) Shear compression.

A preliminary theoretical investigation suggested that an I - section as described in section 3.3a would give both types of failure by varying the Shear span/Effective depth ratio. A series of five preliminary static tests to failure were, therefore, carried out to verify this, the results of which are detailed in section 4.2. The conclusions drawn from these tests were as follows :-

a) A satisfactory and consistent static diagonal tension failure could be obtained from the section at an $^a/d = 3.02$ - these conditions were, therefore, considered satisfactory for fatigue tests and a casting and testing programme was set up.

b) A consistent static shear compression failure could not be obtained at higher $^a/d$ ratios since insufficient bond between the prestressing steel and the concrete prevented the formation of the required flexural - shear cracks, and flexural failures were obtained.

Due to the lack of previous information on the behaviour under repeated load of beams which failed statically in shear it was necessary to carry out preliminary tests under repeated load at an $^a/d = 3.02$, before finalising the test conditions. Three beams were, therefore, tested at various levels of repeated load and from the results it was concluded that, under the conditions of the tests, repeated loading acted to change the type of failure from diagonal tension to flexure.

Two beams were then tested under repeated load at an $^a/d = 3.83$. From the conclusions of the previous paragraph, it was obvious that the beams would fail in flexure since the moment/shear ratio was greater; the constant moment region of the beams was, therefore, reinforced with additional intensioned steel in order to force the occurrence of flexural - shear cracks - in this, the tests were, however, unsuccessful, due to the breakdown of bond between untensioned steel and concrete.

The preliminary tests thus showed that, for the particular section and test conditions chosen, flexure was always the criterion of failure under repeated load, and with this knowledge, the final test programme was formulated and commenced.

The tests were designed to provide information on both flexural cracking and failure under repeated load, and two beams were tested with improved bond conditions between steel and concrete in order to determine the effect of varying bond quality on the fatigue strength. One beam was tested at a very slow rate of loading to see whether the speed of testing had any effect on the fatigue strength.

The results of the first eight beams tested, however, indicated that one further change was necessary in the test conditions. At load levels which approached the fatigue limit, the beam behaviour was satisfactory, but at higher levels of load, the phenomenon of abrasion at flexural cracks created tension in the top flange and eventually caused cracks, which quickly became unstable and led to premature failure - it was not considered that this was a typical type of failure and, therefore, for the final series of fatigue tests, the minimum load level was increased from 10% to 27.5% of the static ultimate strength; with this minimum load level, no cracks occurred in the top flange even after 3×10^6 cycles.

Instrumentation was considered to be vitally important in the investigation and measurements of beam deflections, rotations, and concrete strain distributions were taken at intervals throughout the tests.

4.2) PRELIMINARY STATIC TESTS TO FAILURE

4.2a) TEST PROCEDURE

The loading conditions were as described in section 3.10a. The applied load was increased by increments of approximately 10% of the ultimate load until the first crack was observed, and, thereafter, the load increments were varied so as to give approximately equal increments of deformation in the beam, the magnitude being chosen so as to give about fifteen load stages in all. At load levels greater than about 80% of the ultimate strength, considerable creep occurred, and four or five minutes were allowed to elapse between the application of a load increment and the measurement of deformations and deflections in order to allow the readings to settle down to relatively steady values.

Instrumentation consisted of dial gauges to measure the deflections on the centre line, and under the load points, clinometers to measure the rotation between the ends of the beams, and electrical resistance strain gauges to determine the strain distribution on the top surface of the beams.

4.2b) TEST RESULTS

Beam F1 was tested at an $^{a}/d = 3.83$. The crack pattern consisted of three flexural cracks in the constant moment zone, and one flexural - shear crack in each of the shear spans. As the test progressed, the two flexural - shear cracks opened considerably more than the other flexural cracks and when the concrete in the top flange started to spall it appeared that a shear - compression failure was imminent. However, at this point, an unstable diagonal crack formed suddenly in the web of one of the shear spans, and complete collapse occurred as the crack propagated immediately to the load point and the support point.

The above result indicated that an increase in the $^a/d$ ratio (and hence an increase in the moment/shear ratio) would provide a satisfactory shear - compression failure before a diagonal tension failure occurred, and hence beam F3 was tested at an $^a/d = 4.75$. In this test, one flexural crack occurred in the centre of the constant moment zone and continued to open up until crushing of the concrete in the compression zone occurred. The fact that only one crack occurred indicated that the bond between steel and concrete was insufficient for the formation of flexural - shear cracks. Beam F7 was, therefore, tested at an $^a/d = 3.83$, in order to verify this fact - two flexural cracks were obtained in the constant moment zone and failure eventually occurred in diagonal tension. This confirmed that flexural - shear cracks would not consistently occur in the chosen section.

On the basis of the failures obtained in beams F1 and F3, it was expected that at a lower $^a/d$ ratio a diagonal tension failure could be consistently obtained, and beam F2 was tested at an $^a/d = 3.02$ to confirm this - the beam failed in diagonal tension as expected, and the result indicated that the test conditions were suitable for testing under repeated load.

Beam F18 contained $\frac{1}{8}$" diameter mild steel stirrups at 6" centres in the web and was tested at an $^a/d = 3.83$ in order to determine whether the section could be used to investigate the effect of repeated loading on beams containing web reinforcement. The beam failed by crushing of the concrete in the constant moment zone, and the width of the inclined web - shear (diagonal tension) cracks which occurred indicated that failure of the web reinforcement would not occur under repeated load, and therefore, a different beam section was required for test series S.

The summarised results are included in table 4.1.

4.3) PRELIMINARY FATIGUE TESTS

4.3a) TEST PROCEDURE

The equipment used for applying the repeated load to the specimens is fully detailed in section 3.10b.

The first ten cycles of load were always applied manually to the beam by means of the constant minimum load device - the reason for this was that the response of the beams always changed rapidly during the first few load cycles and, therefore, it was necessary to take readings at small increments of load cycles in the early part of the test - cycle increments of this size were not possible using the Amsler pulsator at a a speed of 300 cycles/min. Throughout the tests, sets of readings were taken at approximately those intervals such that the increase in the logarithm (to the base 10) of the number of load cycles completed remained constant; i.e. after 1, 3, 10, 32, 100, 316, 1000, 3160, 10,000 cycles etc. If the test continued for longer than 500,000 cycles, readings were then taken approximately every 500,000 load cycles. Generally, it was found that, after about 25,000 load cycles, the response of the beam settled down to a value which only changed slowly with cycles until failure occurred. In order to take readings, the load cycling was stopped by reducing the pulsating oil volume to zero; the load was then increased up to the maximum cycling value by means of the constant minimum load device, and a set of readings taken. It was then reduced to the minimum cycling value, and another set of readings taken. The beams were, therefore, never unloaded below the value of the minimum load at any stage until failure, once the load cycling had commenced.

Due to the dynamic forces set up in the moving parts of the jacks and test beam, it was necessary to correct the loads shown on the maximum and minimum pressure gauges of the pulsator. To this end, the range of deflection between the maximum and minimum loads was measured statically - knowing the weights of the moving parts of the jacks and test beam, and the testing speed, the correction could then be calculated from the formula:-

$$P_b = \frac{W.\ w^2.\ d_a}{g}$$

where : P_b = accelerating force = correction to maximum and minimum loads.

w = angular velocity.

d_a = amplitude of deflection in load cycle.

g = gravitational constant.

W = weight of moving masses.

In three beams, the calculation was checked by comparing the values of strain obtained from dynamic measurements by means of an oscilliscope (as described in section 3.11a), with those obtained by taking the readings statically immediately afterwards - the beam response was at this stage virtually constant, and it could, therefore, be assumed that the change in the response in the interval of about 1000 cycles was quite negligible. As no significant difference was found in all three cases, it was assumed that the calculations were correct, and they were applied without further experimental check in all subsequent dynamic tests. In all tests, after each set of readings had been taken, the correction was recalculated and adjustments to the applied loads made if necessary.

The instrumentation in these preliminary tests consisted of electrical resistance strain gauges to measure the strain distribution on the top surface of the beams, and in the web in each shear span.

4.3b) TEST RESULTS

Beam F4 was subjected to repeated loading at an $^a/d = 3.02$, which created a maximum principal tensile stress in the web of 40% of the static ultimate tensile strength. The latter was calculated as detailed in section 4.5b. After resisting 3,000,000 cycles of this loading without failure or cracking having occurred, the beam was tested statically to failure, which occurred by the formation of an unstable diagonal crack in the web leading to collapse.

In Beam F5, the maximum load level was increased such that the maximum principal tensile stress in the web was 50% of the static ultimate tensile strength, but again 3,000,000 load cycles were completed without cracking or failure, and the beam was then tested statically to failure, which occurred as in Beam F4, in diagonal tension. The $^a/d$ ratio was 3.02 as before. The crack pattern is shown in plate 4.1.

For beam F6, the maximum principal tensile stress in the web was increased to 75% of the static ultimate tensile strength, still at an $^a/d = 3.02$. This load was above the static flexural cracking load and consequently, two flexural cracks occurred in the constant moment zone in the first cycle of loading. With the commencement of repeated loading, the concrete rapidly deteriorated and spalled off around the two flexural cracks - after 11,000 load cycles a crack formed in the top flange and after 15,000 cycles, the concrete crushed at this crack and the beam collapsed.

The results of these three tests thus lead to the conclusion that diagonal tension failures would not be obtained under repeated loading with that particular section, as flexure would always be the criterion of failure in fatigue.

In the tests on Beams F12 and F13 an attempt was made to achieve shear - compression failures in fatigue at an $^a/d = 3.83$, by placing additional untensioned steel in the constant moment zone to force the occurrence of flexural - shear cracks, and prevent flexural failures under repeated loading. In beam F12, two flexural - shear cracks, in addition to flexural cracks, were formed, but failure eventually took place by fracture of the steel prestressing strand at a flexural crack. Examination of the failure point indicated that fretting had taken place between tensioned and untensioned steel - it is, therefore, possible that this led to premature failure. In the test on Beam F13, no flexural - shear cracks were obtained, probably due to insufficient bond between the untensioned steel and the concrete, and the beam was, therefore, tested statically to failure, which occurred in diagonal tension.

The summarised results of these tests are included in Table 4.2.

4.4) STATIC TESTS TO FAILURE

4.4a) TEST PROCEDURE

The test procedure in these tests was identical to that described in section 4.2a.

Instrumentation consisted of dial gauges to measure deflections on the centre line and under the load points, and clinometers to measure the rotation between the ends of the beams. The strain profiles on both sides of the beam were determined by demec gauge readings in the constant moment zone at four levels in the compression flange - the layout of the demec points was as shown in fig. 4.1.

4.4b) TEST RESULTS

Beams F9, F10, F14, F21, and F23 all had a previous history of repeated loading and had endured 3,000,000 load cycles of intensities as given in table 4.3. Since no failure had occurred under repeated loading in these beams, they were then tested statically to failure.

Beam F27 had no prior load history and was used as a control beam. Beam F3 (results are given in section 4.2b) similarly had no load history and, therefore, the static flexural strength, $\bar{M}_u$ of the beams was taken as the mean of the strengths of beams F3 and F27, i.e, $\bar{M}_u$ = 302,830 lbs - ins (34.214×10^6 N - mm).

The cracking patterns of the beams are shown in plates 4.1 to 4.5. Beams F10 and F27 were uncracked at the commencement of the test and the difference between the cracking patterns of these two beams and those which had been subjected to repeated loading in a cracked condition may be clearly seen in the plates. In beams F10 and F27, the two cracks which occurred in each beam were restricted to the constant moment zone and followed an approximately vertical path to a point about 2" below the top flange, where they forked into two opposing inclined cracks - on reaching the top flange, the cracks travelled vertically once again.

All the beams failed in a manner typical of under - reinforced beams by yielding of the steel and then crushing of the concrete in the outer compression fibres at the head of a flexural crack.

Details of prior load histories, flexural cracking moments, ultimate moments and maximum top fibre strains are given in table 4.3.

Details of the concrete strengths are given in table 4.5.

The moment - curvature relationships shown in figs. 4.2 to 4.6 show the effect of the previous load history on the subsequent behaviour of the beams. In beam F10, which was uncracked in fatigue, the linear elastic (uncracked) stiffness has been increased by 6.5% over that of beam F27, but for all the other beams, which were cracked during the previous load history, the linear elastic (before flexural cracks open) stiffness is not significantly different from that of beam F27.

In the beams which were previously cracked, the tangent stiffness (measured at given moments) is lower, from the point at which flexural cracks re-open, up to the point at which flexural cracking occurred in the control beam. Above this moment, the tangent stiffness of the previously fatigued beams is greater than the control beam, although for beam F14, this is only just so - this increase was greater as the level of prior repeated loading was increased. Above about 80% of $\overline{M}_u$, the tangent stiffness of the fatigued beams was much the same as that of the control beam, and decreased at the same rate as that of the control beam. The greatest effect of the prior load history was in the load range between the previous maximum level of repeated loading in any particular beam and a load about 20% of the ultimate load capacity above that - in this portion the stiffness was greatly increased over that of the cracked unfatigued beam. In the range where the cracked tangent stiffnesses were similar, the curvature at a given moment was much greater in the control beam than in the previously fatigued beams.

The relation between the change in ultimate strength and the maximum level of prior repeated loading is shown in fig. 4.7. The results of Sawko and Saha (65) and Venuti (63, 64) are included in the diagram. Although the author's results tend to indicate an increase in strength after repeated loading, this cannot be stated to be conclusive, since the value of $\overline{M}_u$ used is the mean of the values obtained from two tests only - the true mean could, therefore, be somewhat different from this value. Venuti's results are more reliable since he carried out tests on 16 similar beams in order to obtain the mean static ultimate strength, $\bar{M}_u$ - these results lay within a band of $\pm$ 15% of the mean, with a coefficient of variation of 8.5%. He also tested 11 beams which had been subjected to 5×10^6 cycles of loading at 50% of $\bar{M}_u$ - the mean ultimate strength of these beams was 0.3% less than $\bar{M}_u$, and lay within a band 10% above, and 13% below $\bar{M}_u$, with a coefficient of variation of 6.6%. Therefore, all the results shown in fig. 4.7 lie within the limits of the scatter obtained by Venuti for unfatigued beams and do not justify the assumption of any definite relation between change in ultimate strength and level of prior repeated loading as suggested by Sawko and Saha (65).

The relation between the bond factor, F, and the applied moment is shown in fig. 4.8 for beams F21, F23, and F27. The effect of repeated loading is clearly shown by the change of slope of the diagram above the level of prior repeated loading in the curves for beams F21 and F23 - as the load is increased above the maximum level of repeated loading, M^{max}, the bond factor remains virtually constant for an increase in load of about 10% of $\bar{M}_u$, before the bond factor is further reduced by overloading. This indicates that the bond breakdown in fatigue at that load level is equivalent to that which would occur under an overload 10% of $\bar{M}_u$ greater than the level of repeated loading. When the moment is greater than about 20% of $\bar{M}_u$ above the previous maximum level of repeated loading, the rate of bond breakdown is apparently unaffected by the prior repeated loading and follows a path determined by the magnitude of the applied load. The bond factors at ultimate load in beams F21 and F23 are greater than those of the control beam F27, and this could account for the increased ultimate strength of these two beams. However, considerable scatter is to be expected in the bond factors obtained from similar beams, and no significant conclusions can be drawn with regard to the effect of repeated loading on the ultimate strength. The method of evaluation of the bond factor is given in the Appendix.

The moment - steel stress relationship is shown in fig. 4.9 for beams F23 and F27 - as may be seen from the curves, the difference in stiffness and bond factors between the beams has little effect on this relationship.

4.5) FATIGUE TESTS TO INVESTIGATE FLEXURAL AND SHEAR CRACKING

4.5a) TEST PROCEDURE

The test procedure for all these tests was as described in section 4.3a, except that the tests were not stopped at intervals to take readings. The instant of flexural cracking was determined by the drop which occurred in the maximum load on cracking; this operated the automatic cut - out on the pulsator (see section 3.10b). The tests were stopped if cracking had not occurred after 3,000,000 load cycles.

4.5b) TEST RESULTS

Since the beams tested in this part of the investigation were used subsequently in the fatigue tests to failure, it was essential that the history of repeated loading in these tests had no effect on the fatigue strength of the beams. Even under the greatest maximum load applied in these tests the stress range in the steel was only 2.2% of the static ultimate strength, and as the fatigue limit stress range was 13.5% of $\bar{f}_{su}$, it could be assumed that the prior repeated loading up to flexural cracking had no significant effect on the subsequent fatigue strength of the steel.

In all fatigue tests on concrete, determination of the static ultimate strength of the specimen is vitally important since the fatigue strength is directly related to it - unfortunately, the static and fatigue strength of a single specimen cannot be obtained - the static strength must, therefore, be estimated from associated control specimens, and this estimate may be in considerable error since the strength of these control specimens may vary from that of the fatigued specimen. When the tests involve concrete in tension, the problem is further exaggerated, since the tensile strength is extremely sensitive to flaws, notches and other possible irregularities, which obviously cannot be reproduced in control specimens. In prestressed beams, the static flexural cracking load is dependent upon the effective prestress as well as the tensile strength of the concrete. For all the beams reported, the initial prestress (after elastic and wedge slip losses) was known accurately, and since creep and shrinkage losses were measured, the effective prestress could be accurately estimated. The static flexural cracking load was measured in the tests on 17 beams, and from these results (see table 4.6), the flexural cracking stress in the bottom fibre, f_{crf}, could be calculated; these values are plotted against the cube strength, f_{cu}, and the modulus of rupture strength f_r, in figs. 4.10 and 4.11 respectively. The results show considerable scatter and do not justify the assumption of a relationship more complex than :-

$$\text{Flexural cracking strength, } f_{crf} = K \times f_{cu}$$

where: K = a constant = the mean of the ratio f_{crf}/f_{cu} for the 17 beams tested.

$= 0.0762.$

Using this relationship, the actual and predicted values of the flexural cracking stress are compared in table 4.6 - the coefficient of variation of the results is 11.5%.

This relationship was then used to predict the static flexural cracking stress of the beams tested in fatigue - these estimates, together with the maximum stress levels and number of cycles to cracking, are given in table 4.7. In the tests on beams F9, F10, and F16, the minimum moment level was 10% of $\bar{M}_u$, whereas for all the other beams, the minimum moment level was 27.5% of $\bar{M}_u$; these moments created stresses in the bottom fibre of 1210 and 510 lbs/in^2 (compression) respectively. On the basis of the results given in section 2.1c, as indicated in fig. 2.2, it was assumed that this difference had no effect on the fatigue strength of the concrete in tension. The results are plotted as an S - N curve in fig. 4.12. Considerable scatter is evident in the results, which indicate that the fatigue strength at 3×10^6 cycles is about 65% of the static flexural cracking strength. Beams F4, F5, F10, and F29, which endured 3×10^6 cycles without cracking were subsequently loaded statically up to flexural cracking - the flexural cracking stresses and previous load histories are given in table 4.6 & 4.7. The differences between the actual and predicted strengths (assuming no previous load history), are within the expected scatter, and the beams showed a mean increase in strength of 1.5%, based on their predicted strengths; no significant conclusions can be drawn from this result.

Although no diagonal tension shear cracking occurred in fatigue in any of the tests, the principal tensile stresses existing in the web in the fatigue tests were calculated in order to obtain a lowerbound estimate of the fatigue strength. The calculated stresses (assuming a homogeneous elastic material with the maximum principal tensile stress existing at the centroid of the section) are given in table 4.8. The results showed that the fatigue strength at 3×10^6 cycles of the concrete in tension in the web of the beams was not less than 53% of the static tensile strength. The static tensile strengths were predicted in a similar manner to the prediction of the static flexural cracking strengths, on the basis of the principal tensile stresses at failure, as given in table 4.8, for the beams which failed in diagonal tension. Beams F4 and F5, which were subsequently tested statically to failure in diagonal tension, showed a mean increase in strength of 0.1%, based on their predicted static tensile strengths. The previous load history thus appeared to have no significant effect on the static ultimate strength.

4.6) FATIGUE TESTS TO FAILURE, WITH MINIMUM LOAD = 10% OF MEAN STATIC ULTIMATE STRENGTH.

The experimental procedure and instrumentation in these tests was as described in section 4.3a.

Seven beams were tested under these conditions, at three different values of the maximum load level.

4.6a) BEAM BEHAVIOUR WITH MAXIMUM LOAD LEVEL = 58.0% OF $\overline{M}_u$

One beam, F9, was tested with the maximum load level = 58.0% of $\overline{M}_u$. The first two cycles of loading were applied manually to the beam - no flexural cracking occurred. The pulsating load was then applied to the beam, and after 500 cycles, two flexural cracks appeared, which propagated rapidly upwards and forked into opposing inclined cracks at the centroid of the beam. After about 30,000 load cycles, the crack propagation was virtually complete, and no visible extension of the cracks was observed after this. The two flexural cracks did not propagate sufficiently to join together as observed in the beams tested at higher levels of the maximum load. After 3,156,000 load cycles, no failure had occurred in the beam, and the fatigue test was, therefore, stopped, and the beam loaded statically to failure as described in section 4.4.

4.6b) BEAM BEHAVIOUR WITH MAXIMUM LOAD LEVEL = 64.1% of $\overline{M}_u$

Four beams were tested with this level of maximum load.

In the test on beam F8, two flexural cracks occurred in the first cycle of loading; with the onset of the pulsating load, the two flexural cracks propagated horizontally along the top of the web, and after 25,000 cycles had joined together. After 2,375,000 load cycles a fracture occurred in one of the strands at a point 5" away from a flexural crack, indicating considerable bond breakdown.

The behaviour of beam F14 was virtually identical with that of F8, but after 3,052,000 load cycles, no failure had yet occurred and the beam was, therefore, tested statically to failure as described in section 4.4.

Beam F17 was subjected to an overload in the first cycle of loading equal to 90% of the static ultimate strength - the load was then reduced, and the beam subjected to repeated loading with the maximum load level $= 64.1\%$ of $\bar{M}_u$. The pulsating load appeared to have a more detrimental effect in this test than in the case of F8 and F14; the concrete at the flexural cracks spalled off quite markedly due to the closing of the cracks under minimum load and considerable wearing away of the concrete at the crack surfaces was observed. The tension thus created in the top flange eventually led to the initiation of a crack there after 160,000 cycles which reduced the stiffness of the beam considerably. It continued to sustain the repeated load until 255,000 load cycles had been completed when fatigue fracture of one of the strands occurred. Examination of the grout - concrete interface revealed that extensive bond breakdown had occurred, possibly in the first cycle of overloading. The low fatigue life of this beam could be partly explained by the fact that the steel stress under minimum load was considerably less than that of F8 and F14, due to larger creep and shrinkage losses; the reduction was possibly also due to the decrease in the bond factor caused by overloading, for the reasons given in section 4.7.

In the first cycle of loading applied to beam F15, only one flexural crack occurred; although four further load cycles were applied manually to the beam, no more cracks appeared. With the commencement of pulsating loading, the one crack rapidly propagated sideways and after 2,000 load cycles, had travelled a distance of 10" horizontally along the top of the web. The deflection of the beam continued to increase considerably and after 2,500 load cycles, a crack appeared in the top flange above the flexural crack. With the completion of 4,000 cycles, the horizontal crack had travelled 18" along the top of the web and had started to propagate upwards into the top flange. Complete collapse occurred after 4,700 cycles. The unusual propagation of cracks in this test was caused by the unsymmetrical position of the one flexural crack which occurred and, although it is not typical of flexural fatigue failures, the result is important for illustrating the behaviour which may occur under certain conditions of repeated loading. The failure is clearly shown in plate 4.2.

4.6c) BEAM BEHAVIOUR WITH MAXIMUM LOAD LEVEL = 73.8% OF $\bar{M}_u$

Two beams, F11 and F16, were tested at this load level and, although the fatigue lives of the two were significantly different, the overall mode of failure was very similar in both cases.

Two flexural cracks occurred in F11 in the first cycle of loading, and when the pulsating load was commenced, the condition of the concrete at the flexural cracks rapidly deteriorated and extensive spalling off of fragments occurred, causing tension in the top flange above the flexural cracks, with the result that a crack appeared in the top flange after 14,000 cycles. Spalling off of concrete then commenced at this crack and, after 32,000 cycles, the top flange collapsed at the crack as shown in plate 4.1.

Two flexural cracks were also observed in the first cycle of loading on beam F16, and after 10,000 cycles these two cracks had propagated horizontally along the top of the web and joined together. When 38,000 cycles had been completed, a crack occurred in the top flange and after 110,000 cycles, it was obvious that failure was imminent - the test was, therefore, terminated before the top flange collapsed completely. The crack pattern is shown in plate 4.3. The relation between the top fibre strain in the flange above a flexural crack and the number of load cycles is shown in fig.4.14. The curve shows clearly the effect of abrasion at a flexural crack under minimum load. Up to about 8,500 cycles, the top fibre was under compression, but after this, the rapid wearing away of the concrete at the cracks caused the top fibres to be put into tension, reaching a maximum after 40,000 cycles, after which the abrasion had little further effect, having reached a virtually steady state. The abrasion thus caused an increase in tensile strain in the top fibre of 0.00031.

4.6d) DISCUSSION OF RESULTS

The results of the fatigue tests to failure carried out with a minimum load level of 10% of the mean static ultimate strength vary greatly, both in nature, and in magnitude, as shown in the S - N diagram in fig. 4.15. However, the main value of the results lies in the qualitative nature of the type of failures obtained, because, although they are not generally typical of flexural fatigue failures, they form important exceptions that are possible under certain conditions, which should obviously be avoided in practice. The stress conditions existing in the concrete under dead load and prestress only, under a load of 10% of $\overline{M}_u$ (assuming no abrasion of concrete at cracks), and under a load of 27.5% of $\overline{M}_u$, are given in fig. 4.16. In order to obtain failures which were more typical of flexural fatigue failures, it was obviously necessary to increase the level of the minimum load as this would reduce the compressive stress on the bottom fibre and less abrasion would be caused. At the same time, the compressive stress on the top fibre would be increased, thus allowing a greater increase in tensile strain before the onset of cracking. For the series of tests described in section 4.7, the minimum load level was, therefore, increased to 27.5% of $\overline{M}_u$. It is important to note that in no case did any new flexural cracks occur under repeated loading.

The discussion of the results of the beams which failed by fatigue fracture of the strand is included in section 4.7.

The results are summarised in table 4.9.

4.7) FATIGUE TESTS TO FAILURE WITH MINIMUM LOAD = 27.5% OF THE MEAN STATIC ULTIMATE STRENGTH

4.7a) TEST PROCEDURE

The experimental procedure in all these tests was as described in section 4.3a.

The instant at which the first wire in the strand fractured was determined by the decrease in the maximum load which occurred instantaneously due to the reduced stiffness of the beam. This decrease in load operated the automatic cut - out which removed the pulsating load, but left the beam under the minimum load. The test was then started again and continued until subsequent wire failures reduced the resistance of the beam to the level of the maximum repeated load - the beam was then unloaded. If no failure had taken place after 3,000,000 load cycles, the fatigue test was stopped and the beam loaded statically to failure.

Instrumentation consisted of dial gauges to measure deflections, and clinometers to measure rotations between the ends of the beams. The strain profiles on both sides of the beam at five adjacent sections in the constant moment zone were determined by demec gauge readings at four levels in the compression flange - the layout of the demec points was as shown in fig. 4.1.

4.7b) BEAM BEHAVIOUR

The behaviour of the ten beams tested in this series followed a similar pattern in all cases and, therefore, the descriptions are not divided into sub - sections for each level of the maximum load. The patterns of behaviour are detailed in terms of crack patterns, deformations, and the characteristics of failure. The level of the maximum load varied from 74.0% of the mean static ultimate strength, $\bar{M}_u$, which caused failure after approximately 100,000 load cycles, to 66.6% of $\bar{M}_u$, at which level, no failure occurred after 3,000,000 load cycles.

The final stable state crack patterns for all the beams are shown in plates 4.3, 4.4 and 4.5. The overall crack patterns were generally similar to those observed in the static tests to failure, the greatest variation from these being in the tests with the highest levels of maximum load. In all the beams, the cracks had either been formed during the previous repeated loading, or occurred in the first cycle of load; in no case did any new cracks form as a result of the repeated loading. In the first cycle of loading, the cracks propagated to within about 1" of the top flange, normally after forking into opposing inclined cracks in the region of the centroid of the web. Some extension of the cracks took place during the repeated loading, particularly during the early load cycles, but after about 10,000 cycles, no visible propagation of cracks was observed until fracture of the strand took place. In beams F19, F20, F26, and F22, the cracks propagated horizontally along the top of web and by 10,000 cycles, had joined together as shown in plates 4.3 and 4.4. When three or more flexural cracks formed in the constant moment zone (beams F23, F24, F29 and F30), the tendency to propagate horizontally under repeated loading was not so marked. The crack pattern of beam F28, which was tested under slow - cycling conditions (see section 3.10c) was significantly different from that of beam F19, which was tested with the same maximum load and also had only two flexural cracks; in F28, the cracks did not propagate sufficiently to join together at the top of the web, and it was, therefore, apparent that dynamic forces had some effect on the propagation of cracks. Some spalling and wearing away of concrete at flexural cracks was observed on closing of the cracks under minimum load, but in no case was it particularly severe, and did not lead to tension in the top flange as described in section 4.6c.

The crack patterns of beams F29 and F30 were significantly different from the rest of the beams due to the improved bond conditions between steel and concrete, created by forming the ducts with corrugated metal ductube (see section 3.3a). The crack spacing was considerably less, and in beam F30, inclined flexural - shear cracks occurred in both shear spans.

The deformations in the beams altered quite considerably under repeated loading, with the major portion of the change occurring in the early load cycles - by the time 30,000 load cycles had been completed, the response of the beam to load had reached a virtually stable state and continued to change only slowly with increasing numbers of load cycles. This is illustrated clearly by the relationship between curvature and number of load cycles as shown in figs. 4.17 to 4.26 for the ten beams. The magnitude of the absolute values (with the same maximum load level) show considerable variation, both in the early part of the test and in the stable state values, with the increase in the curvature due to repeated loading (stable state values) varying by between 40% and 110% of the value in the first cycle of loading.

The effect of repeated loading on the bond factor, F, at the final failure sections is shown in figs. 4.27 to 4.32. All the curves on each figure apply to beams tested with the same level of the maximum load. The effect of repeated loading was, thus, to reduce the efficiency of the bond in all cases - this occurred by progressive breakdown of bond at the grout - concrete interface at some distance from flexural cracks. Although the absolute values of the bond factor are considerably higher for beams F29 and F30, the proportionate reduction due to repeated loading was no less than for the remaining beams, as shown in table 4.11. The mean reduction in the bond factor for all the beams was 30.6% of value in the first cycle of loading.

The steel stress at critical (cracked) sections under maximum load was little affected by repeated loading as shown in figs. 4.33 to 4.37. The reduction in stress was due to the breakdown in bond with consequent rise in the neutral axis and increase in the internal lever arm. In most cases, the reduction from the value in the first cycle of loading amounted to about 1% of the static ultimate strength and in no case did it exceed 2%. After about 10,000 cycles, the steel stress was virtually constant and it was, therefore, assumed in calculations of the fatigue strength of the steel, that this stable state stress existed for the whole length of the fatigue test.

From the deformation readings it is, therefore, obvious that after a short initial period, the beams settled down to give a fairly consistent and virtually constant response to load. In no case was there any prior indication that a strand fatigue failure was imminent. The fracture of a wire in the strand was always detected by the sudden decrease in the maximum load which operated the pulsator cut - out - the fracture was accompanied by a distinctive sound as the wire broke. When the test was started again, the deformations were found to be significantly increased but, after a short period, the beam again settled down to give a fairly constant response to load. Often, a reasonably large number of cycles separated the first and second wire failures, but as the number of failed wires increased, the interval between successive failures was reduced progressively. The wire fractures also caused the existing cracks to extend in a vertical direction. The test was continued until the concrete in the top fibres began to crush and the beam was unable to resist the maximum load. In beam F19, the concrete in the bottom flange spalled off in the vicinity of the ruptured wire. In beams F29 and F30, horizontal cracks along the level of the steel were observed in the fracture region - this was probably due to the release of energy which accompanied a wire fracture.

In the beams with the smooth concrete ducts, the fractures did not always occur at flexural cracks, and in some cases, the strand was fractured as much as 5" away from a crack, indicating considerable bond breakdown. The failures in the beams with the corrugated metal ducts (F29 and F30) were all at flexural cracks, although not at the same cracks. It is significant to note that, in beam F30, no fracture occurred at either of the flexural - shear cracks.

The results of the beam fatigue tests are given in table 4.10.

The theory for the evaluation of the curvatures, maximum and minimum steel stresses, and the bond factors, is given in the Appendix.

4.7c) DISCUSSION OF RESULTS

Within the range of the maximum load levels chosen, fatigue fracture of the prestressing strand was, in all cases, the criterion of failure under repeated loading. With these stress levels, the number of cycles to failure fell within the range of 100,000 cycles to 3,000,000 cycles, or ran - out after 3×10^6 cycles - this may be considered to cover the range of load cycles which are likely to be applied to all normal structures subject to fatigue loading. At load levels higher than 74.0% of $\bar{M}_u$, it is likely that concrete fatigue would be the criterion of failure, but repeated load levels of this order cannot be considered as typical of practical structures. The section tested, forms an example of a normally designed under - reinforced beam.

From the S - N curve in figure 4.38, the fatigue limit for the section was found to be approximately 67% of the static ultimate strength. Therefore, considering a load factor of 2, the factor of safety against fatigue failures under working load was 1.34.

The maximum, minimum and range of steel stresses in the beams are given in table 4.10 and plotted on the S - N diagram in fig. 4.39. Also plotted on this diagram are the results obtained from the tests on the steel strand in air as described in section 4.8 - the curve plotted is for a probability of failure of 0.293 in an individual strand; since the beam contains two strands, this is equivalent to a probability of beam failure of 0.5, i.e. mean fatigue life (see section 5.5). From the diagram, it is clear that the fatigue strength of the strand at all stress levels is considerably reduced when embedded in a beam. The fatigue limit stress range of the strand in air was approximately 13.5% of the ultimate strength, whereas, in the beams tested, it was only about 8% of the ultimate strength - a reduction of 40%. It was also apparent that, as the stress level increased, the reduction in the fatigue strength also increased. The scatter of results appeared to be excessive, particularly when the results of beams F29 and F30 were included in the diagram, and it was, therefore, obvious that the maximum and minimum stress levels were not the only parameters which defined the number of cycles to failure of the strand when embedded in a beam. The reduction in the fatigue strength was clearly influenced by the quality of the bond as may be seen in fig. 4.40. The results obtained by Warner and Hulsbos (38, 48) are included in this figure which suggests a linear relationship between the reduction in the fatigue strength of the strand and the bond factor, F, as measured at the critical (failure) sections in the beams. Similar evidence of the effect of slip on the fatigue strength was found by Harris (40), and Cox and Fenners (cited in (40)), who found, experimentally, that the reduction in the fatigue strength was directly related to the magnitude of the relative slip between the two surfaces; the bond factor, F, is directly associated with the relative magnitudes of the deformation in the steel and adjacent concrete. The results of Warner and Hulsbos (38, 48) indicated that with a bond factor greater than about 0.8, there was no reduction in the fatigue strength, but further results are required to verify this. The method of least squares was used to give the best straight - line fit to the data - the resulting relationship is :-

$$\text{For } F < 0.765 \quad : \quad K = 1.0645F + 0.1833 \quad \ldots (4.1)$$

$$\text{or for } F \geqslant 0.765 \quad : \quad K = 1.00 \quad \ldots (4.2)$$

A detailed physical explanation of the occurrence of fretting between concrete and steel is not yet possible, but it is likely that the phenomenon is not the same as that which occurs between metallic surfaces. It appears that abrasion makes the steel surface chemically active, leading to oxidation in the presence of air as shown in plate 6.9. Since the fatigue strength is extremely sensitive to irregular surface conditions, it is probable that this oxidation leads to the premature initiation of fatigue cracks in the surface. The effect of heat is probably also involved in the phenomenon since the abrasion causes high local temperatures and an increase in temperature is detrimental to the fatigue strength of steel. Lateral pressure on the strand is also likely to be a contributory factor.

The factor, K, is thus an essential addition to any theory for the prediction of the fatigue life of flexural members - the necessity of this is further emphasised when it is realised that neglect of the factor will lead to unsafe results.

The slow - cycling test on beam F28 showed that the test speed within the range of 4 cycles/min to 300 cycles/min had no significant effect on either the behaviour of the beam, or the fatigue life of the beam. It had been expected that some difference might be found, since it appeared reasonable to suppose that the effect of fretting would be influenced by the test speed.

4.8) STATIC AND FATIGUE TESTS ON $\frac{3}{8}$" DIAMETER PRESTRESSING STRAND

4.8a) OBJECT AND SCOPE OF TESTS.

The main purpose of the tests was to provide an empirical relationship between the stress range and the probable fatigue life of the strand for one particular value of the minimum stress which was kept constant in all the fatigue tests. The four maximum stress levels were chosen (on the basis of preliminary tests) to give fatigue lives varying between approximately 100,000 cycles and 1,000,000 cycles - this covered completely the range of fatigue lives obtained in the beam tests. Ten specimens were tested at each chosen level of the maximum stress; the result of any specimens which failed at the grips was ignored in the analysis, and the test repeated. The value of the minimum stress (45% of the mean static ultimate strength) used in the tests was the mean of the values of the steel stress under minimum load in the beams which were tested with the minimum load level = 27.5% of the static ultimate strength of the beams. The specimens were taken from one continuous length of strand, selected at random from the same batch of strand which was used in the beam tests. The specimens were then randomly selected from this length, and assigned to a random order of testing.

Static tests to failure were conducted on ten specimens to determine the mean ultimate strength of the strand.

4.8b) RESULTS OF STATIC TESTS

The results of the static ultimate strength tests are given in table 4.12. All specimens failed in the open length of strand between the end grips. An example of the fracture is given in plate 4.7.
A stress - strain relationship obtained from electrical resistance strain gauges attached to individual wires is given in fig. 3.2. The mean ultimate strength of the strand was 22,570 lbs (100,370 Newtons) with a coefficient of variation of 0.1%. Based on an area of 0.08 sq. ins, this is equivalent to a stress at ultimate of 282,070 lbs/in^2 (1,944.8 N/mm^2).

4.8c) FATIGUE TEST RESULTS

The fatigue test results are given in table 4.12, where N_1 is the number of load cycles at which the first wire in the strand fractured. The results are summarised for the purpose of analysis in table 4.13.

One of the six outside wires was always the first to fail in fatigue - this was probably due to the following two factors :-

i) Since all load had to be transferred by friction from the outer wires to the centre wire, it is likely that some slip occurred and, therefore, the centre wire was stressed to a lower level than the outer wires.

ii) The lay of the outer wires caused torsional stresses to be created in them under load - this did not occur in the straight centre wire.

The fatigue fractures were clearly distinguishable by the typical crescent - shaped fatigue cracks which were always present in the fracture surface as shown in plates 4.6 and 4.7. In 84% of the fractures, the initiating fatigue crack was started at the surface where the adjacent wires were touching each other, 76% of these being initiated where the outer wires were touching; in these cases, the crack had obviously been caused by fretting due to relative movement between the individual wires. In the remaining 16% of cases, the fatigue crack was initiated at the outer surface of the strand and was not due to any fretting action. The low fatigue strength of strand as compared with wire may be attributed to this fretting action between individual wires, as well as to the additional torsional stresses set up in the outer wires of the strand.

4.8d) STATISTICAL ANALYSIS OF FATIGUE TEST DATA

A certain amount of scatter is present in the results of all experimental work and is caused by the inherent variability of the material properties due to flaws and other variations, in addition to the scatter caused by inexact methods of measurement and testing. When the scatter is small compared with the quantity being measured, the mean may be taken to represent the quantity adequately, as in the case of the static ultimate strength of the strand, where the coefficient of variation of the results is only 0.1%.

However, in the fatigue life data, the scatter is considerable, and in the tests with the stress range $= 15.6\%$ of the ultimate strength, the coefficient of variation of the fatigue life is 43%. The mean S - N curve is, therefore, obviously an inadequate representation of the fatigue properties of the strand, and although a portion of the scatter of the results is attributable to experimental technique (see section 3.12b), it is generally accepted that a considerable variation in results is inherent the phenomenon of fatigue failure. It is, therefore, necessary to assume that the test results at each stress level form a representative sample taken from an infinite population of values which are distributed about a certain mean value.

Several investigators have carried out tests to determine the shape of the frequency distributions obtained for the fatigue life of test specimens. Venuti (63, 64), Warner & Hulsbos (37, 38) and Bo and Leporati (cited in (36)), all found that the logarithm of the fatigue life is practically normally distributed. In this analysis, it has, therefore, been assumed that the log - normal distribution is applicable to the test data at each stress level. Thus, for each stress level, the probability that failure will occur at a number of cycles equal to or less than N, is PR. The probability, PR, is given by the cumulative normal distribution function :

PR = ...

$$PR = \frac{1}{S\sqrt{2\pi}} \int_{-\infty}^{x} e^{-\frac{(x - \bar{x})^2}{2S^2}} dx \qquad \ldots (5.28)$$

where : x = log N_1.

$\bar{x}$ = mean of the sample of log N_1 values.

S = standard deviation of the sample of log N_1 values.

Therefore, once the values of $\bar{x}$ and S have been determined, equation (5.28) may be used to determine the probability of failure for any particular value of x and vice versa. Since the integral can only be evaluated by numerical means, the values are most easily obtained from standard tables (33). The resulting curves for probabilities ranging from 0.01 to 0.99 are given in fig.4.41; the curve for a probability of 0.293 is included in figure 4.41 since this is equivalent to a probability of failure of 0.5 in an individual strand, when two identical strands are tested together (see section 5.5), which is the condition existing in the beams tested, as described in section 4.7.

The relationship between the coefficient of variation, C_v, of N_1, and the applied stress range is given in fig. 4.42. The relation shows a similar pattern to that obtained by Warner and Hulsbos (37, 38) although the increase in C_v at high values of the fatigue life is more marked than that obtained by Warner and Hulsbos - this was probably due to some increase in the error of application of the load range at lower values of the pulsating load (see section 3.12b). It is significant to note that in Venuti's tests on pretensioned beams (63, 64), the coefficient of variation of N was directly proportional to the value of the load range, which is contrary to both the author's and Warner and Hulsbos' results for prestressing strand. The static strength of Venuti's beams was, however, subject to considerable variation ($C_v = 8.5\%$), and it is, therefore, possible that, at high load levels, the true value of the maximum load (as a proportion of the actual static ultimate strength) varied considerably from that used in the calculations.

The relation between the standard deviation, S, of log N_1, and $\overline{\log N_1}$ is shown in fig. 4.43 for both the author's tests and those of Hulsbos and Warner (37, 38). The relationships appear to be almost linear in all cases (if the value of S, with $\overline{\log N_1} = 5.8171$ in the author's tests, is ignored due to possible errors in load application), and would also appear to be dependent on the level of the minimum stress. The relations show reasonable agreement, and when further results become available, it may be possible to obtain a general relationship between S, σ_s^{min} and $\overline{\log N_1}$, which is applicable in all cases.

TABLE 4.1

RESULTS OF PRELIMINARY STATIC TESTS

Beam No.	Prior load history		Flexural Cracking Moment M_{crf}	Failure Mode	Shear force at diagonal tension cracking V_{crws}	Moment at ultimate load M_u
	$\frac{M^{max}}{\bar{M}_u}$	No. of cycles endured				
			lb-ins		lbs	lb-ins
F1	-	-	191,670	Diagonal tension	8,980	296,340
F2	-	-	193,650	Diagonal tension	9,180	238,780
F3	-	-	194,470	Flexure	-	306,290
F4	46.6	3,025,000	188,410	Diagonal tension	8,870	230,630
F5	52.1	3,085,000	188,700	Diagonal tension	10,190	264,990
F7	-	-	182,950	Diagonal tension	8,900	293,830
F13	66.8	300,000	181,100	Diagonal tension	9,580	316,010
F18	-	-	171,500	Flexure	-	325,250

TABLE 4.2

RESULTS OF PRELIMINARY FATIGUE TESTS

Beam No.	a/d	Maximum Moment Level, $\frac{M^{max}}{\bar{M}_u}$ %	Number of cycles to failure, N	Failure mode	Remarks
F4	3.02	46.6	3,025,000	-	-
F5	3.02	52.1	3,085,000	-	-
F6	3.02	72.4	15,000	At top flange crack	-
F12	3.83	66.8	887,000	Fatigue fracture of strand	Beam contained untensioned steel
F13	3.83	66.8	300,000	-	Beam contained untensioned steel

($\bar{M}_u$ = 302,830 lb-ins)

TABLE 4.3

RESULTS OF STATIC TESTS TO FAILURE

Beam No.	Prior Load History		Static Flexural Cracking Moment M_{crf}	Static Ultimate Moment M_u	Maximum top fibre strain, ε_{c2u}	$\frac{M_u}{\bar{M}_u}$
	Maximum Moment Level $\frac{M^{max}}{\bar{M}_u}$	Number of cycles endured, N				
	%		lb-ins	lb-ins		%
F3	-	-	194,470	306,290	0.0430	101.1
F9	58.0	3,156,000	-	330,790	0.0445	109.2
F10	54.9	3,635,000	192,930	324,140	0.0524	107.0
F14	64.1	3,052,000	193,300	288,290	0.0457	95.2
F21	66.6	3,052,000	-	336,340	0.0476	111.1
F23	68.3	3,030,000	-	334,120	0.0510	110.3
F27	-	-	181,470	299,380	0.0438	98.9

($\bar{M}_u$ = 302,830 lb-ins)

TABLE 4.4

PRESTRESSING DETAILS - SERIES F

Beam No.	Initial Prestressing force, P_o		Final Prestressing force, P_e		Steel Prestrain ε_{sp}	Concrete Strain ε_{csp}
	lbs	Newtons	lbs	Newtons	$x\ 10^{-6}$	$x\ 10^{-6}$
F1	21,560	95,900	21,080	93,760	4110	342
F2	21,560	95,900	21,000	93,410	4094	336
F3	21,560	95,900	20,960	93,230	4087	334
F4	21,560	95,900	21,030	93,540	4100	305
F5	21,560	95,900	21,030	93,540	4100	294
F6	21,560	95,900	20,680	91,980	4032	330
F7	21,560	95,900	20,640	91,810	4024	302
F8	21,560	95,900	20,930	93,100	4081	332
F9	21,560	95,900	20,530	91,320	4003	342
F10	21,560	95,900	20,490	91,140	3995	317
F11	21,560	95,900	20,170	89,720	3933	325
F12	21,560	95,900	21,380	95,100	4167	296
F13	21,560	95,900	21,110	93,900	4116	310
F14	21,560	95,900	21,080	93,760	4110	345
F15	21,560	95,900	20,680	91,980	4032	320
F16	21,560	95,900	20,250	90,070	3948	335
F17	21,560	95,900	18,470	82,150	3601	350
F18	21,560	95,900	19,290	85,800	3761	362
F19	21,560	95,900	20,690	92,030	4034	337
F20	21,560	95,900	20,490	91,140	3994	327
F21	21,560	95,900	21,020	93,500	4097	342
F22	21,560	95,900	20,580	91,540	4012	327
F23	21,560	95,900	20,690	92,030	4034	317
F24	21,560	95,900	20,720	92,160	4039	305
F26	21,560	95,900	21,430	95,320	4178	322
F27	21,560	95,900	20,920	93,050	4077	337
F28	21,560	95,900	21,280	94,650	4148	347
F29	21,560	95,900	20,820	92,600	4059	327
F30	21,560	95,900	20,430	90,870	3982	390

TABLE 4.5

CONCRETE PROPERTIES - SERIES F

Beam No.	6" Cube strength f_{cu}		Modulus of rupture strength f_r		Cylinder splitting strength f_t	
	lbs/in^2	N/mm^2	lbs/in^2	N/mm^2	lbs/in^2	N/mm^2
F1	8234	56.8	865	5.96	628	4.33
F2	9091	62.7	757	4.94	531	3.66
F3	8286	57.1	890	6.14	623	4.30
F4	9163	63.2	937	6.46	629	4.34
F5	8870	61.1	788	5.43	536	3.69
F6	9375	64.6	831	5.73	556	3.83
F7	8915	61.5	885	6.10	576	3.97
F8	7940	54.7	862	5.94	590	4.07
F9	8688	59.9	853	5.88	581	4.01
F10	8651	59.6	915	6.31	623	4.30
F11	8707	60.0	922	6.36	646	4.45
F12	9093	62.7	750	5.17	558	3.85
F13	8056	55.5	823	5.61	565	3.90
F14	8562	59.0	803	5.54	531	3.66
F15	8327	57.4	841	5.80	567	3.91
F16	8649	59.6	848	5.85	565	3.90
F17	8995	62.0	785	5.41	538	3.71
F18	8643	59.6	635	4.38	512	3.5[illegible]
F19	9242	63.7	931	6.42	630	4.34
F20	10024	69.1	875	6.03	603	4.15
F21	9837	67.8	882	6.08	594	4.09
F22	9379	64.7	985	6.79	613	4.31
F23	9153	63.1	974	6.72	645	4.45
F24	8821	60.8	1077	7.43	661	4.56
F26	9398	64.8	965	6.65	627	4.32
F27	9292	64.1	915	6.31	611	4.21
F28	9599	66.2	894	6.16	628	4.33
F29	8867	61.1	878	6.05	609	4.20
F30	8230	56.7	718	4.95	501	3.45

TABLE 4.6

STATIC FLEXURAL CRACKING DETAILS

Beam No.	Flexural Cracking Moment, M_{crf}	Actual Flexural Cracking Stress, f_{crf}	Estimated Flexural Cracking Stress, $f_{crf} = 0.0762\, f_{cu}$	$\frac{\text{Actual } f_{crf}}{\text{Estimated } f_{crf}}$
	lb-ins	lb/in^2	lb/in^2	
F1	191,670	736	627	1.172
F2	193,650	742	693	1.071
F3	194,470	756	631	1.198
F4	188,410	674	698	0.966
F5	188,700	683	676	1.010
F6	194,230	771	714	1.080
F7	182,950	634	679	0.934
F8	187,760	663	605	1.096
F10	192,930	774	659	1.174
F11	184,060	677	663	1.021
F12	186,650	626	693	0.903
F13	181,100	568	614	0.925
F14	193,300	720	652	1.104
F15	193,300	761	635	1.198
F17	175,560	708	685	1.034
F18	171,500	563	659	0.854
F27	181,470	576	708	0.814
F28	179,630	518	731	0.709
F29	183,320	614	676	0.908
F30	179,320	562	627	0.896

TABLE 4.7

DETAILS OF FLEXURAL CRACKING IN FATIGUE

Beam No.	Maximum moment level M^{max}	Bottom fibre stress under maximum moment σ_{c1}^{max}	Estimated static flexural cracking strength f_{crf}	$\frac{\sigma_{c1}^{max}}{f_{crf}}$	Number of cycles to flexural cracking N
	lb-ins	lbs/in^2	lbs/in^2	%	
F4	141,230	3	698	0.4	$\overrightarrow{3,025,000}$
F5	157,830	268	676	39.6	$\overrightarrow{3,085,000}$
F9	175,930	532	662	80.4	500
F10	166,320	416	659	63.1	$\overrightarrow{3,635,000}$
F16	180,120	575	659	87.2	5,500
F19	175,560	516	704	73.3	2,625,000
F20	176,670	551	764	72.1	55,000
F21	173,710	463	750	61.7	450,000
F22	175,560	528	715	73.8	6,000
F23	166,320	400	697	57.4	$\overrightarrow{3,013,000}$
F24	166,320	402	672	59.8	6,900
F26	166,320	544	716	76.0	600
F29	158,930	286	676	42.3	$\overrightarrow{3,016,000}$

TABLE 4.8

DETAILS OF PRINCIPAL TENSILE STRESSES IN WEB

Beam No.	Principal tensile stress under V^{max} σ_{cg}^{max}	Estimated static diagonal tension cracking strength $f_{crws} = 0.0502\, f_{cu}$	$\frac{\sigma_{cg}^{max}}{f_{crws}}$	Number of cycles endured, N	Principal tensile stress at diagonal tension failure f_{crws}	$\frac{\text{Actual } f_{crws}}{\text{Estim. } f_{crws}}$
	lbs/in^2	lbs/in^2	%		lbs/in^2	
F1	-	413	-	-	482	1.167
F2	-	456	-	-	427	0.936
F4	184	460	39.9	3,025,000	406	0.883
F5	225	445	50.6	3,085,000	498	1.119
F6	379	470	80.6	15,000	-	-
F7	-	447	-	-	412	0.922
F8	214	398	53.5	2,375,000	-	-
F9	183	436	42.0	3,156,000	-	-
F10	167	434	38.5	3,635,000	-	-
F11	275	437	62.9	32,000	-	-
F12	227	456	49.8	887,000	-	-
F13	-	404	-	-	454	1.124
F14	213	430	49.5	3,052,000	-	-
F17	-	451	-	-	377	0.836
F18	-	434	-	-	441	1.016
F23	240	459	52.3	3,030,000	-	-

TABLE 4.9

RESULTS OF FATIGUE TESTS WITH MINIMUM LOAD = 10% OF MEAN STATIC ULTIMATE STRENGTH

Beam No.	Minimum moment level, $\frac{M^{min}}{\bar{M}_u}$	Maximum moment level, $\frac{M^{max}}{\bar{M}_u}$	Number of cycles to failure N	Failure mode
	%	%		
F9	10	58.0	$\overrightarrow{3,156,000}$	-
F8	10	64.1	2,375,000	Fatigue fracture of strand
F14	10	64.1	$\overrightarrow{3,052,000}$	-
F17	10	64.1	255,000	Fatigue fracture of strand
F15	10	64.1	4,700	At top flange crack
F11	10	73.8	32,000	At top flange crack
F16	10	73.8	110,000	At top flange crack

($\bar{M}_u$ = 302,830 lb-ins)

TABLE 4.10

RESULTS OF FATIGUE TESTS WITH MINIMUM LOAD = 27.5% OF MEAN STATIC ULTIMATE STRENGTH

Beam No.	Minimum moment level, $\frac{M^{min}}{\bar{M}_u}$	Maximum moment level, $\frac{M^{max}}{\bar{M}_u}$	Number of cycles to first fracture, N_1	Minimum steel stress, $\frac{\sigma_s^{min}}{\bar{f}_{su}}$	Maximum steel stress, $\frac{\sigma_s^{max}}{\bar{f}_{su}}$	Steel stress range $\frac{\sigma_s^r}{\bar{f}_{su}}$
	%	%		%	%	%
F21	27.5	66.6	3,052,000 →	45.13	52.64	7.51
F23	27.5	68.3	3,030,000 →	44.45	54.37	9.91
F22	27.5	68.3	535,000	43.98	53.21	9.23
F20	27.5	71.0	340,000	44.04	54.79	10.75
F26	27.5	71.0	313,000	45.97	54.45	8.48
F30	27.5	71.0	458,000	43.92	56.53	12.61
F19	27.5	74.0	134,000	44.46	56.78	12.32
F24	27.5	74.0	95,000	44.52	56.85	12.33
F28	27.5	74.0	98,000	45.66	57.11	11.45
F29	27.5	74.0	492,000	44.72	58.74	14.02

($\bar{M}_u$ = 302,830 lb-ins)

($\bar{f}_{su}$ = 282,070 lbs/in^2)

TABLE 4.11

BOND FACTORS AND FATIGUE STRENGTH REDUCTIONS

Beam No.	Minimum bond factor, F, under M^{max} in first load cycle	Minimum value of stable state bond factor, F, under M^{max}	Number of cycles to first fracture N_1	Steel stress range in beam $\frac{\sigma_s^r}{\bar{f}_{su}}$	Steel stress range when tested in air $\frac{\sigma_s^r}{\bar{f}_{su}}$	Factor, K.
				%	%	
F21	0.81	0.52	$\overrightarrow{3{,}052{,}000}$	7.51	13.50	0.556(+)
F23	0.72	0.54	$\overrightarrow{3{,}030{,}000}$	9.91	13.50	0.735(+)
F22	0.67	0.45	535,000	9.23	15.50	0.596
F20	0.54	0.39	340,000	10.75	16.95	0.634
F26	0.44	0.34	313,000	8.48	17.25	0.492
F30	0.76	0.54	458,000	12.61	15.95	0.791
F19	0.66	0.34	134,000	12.32	20.90	0.590
F24	0.61	0.33	95,000	12.33	23.35	0.528
F28	0.44	0.28	98,000	11.45	23.10	0.496
F29	0.93	0.68	492,000	14.02	15.75	0.890

(+) Lowerbound values

TABLE 4.12

RESULTS OF STATIC AND FATIGUE TESTS ON $\frac{3}{8}$" DIAMETER STEEL STRAND

	Static failure load lbs.	Number of cycles to first wire fracture, N_1			
		$\frac{\sigma_s^r}{\bar{f}_{su}} = 15.6\%$	$\frac{\sigma_s^r}{\bar{f}_{su}} = 17.7\%$	$\frac{\sigma_s^r}{\bar{f}_{su}} = 20.6\%$	$\frac{\sigma_s^r}{\bar{f}_{su}} = 23.6\%$
	22,580	662,000	315,000	149,000	110,000
	22,560	371,000	357,000	158,000	86,000
	22,560	1,046,000	346,000	180,000	121,000
	22,580	928,000	283,000	154,000	100,000
	22,580	401,000	277,000	123,000	109,000
	22,570	1,251,000	414,000	194,000	80,000
	22,570	947,000	329,000	181,000	123,000
	22,490	610,000	210,000	122,000	114,000
	22,580	418,000	302,000	136,000	87,000
	22,600	514,000	334,000	139,000	89,000
Mean	22,570	714,800	316,700	153,600	101,900

$$\frac{\sigma_s^{min}}{\bar{f}_{su}} = 45.0\%$$

TABLE 4.13

SUMMARY OF STRAND FATIGUE TEST RESULTS

Steel stress range, $\frac{\sigma_s^r}{\bar{f}_{su}}$	Mean fatigue life, $\bar{N}$	Standard deviation of N, S	Coefficient of variation of N, C_v	Mean value of Log N, $= \overline{\log N}$	$\log^{-1} \overline{(\log N)}$	Standard deviation of log N, s
%			%			
15.6	714,800	308,300	43.1	5.8171	656,300	0.1901
17.7	316,700	54,770	17.3	5.4945	312,400	0.0790
20.5	153,600	24,900	16.2	5.1813	151,800	0.0701
23.6	101,900	15,620	15.3	5.0035	100,800	0.0676

$$\frac{\sigma_s^{min}}{\bar{f}_{su}} = 45.0\%$$

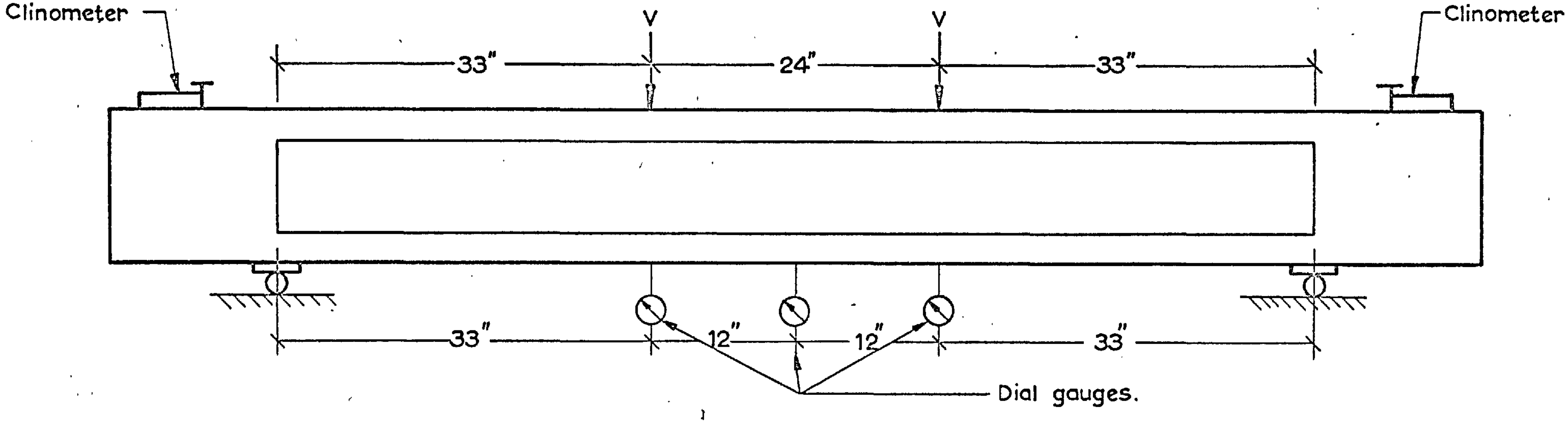

LAYOUT OF DIAL GAUGES AND CLINOMETERS - SERIES F

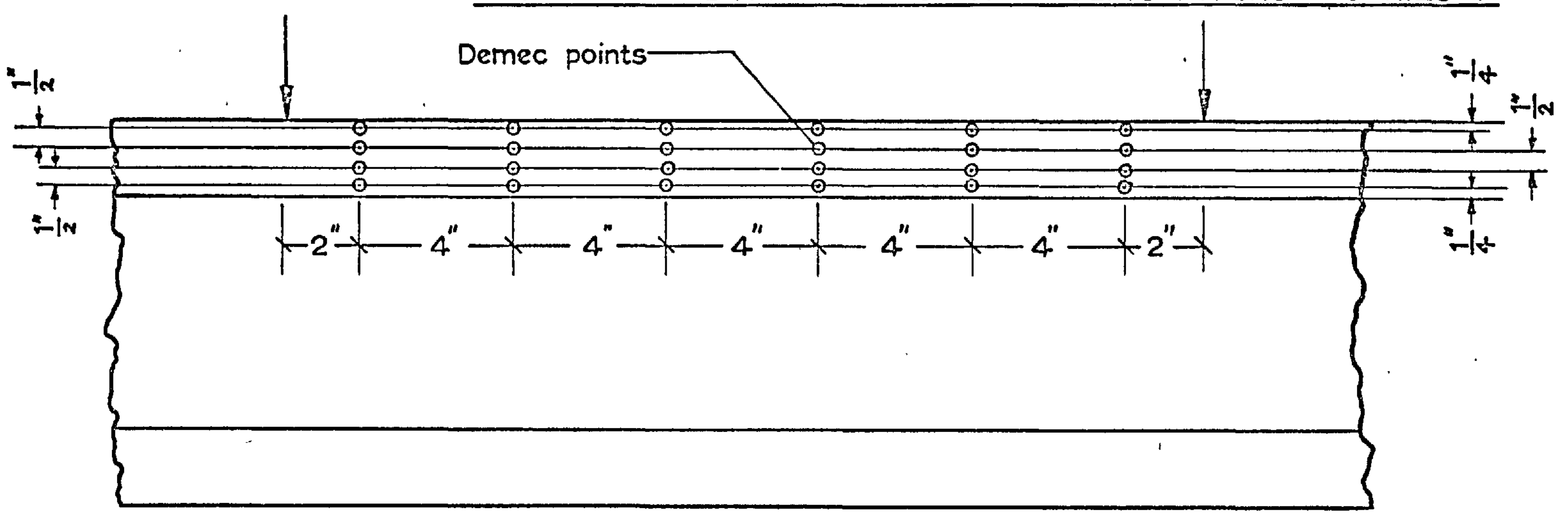

LAYOUT OF DEMEC POINTS - SERIES F

Fig. 4.1

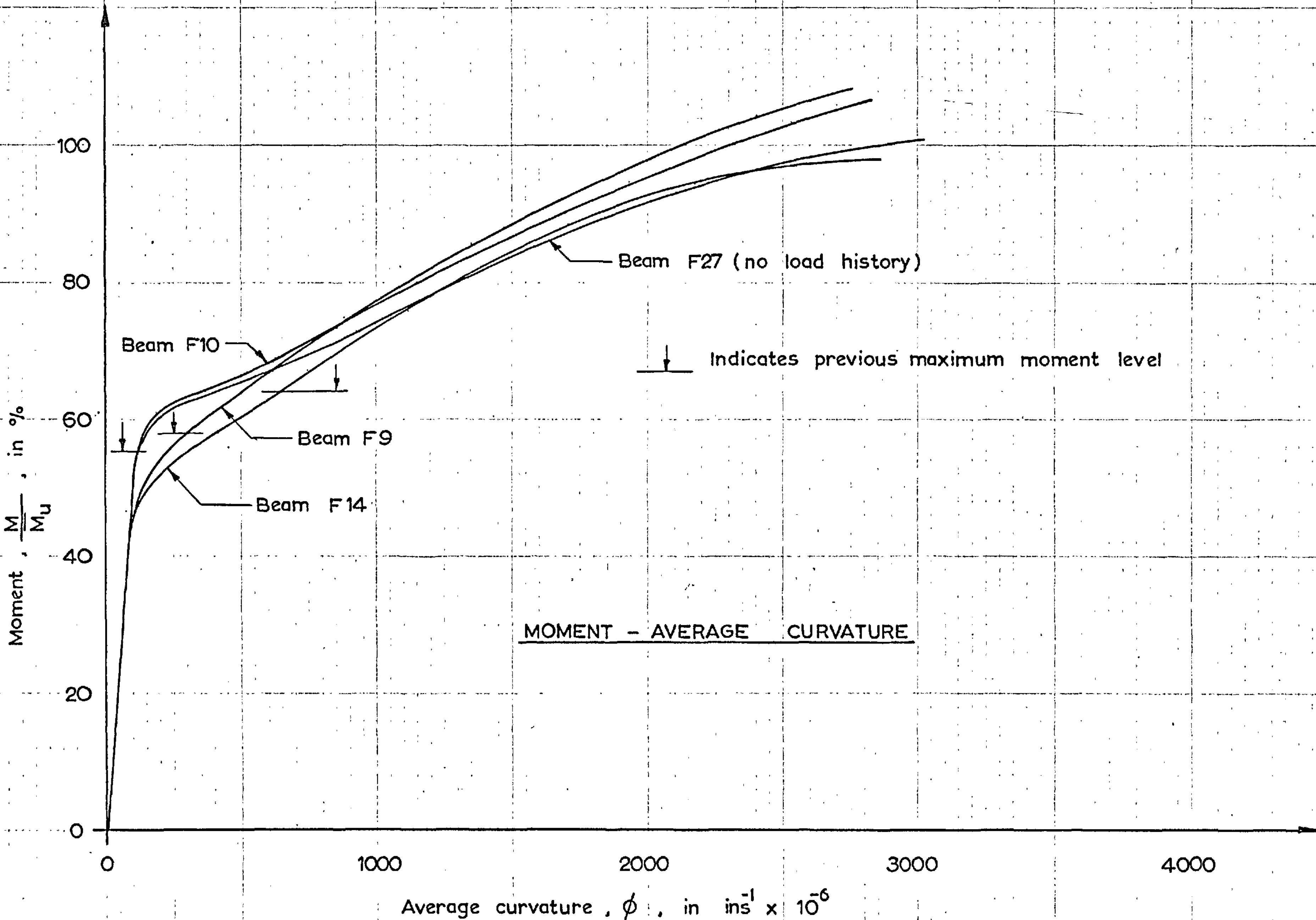
100
80
60
40
20
0
0
1000
2000
3000
4000
Moment , M/Mu , in %
Average curvature , φ , in ins⁻¹ x 10⁻⁶
Beam F27 (no load history)
Beam F10
Beam F9
Beam F14
Indicates previous maximum moment level
MOMENT - AVERAGE CURVATURE

Fig. 4.2

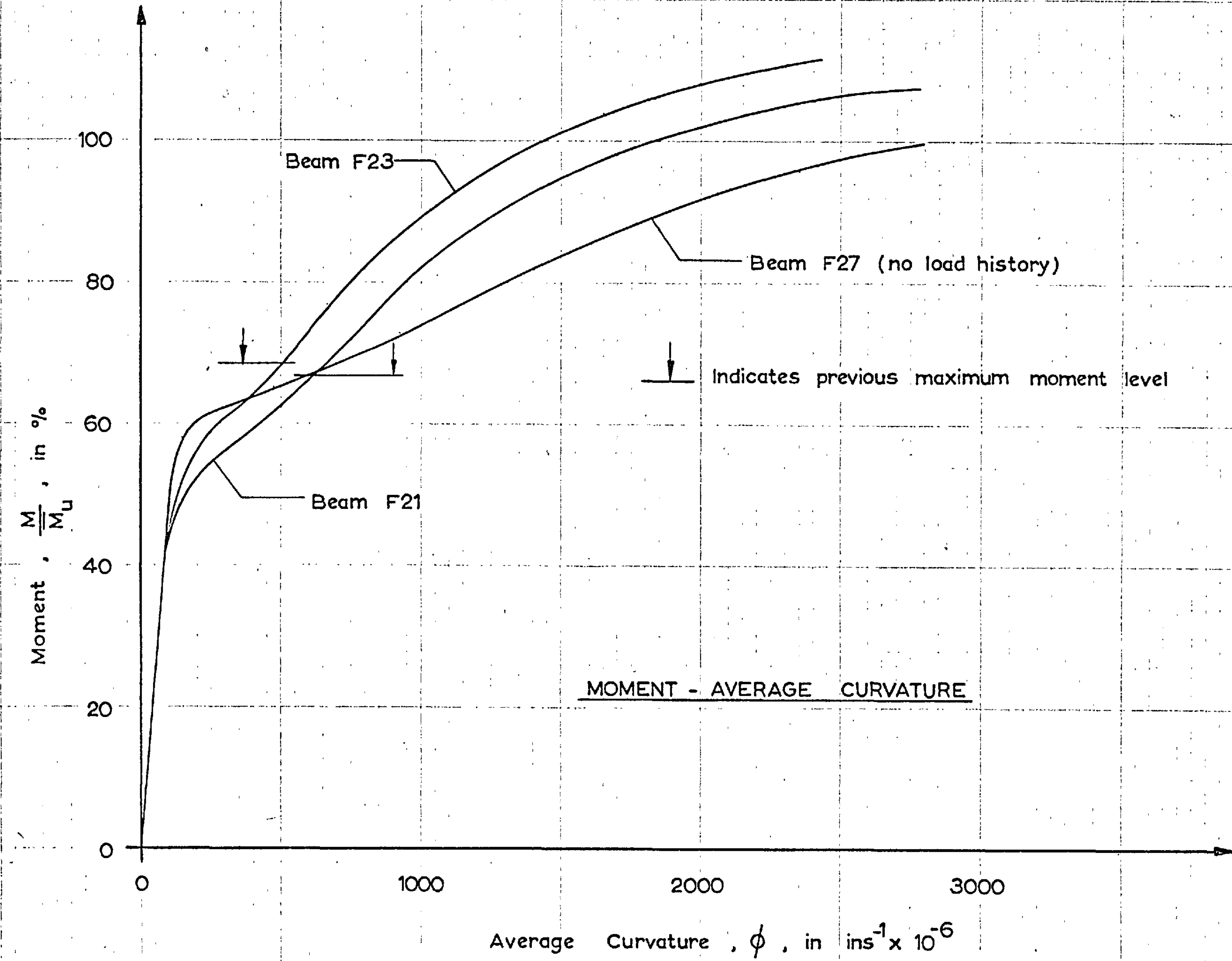
Beam F23
Beam F27 (no load history)
Indicates previous maximum moment level
Beam F21
MOMENT - AVERAGE CURVATURE
Moment, $\frac{M}{M_u}$, in %
0
20
40
60
80
100
1000
2000
3000
Average Curvature, ϕ, in $ins^{-1} \times 10^{-6}$

Fig. 4.3

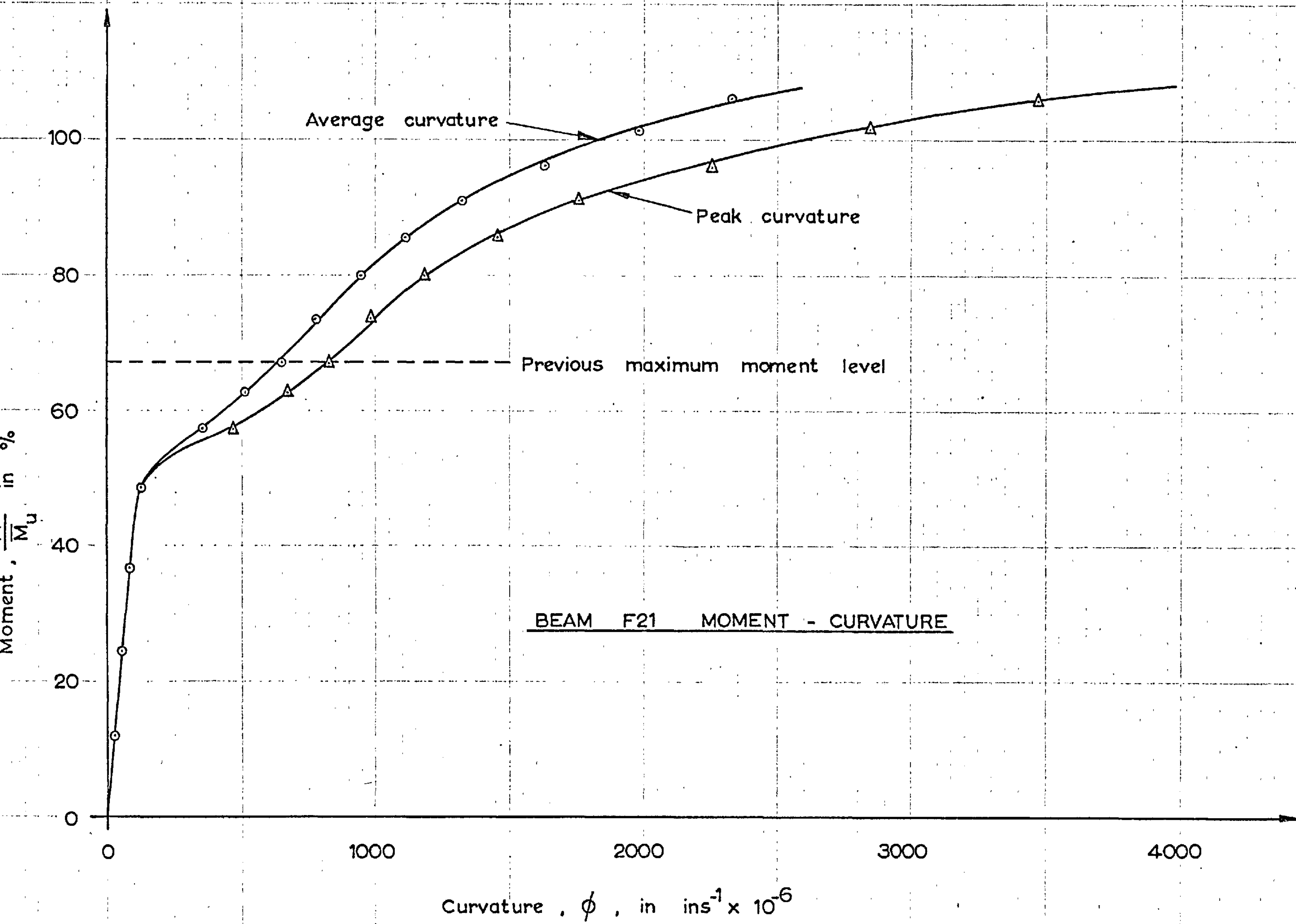
Average curvature
Peak curvature
Previous maximum moment level
BEAM F21 MOMENT - CURVATURE
Moment , $\frac{M}{M_u}$ in %
0
20
40
60
80
100
0
1000
2000
3000
4000
Curvature , ϕ , in $ins^{-1} \times 10^{-6}$

Fig. 4.4

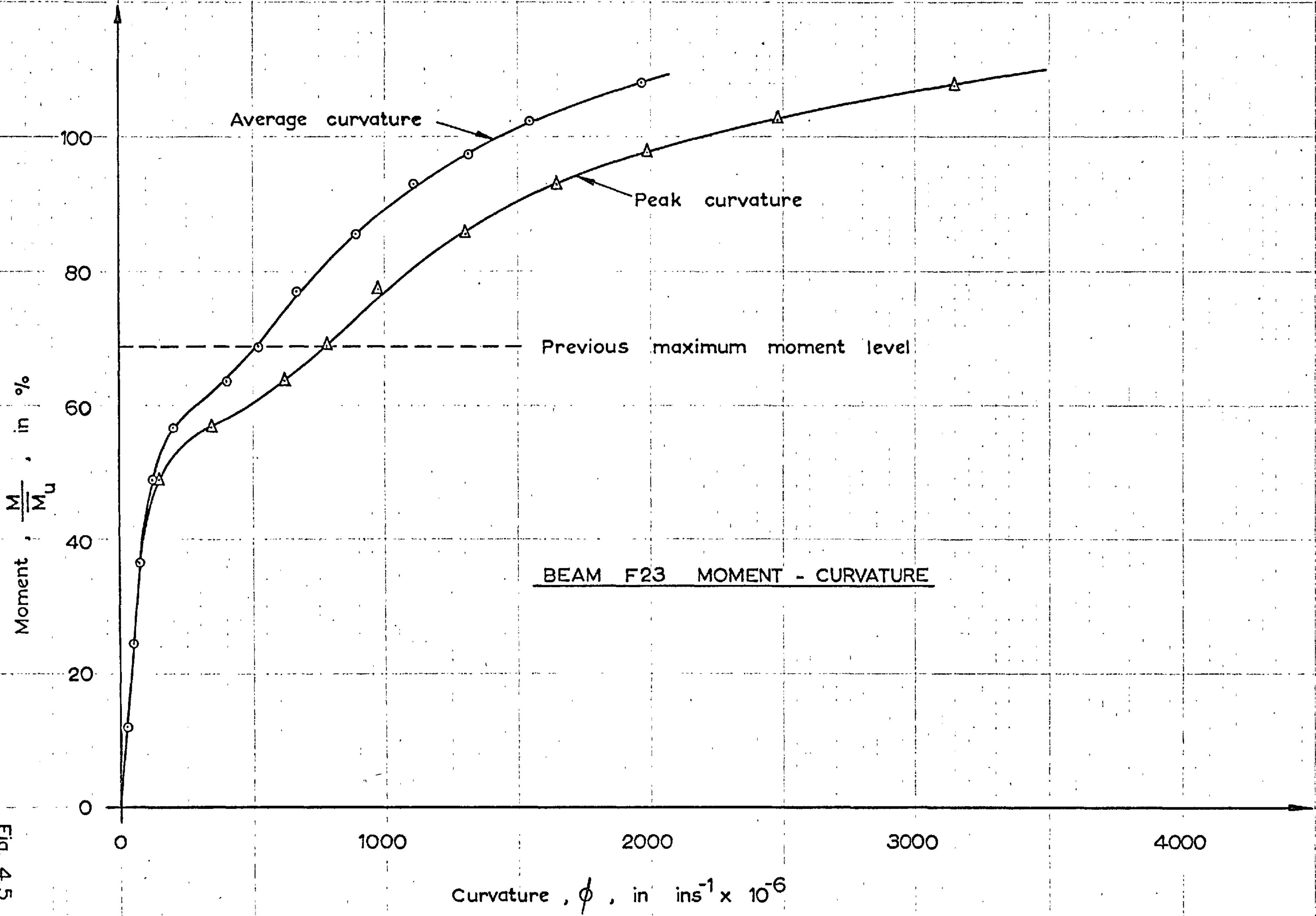
Average curvature
Peak curvature
Previous maximum moment level
BEAM F23 MOMENT - CURVATURE
Moment , $\frac{M}{M_u}$, in %
0
20
40
60
80
100
0
1000
2000
3000
4000
Curvature , ϕ , in ins^{-1} x 10^{-6}

Fig. 4.5

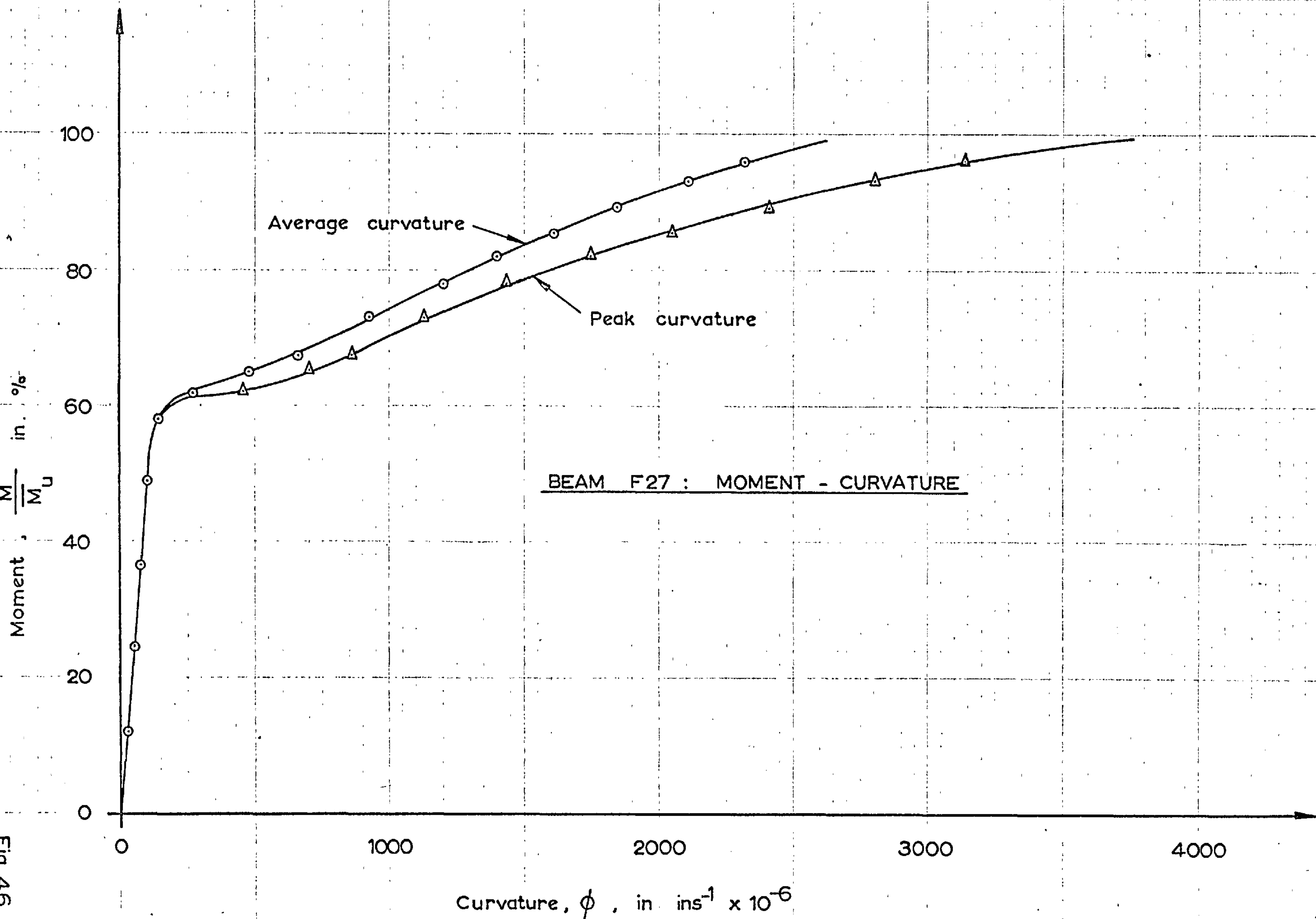
Average curvature
Peak curvature
BEAM F27 : MOMENT - CURVATURE
Moment , $\frac{M}{M_u}$ in. %
Curvature, ϕ , in ins^{-1} x 10^{-6}
0
20
40
60
80
100
1000
2000
3000
4000

Fig. 4.6

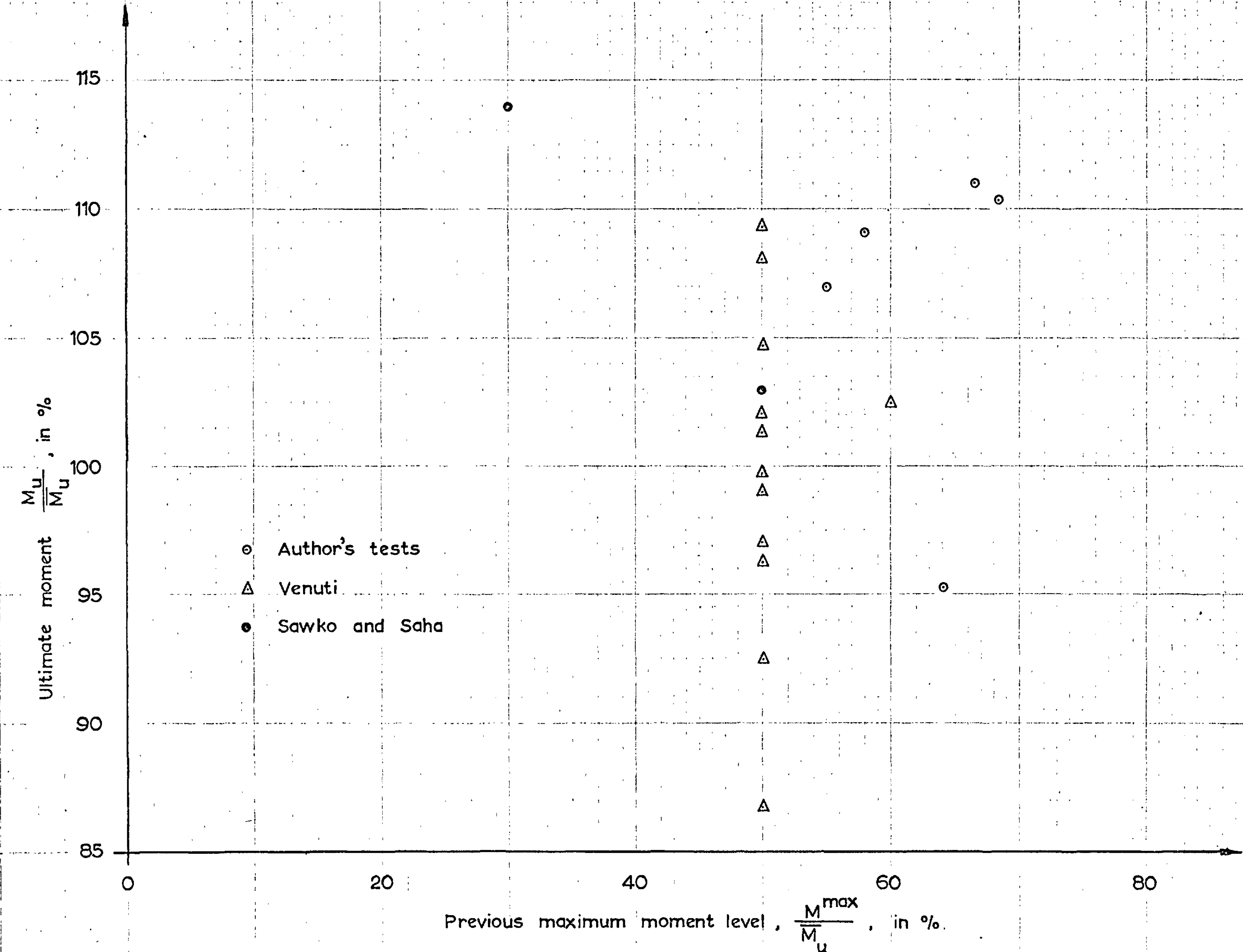
Ultimate moment $\frac{M_u}{\bar{M}_u}$, in %
115
110
105
100
95
90
85
0
20
40
60
80
Previous maximum moment level, $\frac{M^{max}}{\bar{M}_u}$, in %
Author's tests
Venuti
Sawko and Saha

Fig. 4.7

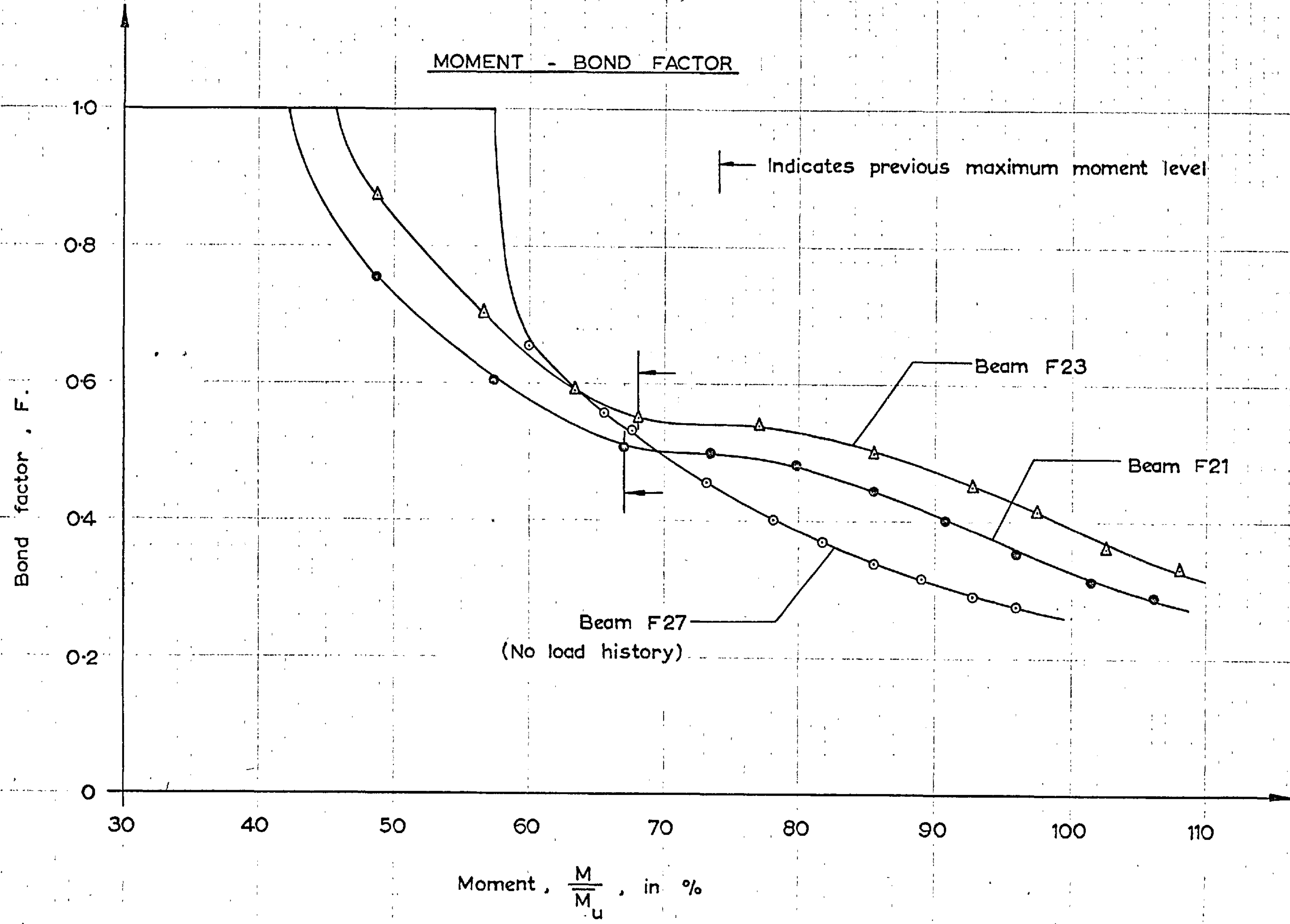
MOMENT - BOND FACTOR
Indicates previous maximum moment level
Beam F23
Beam F21
Beam F27
(No load history)
Bond factor , F.
1·0
0·8
0·6
0·4
0·2
0
30
40
50
60
70
80
90
100
110
Moment , $\frac{M}{\overline{M}_u}$, in %

Fig. 4.8

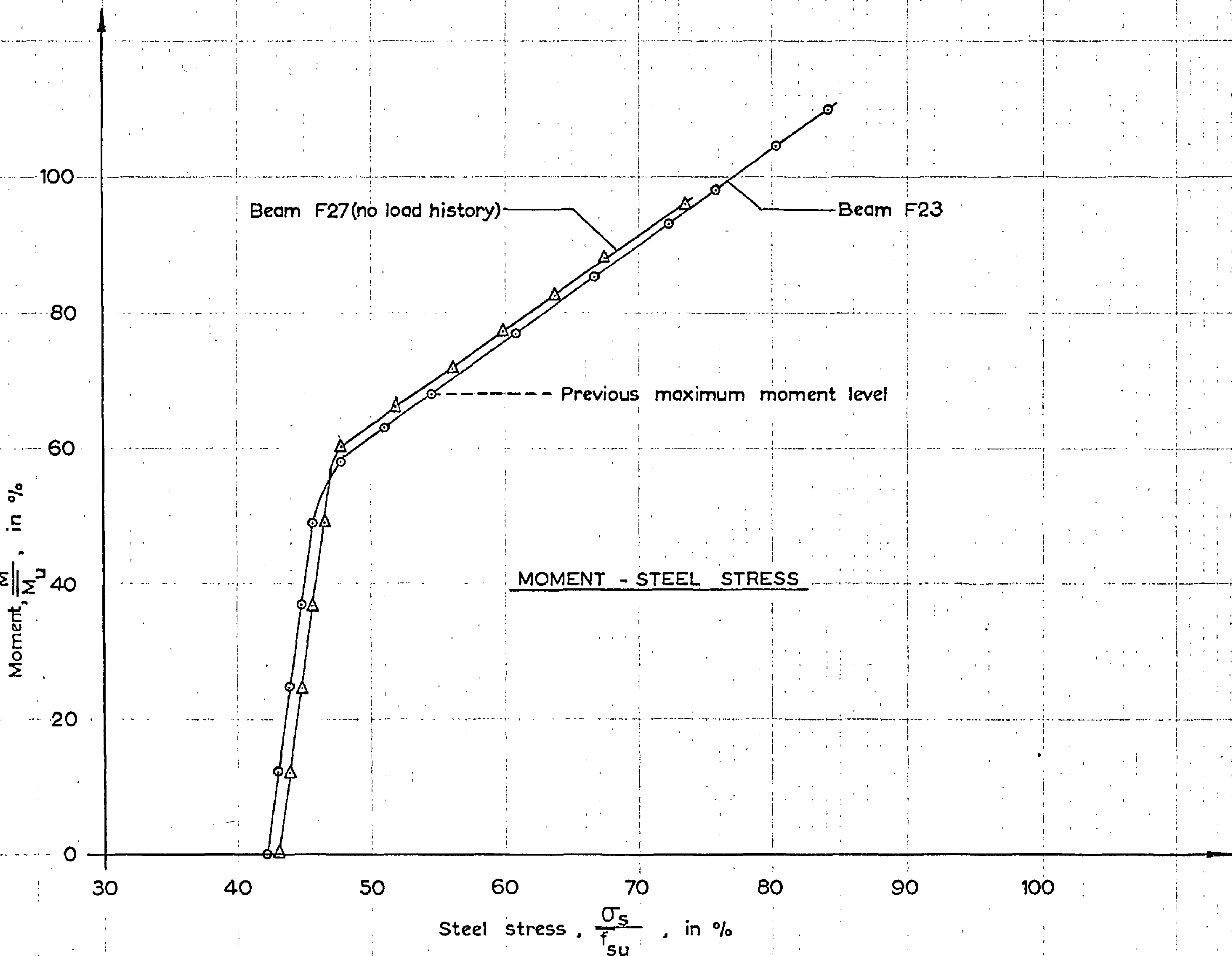
MOMENT - STEEL STRESS
Beam F27(no load history)
Beam F23
Previous maximum moment level
Moment, $\frac{M}{M_u}$, in %
Steel stress, $\frac{\sigma_s}{f_{su}}$, in %
0
20
40
60
80
100
30
40
50
60
70
80
90
100

Fig. 4.9

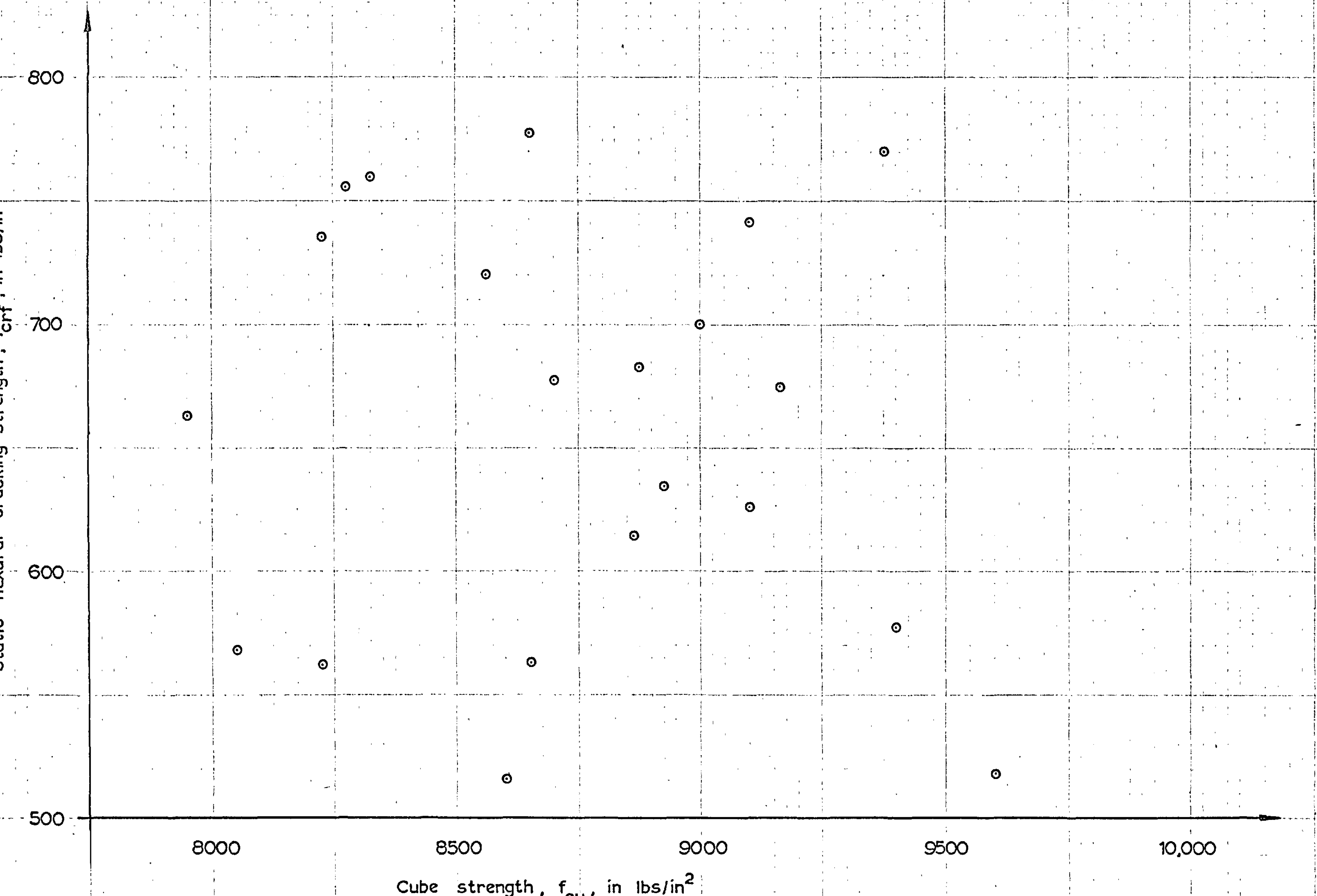
Static flexural cracking strength, f_{crf}, in lbs/in^2
800
700
600
500
8000
8500
9000
9500
10,000
Cube strength, f_{cu}, in lbs/in^2

Fig. 4.10

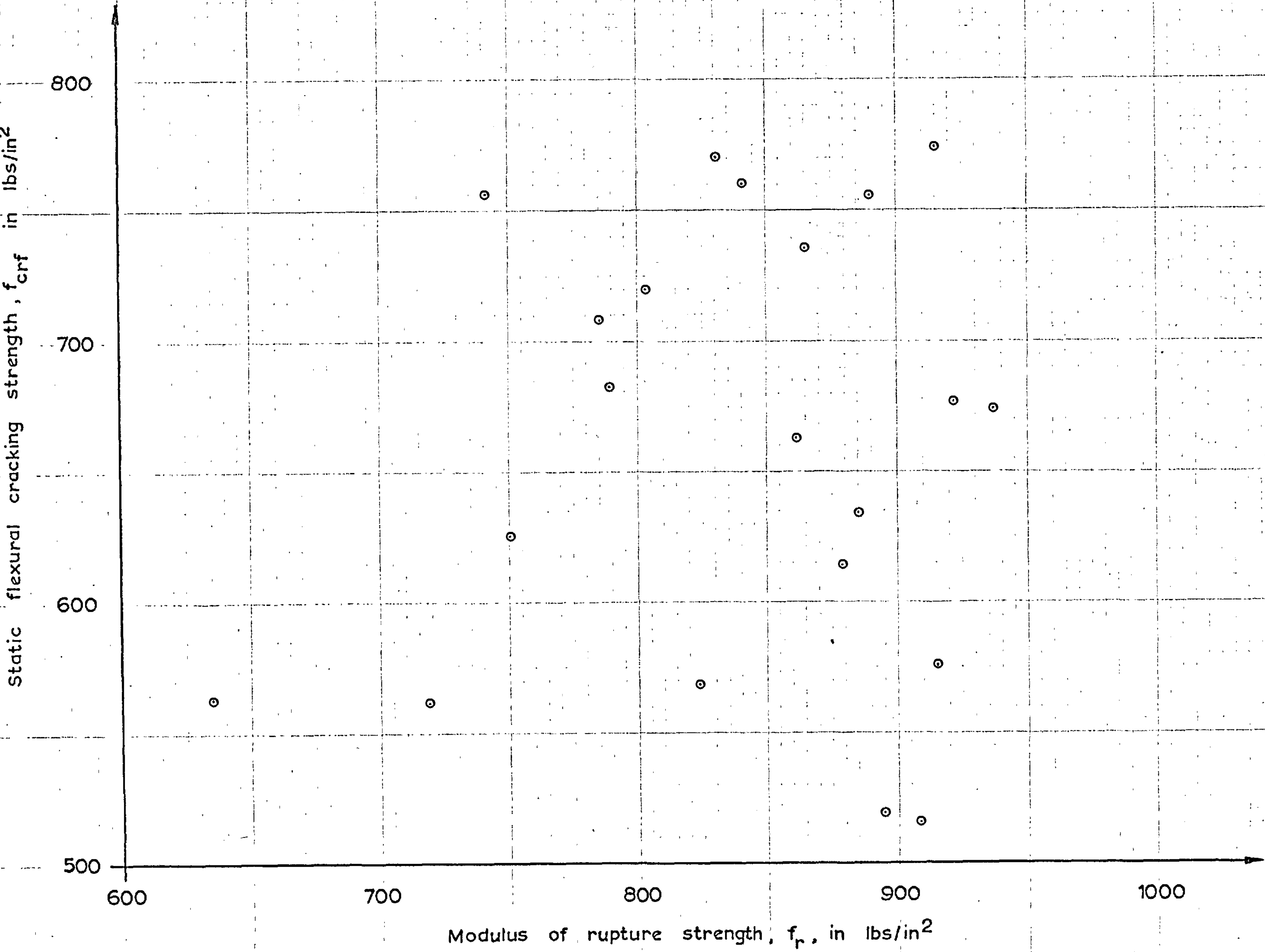

800
700
600
500
600
700
800
900
1000
Static flexural cracking strength, f_{crf} in lbs/in^2
Modulus of rupture strength, f_r, in lbs/in^2

Fig. 4.11

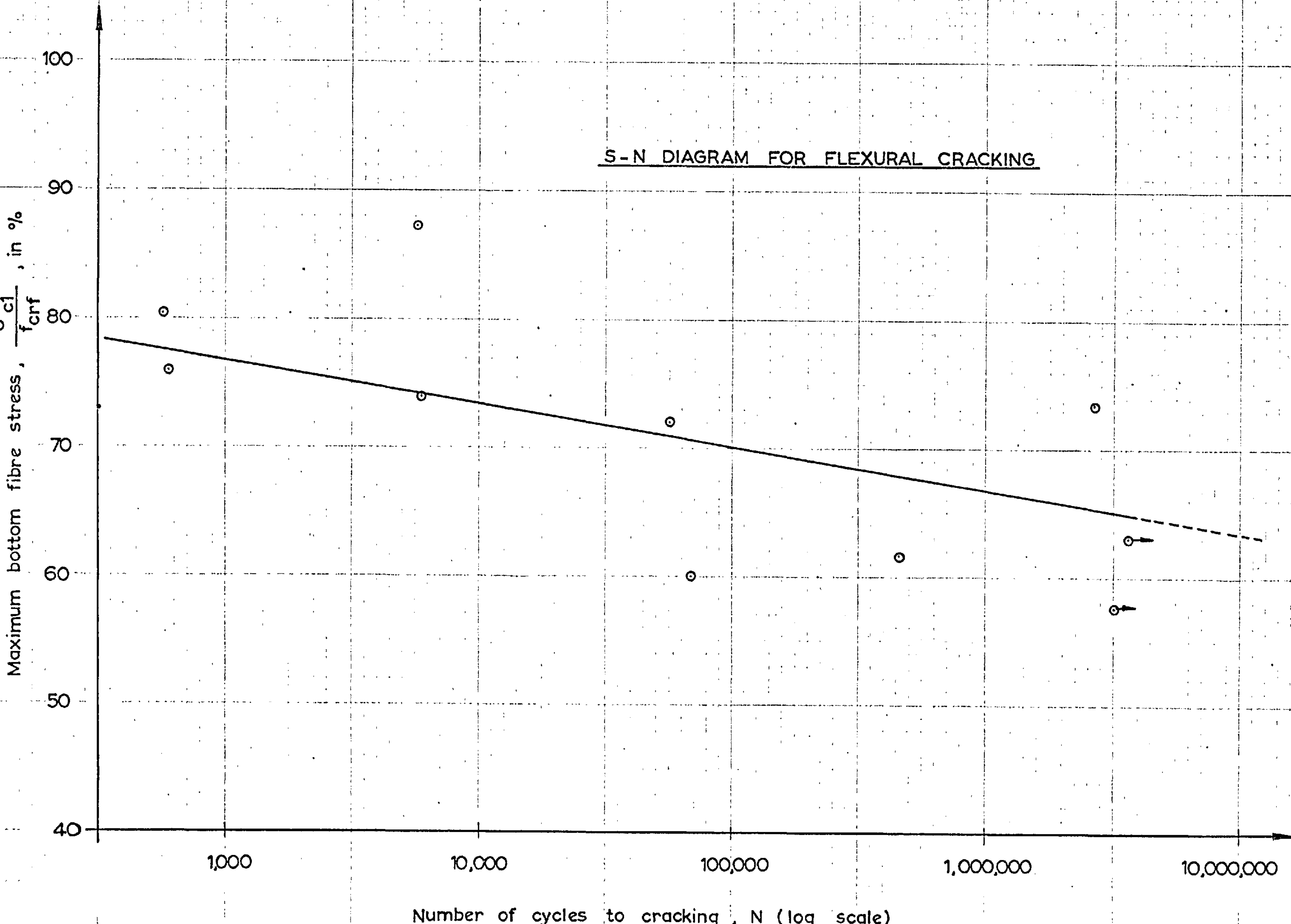

S-N DIAGRAM FOR FLEXURAL CRACKING
Maximum bottom fibre stress, $\frac{\sigma_{c1}^{max}}{f_{crf}}$, in %
100
90
80
70
60
50
40
1,000
10,000
100,000
1,000,000
10,000,000
Number of cycles to cracking, N (log scale)

Fig. 4.12

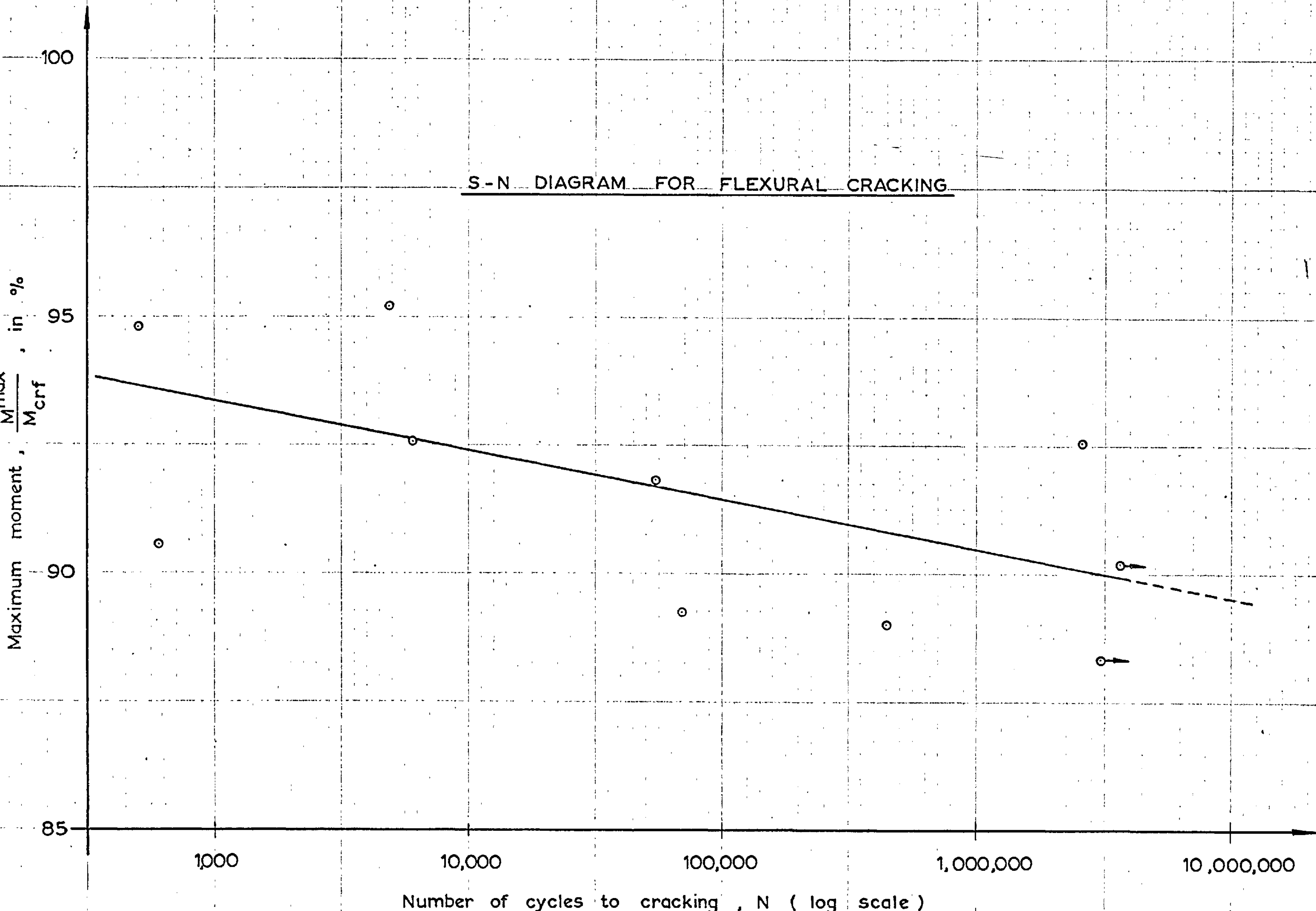
S-N DIAGRAM FOR FLEXURAL CRACKING
Maximum moment , $\frac{M^{max}}{M_{crf}}$, in %
100
95
90
85
1,000
10,000
100,000
1,000,000
10,000,000
Number of cycles to cracking , N (log scale)

Fig. 4.13

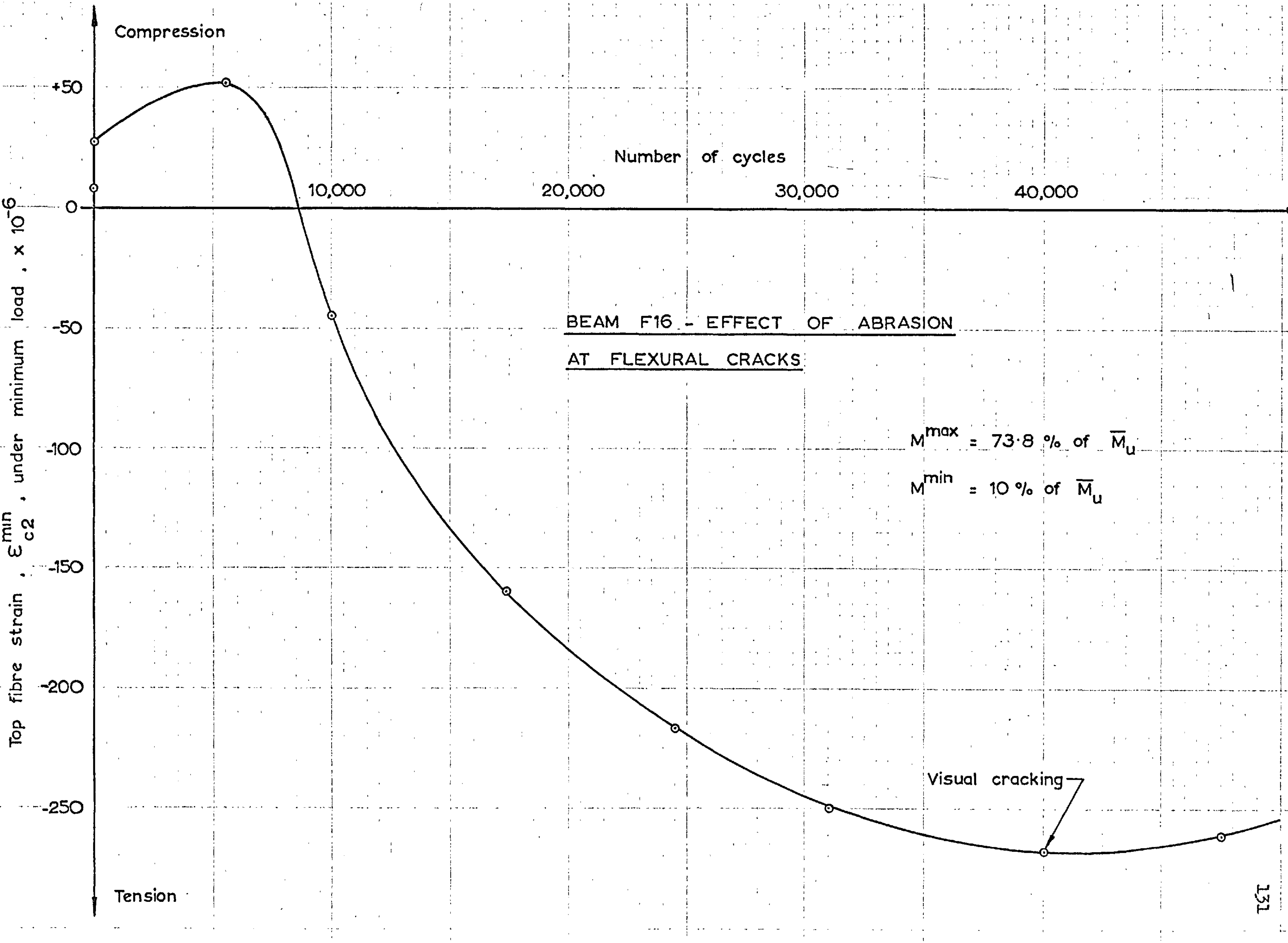
Compression
Tension
Top fibre strain , ε_{c2}^{min} , under minimum load , x 10^{-6}
+50
0
-50
-100
-150
-200
-250
Number of cycles
10,000
20,000
30,000
40,000
BEAM F16 - EFFECT OF ABRASION
AT FLEXURAL CRACKS
M^{max} = 73·8 % of $\overline{M}_u$
M^{min} = 10 % of $\overline{M}_u$
Visual cracking

Fig. 4.14

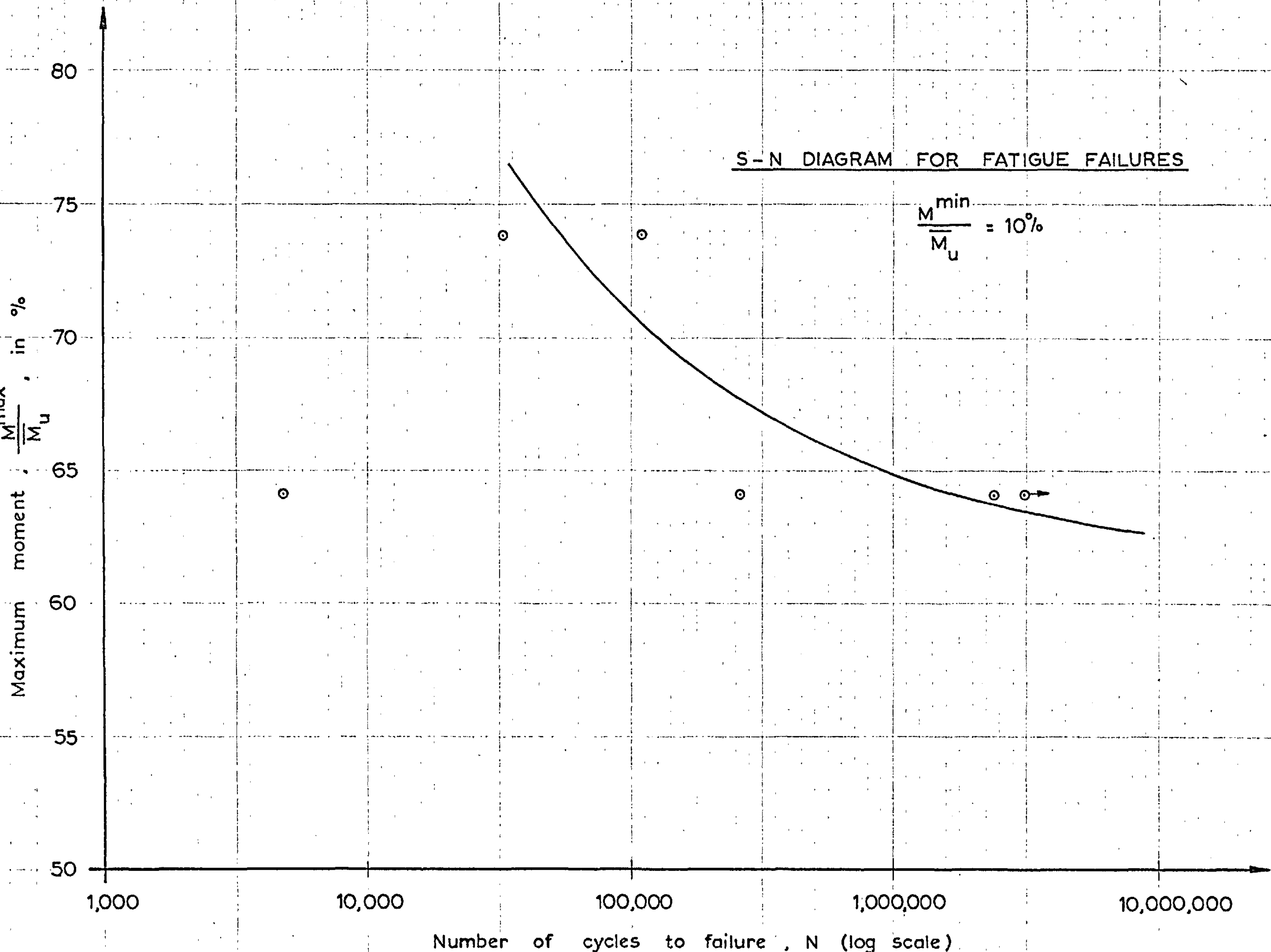
S-N DIAGRAM FOR FATIGUE FAILURES
M^min / M̄_u = 10%
Maximum moment, M^max / M̄_u, in %
80
75
70
65
60
55
50
1,000
10,000
100,000
1,000,000
10,000,000
Number of cycles to failure, N (log scale)

Fig. 4.15

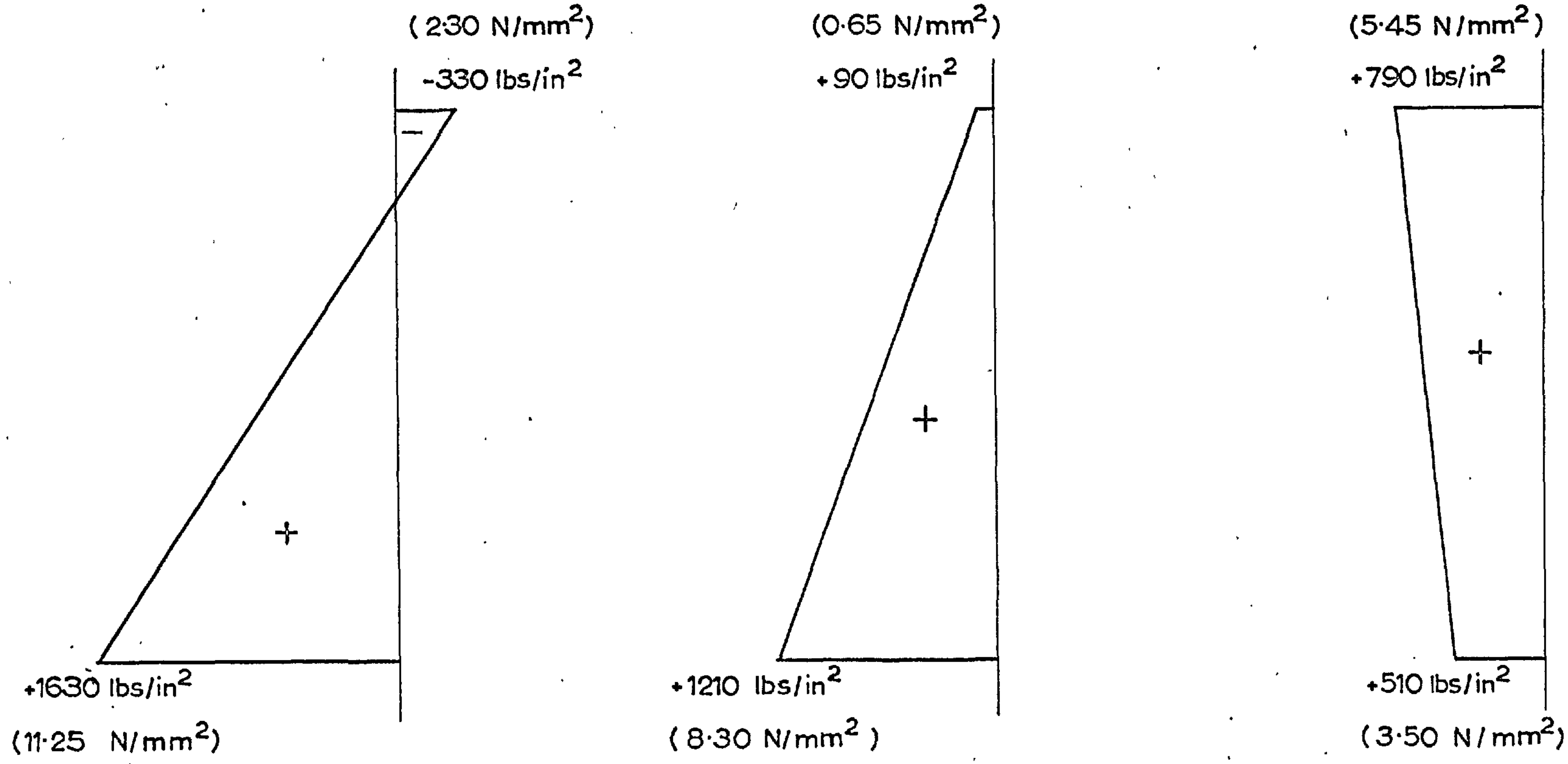

a) Stress distribution under dead load and prestress only

b) Stress distribution with $M^{min} = 10\%$ of $\overline{M}_u$

c) Stress distribution with $M^{min} = 27{\cdot}5\%$ of $\overline{M}_u$

CONCRETE STRESS DISTRIBUTIONS - SERIES F

Fig. 4.16

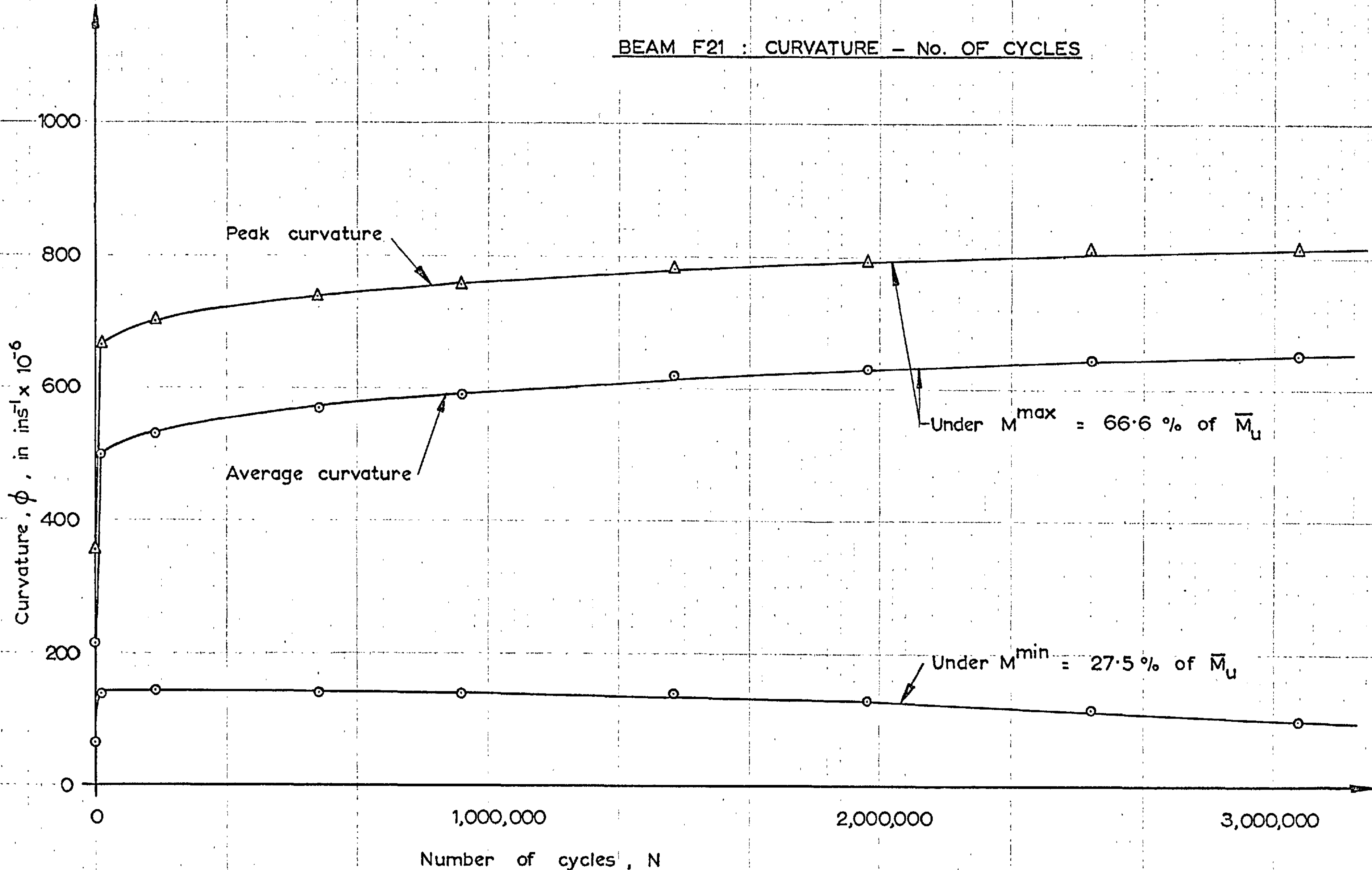
BEAM F21 : CURVATURE – No. OF CYCLES
Peak curvature
Average curvature
Under M^{max} = 66·6 % of $\overline{M}_u$
Under M^{min} = 27·5 % of $\overline{M}_u$
Curvature, ϕ, in $ins^{-1} \times 10^{-6}$
1000
800
600
400
200
0
Number of cycles, N
0
1,000,000
2,000,000
3,000,000

Fig. 4.17

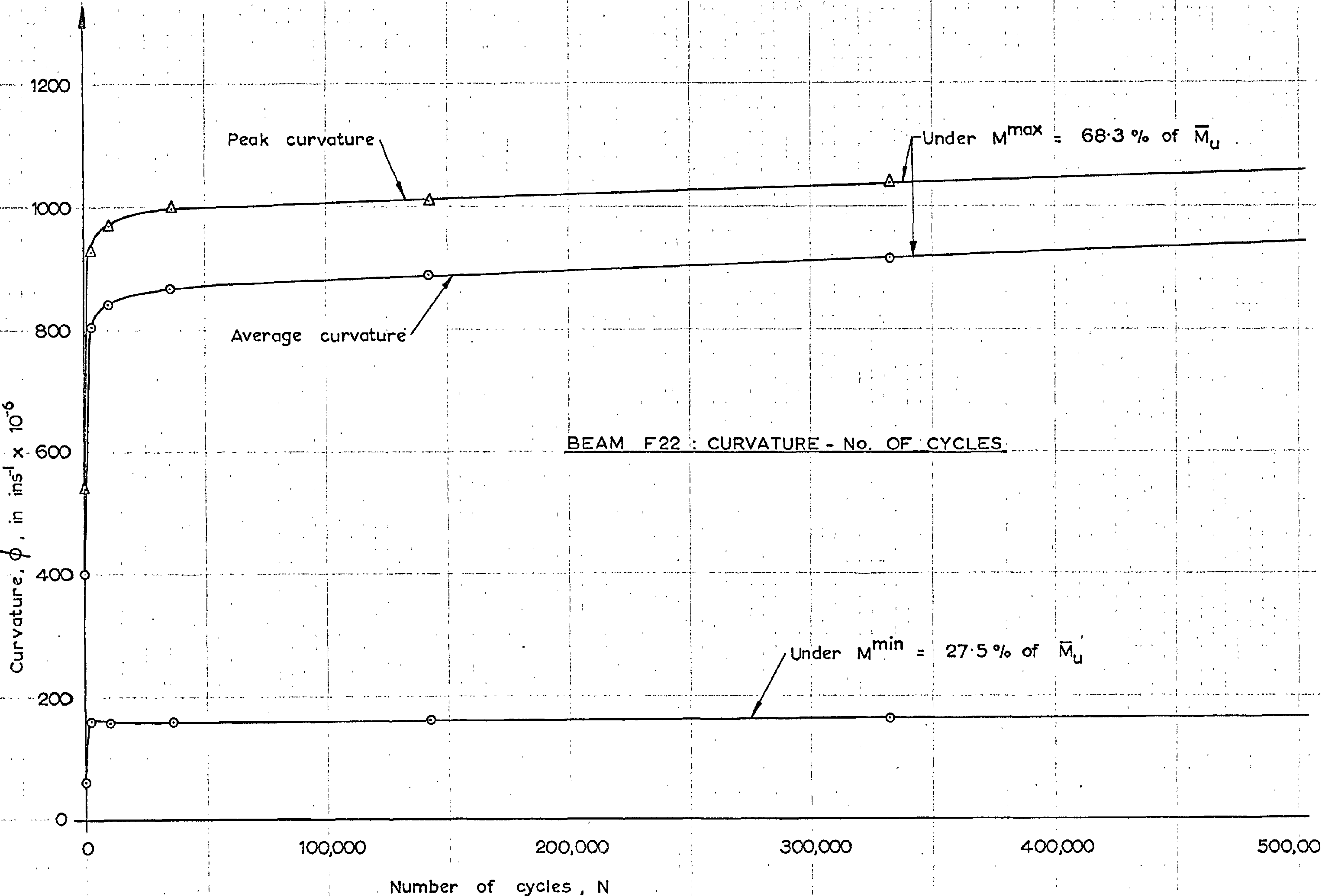

Peak curvature
Under M^{max} = 68·3 % of $\overline{M}_u$
Average curvature
BEAM F22 : CURVATURE - No. OF CYCLES
Under M^{min} = 27·5 % of $\overline{M}_u$
Curvature, ϕ, in $ins^{-1} \times 10^{-6}$
1200
1000
800
600
400
200
0
0
100,000
200,000
300,000
400,000
500,00
Number of cycles , N

Fig. 4.18

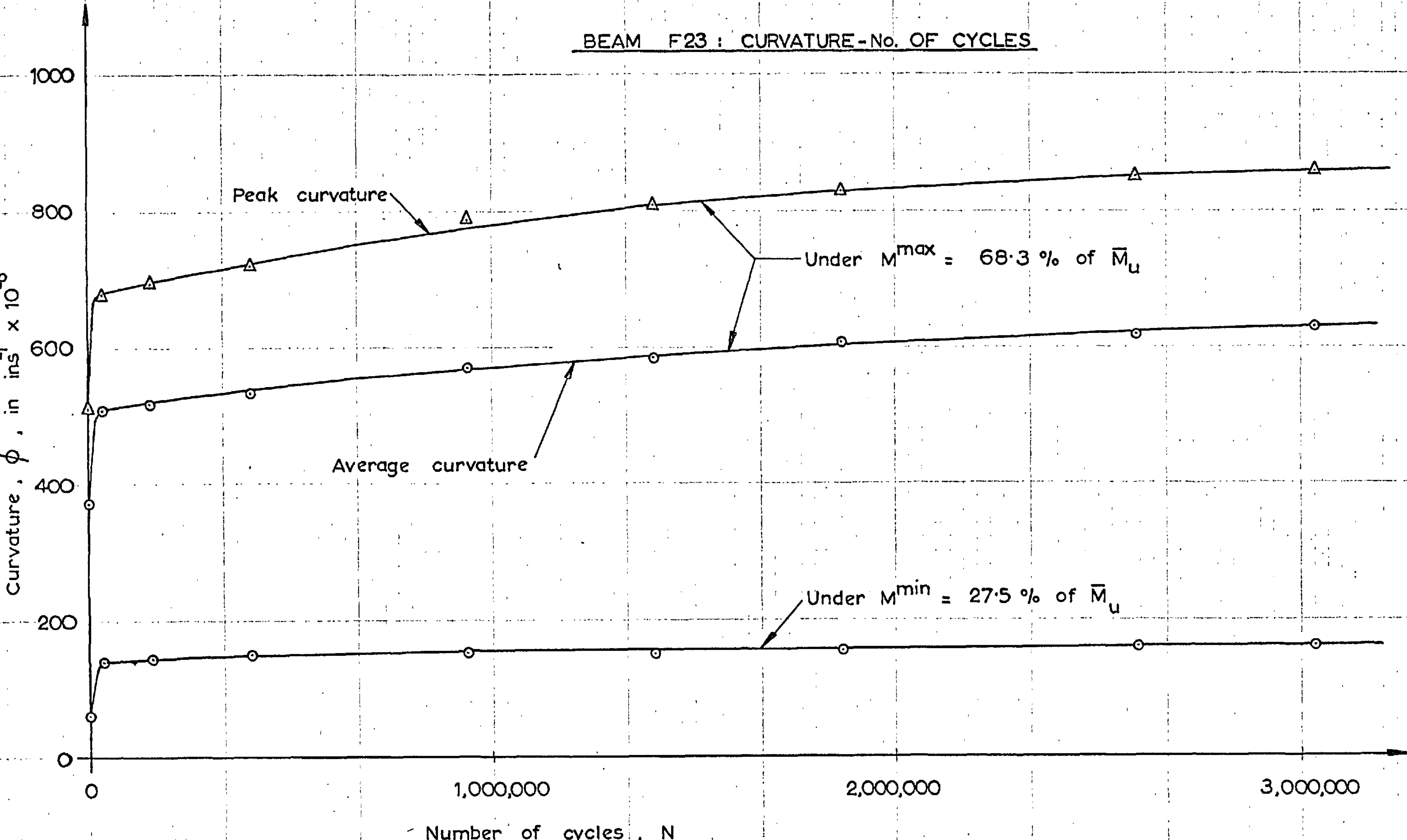
BEAM F23 : CURVATURE-No. OF CYCLES
Peak curvature
Under M^{max} = 68·3 % of $\overline{M}_u$
Average curvature
Under M^{min} = 27·5 % of $\overline{M}_u$
Curvature, ϕ, in $ins^{-1} \times 10^{-6}$
1000
800
600
400
200
0
0
1,000,000
2,000,000
3,000,000
Number of cycles, N

Fig. 4.19

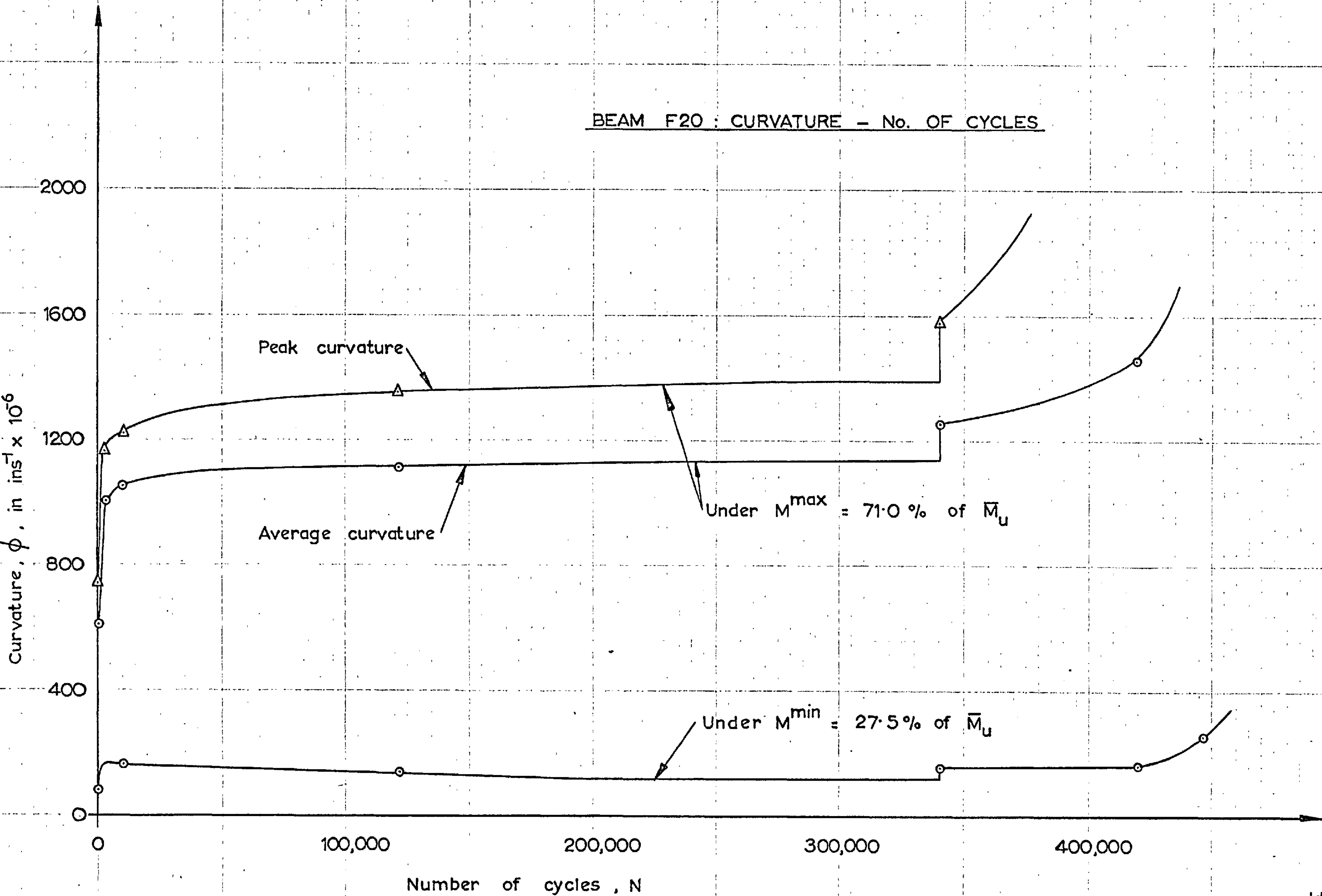
BEAM F20 : CURVATURE – No. OF CYCLES
Peak curvature
Average curvature
Under M^{max} = 71·0 % of $\overline{M}_u$
Under M^{min} = 27·5 % of $\overline{M}_u$
Curvature, ϕ, in $ins^{-1} \times 10^{-6}$
2000
1600
1200
800
400
0
0
100,000
200,000
300,000
400,000
Number of cycles , N

Fig. 4.20

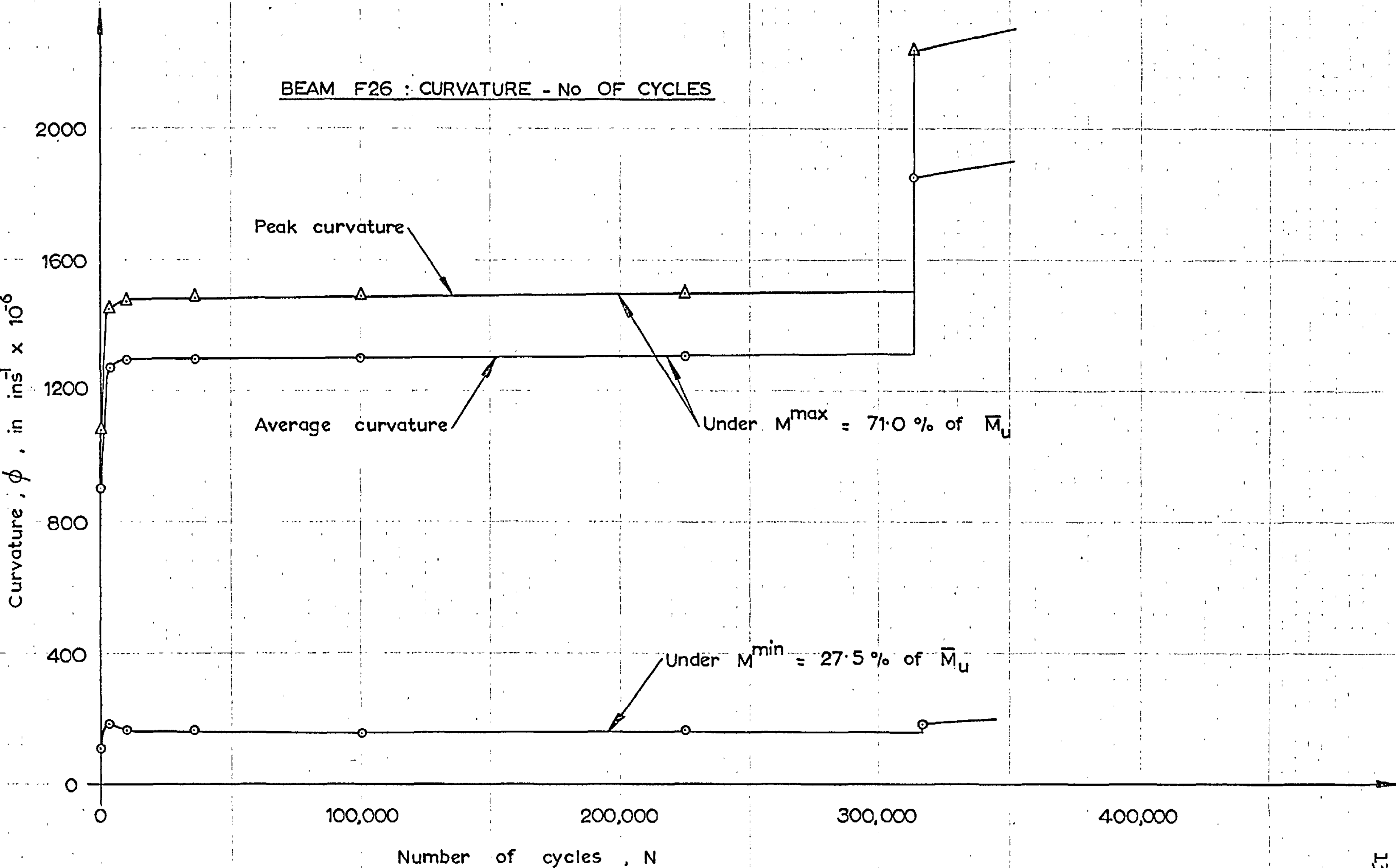

BEAM F26 : CURVATURE - No OF CYCLES
Peak curvature
Average curvature
Under M^{max} = 71·0 % of $\overline{M}_u$
Under M^{min} = 27·5 % of $\overline{M}_u$
Curvature, ϕ, in ins^{-1} x 10^{-6}
0
400
800
1200
1600
2000
100,000
200,000
300,000
400,000
Number of cycles , N

Fig. 4.21

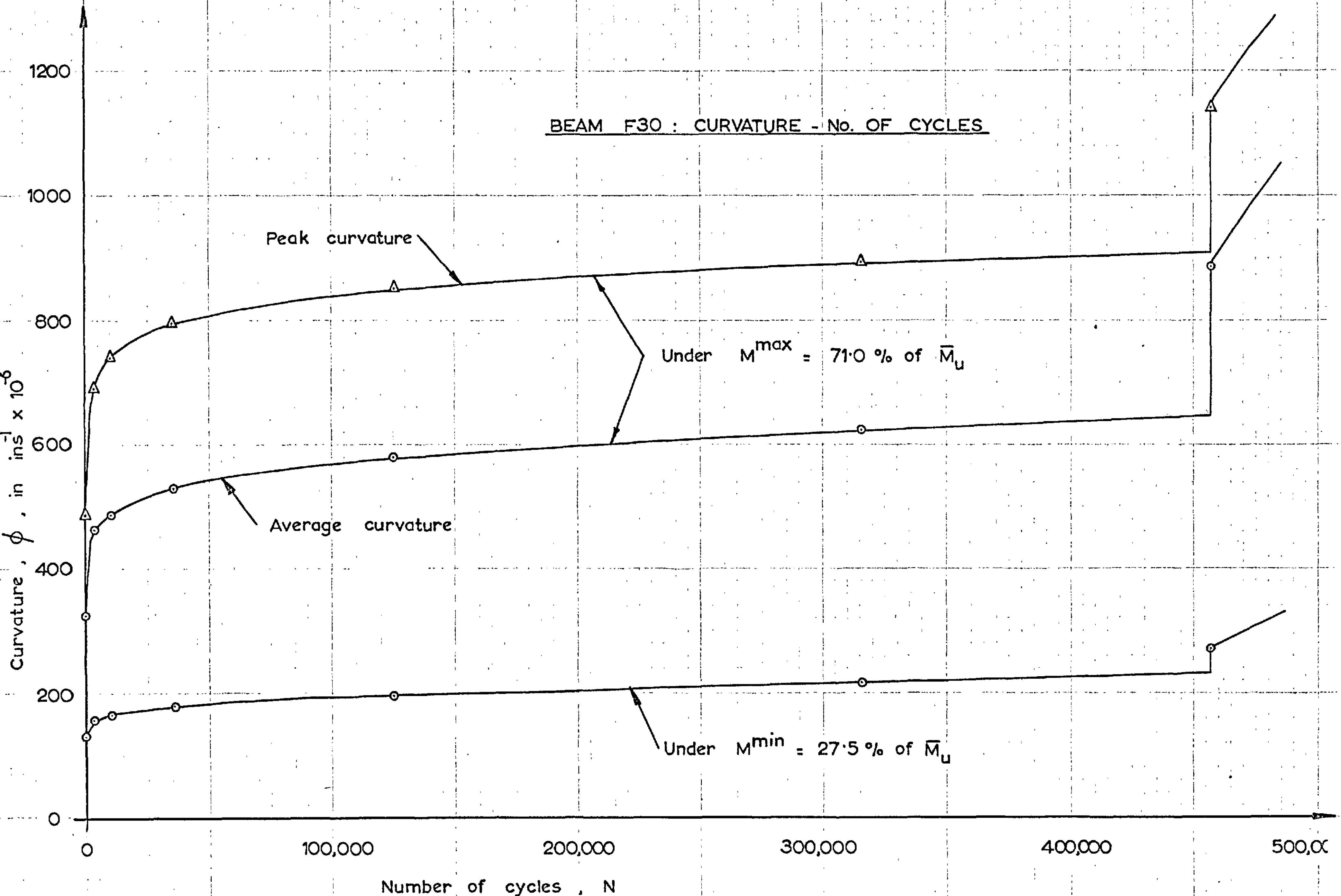

BEAM F30 : CURVATURE - No. OF CYCLES
Peak curvature
Under M^max = 71·0 % of M̄u
Average curvature
Under M^min = 27·5 % of M̄u
Curvature , φ , in ins^-1 x 10^-6
1200
1000
800
600
400
200
0
0
100,000
200,000
300,000
400,000
500,0
Number of cycles , N

Fig. 4.22

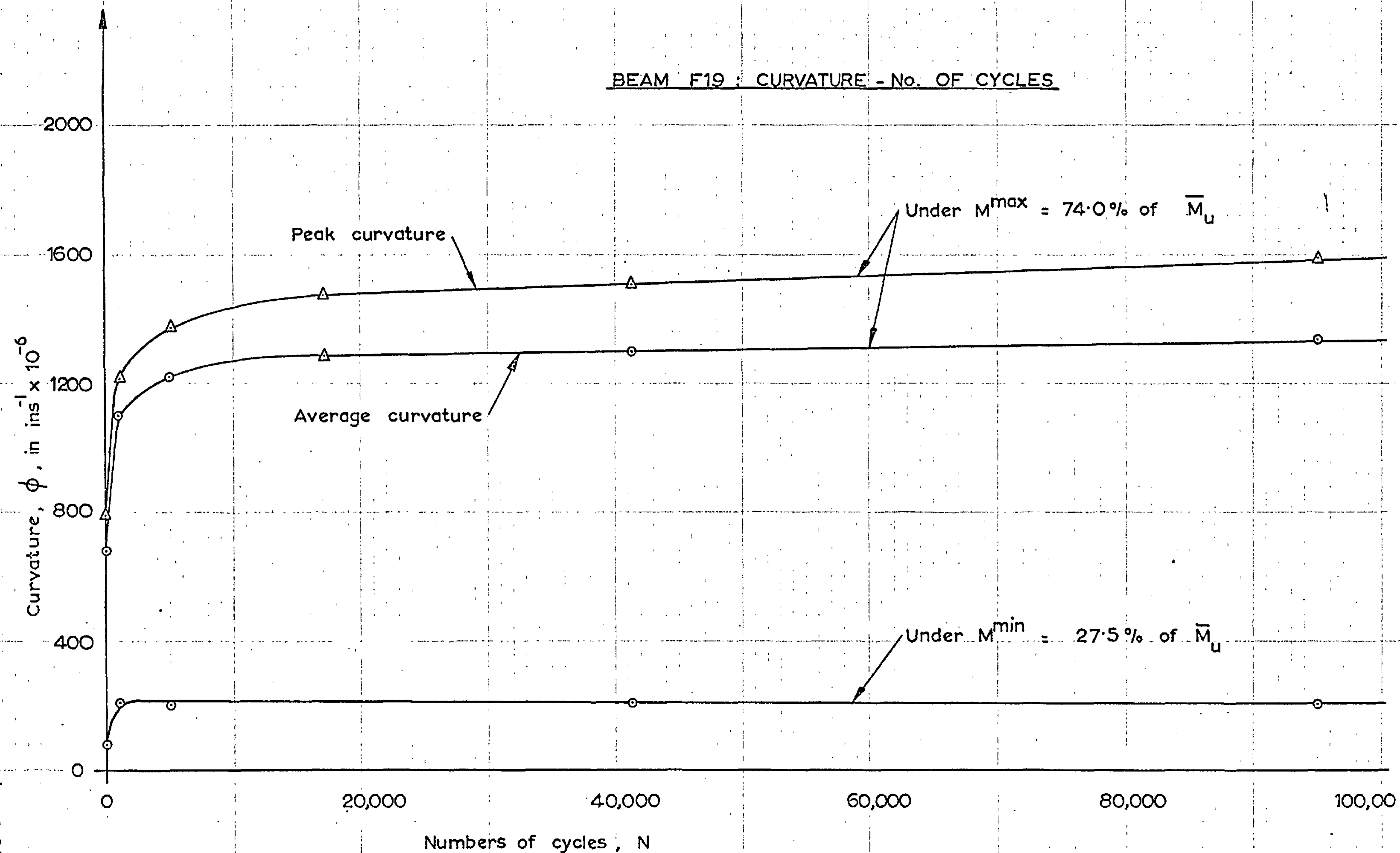
BEAM F19 : CURVATURE - No. OF CYCLES
Peak curvature
Average curvature
Under M^{max} = 74·0 % of $\overline{M}_u$
Under M^{min} = 27·5 % of $\overline{M}_u$
Curvature, ϕ, in $ins^{-1} \times 10^{-6}$
Numbers of cycles , N
0
400
800
1200
1600
2000
0
20,000
40,000
60,000
80,000
100,00

Fig. 4.23

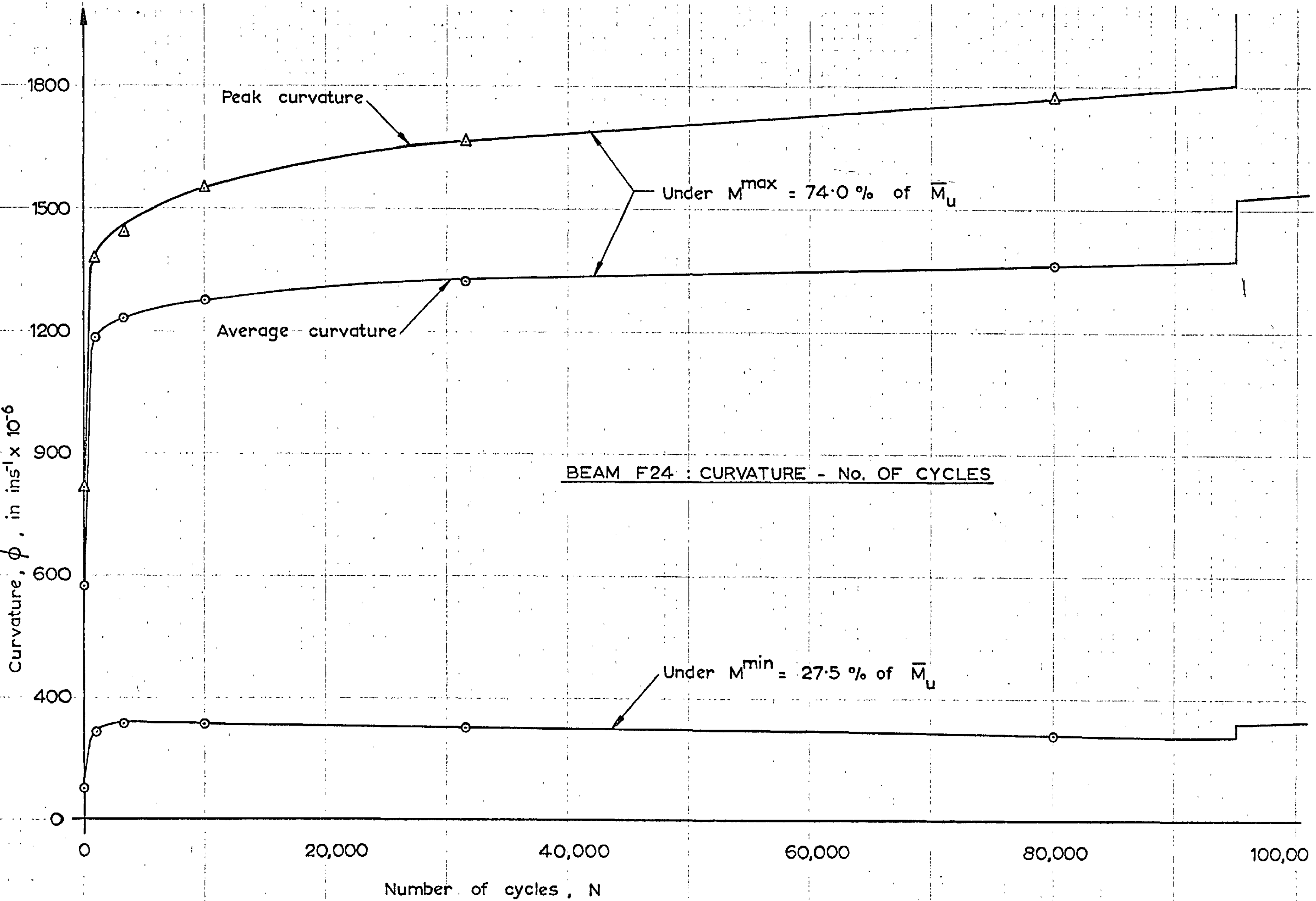
BEAM F24 : CURVATURE - No. OF CYCLES
Peak curvature
Average curvature
Under M^{max} = 74·0 % of $\overline{M}_u$
Under M^{min} = 27·5 % of $\overline{M}_u$
Curvature, ϕ, in $ins^{-1} \times 10^{-6}$
1800
1500
1200
900
600
400
0
Number of cycles, N
0
20,000
40,000
60,000
80,000
100,00
Fig. 4.24

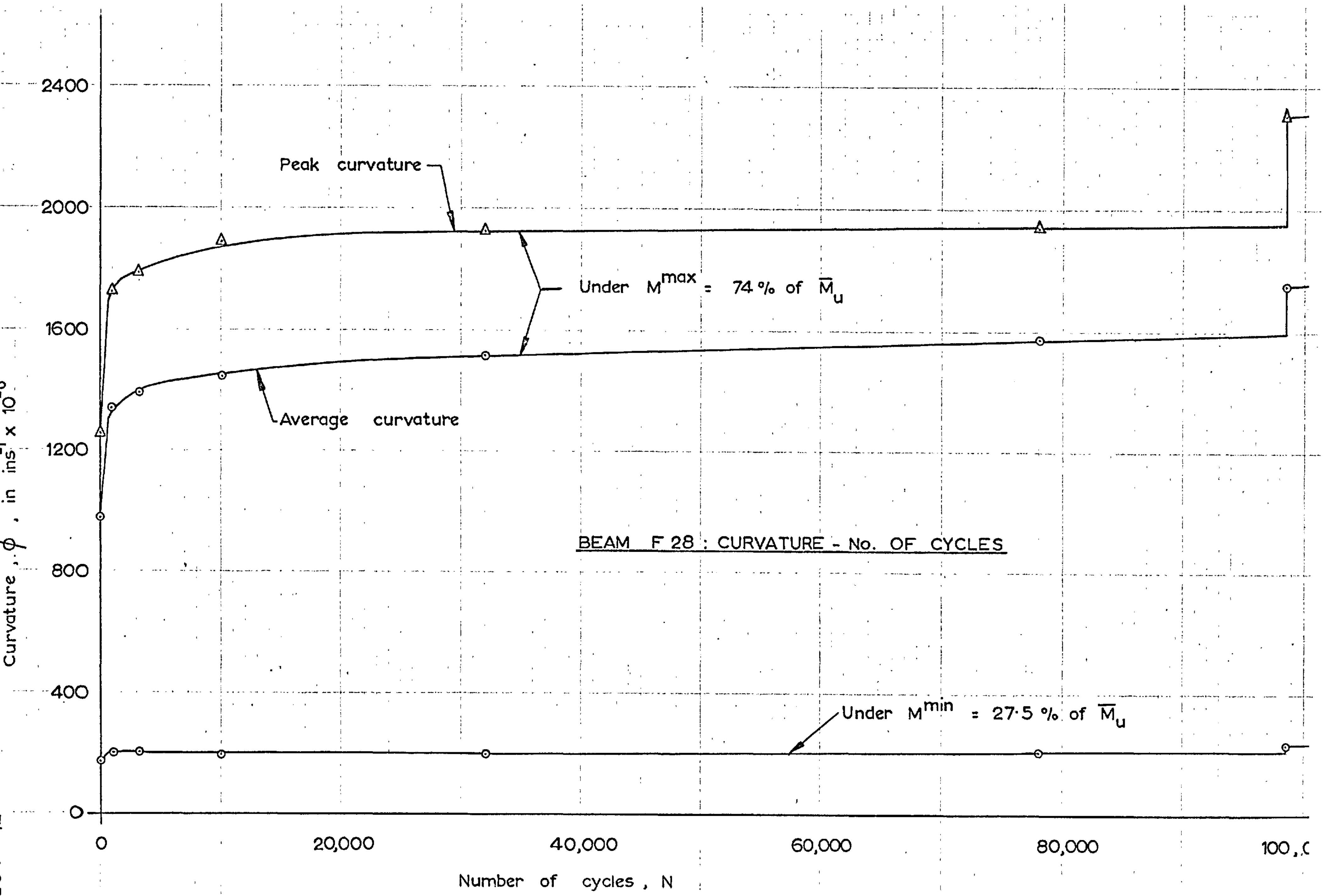
BEAM F 28 : CURVATURE - No. OF CYCLES
Peak curvature
Average curvature
Under M^max = 74 % of M̄u
Under M^min = 27·5 % of M̄u
Curvature, φ, in ins^-1 x 10^-6
Number of cycles, N
2400
2000
1600
1200
800
400
0
20,000
40,000
60,000
80,000
100,0

Fig. 4.25

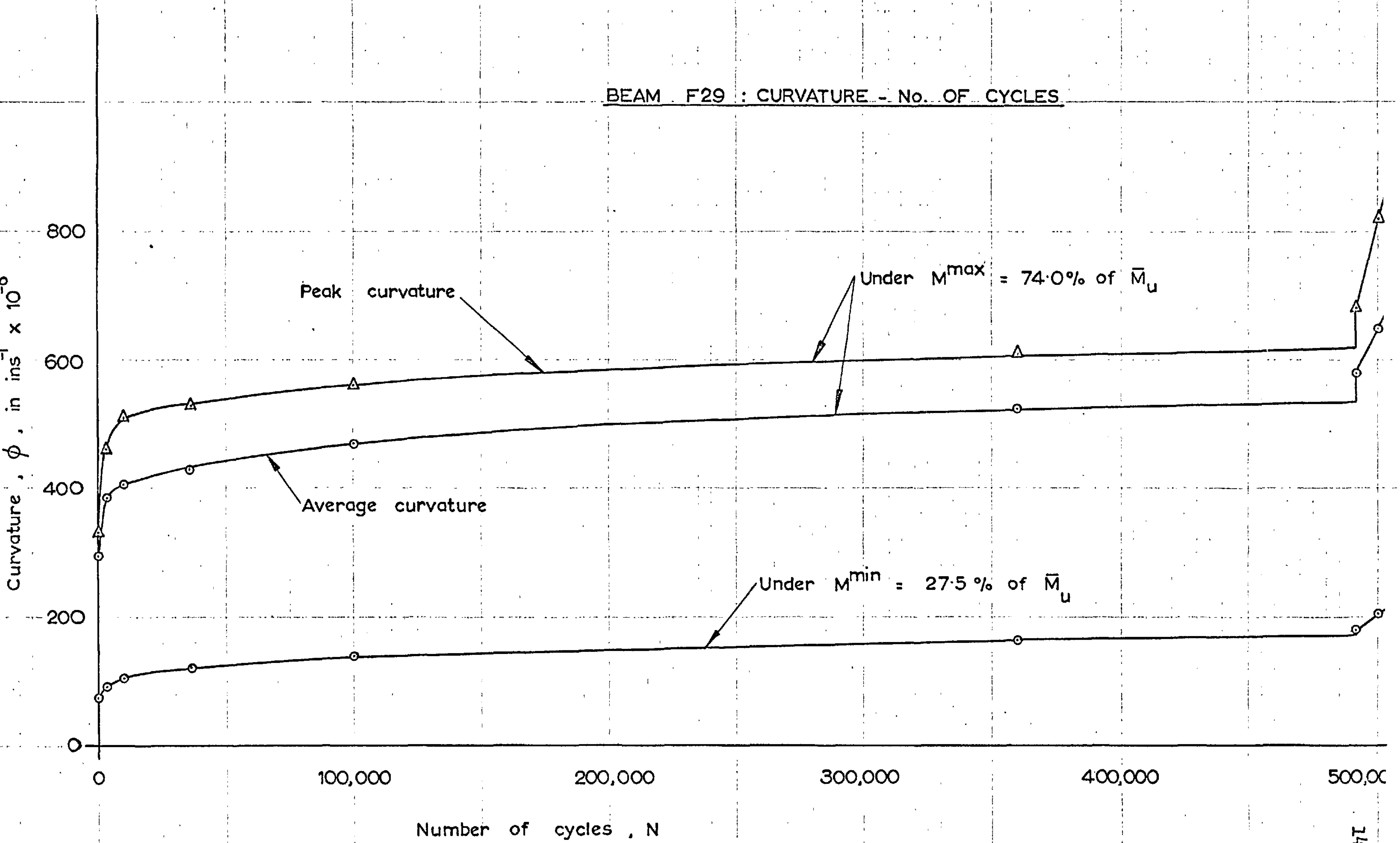
BEAM F29 : CURVATURE - No. OF CYCLES
Peak curvature
Average curvature
Under M^{max} = 74·0% of $\bar{M}_u$
Under M^{min} = 27·5 % of $\bar{M}_u$
Curvature , ϕ , in ins^{-1} x 10^{-6}
0
200
400
600
800
0
100,000
200,000
300,000
400,000
500,00
Number of cycles , N

Fig. 4.26

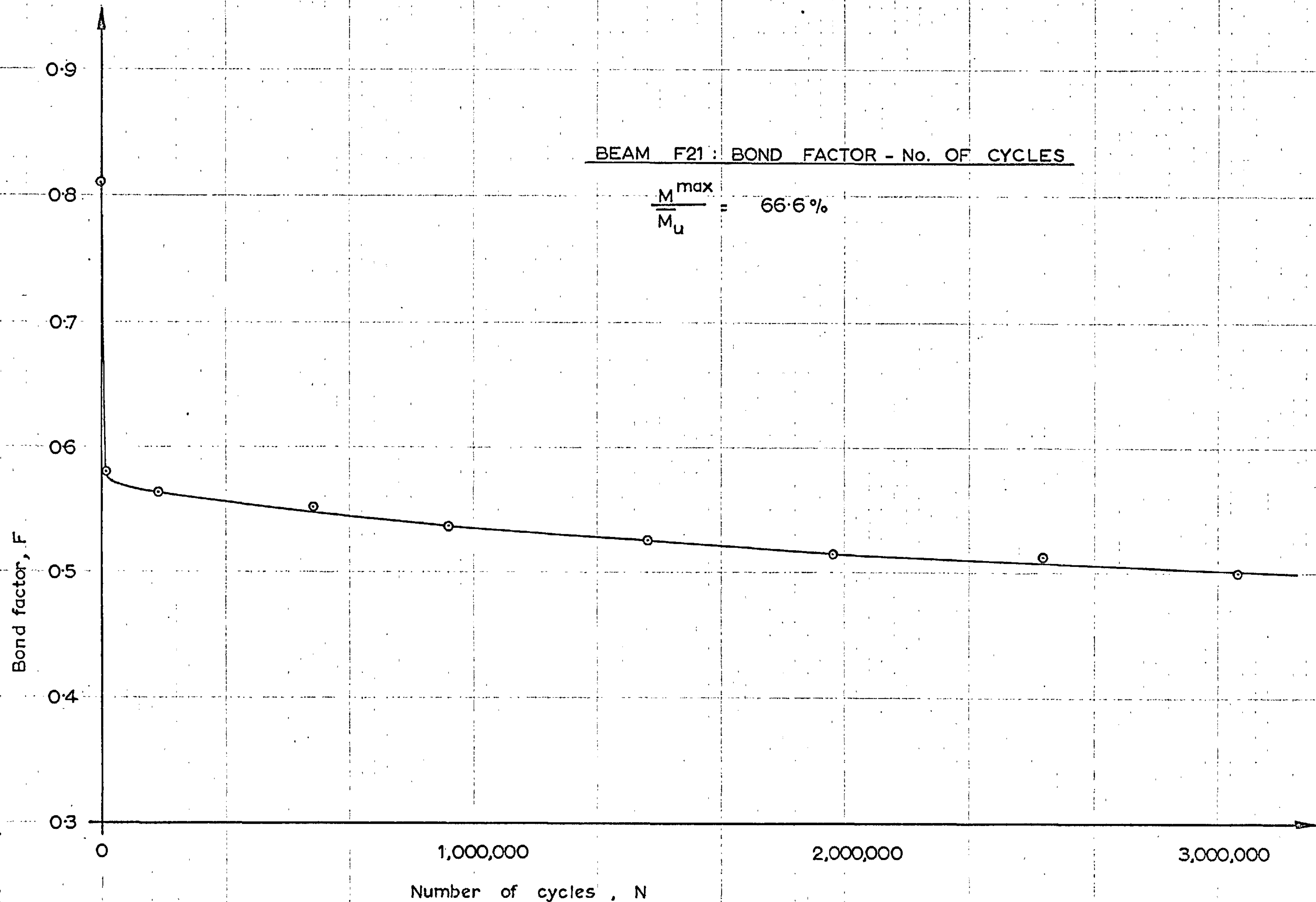
BEAM F21 : BOND FACTOR - No. OF CYCLES
$\frac{M^{max}}{M_u}$ = 66·6 %
0·9
0·8
0·7
0·6
0·5
0·4
0·3
Bond factor, F
0
1,000,000
2,000,000
3,000,000
Number of cycles , N

Fig. 4.27

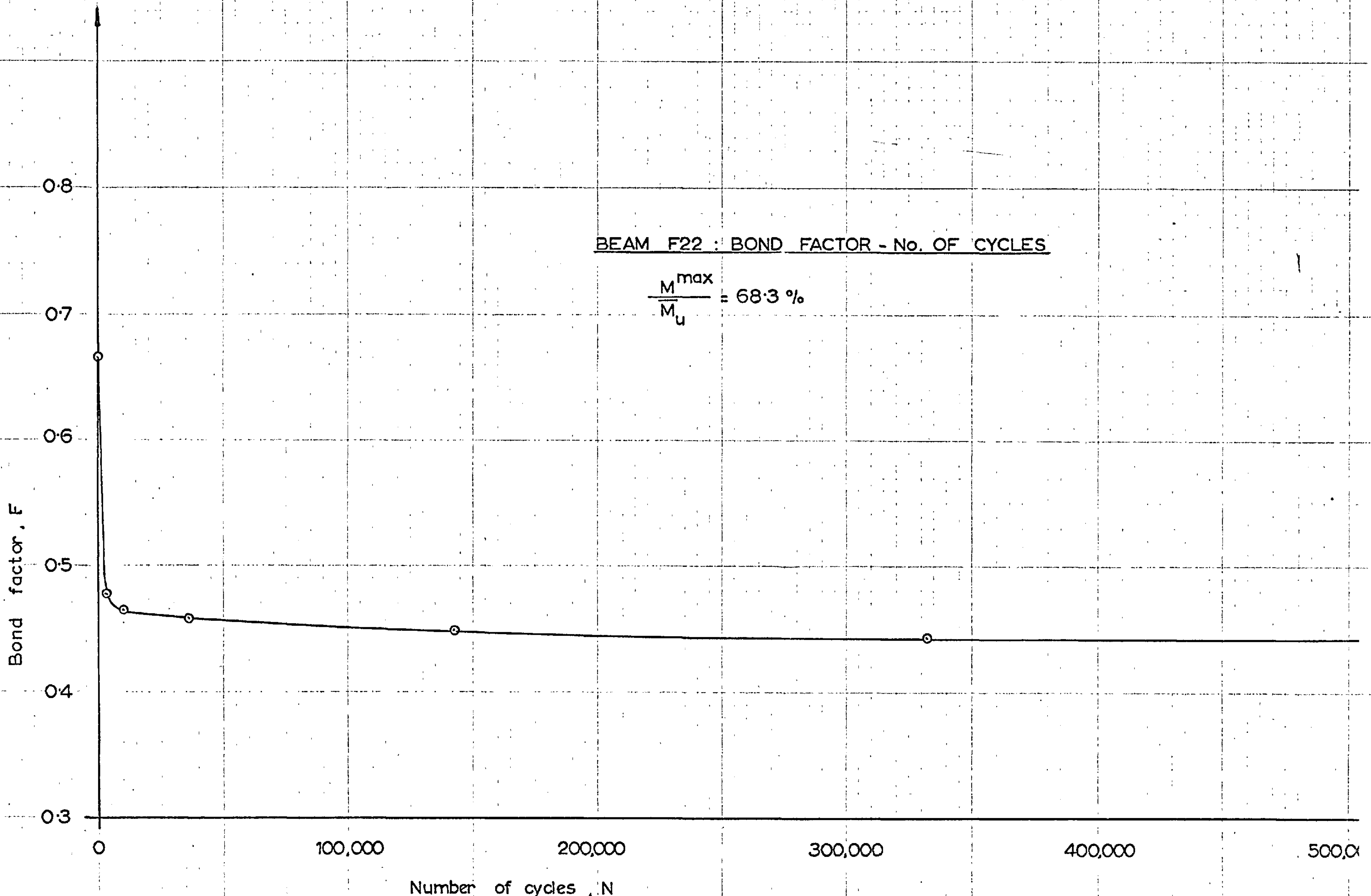
BEAM F22 : BOND FACTOR - No. OF CYCLES
$\frac{M^{max}}{\overline{M}_u} = 68{\cdot}3\ \%$
Bond factor, F
0·8
0·7
0·6
0·5
0·4
0·3
0
100,000
200,000
300,000
400,000
500,0
Number of cycles, N

Fig. 4.28

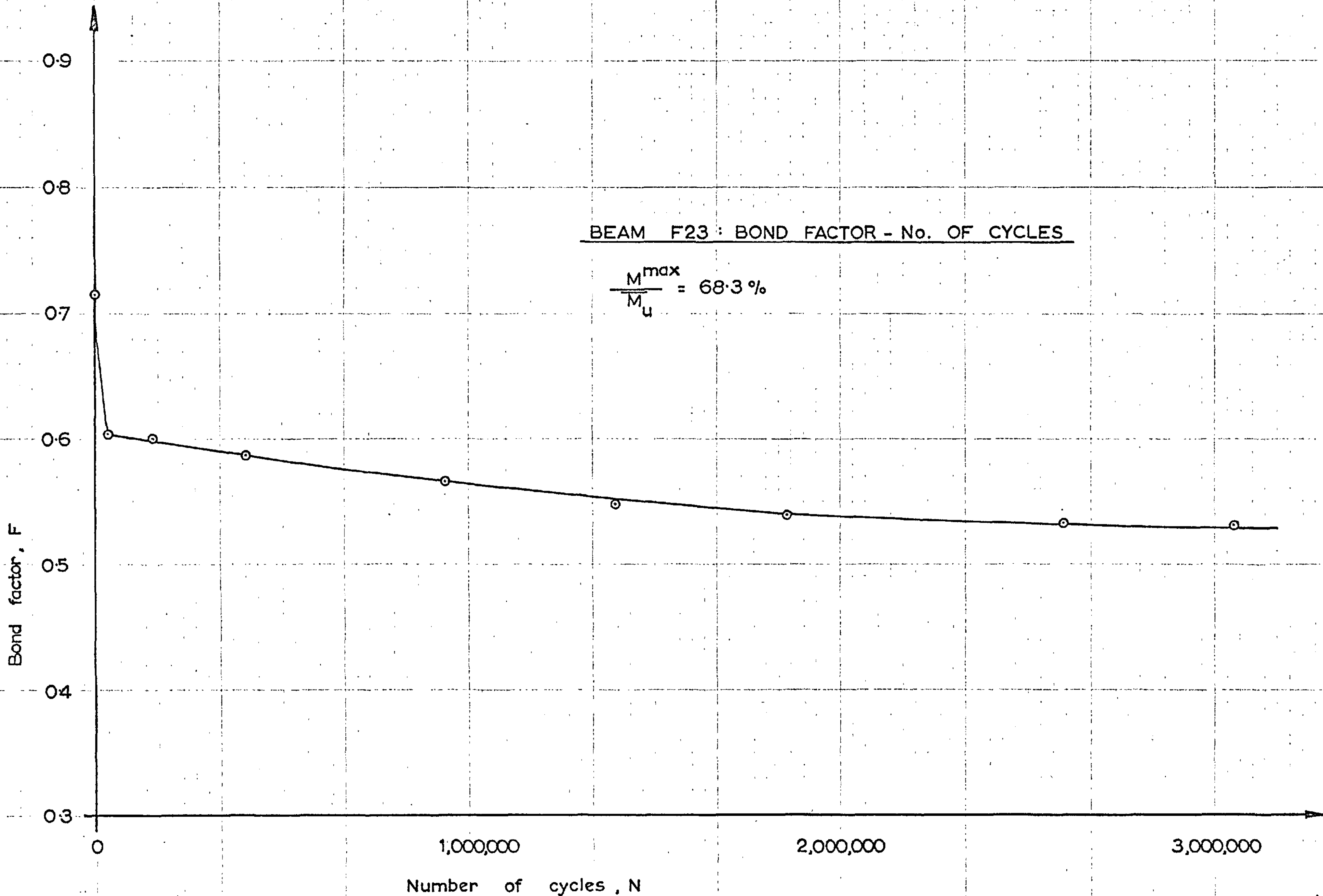
BEAM F23 : BOND FACTOR - No. OF CYCLES
$\frac{M^{max}}{M_u}$ = 68·3 %
0·9
0·8
0·7
0·6
0·5
0·4
0·3
Bond factor, F
0
1,000,000
2,000,000
3,000,000
Number of cycles , N

Fig. 4.29

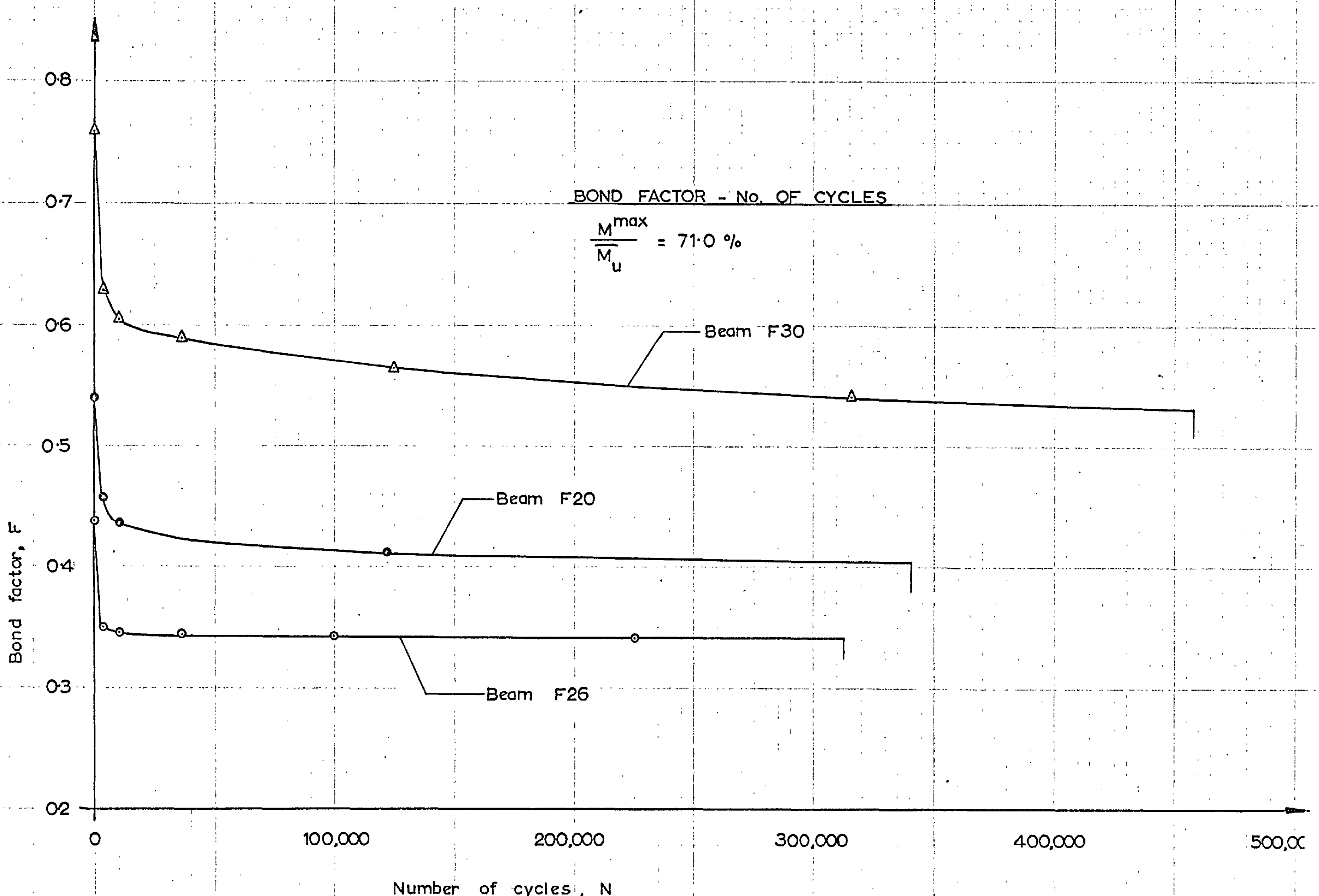

BOND FACTOR - No. OF CYCLES
$\frac{M^{max}}{M_u} = 71{\cdot}0\ \%$
Beam F30
Beam F20
Beam F26
0·8
0·7
0·6
0·5
0·4
0·3
0·2
Bond factor, F
0
100,000
200,000
300,000
400,000
500,0C
Number of cycles, N

Fig. 4.30

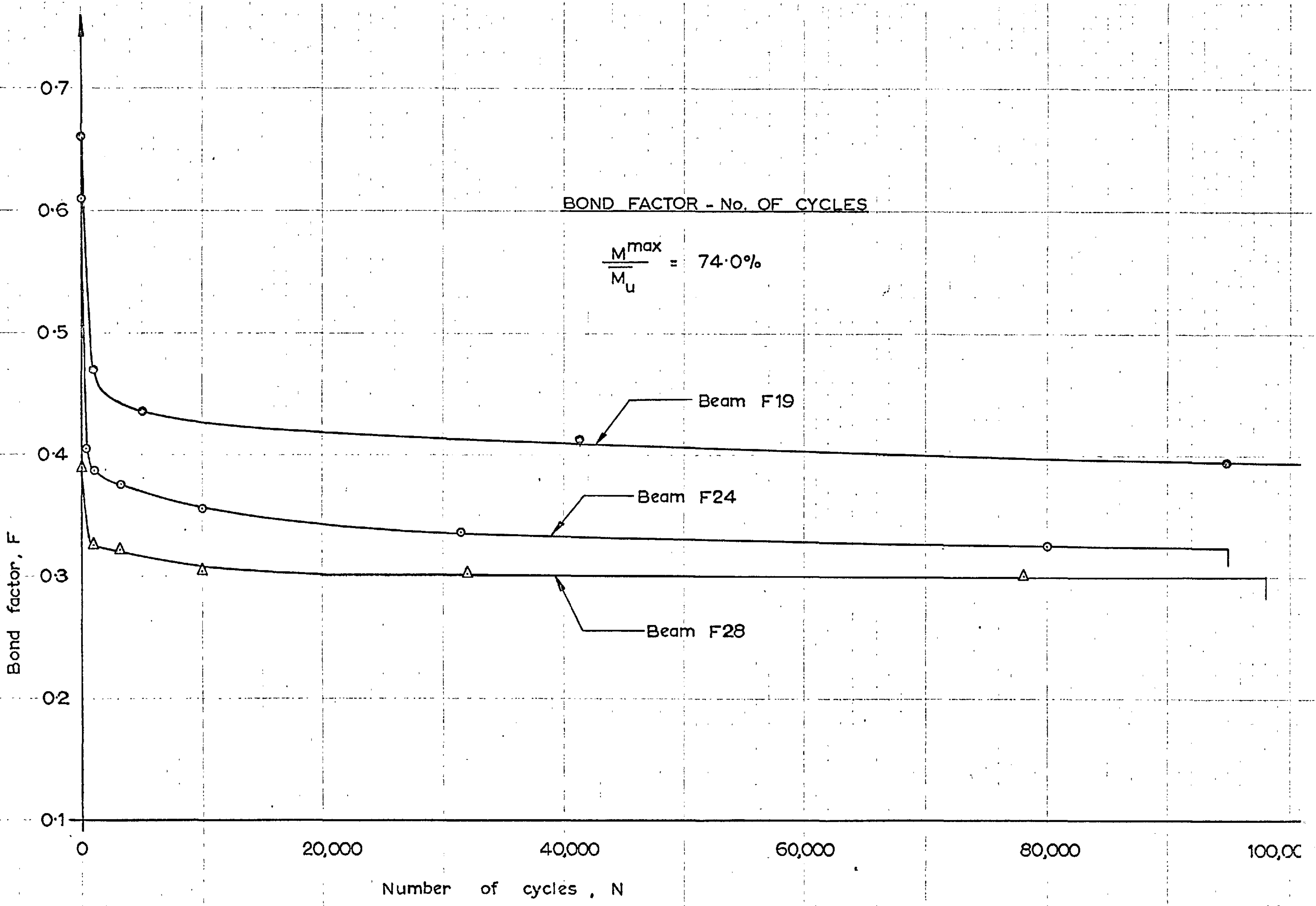
BOND FACTOR - No. OF CYCLES
$\frac{M^{max}}{M_u}$ = 74·0%
Beam F19
Beam F24
Beam F28
Bond factor, F
0·7
0·6
0·5
0·4
0·3
0·2
0·1
0
20,000
40,000
60,000
80,000
100,00
Number of cycles, N

Fig. 4.31

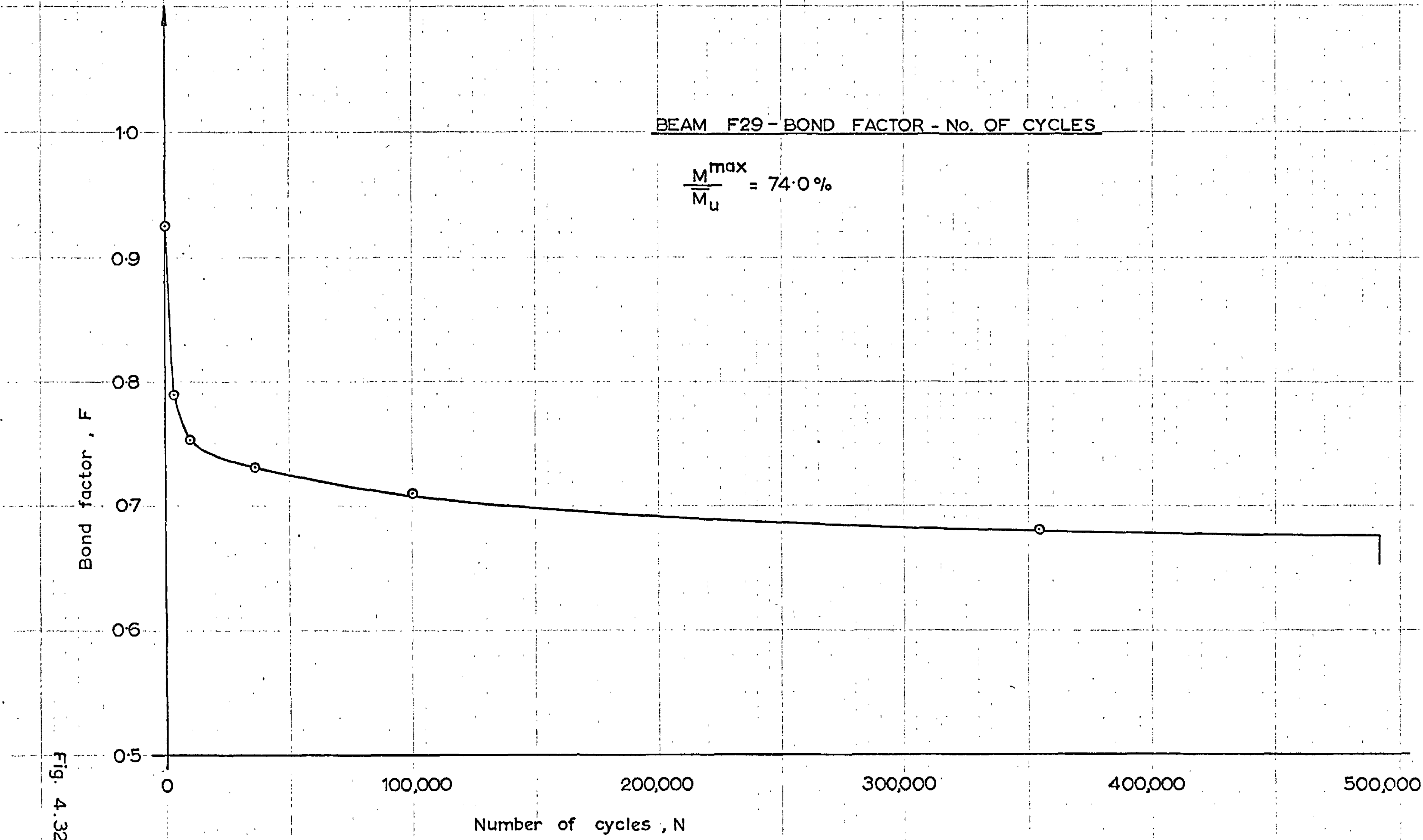
BEAM F29 - BOND FACTOR - No. OF CYCLES
$\frac{M^{max}}{M_u}$ = 74·0 %
1·0
0·9
0·8
0·7
0·6
0·5
Bond factor , F
0
100,000
200,000
300,000
400,000
500,000
Number of cycles , N

Fig. 4.32

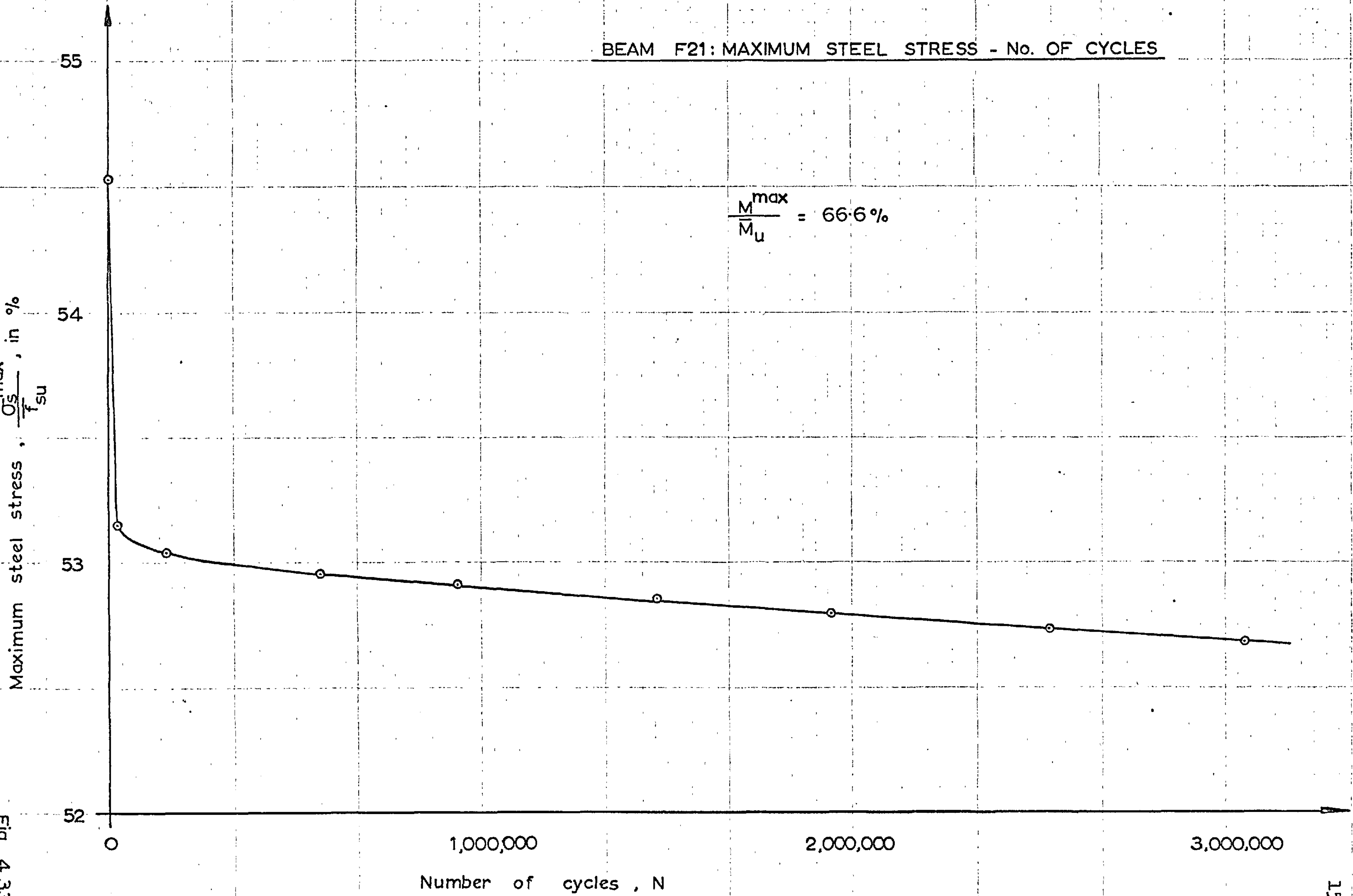
BEAM F21: MAXIMUM STEEL STRESS - No. OF CYCLES
$\frac{M^{max}}{\bar{M}_u}$ = 66·6 %
Maximum steel stress, $\frac{\sigma_s^{max}}{f_{su}}$, in %
55
54
53
52
0
1,000,000
2,000,000
3,000,000
Number of cycles, N

Fig. 4.33

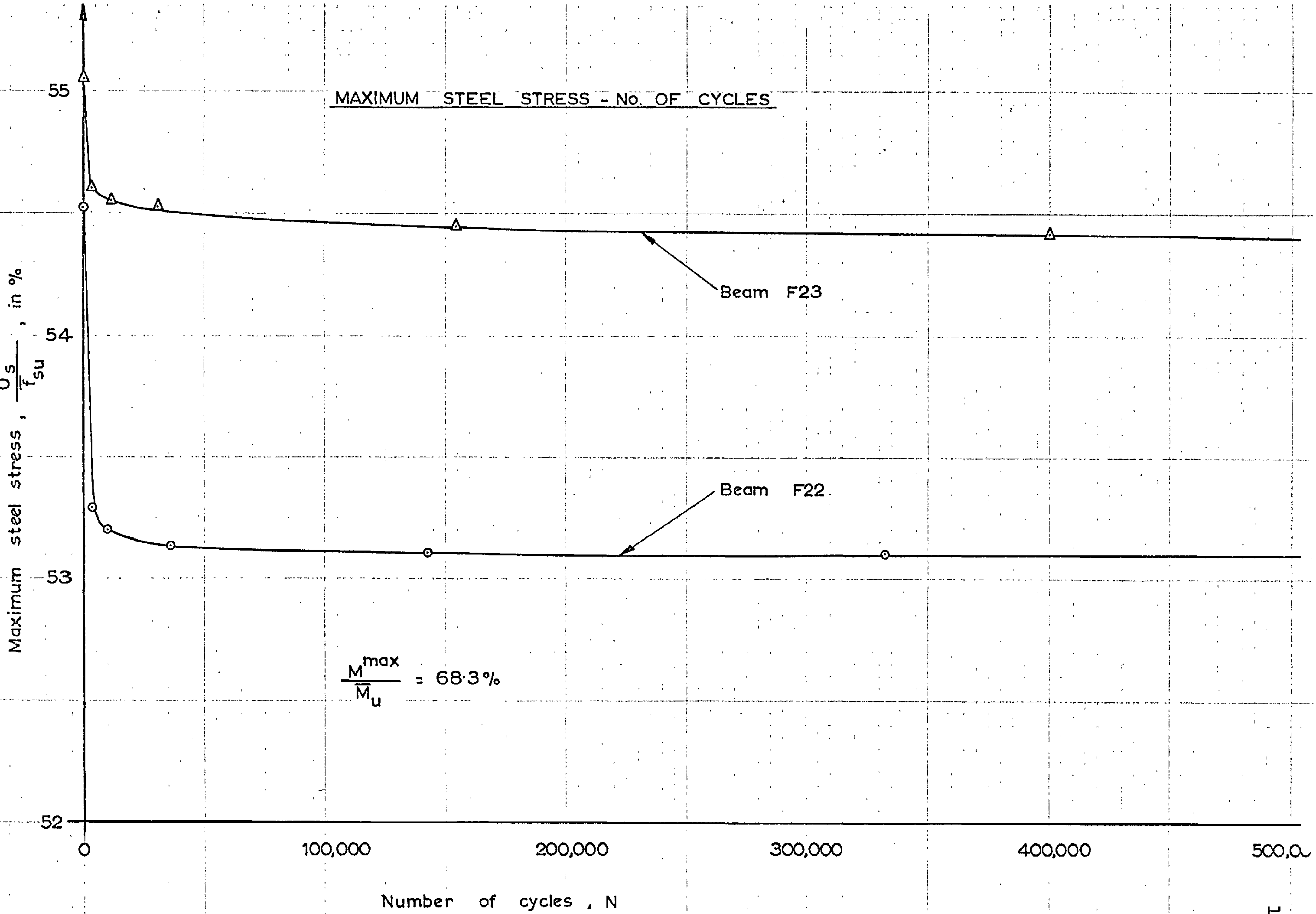
MAXIMUM STEEL STRESS - No. OF CYCLES
Maximum steel stress, $\frac{\sigma_s^{max}}{f_{su}}$, in %
55
54
53
52
Beam F23
Beam F22
$\frac{M^{max}}{\overline{M}_u} = 68{\cdot}3\%$
0
100,000
200,000
300,000
400,000
500,0
Number of cycles, N

Fig. 4.34

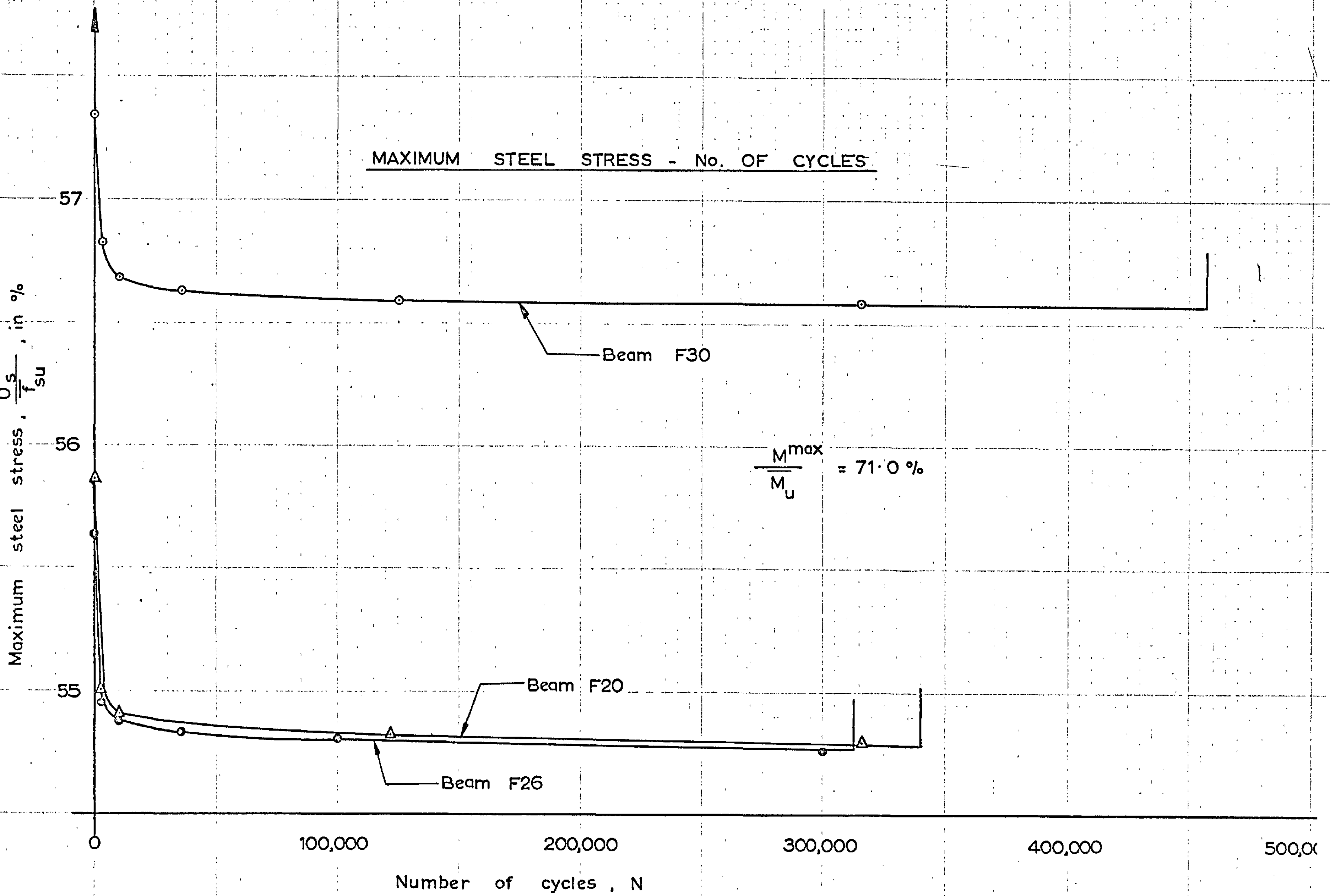
MAXIMUM STEEL STRESS - No. OF CYCLES
$\frac{M^{max}}{M_u} = 71 \cdot 0\ \%$
Beam F30
Beam F20
Beam F26
57
56
55
0
100,000
200,000
300,000
400,000
500,00
Number of cycles , N
Maximum steel stress , $\frac{\sigma_s^{max}}{f_{su}}$, in %

Fig. 4.35

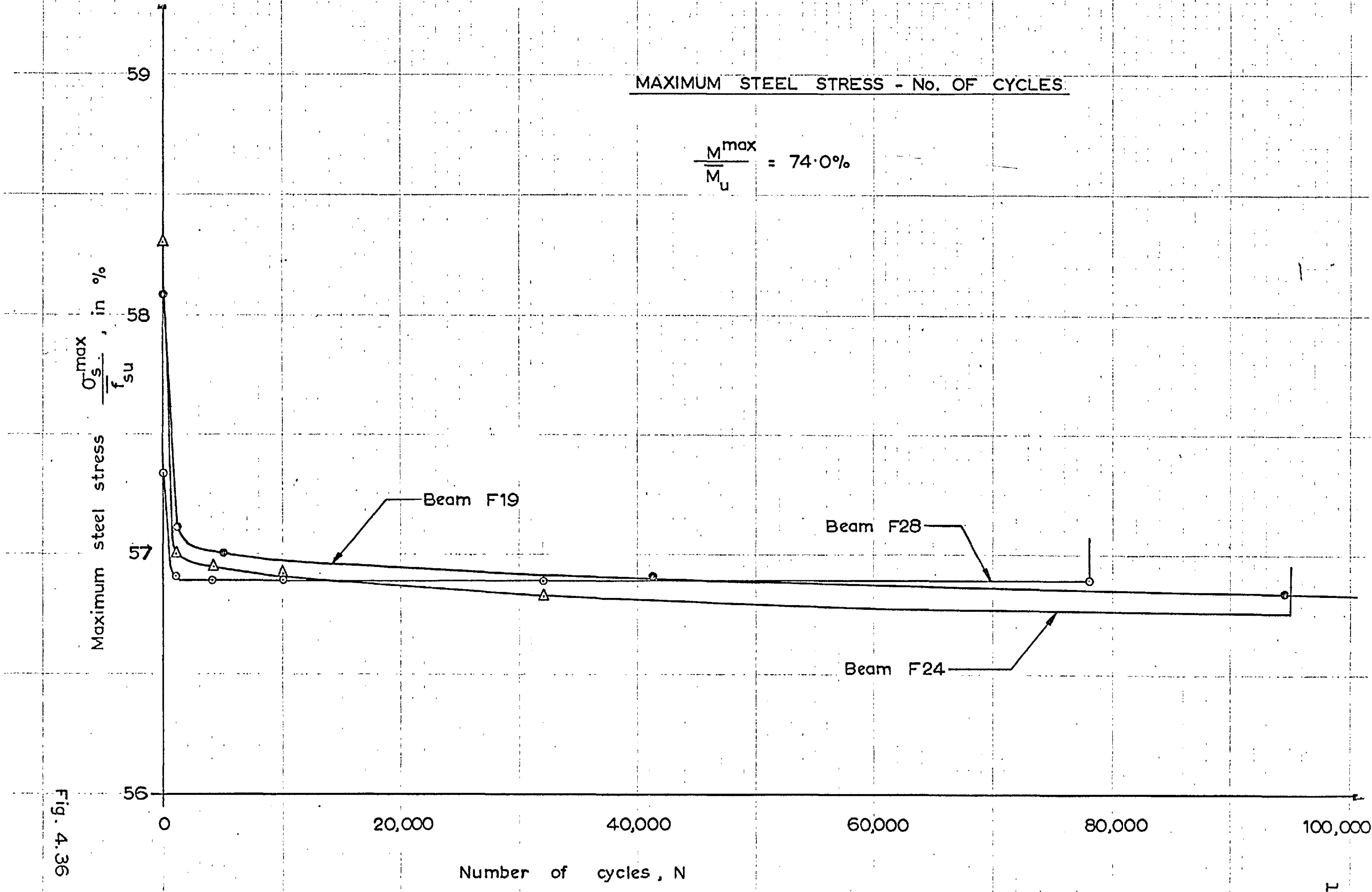
MAXIMUM STEEL STRESS - No. OF CYCLES
$\frac{M^{max}}{M_u}$ = 74·0%
59
58
57
56
Maximum steel stress $\frac{\sigma_s^{max}}{f_{su}}$, in %
Beam F19
Beam F28
Beam F24
0
20,000
40,000
60,000
80,000
100,000
Number of cycles, N

Fig. 4.36

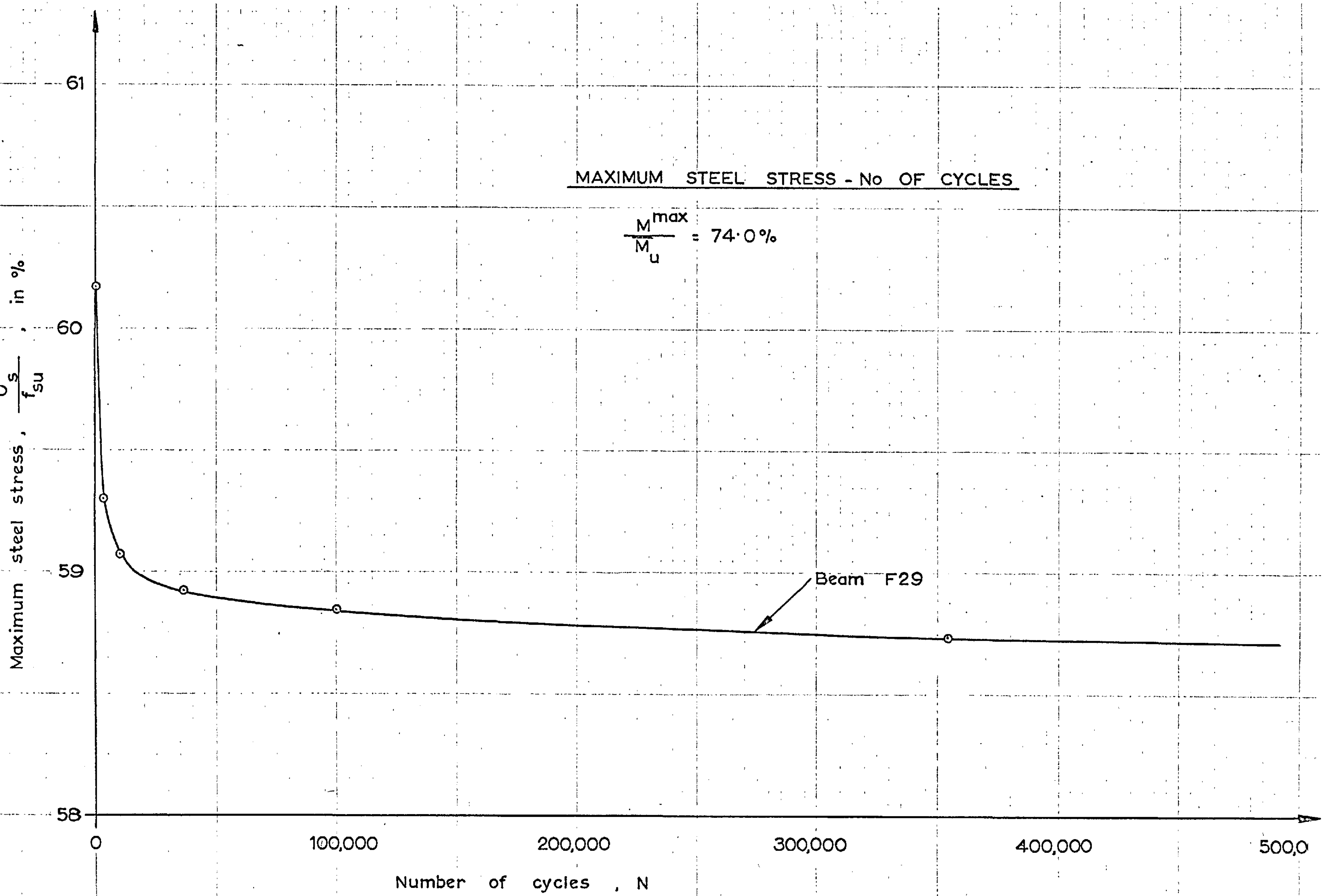

MAXIMUM STEEL STRESS - No OF CYCLES
$\frac{M^{max}}{M_u} = 74{\cdot}0\%$
Beam F29
61
60
59
58
Maximum steel stress, $\frac{\sigma_s^{max}}{f_{su}}$, in %
0
100,000
200,000
300,000
400,000
500,0
Number of cycles , N

Fig. 4.37

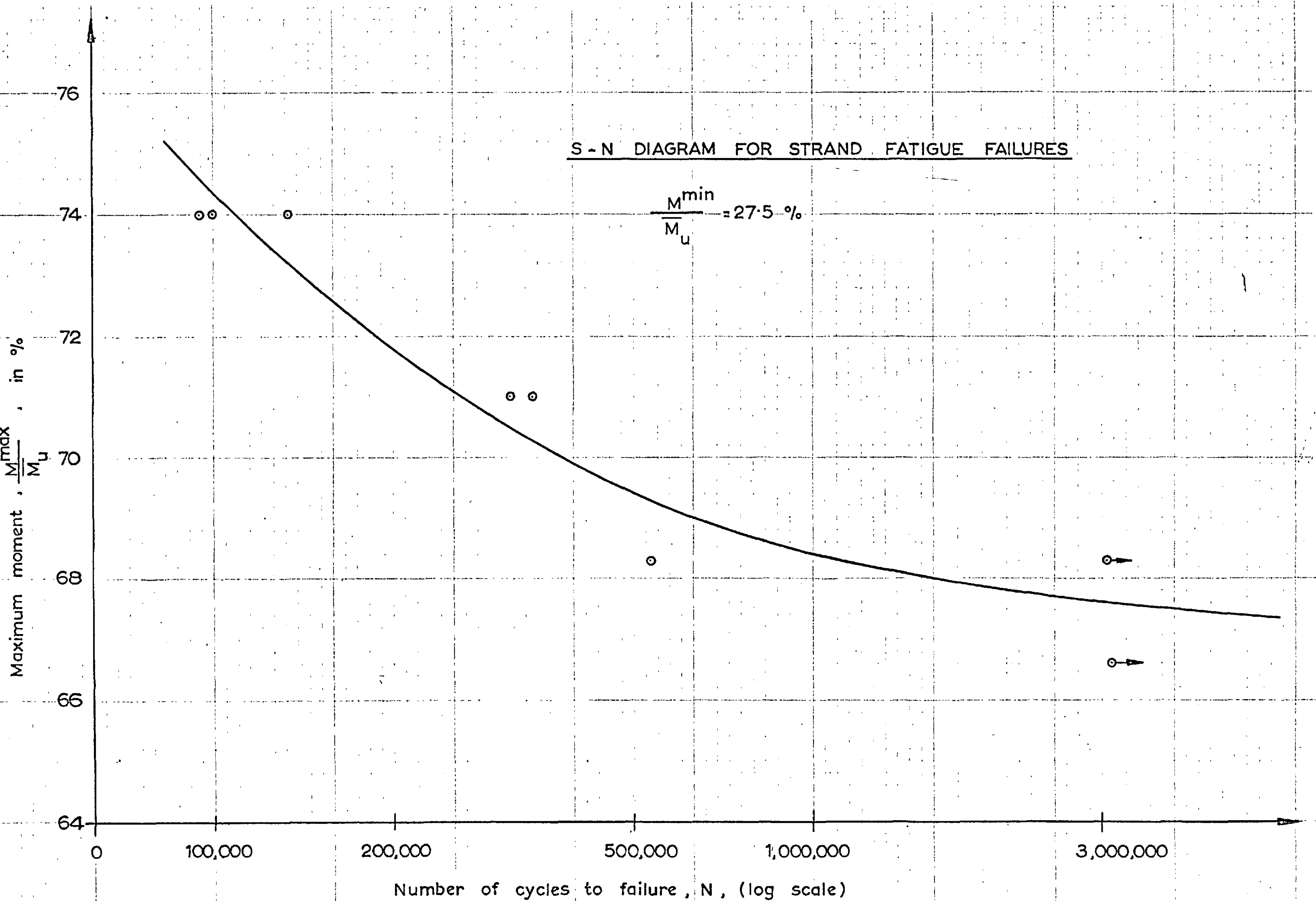

S - N DIAGRAM FOR STRAND FATIGUE FAILURES
$\frac{M^{min}}{M_u} = 27{\cdot}5\ \%$
Maximum moment , $\frac{M^{max}}{M_u}$, in %
76
74
72
70
68
66
64
0
100,000
200,000
500,000
1,000,000
3,000,000
Number of cycles to failure , N , (log scale)

Fig. 4.38

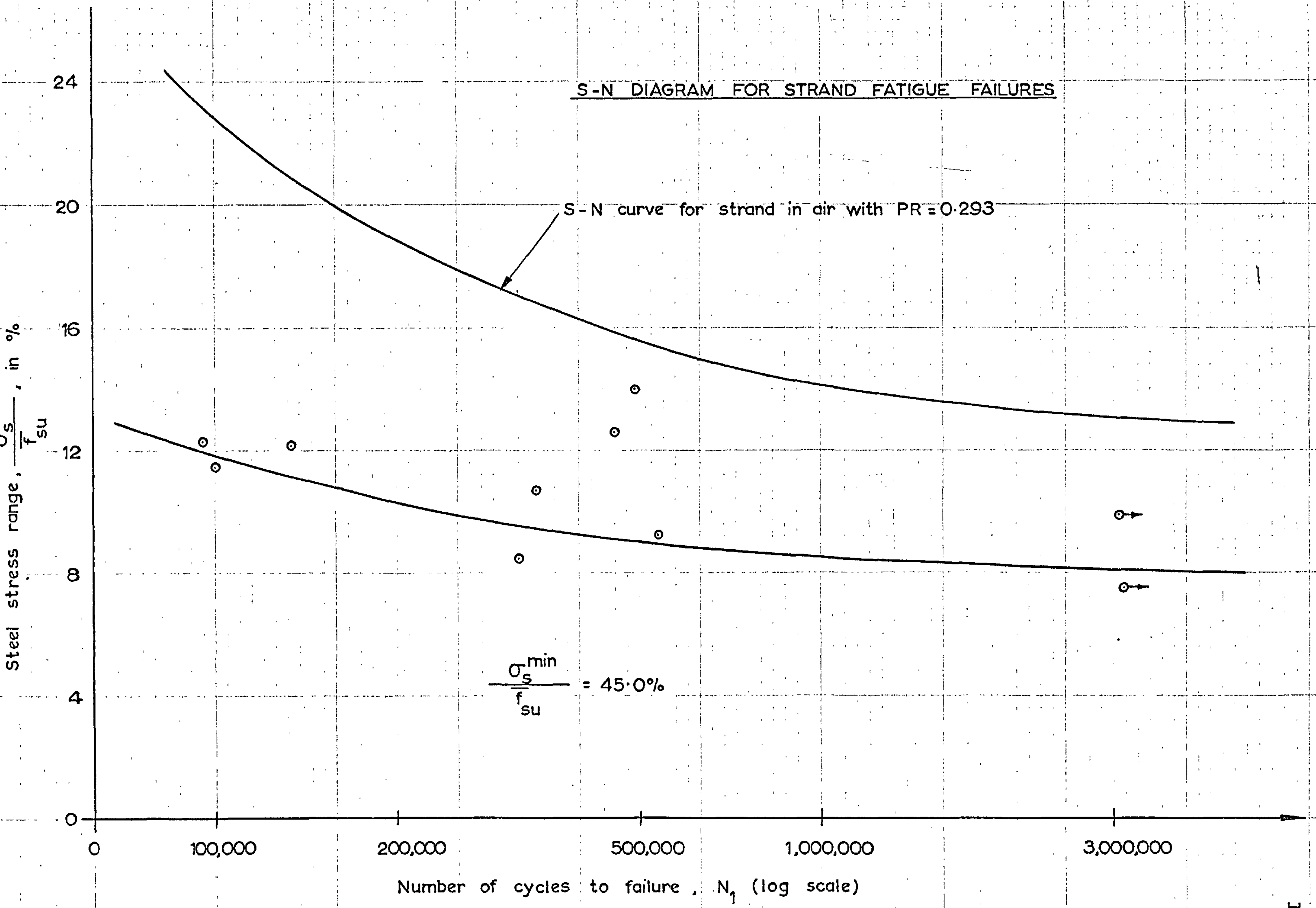
S-N DIAGRAM FOR STRAND FATIGUE FAILURES
S-N curve for strand in air with PR = 0·293
$\frac{\sigma_s^{min}}{f_{su}}$ = 45·0%
Steel stress range, $\frac{\sigma_s^r}{f_{su}}$, in %
24
20
16
12
8
4
0
0
100,000
200,000
500,000
1,000,000
3,000,000
Number of cycles to failure, N_1 (log scale)

Fig. 4.39

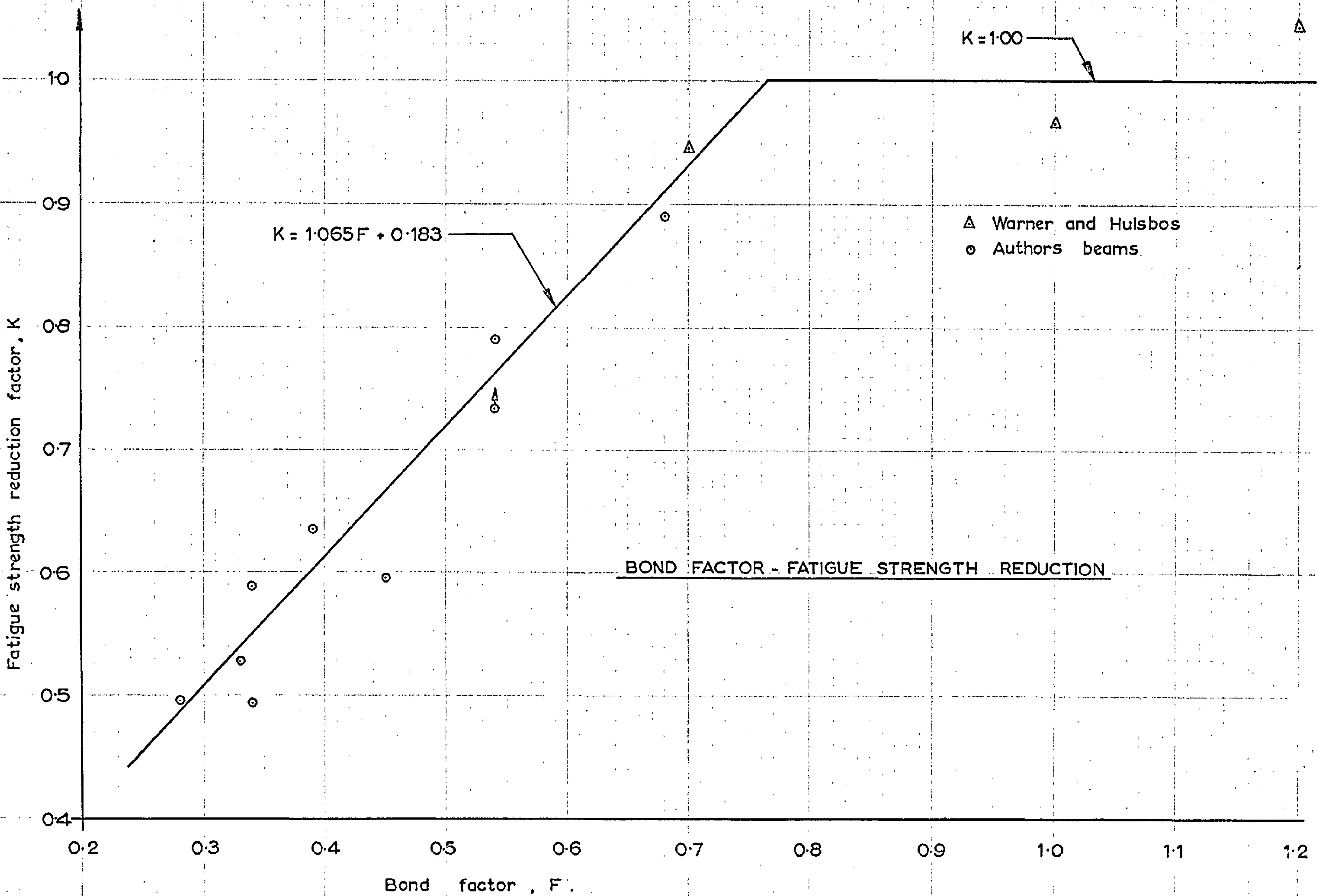
K = 1·00
K = 1·065F + 0·183
Warner and Hulsbos
Authors beams
BOND FACTOR - FATIGUE STRENGTH REDUCTION
Fatigue strength reduction factor, K
1·0
0·9
0·8
0·7
0·6
0·5
0·4
0·2
0·3
0·4
0·5
0·6
0·7
0·8
0·9
1·0
1·1
1·2
Bond factor, F.

Fig. 4.40

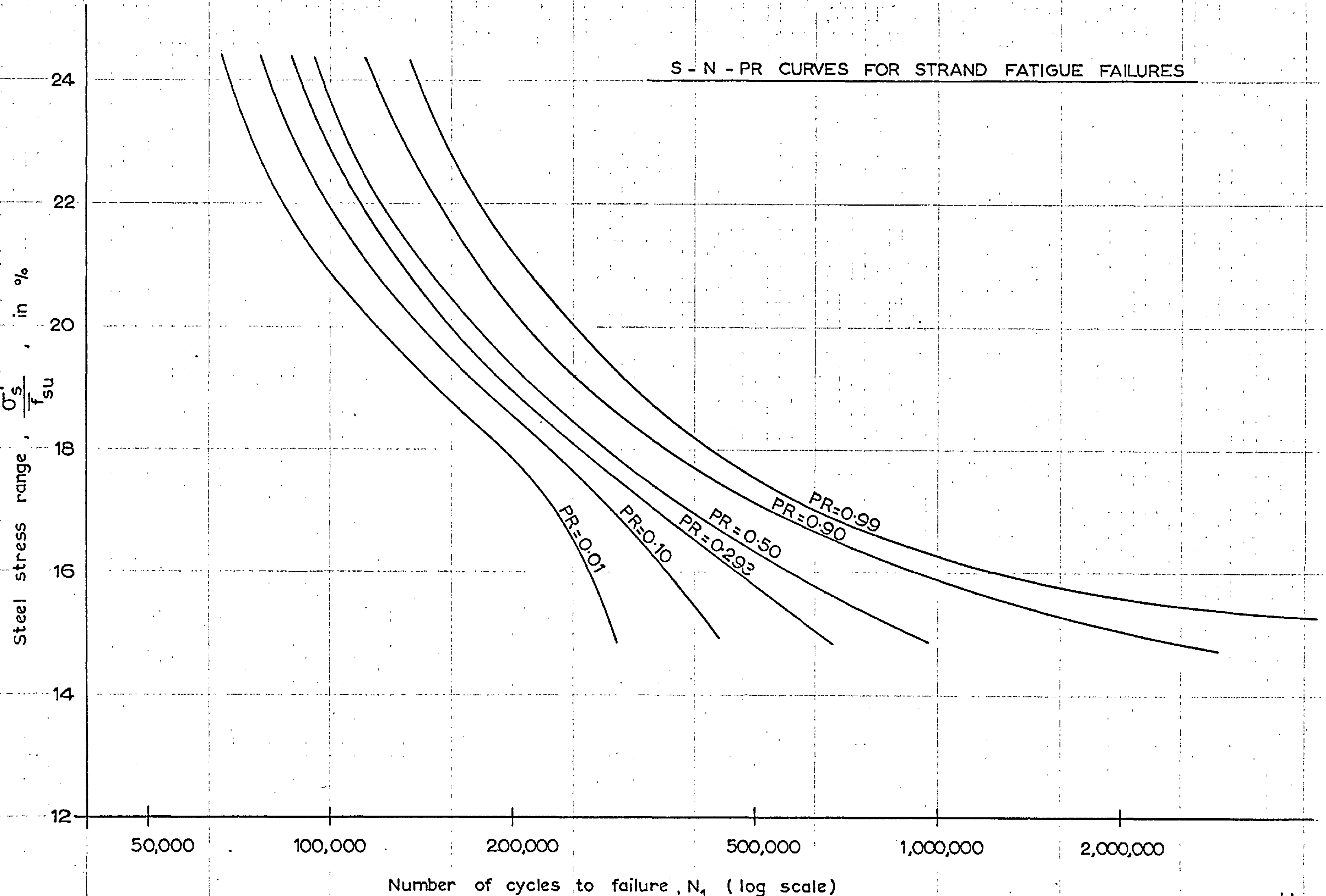
S - N - PR CURVES FOR STRAND FATIGUE FAILURES
Steel stress range , $\frac{\sigma_s^r}{f_{su}}$, in %
24
22
20
18
16
14
12
PR=0·01
PR=0·10
PR=0·293
PR=0·50
PR=0·90
PR=0·99
50,000
100,000
200,000
500,000
1,000,000
2,000,000
Number of cycles to failure , N_1 (log scale)

Fig. 4.41

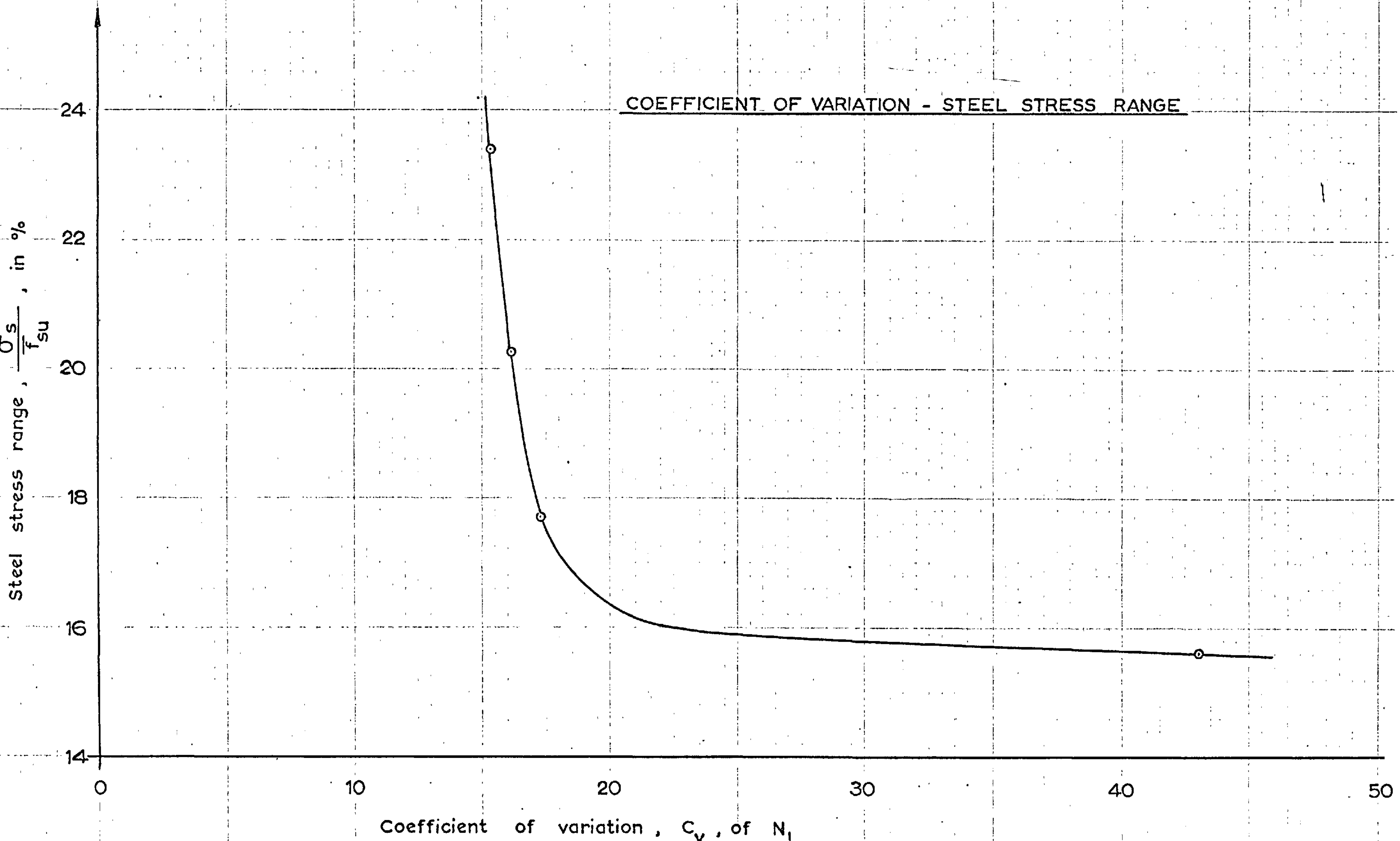
COEFFICIENT OF VARIATION - STEEL STRESS RANGE
Steel stress range , $\frac{\sigma_s^r}{f_{su}}$, in %
24
22
20
18
16
14
0
10
20
30
40
50
Coefficient of variation , C_v , of N_1

Fig. 4.42

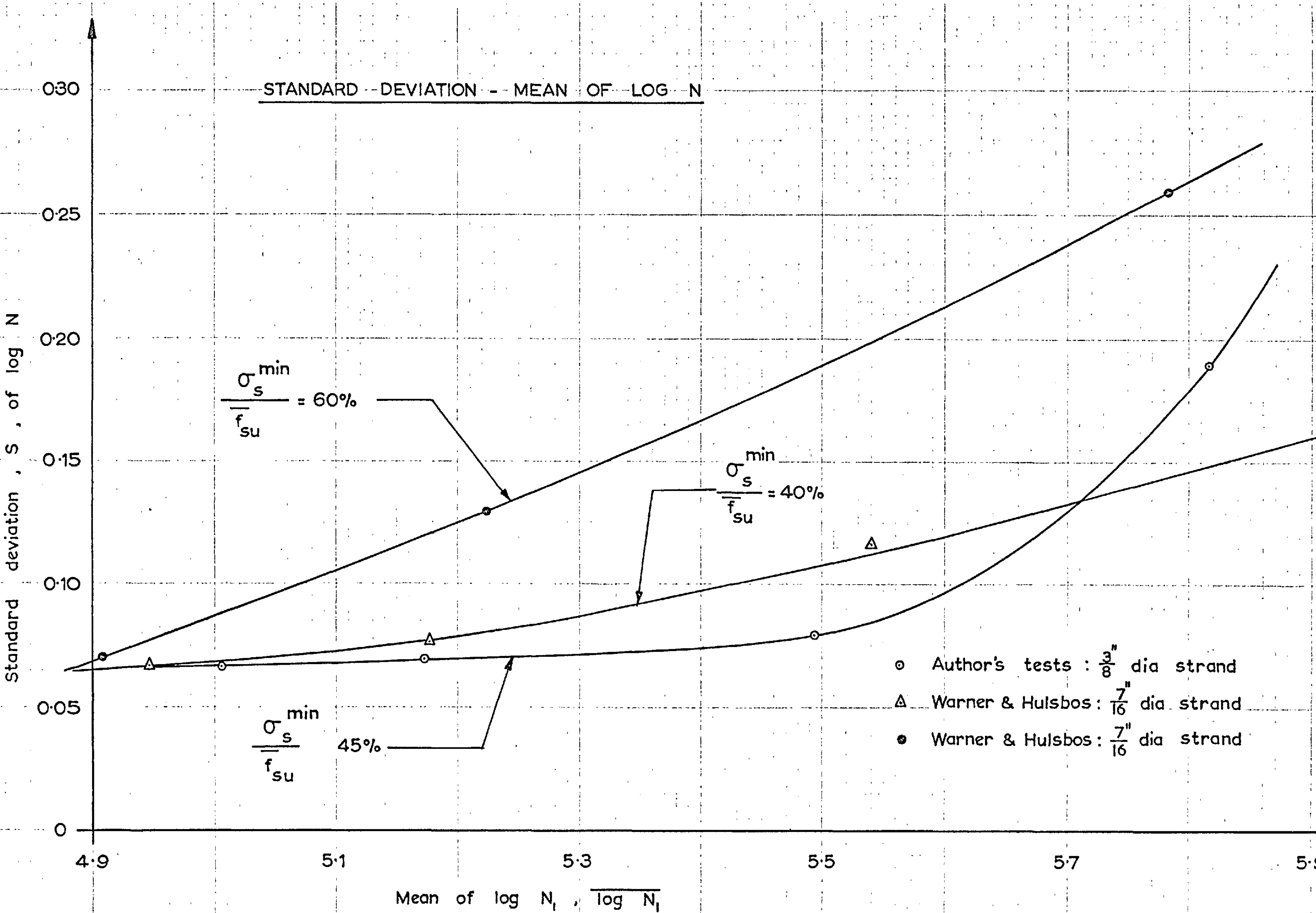

STANDARD DEVIATION - MEAN OF LOG N
Standard deviation, S, of log N
0·30
0·25
0·20
0·15
0·10
0·05
0
4·9
5·1
5·3
5·5
5·7
5·9
Mean of log N_1, $\overline{\log N_1}$
$\frac{\sigma_s^{min}}{\overline{f}_{su}}$ = 60%
$\frac{\sigma_s^{min}}{\overline{f}_{su}}$ = 40%
$\frac{\sigma_s^{min}}{\overline{f}_{su}}$ 45%
Author's tests : $\frac{3}{8}''$ dia strand
Warner & Hulsbos : $\frac{7}{16}''$ dia strand
Warner & Hulsbos : $\frac{7}{16}''$ dia strand

Fig. 4.43

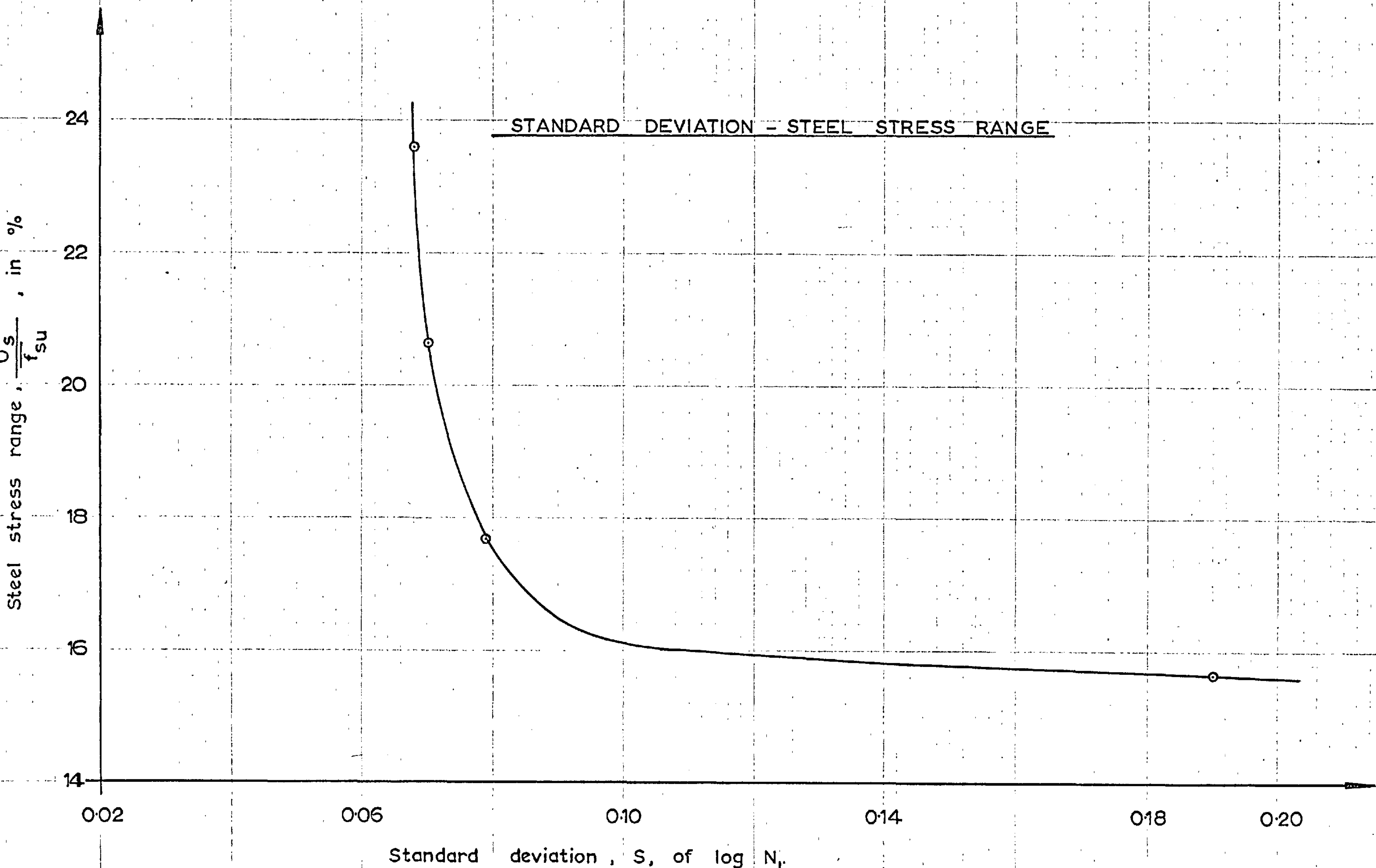
STANDARD DEVIATION - STEEL STRESS RANGE
Steel stress range, $\frac{\sigma_s^r}{f_{su}}$, in %
24
22
20
18
16
14
0·02
0·06
0·10
0·14
0·18
0·20
Standard deviation, S, of log N_1.

Fig. 4.44

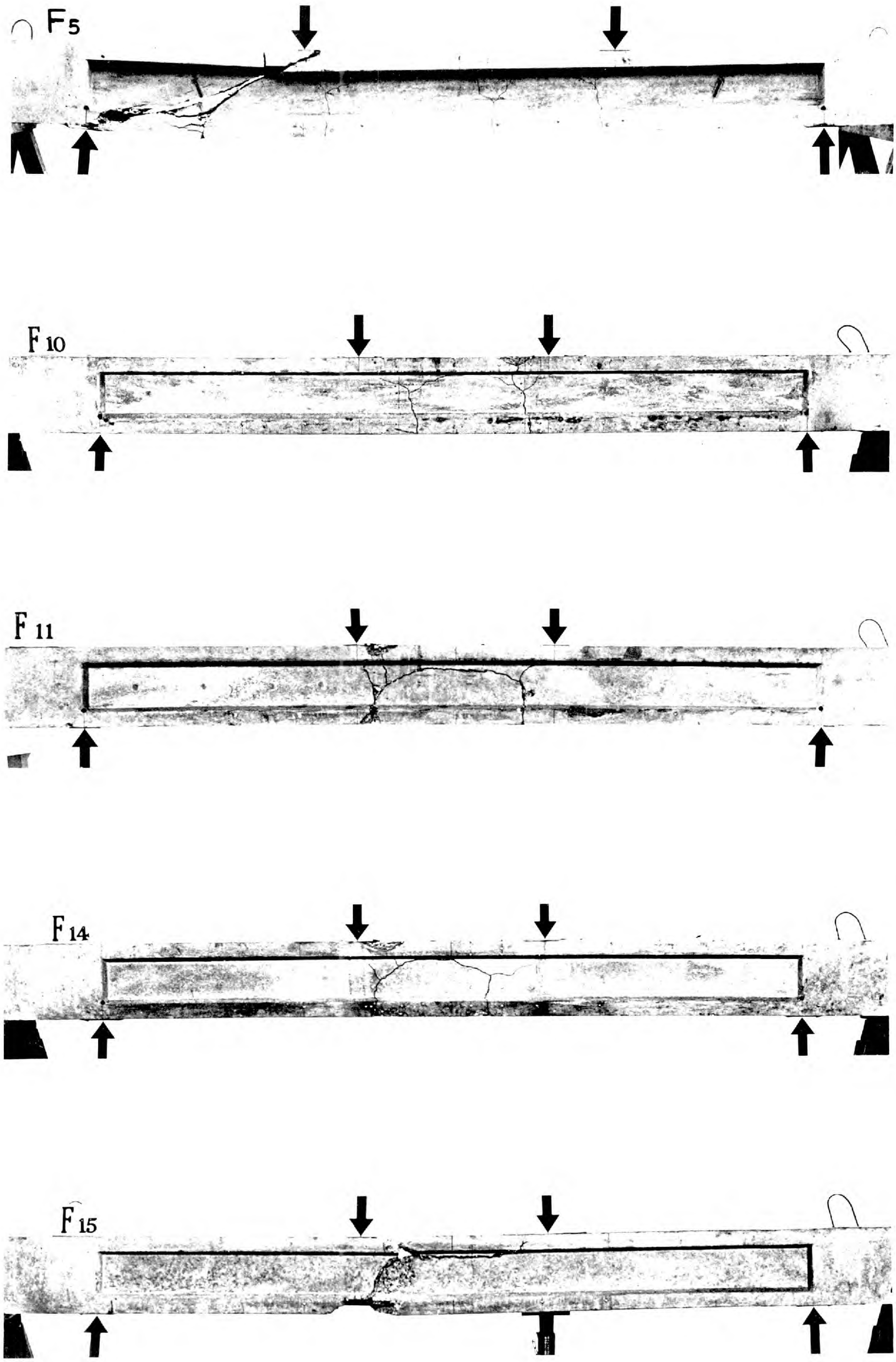

PLATE 4.1

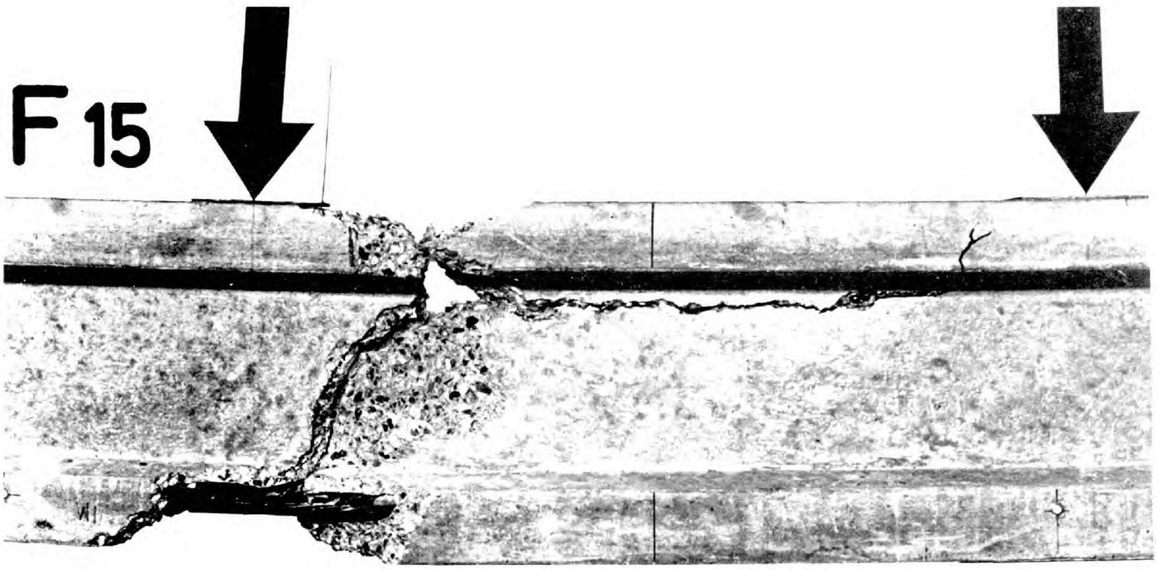

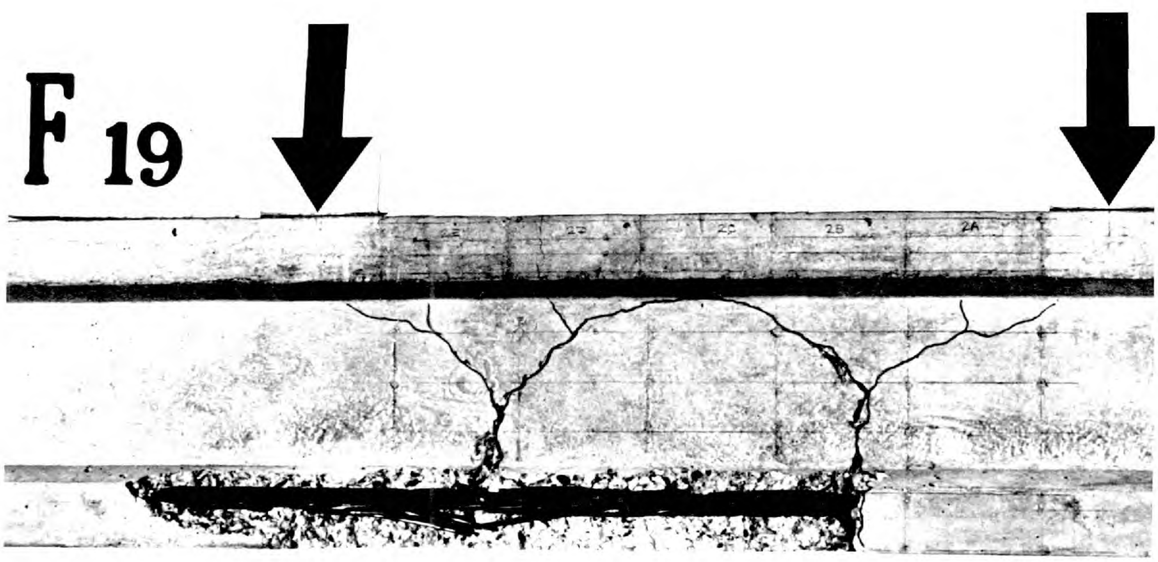

CLOSE-UP OF FAILURE SECTIONS

PLATE 4.2

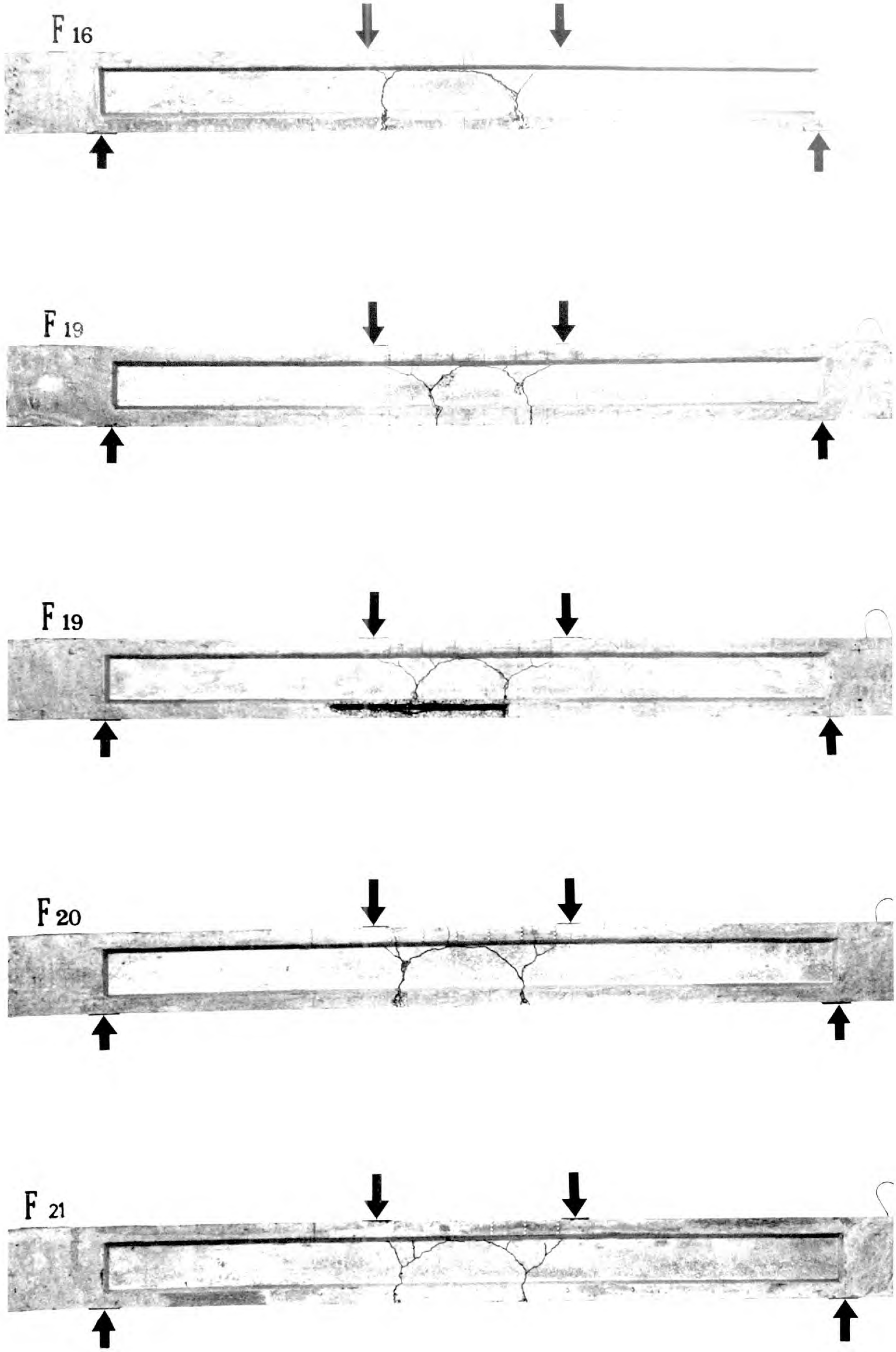

PLATE 4.3

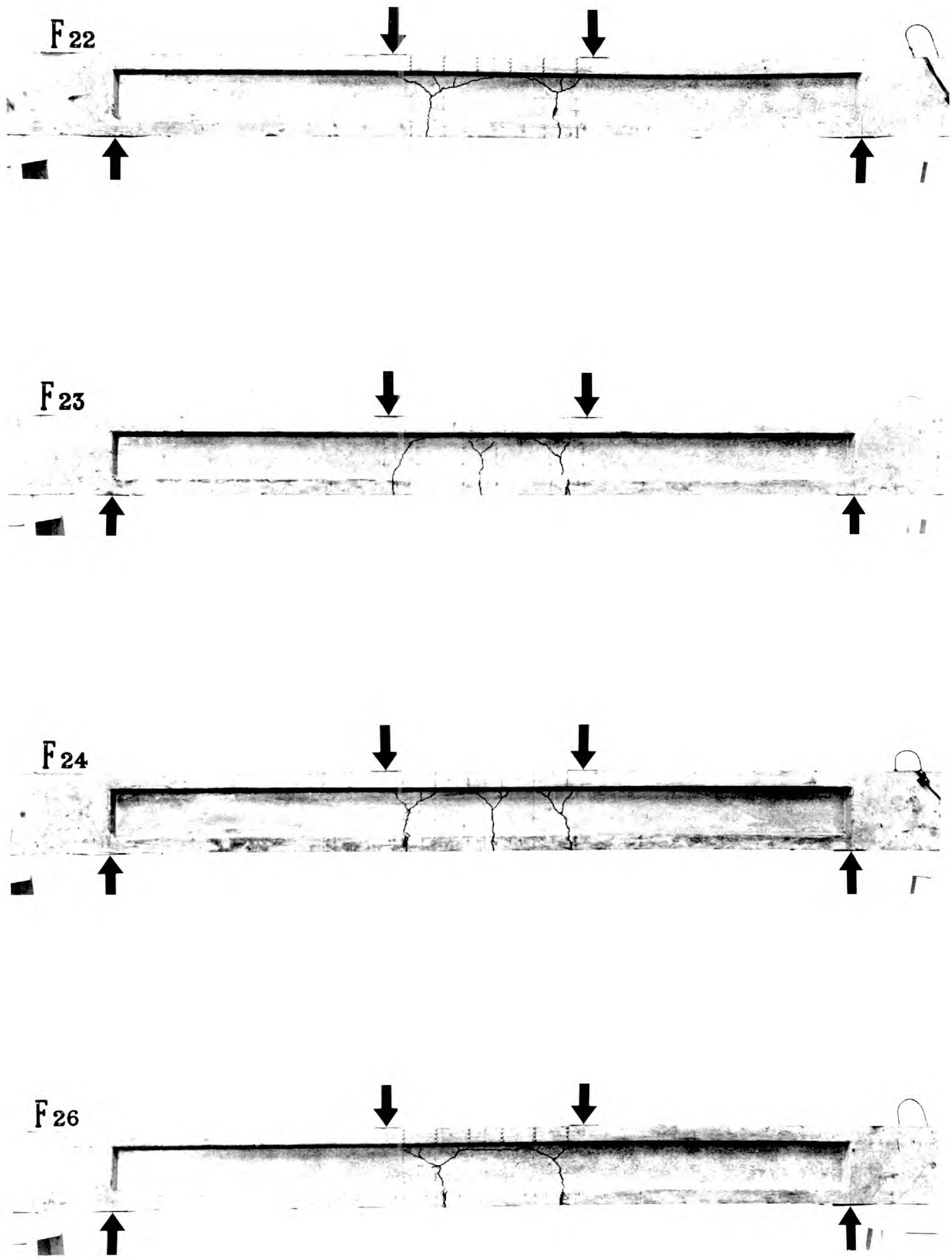

PLATE 4.4

F27

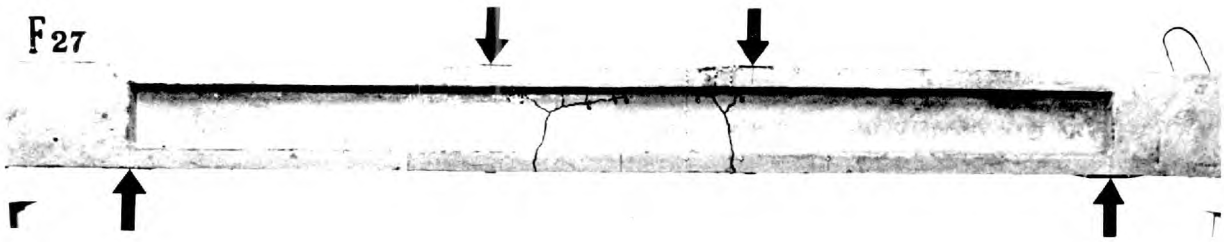

F28

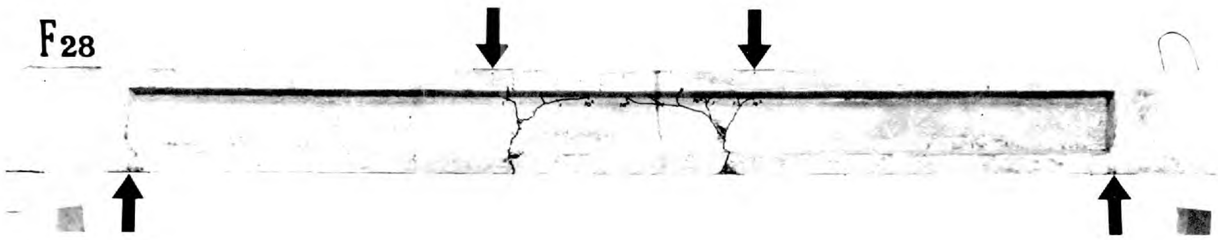

F29

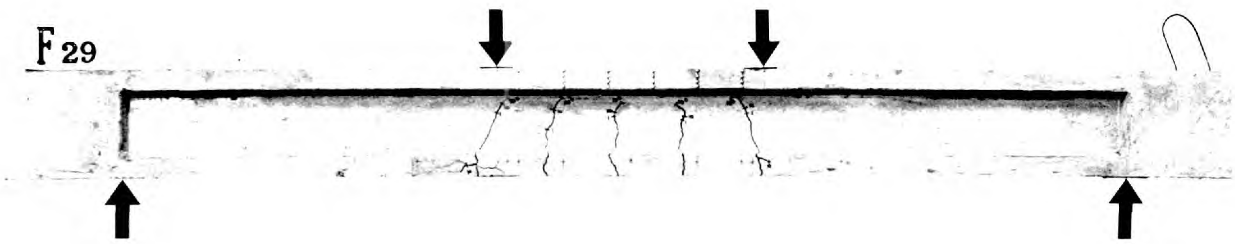

F30

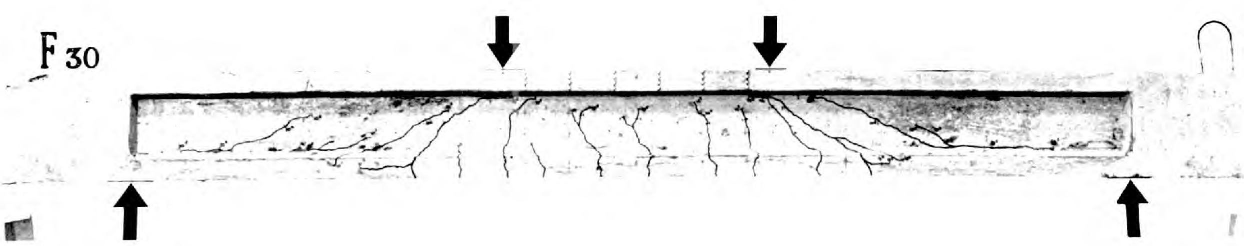

PLATE 4.5

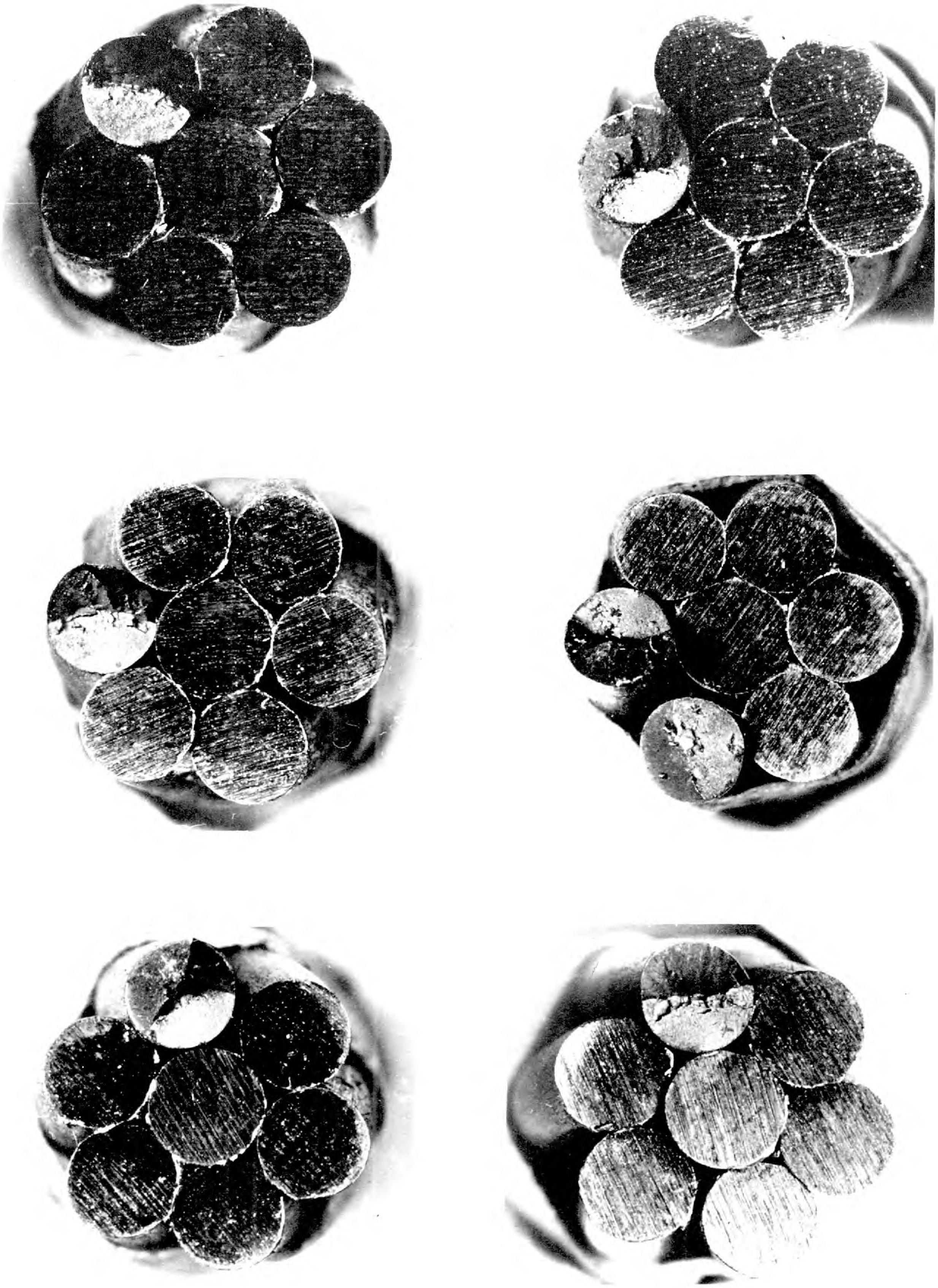

EXAMPLES OF STRAND FATIGUE FRACTURES

PLATE 4.6

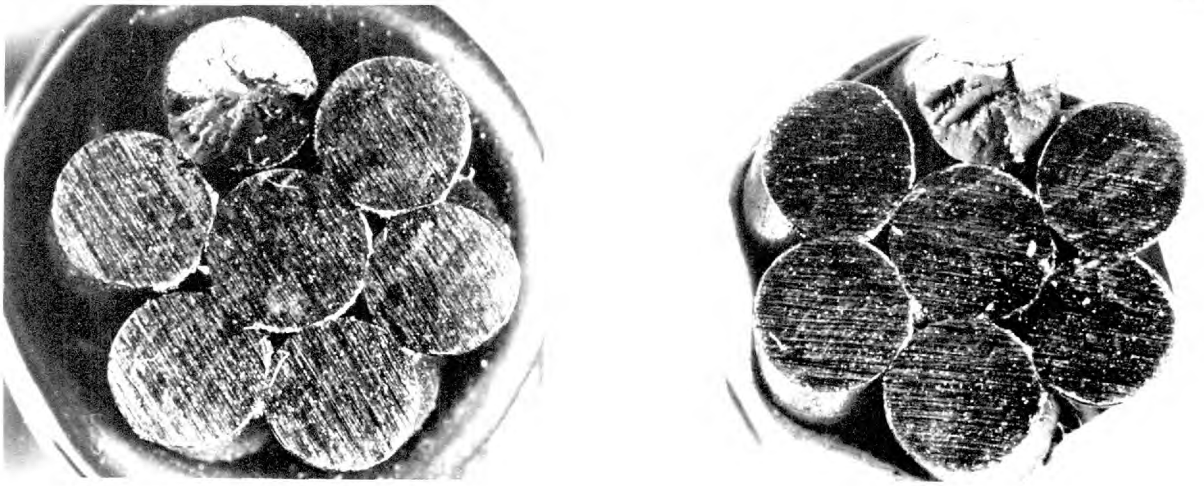

EXAMPLES OF STRAND FATIGUE FRACTURES

EXAMPLES OF STATIC DUCTILE FRACTURES

PLATE 4.7

CHAPTER 5

PREDICTION OF FLEXURAL CRACKING AND FAILURE IN FATIGUE IN PRESTRESSED CONCRETE STRUCTURES

5.1) INTRODUCTION

In order to be able to predict the fatigue life of any structure, it is necessary to know accurately the state of stress existing in the elements of the members at critical sections under the extremes of loading likely to be applied to the structure. In the analysis which follows, it has been assumed that the applied loading varies between two extreme limits which remain constant throughout the life of the structure - this is obviously a simplification of the conditions existing in practice, but the state of knowledge of fatigue of prestressed concrete flexural members is not yet at such a stage that any extension to the theory can be made with any confidence.

In the theoretical study given here it has been found convenient to separate the response of a member to load into three stages :-

Stage I : The structure is uncracked, and the response to load is linear and elastic. Increments of steel and concrete strain are relatively small and linear stress - strain relations may be assumed for both materials.

Stage II : The concrete in the tension zone is now assumed to be cracked (either by previous repeated loading or by a static overload). The load level is less than M^{tr}, which is the moment at which flexural cracks begin to open and, therefore, the structure still behaves in a linear elastic manner, and linear stress - strain relations may be assumed for steel and concrete. The previously formed flexural cracks are closed by the prestressing force and, therefore, as long as the stresses in the cracked fibres remain compressive, the structure behaves elastically.

<u>Stage III</u> : In this stage, the tension zone is assumed to be cracked, and the load level is greater than M^{tr}. Flexural cracks have now opened, and the response of the beam to load can no longer be assumed to be linear. Non - linear stress - strain relations must be assumed for both steel and concrete, and the conditions of equilibrium of internal and external forces, and compatibility of deformations must be satisfied at cracked sections.

The calculations involved in Stage III are considerably more complicated than those required for Stages I and II, and furthermore, must be open to greater error due to the greater number of parameters involved for which values must be assumed in practice. In particular, the bond factor, F, is likely to vary considerably, even between similar beams, as shown in figs. 4.27 to 4.32. Variations in F have a considerable effect on the fatigue life of flexural members (see section 4.7c).

5.2) STAGE I : PREDICTION OF FLEXURAL CRACKING, BOTH STATICALLY AND IN FATIGUE.

The following assumptions are made in the analysis for this stage :-

i) Linear stress - strain relations for steel and concrete.

ii) Plane sections remain plane, i.e. the strains vary linearly with depth in the beam.

iii) The bond strain compatibility factor, F, is assumed to be equal to 1.0.

iv) The modulus of elasticity of concrete, E_c, is the same in tension and compression.

After losses, the extreme fibre stresses due to prestress only are :-

$$\sigma_{c2p} = \frac{P_e}{A} + \frac{P_e e_s}{Z_2} \qquad \text{... (5.1)}$$

$$\sigma_{c1p} = \frac{P_e}{A} + \frac{P_e e_s}{Z_1} \qquad \text{... (5.2)}$$

If cracking takes place under static loading, it will occur when the stress in the bottom fibre is f_{crf}. The value of f_{crf}, determined from tests, has been found to be subject to considerable scatter, but it is generally assumed to be a function of the direct compressive strength. Within the limited range of cube strengths (8,000 - 9,600 lbs/in^2) in the author's tests, no more complex relationship than :-

$$f_{crf} = - 0.076 \, f_{cu}$$

was found to be justifiable (see section 4.5b). Somes (104) used a similar relationship for f_{crf} within a range of cube strengths of 4,600 - 6,700 lbs/in^2, i.e. :-

$$f_{crf} = - 0.08 \, f_{cu}$$

Warwaruk, Sozen and Siess (108) have determined the relationship between f_{crf} and the compressive strength, f'_c, for values of f'_c varying between 1,000 - 8,500 lbs/in^2. According to the British Standard Code of Practice, 1881, :

$$f'_c = 0.75\, f_{cu}$$

Using this ratio of $f'_c : f_{cu}$, the relation given by Warwaruk et al agrees well with both the author's and Somes' results in the range of cube strengths applicable. Substituting for f'_c thus gives :-

$$f_{crf} = - \frac{3000}{3 + \frac{16,000}{f_{cu}}} \qquad \ldots (5.3)$$

When flexural cracking is imminent, the strain in the steel will have changed to :-

$$\varepsilon_{scrf} = \varepsilon_{sp} - \frac{(\sigma_{c1p} - f_{crf})\, e_s}{E_c\, e_1} \qquad \ldots (5.4)$$

For E_c, see equation (5.12).

The prestressing force will, therefore, become :-

$$P_{crf} = P_e \frac{\varepsilon_{scrf}}{\varepsilon_{sp}} \qquad \ldots (5.5)$$

Therefore, at this instant :-

$$f_{crf} = \frac{P_{crf}}{A} - \frac{P_{crf}\, e_s}{Z_1} - \frac{M_{crf}}{Z_1} \qquad \ldots (5.6)$$

Re-arranging this expression leads to the flexural cracking moment :-

$$M_{crf} = Z_1 \left[\frac{P_{crf}}{A} - \frac{P_{crf}\, e_s}{Z_1} - f_{crf} \right] \qquad \ldots (5.7)$$

If the value of $M_{crf} > M^{max}$, then cracking may occur in fatigue, and it is necessary to calculate the extreme fibre stresses under both maximum and minimum load. In a similar manner :-

$$\sigma_{c1}^{min} = \frac{P^{min}}{A} - \frac{P^{min}\, e_s}{Z_1} - \frac{M^{min}}{Z_1} \qquad \ldots (5.8)$$

where:
$$P^{min} = P_e \left[1 - \frac{(\sigma_{c1p} - \sigma_{c1}^{min})\, e_s}{E_c\, e_1\, \varepsilon_{sp}} \right] \qquad \ldots (5.9)$$

and:
$$\sigma_{c1}^{max} = \frac{P^{max}}{A} - \frac{P^{max}\, e_s}{Z_1} - \frac{M^{max}}{Z_1} \qquad \ldots (5.10)$$

where:
$$P^{max} = P_e \left[1 - \frac{(\sigma_{c1p} - \sigma_{c1}^{max})\, e_s}{E_c\, e_1\, \varepsilon_{sp}} \right] \qquad \ldots (5.11)$$

Little information is available on the fatigue strength of concrete in tension in prestressed concrete beams, but the author's tests (see section 4.5) have shown that the fatigue properties are only marginally different from those of plain concrete beams subjected to repeated loading when the strength is expressed as a proportion of the static tensile strength. The tensile fatigue strength in prestressed beams appears to show a small increase over that of plain beams, but until further tests have verified this, the fatigue properties may be assumed to be the same as those of plain beams since, on the available information, this will give safe results in design.

The results given in figs. 5.1 and 2.2 cover all likely combinations of maximum and minimum stresses in the extreme fibres and may be used to predict the number of cycles to cracking. In fig. 5.1, the S - N curve given is for the condition in which the minimum stress is zero. When the value of σ_{c1}^{min} is compressive, the same S - N curve may still be used, since the range of stress has no effect on the tensile fatigue strength under these conditions, as shown by fig. 2.2. The data given in figs. 5.1 and 2.2 is based on the results of Clemmer (13), Crepps (14), Hatt (15), Kesler (17), Murdock and Kesler (18), and McCall (19).

The theory put forward here for the prediction of flexural cracking does not include the probability parameter, PR, but at the present time, the information available on the fatigue strength of concrete in tension in a prestressed beam does not warrant the use of such precise analysis.

According to the British Standard Code of Practice, 115, the maximum compressive stress allowable in concrete is 40% of the cube strength, f_{cu}, at 28 days, and the maximum tensile stress allowable is 225 lbs/in^2, for a cube strength of 7500 lbs/in^2 at 28 days. The maximum possible stress range in the concrete is thus :-

$$\sigma_{c1}^{max} - \sigma_{c1}^{min} = (0.4 \times 7500) + 225 = 3,225 \text{ lbs/in}^2$$

Then assuming that:-

$$E_c = \left(4 + \frac{f_{cu} - 4000}{2000}\right) \times 10^6 \text{ lbs/in}^2 \quad \ldots (5.12)$$

$$\therefore \text{ For } \quad f_{cu} = 7,500 \text{ lbs/in}^2, \quad E_c = 5.75 \times 10^6 \text{ lbs/in}^2$$

$$\therefore \quad \varepsilon_{c1}^{max} - \varepsilon_{c1}^{min} = \frac{3,225}{5.75} \times 10^{-6} = 560 \times 10^{-6}$$

If $E_s = 28 \times 10^6$ lbs/in^2, then :-

$$\sigma_s^r = \sigma_s^{max} - \sigma_s^{min} = 15,700 \text{ lbs/in}^2 = \text{stress range in steel.}$$

This is equal to about 6% of the static ultimate strength of prestressing steel and is well below the fatigue limit stress range of all steels used in practice. Fatigue failures of steel will not, therefore, be possible in all practical cases if the concrete is in an uncracked condition.

5.3) STAGE II. ESTIMATION OF STEEL STRESSES IN CONDITION BEFORE CRACKS BEGIN TO OPEN.

The following assumptions are made in the analysis for Stage II:-

i) Linear stress - strain relations for steel and concrete.

ii) Plane sections remain plane.

iii) The bond strain compatibility factor, F, is assumed to be equal to 1.0.

The value of the moment, M^{tr}, at which previously formed cracks begin to open, is given by equation 5.6 with the value of f_{crf} equal to zero, thus :-

$$0 = \frac{P^{tr}}{A} - \frac{P^{tr}\ e_s}{Z_1} - \frac{M^{tr}}{Z_1}$$

where:
$$P^{tr} = P_e \left[1 - \frac{\sigma_{c1p}\ e_s}{E_c\ e_1\ \varepsilon_{sp}} \right] \quad \ldots (5.13)$$

and thus:
$$M^{tr} = Z_1 \left[\frac{P^{tr}}{A} - \frac{P^{tr}\ e_s}{Z_1} \right] \quad \ldots (5.14)$$

If $M^{min} < M^{tr}$, the bottom fibre stress under minimum load, σ_{c1}^{min}, may then be calculated from equation 5.8.

The steel stress under M^{min}, is then given by:-

$$\sigma_s^{min} = E_s \left[\varepsilon_{sp} - \frac{(\sigma_{c1p} - \sigma_{c1}^{min})\, e_s}{E_c\, e_1} \right] \qquad \ldots (5.15)$$

It is imperative that the value of ε_{sp} used in the calculations is determined accurately since the fatigue strength of the steel is extremely sensitive to changes in the value of σ_s^{min}. Appropriate values of ε_{sp} must, therefore, be determined in each case on the basis of an analysis for creep and shrinkage losses and an estimation of all other possible effects.

If both M^{min} and $M^{max} \nless M^{tr}$, then on the same reasoning given in section 5.2, fatigue failures of steel are extremely improbable in all practical cases in Stage II.

5.4) STAGE III : ESTIMATION OF STEEL STRESSES IN LOADING CONDITION WHERE $M > M^{tr}$

The following assumptions are made in the analysis for Stage III:-

i) In the compression zone, the change in strain varies linearly with the distance from the neutral axis.

ii) The stress - strain relations for steel and concrete are non - linear.

iii) The contribution of concrete tensile stresses to the moment of resistance is negligible.

5.4a) STEEL STRESS - STRAIN RELATION

Determination of the steel stress - strain relation under repeated loading is relatively simple since it has been found that the relationship is independent of the number of cycles of applied loading, and is dependent only on the level of the maximum applied stress in previous load cycles. The complete stress - strain curve is given (with examples of unloading and reloading curves) in fig. 5.2 for the $\frac{3}{8}$" diameter strand used in the author's beam tests. At stress levels above about 90% of the ultimate strength, the modulus of elasticity on reloading may be reduced by about 5% of the initial value but since the maximum stress will seldom reach this level under repeated loading, the reduction may be neglected, and the static modulus of elasticity assumed to apply in all cases.

5.4b) CONCRETE STRESS - STRAIN RELATION

Evaluation of the stress - strain relation for concrete under repeated loading is considerably more complicated than that for steel since the relationship has been shown by many investigators to be dependent on both the number of cycles of repeated loading and on the maximum stress level in a load cycle. Examples of this variation with N are shown in figs. 5.3 and 5.4, for two different levels of the maximum stress. When the maximum stress level is below the fatigue limit, the relation becomes linear after about 10,000 load cycles and no further change takes place with increasing number of load cycles.

At each level in the compression zone of a beam, the fibres are being subjected to a different maximum stress and, therefore, the stress - strain relationship is different for each level. On this basis, a series of isocyclic envelope curves may be drawn, as shown in fig. 5.5, where each curve relates the stress and strain in concrete elements which have been subjected to varying maximum stresses (of magnitude given by the ordinate of the curve) for the same number of load cycles. The maximum stress for each curve is the fatigue strength for that number of load cycles. Thus, in the compression zone of a beam, the maximum stress that can exist in the concrete after a certain number of load cycles is given by the fatigue strength for that particular number of cycles. It must be emphasized that the curves given in fig. 5.5 are only possible hypothetical relationships based on the co-ordinated results of several investigators - no investigation has been carried out to date to determine the exact relations from one complete series of tests. Once obtained, the envelope curves may be used directly to determine the stress - distribution in the compression zone of a beam which has been subjected to any number of load cycles. The stress and strain for a particular envelope curve (for a number of cycles of loading, N) are assumed to be related by the function:-

$$\sigma_c = F(\varepsilon_c) \qquad \ldots (5.16)$$

If the section is rectangular, or, in the case of an I - beam, the neutral axis lies within the top flange, the compressive force, C, is given by :-

$$C = b' \int_0^{d_n} \sigma_c \, dy$$

But : $y = \dfrac{d_n \varepsilon_c}{\varepsilon_{c2}}$, and substituting for σ_c :-

$$C = \frac{b\, d_n}{\varepsilon_{c2}} \int_0^{\varepsilon_{c2}} F(\varepsilon_c)\, d\varepsilon_c \qquad \ldots (5.17)$$

The depth of the centre of compression, d_c, is given by :-

$$d_c = k_2 \, d_n \qquad \ldots (5.18)$$

The value of k_2 is determined from the position of the centre of gravity of the area of the stress block:-

i.e. $$k_2 \, \varepsilon_{c2} = \varepsilon_{c2} - \frac{b \int_0^{\varepsilon_{c2}} F(\varepsilon_c) \, \varepsilon_c \, d\varepsilon_c}{b \int_0^{\varepsilon_{c2}} F(\varepsilon_c) \, d\varepsilon_c}$$

which leads to:

$$k_2 = 1 - \frac{\int_0^{\varepsilon_{c2}} F(\varepsilon_c) \, \varepsilon_c \, d\varepsilon_c}{\varepsilon_{c2} \int_0^{\varepsilon_{c2}} F(\varepsilon_c) \, d\varepsilon_c} \qquad \ldots (5.19)$$

If the neutral axis lies within the web of an I - beam, the compressive force, C, is given by :-

$$C = b_o \int_0^{d_n - d_f} \sigma_c \, dy + b \int_{d_n - d_f}^{d_n} \sigma_c \, dy$$

Substituting, as in equation (5.17) :-

... (5.20) ......

$$C = \frac{b_o\, d_n}{\varepsilon_{c2}} \int_{o}^{\varepsilon_{c3}} F(\varepsilon_c)\, d\varepsilon_c + \frac{b\, d_n}{\varepsilon_{c2}} \int_{\varepsilon_{c3}}^{\varepsilon_{c2}} F(\varepsilon_c)\, d\varepsilon_c \quad \ldots (5.20)$$

Similarly, the factor, k_2, is given by :-

$$k_2 = 1 - \frac{b_o \int_{o}^{\varepsilon_{c3}} F(\varepsilon_c)\, \varepsilon_c\, d\varepsilon_c + b \int_{\varepsilon_{c3}}^{\varepsilon_{c2}} F(\varepsilon_c)\, \varepsilon_c\, d\varepsilon_c}{\varepsilon_{c2}\, b_o \int_{o}^{\varepsilon_{c3}} F(\varepsilon_c)\, d\varepsilon_c + \varepsilon_{c2}\, b \int_{\varepsilon_{c3}}^{\varepsilon_{c2}} F(\varepsilon_c)\, d\varepsilon_c}$$

$$\ldots (5.21)$$

5.4c) COMPATIBILITY OF DEFORMATIONS AT CRACKED SECTIONS

The deformation existing in the concrete at cracked sections may be represented by a linear distribution of strains throughout the depth of the section; above the neutral axis, the strains represent actual compression strains in the concrete, and below the neutral axis, the apparent tensile strains represent the finite width of the cracks. Since infinite strains cannot exist in the steel reinforcement, some bond breakdown must be assumed to occur between steel and concrete on either side of the crack. In analysis, it is, therefore, convenient to associate the linear distribution of concrete strain throughout the depth of the section with the actual increase in strain in the reinforcement, $d\varepsilon_s$, due to the opening of the crack. This is done by relating the apparent tensile strain in the concrete at the level of the steel, ε_{cs}^{m}, to the actual increase in strain in the steel, $d\varepsilon_s$ by a bond strain compatibility factor, F.

Thus, at a cracked section, the total steel strain is given by:-

$$\varepsilon_s^m = \varepsilon_{sp} + \varepsilon_{csp} + F\,\varepsilon_{cs}^m$$

or : $$\varepsilon_s^m = \varepsilon_{sp} + \varepsilon_{csp} + F\,\varepsilon_{c2}\,\frac{d - d_n}{d_n} \qquad \ldots (5.22)$$

where: ε_{sp} = effective prestrain in the steel.

ε_{csp} = elastic strain in the concrete at the level of the steel due to the prestress, P_e.

i.e. : $$\varepsilon_{csp} = \frac{\sigma_{c1p}\,e_s}{E_c\,e_1} \qquad \ldots (5.23)$$

In practice, the value of the bond factor, F, is found to be subject to considerable scatter, and does not necessarily lie between zero and unity. In conditions of excellent bond, it may be greater than unity. The value of F is influenced by both the breakdown in local bond between steel and concrete, as well as by the distribution of strain concentrations in the concrete due to the spacing of cracks, etc. In pretensioned beams, reinforced with strand, the bond factor is likely to be greater than unity, whereas in post - tensioned beams, with good bond, it is likely to be approximately equal to one, and in post - tensioned beams with poor bond, it is likely to be as low as 0.5. It should also be noted (see section 4.7b) that F is cycle dependent, and the stable state bond factor is about 70% of its initial value; allowance should be made for this when estimating the value of F.

5.4d) CONDITIONS OF EQUILIBRIUM

The conditions of equilibrium may be used to provide two equations which must be satisfied under all conditions of loading in Stage III.

The force in the steel, T, is given by:-

$$T = A_s\,\sigma_s^m$$

Using equation (5.17) (or 5.20 for an I - beam), the summation of forces in the longitudinal direction yields :-

$$C = T$$

i.e. : $$A_s \sigma_s^m = \frac{b\, d_n}{\varepsilon_{c2}} \int_o^{\varepsilon_{c2}} F(\varepsilon_c)\, d\varepsilon_c$$

i.e. : $$\sigma_s^m = \frac{b\, d_n}{A_s\, \varepsilon_{c2}} \int_o^{\varepsilon_{c2}} F(\varepsilon_c)\, d\varepsilon_c \qquad \ldots (5.24)$$

Equating internal and external moments about the centroid of the compressive force gives :-

$$M = A_s\, \sigma_s^m\, (d - k_2\, d_n) \qquad \ldots (5.25)$$

where k_2 is given in terms of ε_{c2} by equation (5.19).

5.4e) COMPUTATION OF STRESSES

Equations (5.19), (5.22), (5.24), and (5.25) may now be used, in conjunction with the steel stress - strain relation, to evaluate for a moment, M, the quantities σ_s^m , ε_s^m , k_2 , d_n and ε_{c2} in Stage III after any number of load cycles, N.

If it is required to determine the steel stress, σ_s^{max}, for one particular value of M^{max}, the calculation is most easily performed by assuming an approximate value for the internal lever arm, l_a :-

i.e. : $l_a \doteqdot 0.85\, d$

An approximate value of σ_s^{max} is thus obtained :-

$$\sigma_s^{max} \doteq \frac{M^{max}}{A_s \, l_a} = \sigma_s^m$$

which may then be substituted in equations (5.22) and (5.24) (using the steel stress - strain curve to evaluate ε_s^m). The two resulting equations may then be solved by trial and error for the unknowns, d_n and ε_{c2}, which are then substituted in equations (5.19) and (5.25) to determine the correct value of M pertaining to the chosen value of σ_s^m. The process is then repeated for different values of σ_s^m so that the relation between σ_s^m and M may be plotted in the range including M^{max} - from this, the actual value σ_s^{max} corresponding to M^{max} may be read off.

5.5) PREDICTION OF THE FATIGUE LIFE OF PRESTRESSED CONCRETE STRUCTURES

By means of the theoretical analysis given in sections 5.2, 5.3, and 5.4 it is possible to determine the stress existing in the steel at a critical section under any conditions of loading. Since the response of the beam to load remains virtually constant throughout the major portion of its fatigue life, it will normally only be necessary to calculate the stresses existing in the stable state condition of response to load; it may then be assumed that these stresses exist throughout the load history of the structure.

If it is found that flexural cracking occurs in fatigue (from the analysis given in section 5.2) after a certain number of load cycles, it may safely be assumed that this stress history has no effect on the subsequent fatigue strength, since the maximum stress range possible in the steel before flexural cracking is below the fatigue limit of all prestressing steels, as shown in section 5.2.

The information obtained from a theoretical analysis of the stresses, may then be used in conjunction with the experimental results given in chapter 4, and empirical results for the fatigue properties of a single element of the prestressing steel under consideration, to predict the fatigue life in flexure of the structure.

Once the value of the actual stress range in the steel, σ_s^r, which occurs in the structure, has been calculated, it should be divided by the fatigue strength reduction factor, K, to obtain the value of the stress range which would cause fatigue failure in the same number of cycles, N, when the steel is tested free in air,

where: K = ratio of the fatigue strength (stress range) of the steel when embedded in concrete to the fatigue strength (stress range) of the steel in air, for failure after the same number of load cycles.

For: $F < 0.765$: $K = 1.0645\,F + 0.1833$ ... (4.1)

or for : $F \geqslant 0.765$: $K = 1.00$ ... (4.2)

Depending on the availability of statistical results for the fatigue properties of the steel, it is then possible to determine the number of cycles to failure, N, corresponding to any probability level, PR, for any repeated stress cycle.

If the section under consideration contains more than one steel element, the probability of fatigue failure of one wire increases with the number of elements in the cross section. Thus, if there are u similar elements present in the section, the probability of failure in the section, at or before N cycles, is :-

$$QR = 1 - (1 - PR)^{u} \qquad \ldots (5.26)$$

where: PR = probability of failure in a single element.

Therefore, if it is desired to determine the mean fatigue life of the section, $\bar{N}$, the value, $QR = 0.5$, may be substituted, and equation (5.26) solved for PR. Then the mean fatigue life of the section, $\bar{N}$, is equal to the number of cycles corresponding to a probability of failure of :-

$$PR = 1 - (0.5)^{\frac{1}{u}} \qquad \ldots (5.27)$$

in a single steel element.

Then, using the appropriate value of PR, the value of $\bar{N}$ may be obtained from :-

$$PR = \frac{1}{S\sqrt{2\pi}} \int_{-\infty}^{x} e^{-\frac{(x - \bar{x})^2}{2S^2}} \, dx \qquad \ldots (5.28)$$

where: $x = \log N$

$\bar{x}$ = mean of log N for that stress cycle.

i.e. : $$\bar{x} = \overline{\log N} = \frac{\sum_{i=1}^{n} \log N}{n} \qquad \ldots (5.29)$$

S = standard deviation of log N for that stress cycle.

i.e. : $$S = \left[\frac{1}{n-1} \sum_{i=1}^{n} (\log N_i - \overline{\operatorname{Log} N})^2 \right]^{\frac{1}{2}} \qquad \ldots (5.30)$$

n = sample size.

Therefore, once the values for $\bar{x}$ and S have been determined, equation (5.28) may be used to determine the probability of failure for any particular value of x (and thus N), and vice versa. Since the integral in equation (5.28) can only be evaluated by numerical means, the values are most easily obtained from standard tables (33).

5.6) DISCUSSION

5.6a) VARIATIONS IN BEAM RESPONSE

The steel stress under maximum load is extremely sensitive to changes in the bond strain compatibility factor, F, as shown in sections 4.7 and 5.4c. Unfortunately, prediction of the value of F in practice is not possible with any degree of accuracy, since the value is subject to considerable variation, even between similar beams. The ideal approach is a statistical treatment of F, but without extensive experimental results, this is not possible, and at the present time, it is, therefore, necessary to choose conservative values of F.

E_c is another parameter which is open to some doubt, particularly under repeated loading, and further experimental work is required to define more accurately the relation between stress and strain in the concrete compression zone under repeated loading. Adoption of the static stress - strain relationship for concrete will not, however, lead to great errors in the steel stresses, particularly at stress levels of the order of the fatigue limit and below, which is the range most commonly considered in practice.

The significance of creep and shrinkage losses on the fatigue strength has been mentioned in section 5.3, and the importance of accurate analysis for these effects is again emphasized here, since the fatigue strength of prestressing steel is extremely sensitive to small variations in the stress range.

5.6b) VARIATIONS IN THE FATIGUE STRENGTH OF PRESTRESSING STEEL

Although the fatigue properties of the $\frac{3}{8}$" diameter strand used in the author's tests are given as a proportion of the static ultimate strength, it must be emphasized that the results cannot be extrapolated to predict the fatigue behaviour of any prestressing strand; the static ultimate strength is only one of many parameters determing the fatigue strength of prestressing steel. Therefore, at the present time, the fatigue strength of all steels must essentially be based on empirical results (obtained from laboratory tests) supplied by the manufacturers of the particular steel. The fatigue properties are particularly sensitive to changes in the manufacturing processes, such as variations in heat treatment, amount of work - hardening, surface finish, presence of impurities, type of indentations and crimping, relative diameters of centre and outer wires in strand, the lay of the outer wires in strand, and the nominal diameter of the steel. The state of knowledge to date does not allow theoretical evaluation of the effect of these variables.

5.6c) EFFECTS OF EMBEDDING STEEL IN CONCRETE STRUCTURES

Further variations are introduced into the fatigue strength of steel when it is used in a concrete structure. Even before the steel is embedded in concrete, mechanical damage is possible during handling and construction - if the damaged length coincides with a critical section, a significant reduction in the fatigue strength is likely. Corrosion is another factor which has a detrimental effect on the fatigue strength, and although the grout serves to protect the steel, corrosion is still possible at critical cracked sections.

The effect of fretting on the fatigue strength was shown in section 4.7c to be significantly affected by the quality of bond between steel and concrete. Further variations are likely if different grouts and ducts are utilised. It may also be expected that inclined or curved cables will accentuate the effect of fretting due to the increased lateral pressure on the steel; furthermore, where cables pass over saddles, the effect of fretting will be particularly severe due to the interaction of the two metallic surfaces, and since saddle - points normally coincide with regions of maximum moment, the importance of this effect cannot be over - emphasized. It should be noted (see section 2.2c) that reductions of up to 90% in the fatigue strength have been found where fretting occurs between similar metals.

In the cases where unbonded cables are utilised, it may be expected that fatigue failures will always occur at anchorage points, unless the anchorage stresses are significantly reduced by friction forces in the beam. The notch effect caused by wedges is known to significantly reduce the fatigue strength of prestressing steel.

5.6d) SIZE EFFECTS AND DEFINITION OF FAILURE

The effect of a variable number of steel elements in the section on the probability of failure has been included in section 5.5. In the analysis given in sections 5.3, 5.4, and 5.5, it has been assumed that fatigue failure always occurs at a critical cracked section, whereas in the steel fatigue tests, failure always occurs at the weakest point within the test length - since it is improbable that the weakest point in the steel will coincide with a cracked section, this will, in general, give an additional safety factor against failure.

In the author's tests, fatigue failure was defined as the point at which the first wire fractured since this represented a considerable reduction in the stiffness of the beam. When a section contains a large number of steel elements, failure of one wire will not cause a significant reduction in the stiffness of the section, and fatigue failure cannot, therefore, be considered to have occurred. A satisfactory solution would, therefore, be to define fatigue failure as the point at which failure had occurred in a certain fixed proportion of the elements forming the total steel area.

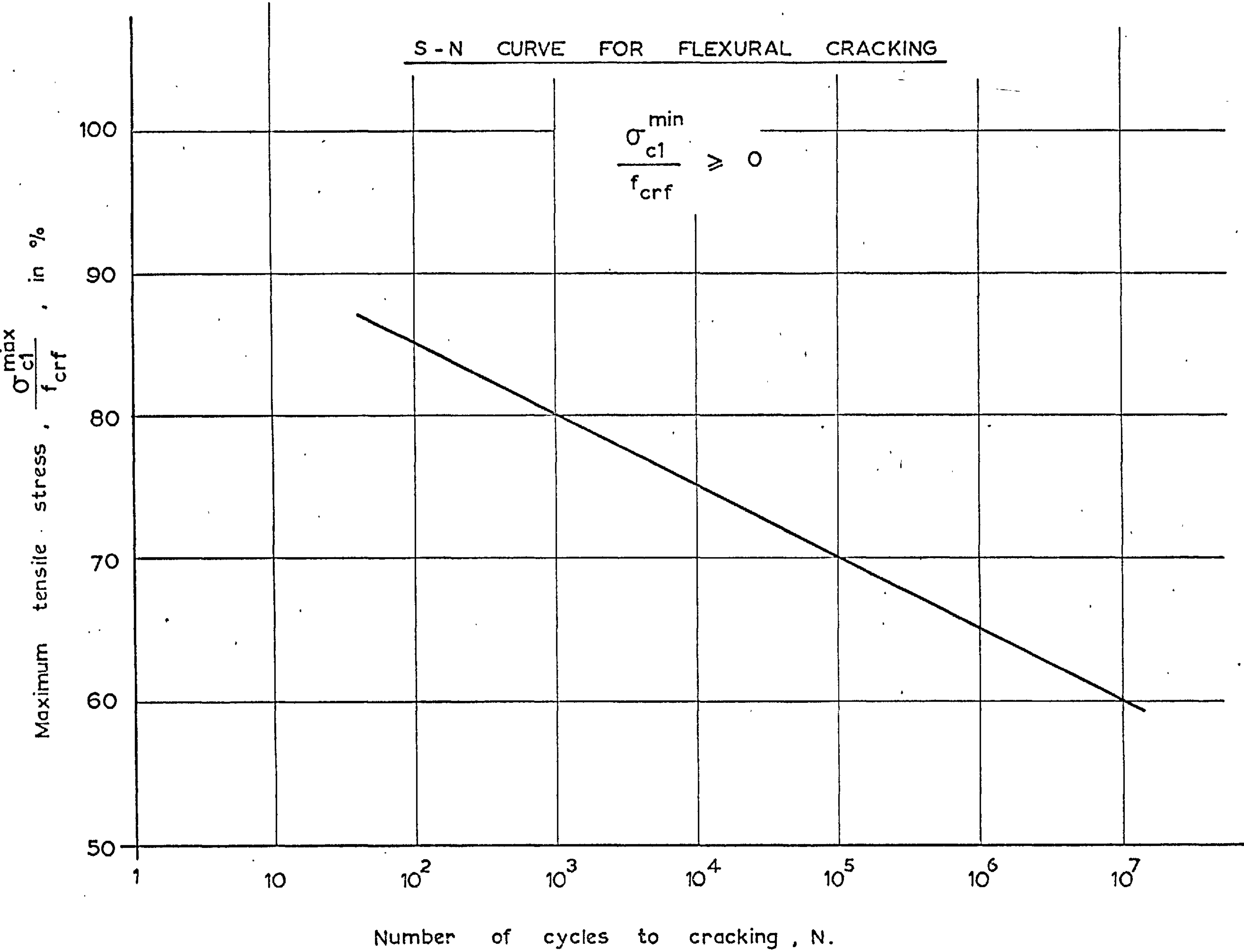

Based on (2 ,13,14, 15, 17, and 19).

Fig. 5.1

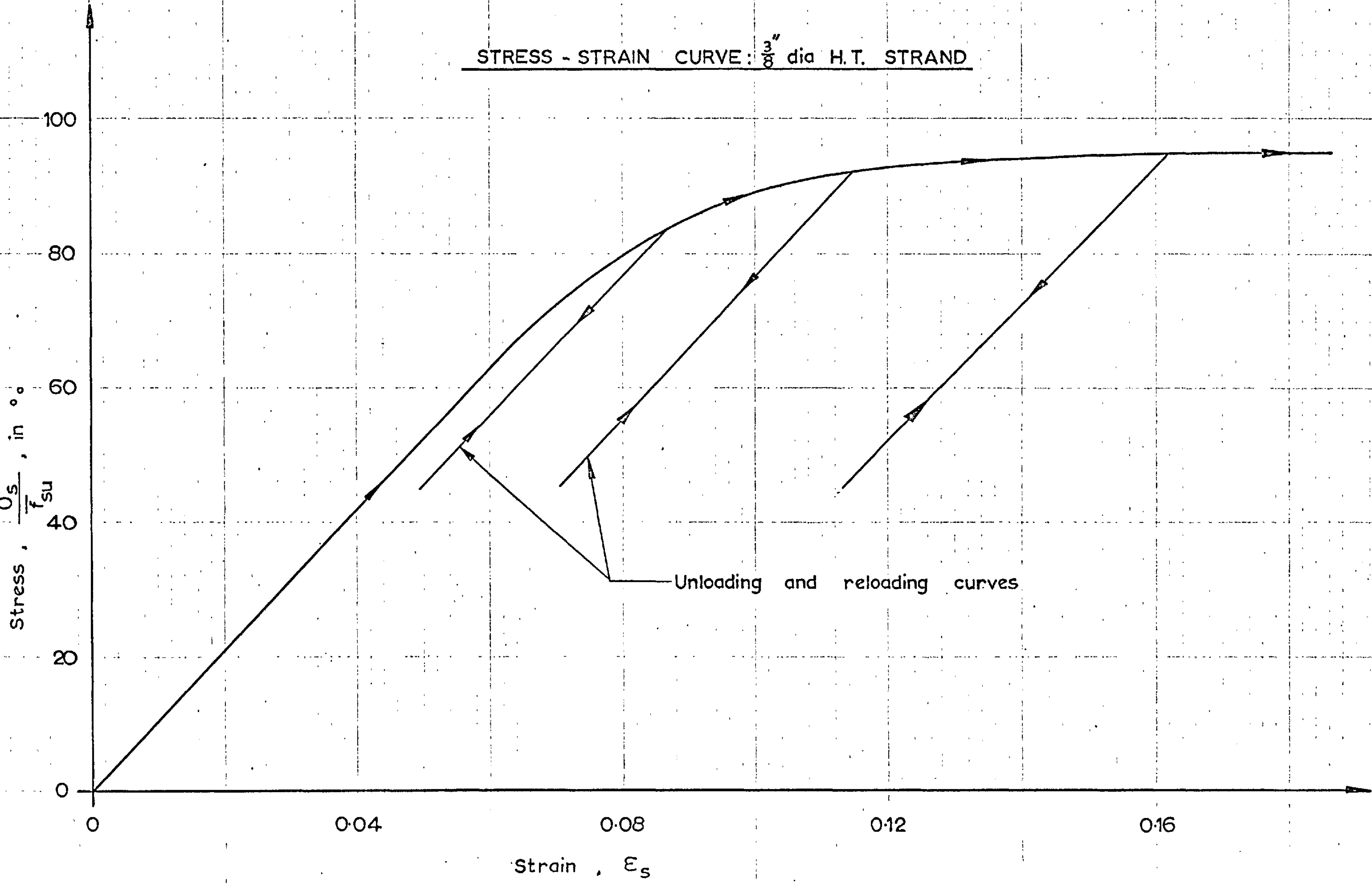
STRESS - STRAIN CURVE: 3/8" dia H.T. STRAND
100
80
60
40
20
0
Stress , σs / fsu , in %
0
0·04
0·08
0·12
0·16
Strain , εs
Unloading and reloading curves

Fig. 5.2

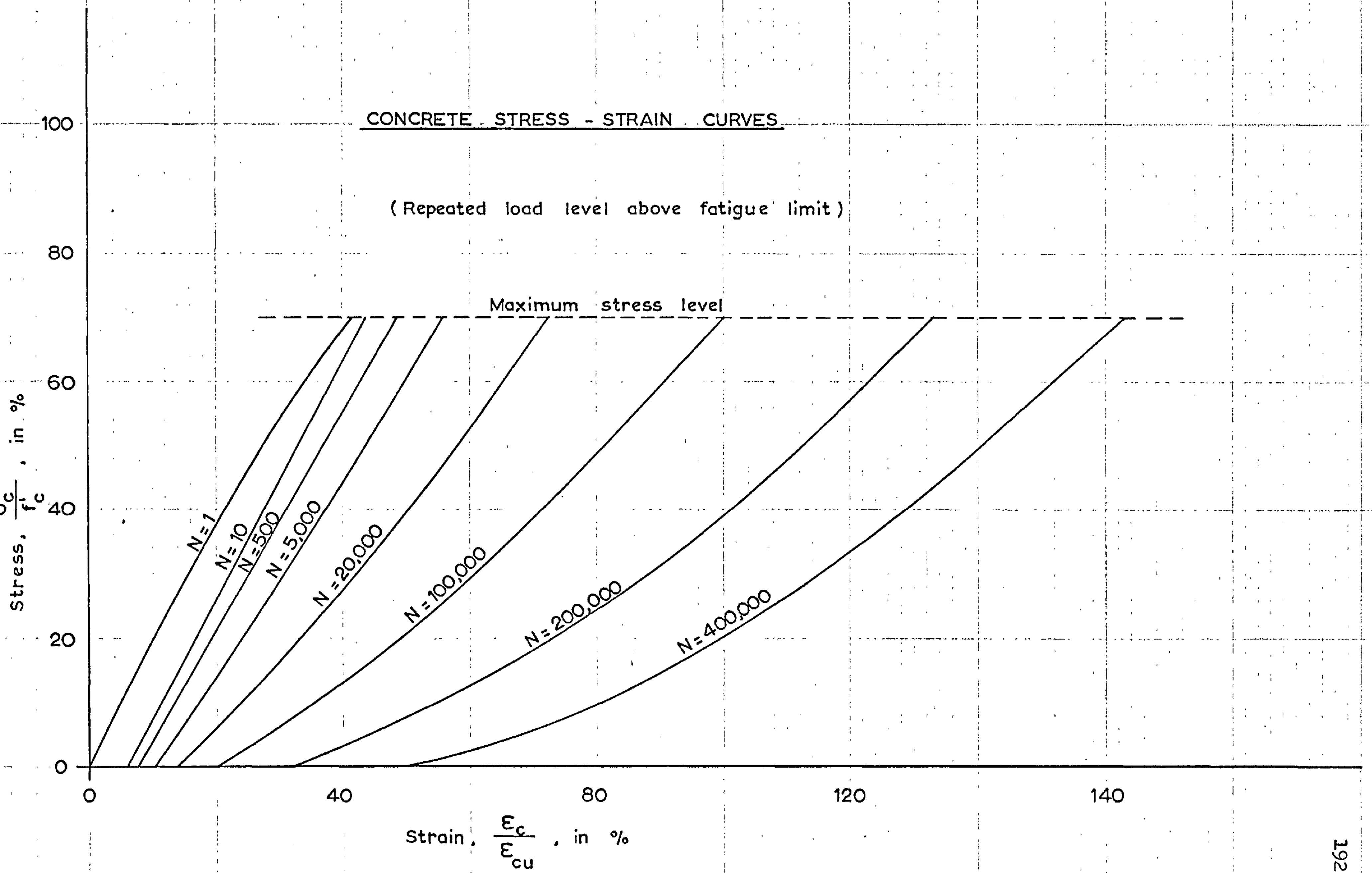
CONCRETE STRESS - STRAIN CURVES
(Repeated load level above fatigue limit)
Maximum stress level
N = 1
N = 10
N = 500
N = 5,000
N = 20,000
N = 100,000
N = 200,000
N = 400,000
Stress, $\frac{\sigma_c}{f'_c}$, in %
Strain, $\frac{\varepsilon_c}{\varepsilon_{cu}}$, in %
0
20
40
60
80
100
0
40
80
120
140

Fig. 5.3

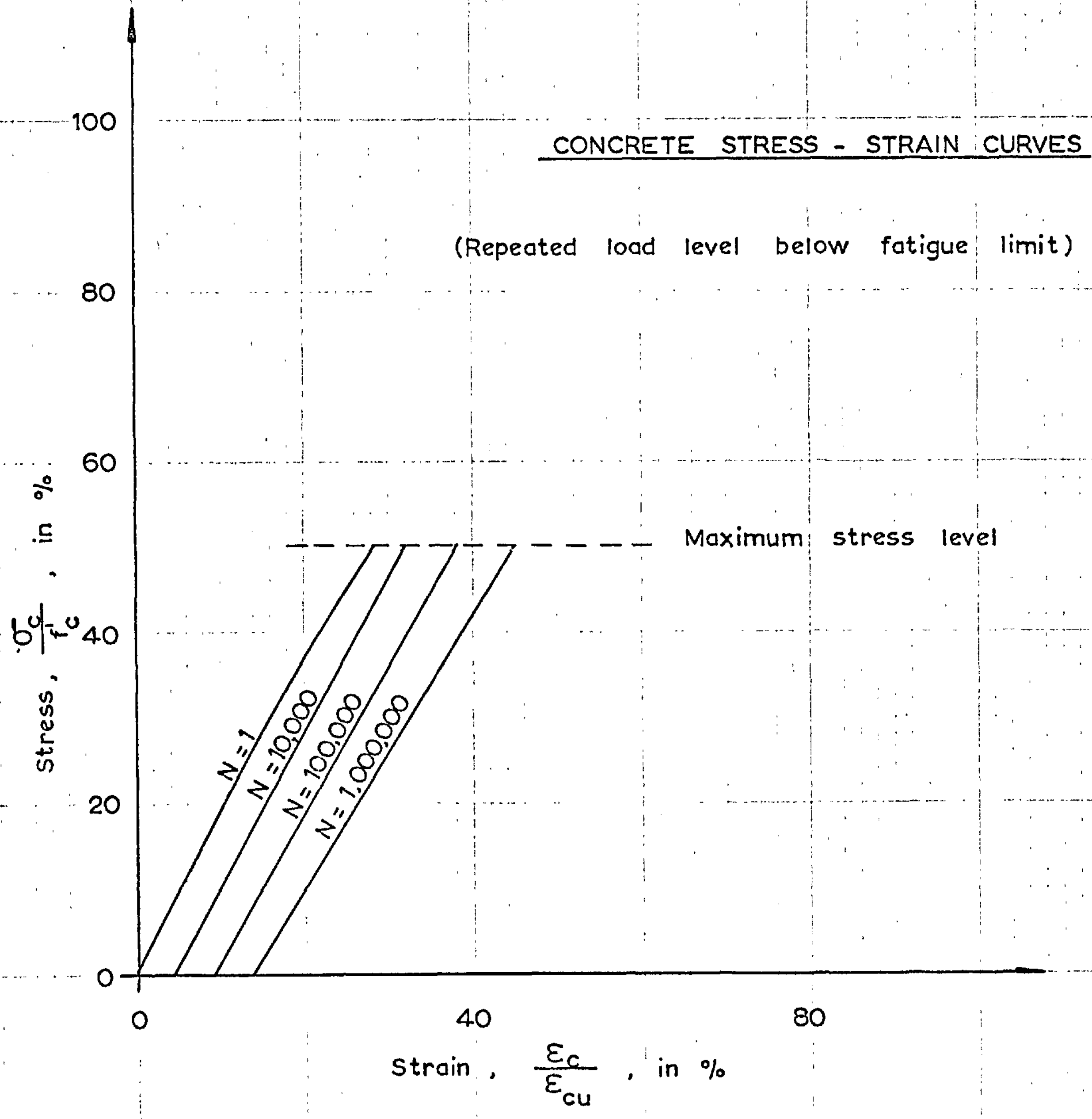
CONCRETE STRESS - STRAIN CURVES
(Repeated load level below fatigue limit)
Maximum stress level
N=1
N=10,000
N=100,000
N=1,000,000
Stress, $\frac{\sigma_c}{f'_c}$, in %
Strain, $\frac{\varepsilon_c}{\varepsilon_{cu}}$, in %
0
20
40
60
80
100
0
40
80

Fig.5.4

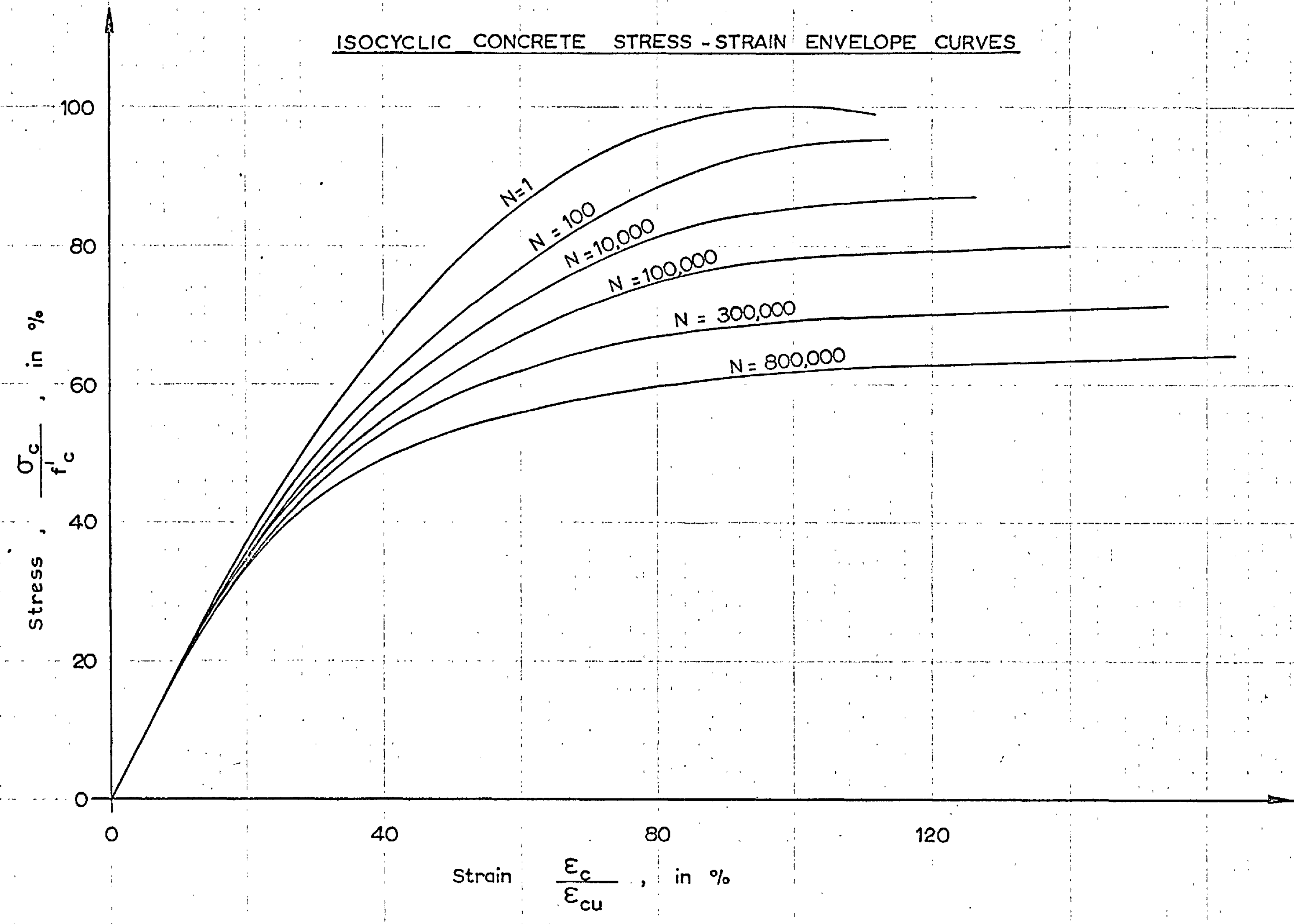
ISOCYCLIC CONCRETE STRESS - STRAIN ENVELOPE CURVES
N=1
N = 100
N = 10,000
N = 100,000
N = 300,000
N = 800,000
100
80
60
40
20
0
Stress , $\frac{\sigma_c}{f'_c}$, in %
0
40
80
120
Strain $\frac{\varepsilon_c}{\varepsilon_{cu}}$, in %

Fig. 5.5

CHAPTER 6

INVESTIGATION OF THE SHEAR STRENGTH IN FATIGUE OF POST-TENSIONED THIN-WEBBED I - BEAMS

TEST SERIES S

6.1) OBJECT AND SCOPE

The purpose of the test programme was to investigate the effect of repeated loading on the behaviour of thin - webbed post - tensioned I - beams with web reinforcement in which static failure occurred in diagonal tension.

It was intended that the diagonal tension cracks should originate entirely within the webs of the beams, and also that they should not be influenced by the presence of flexural - shear cracks in the shear span at any stage up to the ultimate load. It was further intended that an adequate factor of safety against flexural fatigue failure be provided at all possible levels of repeated loading.

Using the above requirements as a basis, a theoretical investigation was carried out to determine a suitable beam section and $^{a}/d$ ratio which satisfied the conditions. This investigation suggested that a beam section, as detailed in section 3.3b (i.e. 14" x 6" I - beam with $1\frac{1}{2}$" web, and 3/16" diameter mild steel stirrups at 8" centres) would be suitable, when tested at an $^{a}/d$ ratio of 3.40.

A preliminary beam, S1, was, therefore, cast and stressed to these specifications, and when tested statically to failure, behaved in a manner which was entirely suitable for the fatigue investigation. Diagonal tension cracking took place within the web in both shear spans before the occurrence of flexural cracking in the constant moment zone, and failure occurred in diagonal tension when a crack lead to instability of the top flange. At failure, the flexural cracks had not opened significantly, and a flexural failure did not appear to be at all imminent. The static ultimate flexural strength was estimated to be 30% greater than the static ultimate shear strength. The results of beam S1 are included in sections 6.2 and 6.4.

It was expected that preliminary fatigue tests would be necessary to determine the approximate values of the maximum load level which caused failure after the desired numbers of load cycles. The test series was designed such that four beams were tested at each of three different levels of the maximum repeated load, with the minimum load constant in all tests. The most practical range of number of load cycles is between 100,000 cycles and 1,000,000 cycles - in general, typical structures would not be designed or expected to fail in fatigue at less than 100,000 cycles, and load levels causing failure at greater than 1,000,000 cycles are very close to the fatigue limit, and a high proportion of non - failures are likely. It was, therefore, desired to obtain failure after approximately 100,000 cycles, 350,000 cycles and 1,000,000 cycles, since these values of N produced equal increments in log N. However, the values of the maximum load levels used in the preliminary fatigue tests were entirely satisfactory, and it was not, therefore, necessary to consider these as preliminary tests.

Beams which endured greater than 3,000,000 cycles of repeated loading in a cracked state were subsequently tested statically to failure. A total of four static tests to failure were carried out on beams which had no previous load history.

The final complete test programme was thus designed to provide information on diagonal tension cracking and failure under static loading and under repeated loading with varying values of the maximum load. The $^{a}/d$ ratio, geometric section properties, reinforcement ratio (prestressing steel and web reinforcement), prestressing force, and minimum repeated load level all remained constant throughout the tests.

Details of the beam section and loading conditions are given in fig. 3.6.

6.2) FATIGUE TESTS TO INVESTIGATE DIAGONAL TENSION CRACKING UNDER REPEATED LOADING.

6.2a) TEST PROCEDURE.

The test procedure was as described in section 4.3a, except that the tests were not stopped at intervals to take readings. Zero readings were taken before the commencement of the test, and again when the test was stopped. The instrumentation was as described in section 6.3a. The instant of diagonal tension cracking was determined by the drop which occurred in the maximum load on cracking - this operated the automatic cut - out on the pulsator (see section 3.10b).

The test speed was 400 cycles/min. The beams were subjected to two point loading as shown in fig 3.6, with an $^a/d$ ratio of 3.40.

The tests were stopped if cracking had not taken place after 3×10^6 load cycles.

6.2b) TEST RESULTS

Two beams, S10 and S11, were tested at repeated load levels below the static diagonal tension cracking load in order to determine the fatigue strength of concrete in tension in the webs of prestressed beams, and also to determine the effect of prior repeated loading on the diagonal tension cracking strength in a subsequent static test.

As discussed in section 4.5b, an accurate estimate of the static cracking strength of the specimen being considered is essential for precise calculations of the fatigue strength. Since all the beams except S10 and S11 were cracked under static loading in the first load cycle, it was possible to calculate the maximum principal tensile stress existing in the web at the instant of diagonal tension cracking in both shear spans for all these 15 beams. Assuming that the line joining the load and support points formed the path of the potential diagonal crack, (the cracks followed this line closely in almost all cases as seen in plates 6.1 to 6.7) it was shown by calculation that within the load range in which diagonal cracking occured in the beams, the maximum principal tensile stress along the line of the potential crack always occurred at the centroid. The principal tensile stresses existing at the centroid at the moment of diagonal cracking, f_{crws}, are given in table 6.1 and plotted against the cube strength, f_{cu}, as a ratio of f_{cu}, in fig. 6.1; they are plotted against the cylinder splitting strength, f_t, in fig. 6.2. The results in fig.6.1 indicate the existence of a relationship between the ratio, f_{crws}/f_{cu}, and f_{cu} - however, the best linear relationship incorporating all the points, as shown by the straight line in fig. 6.1, resulted in the fact that, with the cube strength, f_{cu}, changing from 6500 lbs/in^2 to 9000 lbs/in^2, the principal tensile stress at diagonal cracking changed from 371 lbs/in^2 to 376 lbs/in^2; since the mean principal tensile stress was 374 lbs/in^2, it was considered that the predicted tensile strength could be estimated as the mean tensile strength, $\overline{f_{crws}}$, within the range of concrete strengths considered. A relationship of the form,

$$f_{crws} = k\sqrt{f_{cu}}$$

was also considered, but it led to greater scatter in the values of the ratio, observed tensile strength/predicted tensile strength, and was, therefore, rejected.

In the tests on both S10 and S11, the minimum load level was 25% of the mean static ultimate shear strength, $\overline{V}_u$; under this load, the principal tensile stress in the web at the centroid was 70 lbs/in^2 (or 19.0% of $\overline{f_{crws}}$).

Beam S10 was subjected to repeated loading with a maximum load level of 55.9% of $\overline{V}_u$ - this created a maximum principal tensile stress in the web of 279 lbs/in^2, which was 74.6% of the predicted static tensile strength. After 1,696,000 load cycles, diagonal cracking occurred in the web in shear span W. Under static loading in the first cycle of the subsequent fatigue test, cracking took place in shear span E at a principal tensile stress of 353 lbs/in^2, which was 94.4% of the predicted tensile strength.

The maximum repeated load in the test on beam S11 was 55.0% of $\overline{V}_u$, and the maximum principal tensile stress in the web was 275 lbs/in^2, which was 73.6% of the predicted static tensile strength. The beam resisted 3,088,000 load cycles without the occurrence of diagonal cracking in either shear span, and in a subsequent static loading, cracking occurre in the web at principal tensile stresses of 100.0% and 116.1% of the predicted static tensile strength. As a proportion of these values, the stresses in the web in the repeated load test were 73.6% and 63.4% respectively. The results are included in table 6.1.

The results thus indicate that the fatigue strength at 3×10^6 cycles of concrete in tension in the web of prestressed I - beams is about 75% of the static tensile strength. This is significantly higher than the value of 65% which was obtained for the fatigue strength at 3×10^6 cycles of concrete subjected to reversed flexural stresses in a prestressed beam (see section 4.5b). The difference is even more significant when compared with the value of 60% which is generally accepted as the fatigue strength at 3×10^6 cycles of plain concrete subjected to flexural stresses (see section 2.1c). This increase in the fatigue strength may be due to the varying combined stresses which exist in the web, since the slope of the compressive stress trajectory is continually changing during a repeated load cycle - the effect of this may, therefore, be to restrain the propagation of micro - cracking. However, this cannot be stated to be conclusive since no investigations have been carried out to determine the effect of combined stresses on the fatigue strength of concrete.

The results also show that the prior history of repeated loading had no significant effect on the tensile strength of the concrete in a subsequent static test since the values of observed strength/predicted strength all lie within the expected scatter. However, although the prior history of repeated loading did not affect the tensile strength, it had a significant effect on the propagation of cracks as may be clearly seen from the crack pattern of beam S11 in plate 6.4. Instead of following closely the line joining the load and support points, the cracks were inclined at a much steeper angle to the axis of the beam and followed the line of intersection of the web and top flange over a considerable distance. Throughout the length of the web - flange intersection, it is likely that considerable stresses were in existence in the concrete due to the effects of differential shrinkage, and it is thus possible that the repeated loading advanced the propagation of micro - cracking along this line. Therefore, although the calculated principal tensile stresses at the web - flange interface were less than those at the centroid, the tensile strength was reduced at the top of the web, and cracking took place there before it occurred at the centroid. This change in the crack pattern had a considerable and detrimental effect on the fatigue strength of the beam in a cracked state (see section 6.4).

Both S10 and S11 were subsequently subjected to repeated loading in a cracked state since measurements of stirrup strains had shown that the stirrup stresses were quite negligible before diagonal cracking took place. It was, therefore, assumed that the prior repeated loading had no effect on the subsequent fatigue strength of the steel, fracture of which was the criterion of fatigue failure of the beams in all cases except S11.

6.3) STATIC TESTS TO FAILURE.

6.3a) TEST PROCEDURE

The experimental procedure in these tests was as described in section 4.2a, and the test conditions were identical to those in the fatigue tests described in sections 6.2 and 6.4.

Instrumentation consisted of dial gauges to measure deflections, and clinometers to measure rotations between the ends of the beams. The stirrups in beams S5 and S8 had 20 mm electrical resistance strain gauges attached to them at points which coincided with the line of the potential diagonal cracks, i.e. the line joining the load and support points. The strains on the top surface within the shear spans were determined by means of 8" demec gauges, and the width of diagonal cracks at the stirrups were determined by means of 12" demec gauges; the layout of the demec points is given in fig. 6.3.

All the beams (static and fatigue beams) were assigned to a random order of testing in order to minimize the statistical effects of changes in experimental procedure and manufacture of the specimens.

For the purposes of reference within the text and figures, the stirrups in each beam have been numbered as indicated in fig. 3.6.

6.3b) TEST RESULTS

In all, seven beams were tested statically to failure; four beams (S1, S5, S8 and S17) had no previous load history and were considered to form a sample which was representative of the static behaviour and strength of an infinite population of similar beams.

Beams S10, S12, and S13 all had a previous history of repeated loading and had endured more than 3×10^6 load cycles of intensities as given in table 6.3. Since no failure had occurred under repeated loading in these beams, they were tested statically to failure.

The crack patterns of the static beams are given in plates 6.1 to 6.7. The numbers on the beams in the plates indicate the load stage number - the shear forces corresponding to the load stage numbers are given in table 6.4.

Since all beams except S10 and S11 were cracked under static loading (in the first load cycle in the fatigue tests) it was possible to analyse all these results to determine the static diagonal tension cracking strength of the concrete in the beams - this has been included in section 6.2b.

The diagonal crack patterns in all the static beams were very similar except for S17, in which the cracks in the failure span (shear span, E) were inclined at a somewhat steeper angle to the beam axis than those in the other beams. In general, the cracks were parallel to the line joining the load and support points, and normally occurred close to this line. In all cases, diagonal cracking occurred suddenly without any prior indications, and resulted in a considerable and immediate drop in stiffness in the beam. The cracks always propagated immediately throughout the depth of the web, usually to points on the web - flange join about 5" from the load and support points. Cracking occurred quite independently in the two shear spans, often at considerably different loads. Diagonal cracking caused a major re-distribution of stresses within the shear span and resulted in a considerable increase in the stirrup stresses, which were quite negligible prior to diagonal cracking; yielding of the stirrups did not occur at this stage. Details of the principal tensile stresses in the web at diagonal cracking are given in table 6.1.

With further increase in load, the cracks continued to propagate slowly towards the load and support points, and at failure, they normally extended to within about 1" of these points. At higher loads, additional diagonal cracks often appeared, but the crack opening was generally concentrated at one major crack. Near failure, flexural and flexural - shear cracks occurred within the shear spans, but at no stage did these link up with the diagonal cracks in the web.

The imminence of shear failure in the beams was characterised by the appearance of a crack in the top flange within the shear span, as may be clearly seen in the plates. This crack was caused by the eccentricity of the compression thrust line acting on the concrete above the uppermost diagonal crack as shown in fig.6.4. The magnitude of the tension caused by this thrust was dependent to a large extent on the position and slope of the diagonal cracks - this is shown clearly by the crack patterns in the plates when reference is made to table 6.3, giving the loads at which cracking occurred in the top flange. These cracks occurred in beams S11 and S17 at considerably lower loads than in the remaining beams, and the crack patterns in these two beams were significantly different from the others; in both cases, the diagonal cracks travelled horizontally along the web - top flange interface over some distance before passing through the web. The result of this was to increase the eccentricity of the compressive thrust relative to the concrete above the diagonal cracks, thereby causing cracking in the top flange at lower loads than those in the beams with flatter diagonal cracks. This was undoubtably the reason for the lower static ultimate strength obtained for beam S17, and was the cause of the premature fatigue failure which occurred in beam S11 (see section 6.4). The distribution of strain in the top surface of the shear spans is shown in figs. 6.5 to 6.10 for various values of the shear force.

After the occurrence of cracking, in the top flange, it rapidly became unstable due to the eccentric thrust acting on it, and considerable rotation occurred about the apex of the crack as may be clearly seen in figs. 6.11 to 6.12, which show the deformation within the shear span. This soon led to crushing of the concrete at the head of the top flange crack, and complete collapse of the beam; the crushing may be seen clearly in the plates. This state of instability was accompanied by extensive opening of the diagonal cracks (see the shear force - diagonal crack width relationships in figs. 6.13 to 6.18), and consequent yielding of the stirrups. In all the relationships between the shear force and the diagonal crack width, there appeared to be a point at about 80% of the $\overline{V}_u$ at which the crack width was greater than that expected from the slope of the curves - it did not appear to have any significant effect on the subsequent behaviour of the beams. The shear force - diagonal crack width relationships given in figs. 6.13 to 6.18 are for the shear spans in which failure occurred. In all beams except S17, fracture of the stirrups occurred at failure, but this appeared to be a secondary effect and was not the primary cause of failure. This is borne out by the fact that in beam S17, yielding of the stirrups had not occurred (as shown by the shear force - diagonal crack width relationships in fig. 6.18) when a crack in the top flange led to instability and crushing of the concrete as described above.

The relationships between the shear force and the individual stirrup strains in beam S5 are given in figs. 6.19 and 6.20. Fig. 6.21 shows the relationship between the total shear force and the total stirrup force for beam S5 and all the fatigue test beams in which the stirrup strains were measured under maximum and minimum load during the first load cycle. The results indicate that once diagonal cracks occurred in the beams, the total force in the stirrups was closely approximated by the relationship:-

Total stirrup force $= 0.5\ V$

This relationship is shown by the straight line in fig. 6.21.

Prior to yielding, the strain distribution in the individual stirrups followed closely the distribution of the diagonal crack widths as shown in figs. 6.22 and 6.23. Although few results were obtained after the stirrups yielded, it is likely that this relationship continued to exist, although yielding probably resulted in considerable bond breakdown between the stirrups and adjacent concrete.

The mean static ultimate shear strength, $\bar{V}_u$, of the beams was 7.153 Tons (71.26 KN) with a coefficient of variation of 5.2%. The diagonal cracking loads, principal tensile stresses at diagonal cracking, top flange cracking loads, and ultimate strengths are given in tables 6.1 and 6.3.

Beams S10, S12, and S13 had all endured greater than 3×10^6 cycles of repeated loading in which the maximum load level was 62.9% of $\bar{V}_u$.

In beams S10 and S13, no stirrup fractures had occurred in fatigue, and the subsequent static behaviour of the beams was identical to that of the un - fatigued beams. The mean static ultimate shear strength of the two beams was 7.16 Tons (71.34 KN) - this represented an increase in strength over the mean of the un - fatigued beams of 0.1%; this was well within the expected scatter and indicated that the prior history of repeated loading had no significant effect on the static ultimate shear strength. When the results of S10 and S13 were included with the un - fatigued beams, the mean static ultimate strength was 7.155 Tons (71.29 KN) with a coefficient of variation, C_v, of 4.0%.

Three stirrups which had not fractured in fatigue were subsequently removed from the beams and tested to determine the effect of the repeated loading on the stress - strain characteristics of the steel. The previous load history of the stirrups is given in table 6.5. Only in stirrup E4 from beam S3 was the stress - strain relationship significantly different from that of the non - preloaded steel; it had endured 2,700,000 cycles with a maximum repeated load of 62.9% of $\overline{V}_u$, the stresses in the stirrups varying between 28% and 83% of the static ultimate strength, $\overline{f_{smu}}$, in each load cycle. The initial modulus of elasticity, E_s, was unchanged, but the limit of linearity was reduced considerably to about 50% of $\overline{f_{smu}}$, compared with a value of 90% of $\overline{f_{smu}}$ for the un - fatigued steel. Between 50% and 90% of $\overline{f_{smu}}$ the tangent modulus of elasticity was considerably less than that of the un - fatigued steel, and, furthermore, the bar did not show a definite yield point. The ultimate strength, however, showed an increase of 4.5% over the un - fatigued strength. The other stirrups, which had been subjected to higher stresses for smaller numbers of cycles, also showed a decrease in the limit of linearity, but the magnitude of the decrease in the tangent modulus of elasticity between 60% of $\overline{f_{smu}}$ and the yield stress was not great, and the ultimate strengths were only marginally increased. These changes in the stress - strain relationships of the stirrups appeared to have no significant effect on the static behaviour of the beams. The stress - strain curves are given in fig. 6.24.

Beam S12 had endured 4,962,000 cycles of repeated loading in which the maximum load level was 62.9% of $\overline{V}_u$. During this loading, stirrups W2, W3, and W4 had fractured in fatigue in shear span W, and stirrups E3 and E4 had fractured in shear span E. Thus, in shear span W, only one effective stirrup remained intact across the diagonal cracks. In the static test to failure, the diagonal crack width was considerably greater than that in beams S10 and S13 at all load levels, as may be seen in figs. 6.15 to 6.17. The beam failed in the same manner as all the other static beams at a load of 6.40 Tons (63.76 KN), which was 89.5% of $\overline{V}_u$. Thus, although the effective web reinforcement was reduced by 75%, the ultimate shear strength of the beam was only reduced by 10.5%; this indicates that, for the type of static shear failure obtained in the beams, the web reinforcement acts mainly to reduce the rotation about the apex of the top flange crack. In beam S12, cracking had occurred in the top flange under the maximum repeated load of 62.9% of $\overline{V}_u$, after fracture of the stirrups.

6.4) FATIGUE TESTS ON BEAMS WITH DIAGONAL TENSION CRACKS

6.4a) TEST PROCEDURE

The experimental procedure in these tests was as described in section 4.3a. The beams were tested in a random order as discussed in section 6.3a. The test speed employed was 400 cycles/min, and the beams were subjected to two - point loading as shown in fig.3.6, with an $^a/d$ ratio of 3.40.

If fatigue failure had not taken place after 3×10^6 cycles of repeated loading, the test was stopped, and the beam loaded statically to failure. The test on beam S12 was continued for 4,962,000 cycles since stirrup fractures had taken place before 3×10^6 load cycles had been completed, and it was, therefore, anticipated that complete failure would take place within this additional number of cycles; however, this was not the case, and the beam was loaded statically to failure.

Fracture of one stirrup resulted in only a small decrease in stiffness in the beam, and, therefore, to detect the instant of fracture, it was necessary to set the maximum load cut - out to the position of maximum sensitivity as described in section 3.10b. After the first fracture of a stirrup in the beam, the test was continued until the beam was unable to withstand the maximum applied load, and complete collapse occurred.

The instrumentation in the tests was as described in section 6.3a. The stirrups in beams S2, S3, S4, S6 and S7 had 20 mm electrical resistance strain gauges attached to them at the points which coincided with the line of the potential diagonal cracks (see section 6.2b). However, little success was achieved with these gauges under repeated loading, and few lasted longer than 10 load cycles, many even failing before this.

6.4b) TEST RESULTS

In all, thirteen beams with diagonal cracks were subjected to repeated loading. The only variable in the tests was the level of the maximum repeated load, the minimum load being kept constant at 25.2% of the mean static ultimate shear strength, $\overline{V}_u$. Four beams (S3, S10, S12 and S13) were tested with $V^{max} = 62.9\%$ of $\overline{V}_u$, four beams (S4, S6, S9 and S15) with $V^{max} = 69.9\%$ of $\overline{V}_u$, and five beams (S2, S7, S11, S14 and S16) with $V^{max} = 76.9\%$ of $\overline{V}_u$. Unavoidable variations occurred in the values of the effective prestressing force, P_e, (see table 6.1) and the concrete strengths (see table 6.2) but these differences were small, and it was assumed that they had no significant effect on the fatigue test results. Only beams S10 and S11 had any prior history of repeated loading, and in the test on beam S10, it was assumed that this had no significant effect on the fatigue strength of the beam for the reasons given in section 6.2b.

The behaviour of the beams followed a similar pattern in all cases (except beam S11), and, therefore, the descriptions are not divided into sub - sections for each level of the maximum repeated load. The patterns of behaviour are detailed in terms of crack patterns and crack propagation, deformations, and characteristics and criterion of failure.

The beams were all cracked during the first cycle of load. The descriptions and analysis of diagonal cracking under static loading have been included in section 6.2b and section 6.3b. The crack patterns of the beams are shown in plates 6.1 to 6.7; the numbers on the cracks refer to the limit of the cracks at the number of load cycles stated. Some extension of the cracks towards the load and support points took place under repeated loading, particularly during the early load cycles, but after about 10,000 cycles, no further visible propagation of cracks was observed until stirrup fractures took place. In no case did any new diagonal cracks occur in the web under repeated loading. The spalling and wearing away of concrete which was observed at the flexural cracks in series F (see sections 4.6 and 4.7) did not occur to any great extent, due to the fact that the diagonal cracks did not close under the minimum load. In the beams tested with the maximum load level $= 76.9\%$ of $\overline{V}_u$, flexural cracking occurred in the constant moment zone, but the cracks did not propagate above the level of the bottom flange and no flexural fatigue failures were obtained.

The few results that were obtained for the stirrup strains in the beams indicated that little change occurred in the strains under repeated loading, and in some cases, the strains decreased with load cycling (see figs. 6.25 to 6.26) from the value obtained in the first cycle of load. Contrary to this, the diagonal crack widths (measured at the points where they were crossed by stirrups) increased considerably under repeated loading (see figs. 6.27 to 6.34), reaching a virtually stable state condition after about 10,000 load cycles; after this, the crack widths only increased slowly with increasing numbers of load cycles. In general, the stable state crack width was about twice that in the first cycle of loading, but in some cases, the increases were even greater. The relationships between the diagonal crack widths and the number of cycles given in figs. 6.27 to 6.34 are the maximum values (across the stirrups) which occurred under maximum and minimum load in each shear span of the beam concerned. The results thus indicate that the increase in the diagonal crack width was brought about by progressive bond breakdown between steel and concrete along the length of the stirrups. This is supported by the fact that, in several cases, fatigue fracture of the stirrups took place at some distance from the diagonal cracks, and in two beams, the fracture took place at the bend in the stirrup in the top flange, 8" away from the diagonal crack (see plate 6.9). Visual examination of the stirrups after removal from the beams also showed evidence of the occurrence of slip over a considerable distance.

The measured stirrup strains under maximum and minimum load showed considerable variation between beams which were subjected to repeated loading of the same magnitude; the individual values appeared to be very sensitive to small changes in the crack patterns. Further evidence of this is shown by the variations which occurred in the magnitudes of the diagonal crack widths (see figs. 6.27 to 6.34).

The diagonal crack width - number of cycles relationships thus show that after a short initial period, the deformations within the beams settled down to almost constant values. In no case was there any prior indication of the imminence of a stirrup fracture - the first fracture of a stirrup within the beam resulted in a considerable increase in the diagonal crack width at that point, but the stiffness of the beam was only reduced by about 8%. One of the two stirrups in the centre of the shear span (i.e. W3, W4, E3, or E4) was always the first to fracture in fatigue. After a short period, the beam again settled down to give a fairly constant response to load. Contrary to the behaviour of the beams in the flexural tests in series F, a considerable number of cycles were often resisted between the first and second fatigue fractures.

Complete failure of the beams was considered to have occurred when they were unable to resist the maximum repeated load. Prior indication of the imminence of beam failure was given in all cases by the appearance of vertical cracks in the top flange within the shear span as described in section 6.3b. The occurrence of these top flange cracks was brought about by the extensive opening of the diagonal cracks under maximum load due to the stirrup fractures. The final failure mode was identical to the static failure mode described in section 6.3b; i.e. crushing of the concrete at the apex of the top flange cracks. It is significant to note here the results given in table 6.7 - the results show that, in all beams tested with a maximum load level of 76.9% of $\bar{V}_u$, fatigue fracture of the two centre stirrups led to complete failure of the beam. In the beams subjected to a maximum load of 69.9% and 62.9% of $\bar{V}_u$, fatigue fracture of all four effective stirrups took place before complete failure of the beams occurred. Furthermore, beam S12, which had three fractured stirrups, withstood 89.5% of $\bar{V}_u$ in a subsequent static test, although the beams subjected to repeated loading at 76.9% of $\bar{V}_u$ failed with only two stirrup fractures. This indicates that the final failure of the beams subjected to 76.9% of $\bar{V}_u$ was due to fatigue failure of the concrete at the apex of the top flange crack; after the occurrence of cracking in the top flange, this concrete was subjected to high stresses, which caused failure after a small number of load cycles. The strain distributions in the top surface of the beams are given in figs. 6.35 to 6.38; the curves show that in no case, except S11, did cracks occur in the top flange before fatigue fracture of stirrups took place.

The position of the top flange crack was determined by the diagonal crack pattern within the web - if the diagonal cracks propagated along the top flange - web join for any distance, then the crack occurred in the top flange above the point where the diagonal crack left the web - flange intersection and passed into the web (see beams S1 to S11, S13, S14 and S17). If the diagonal cracks did not travel along the web - top flange join, then several cracks normally occurred in the top flange, the critical crack being a distance of about half the effective beam depth from the support point (see beams S12, S13 and S16).

Therefore, although the final failure always occurred due to crushing of concrete and instability of the top flange, fatigue fracture of the stirrups was the initial criterion of failure in all cases.

Although the individual stirrup stresses and crack widths were subject to considerable variation between beams under the same maximum loads, the values obtained for the fatigue life were in good agreement, considering the presence of the basic scatter which is inherent in the results of all fatigue tests. It appears likely that, when embedded in beams, the stirrups were subjected to several phenomena which had an adverse effect on the fatigue strength of the steel. Visual examination of the stirrups, after the tests, showed the presence of considerable oxidation along the length of the stirrups, indicating that extensive fretting had taken place under repeated loading - this is clearly shown in plate 6.9. Secondly, the opening of the diagonal cracks caused shear deformations in the stirrups - under maximum load, this induced additional bending, as well as shear stresses into the steel. This also served to accentuate the effect of fretting by increasing the lateral pressure on the stirrups. Two fatigue fractures occurred in the bend at the top of the stirrups - this was probably due to the residual stresses induced by bending the bars. The majority of fractures occurred at the diagonal cracks, but several occurred some distance away from the cracks.

The results obtained for the fatigue strength of steel strand when embedded in a concrete beam (see section 4.7c) showed that the parameters which had the greatest effect on the fatigue life of the steel were the maximum stress, minimum stress, and the effect of fretting, represented by the magnitude of the relative slip between steel and concrete. Assuming that the minimum stress in the stirrups was constant for all the beams, the magnitude of the diagonal crack opening in each load cycle was dependent upon the maximum stress in the stirrups, and the relative slip between steel and concrete at the position of the diagonal crack. The measured crack openings (i.e. $w_{cr}^{max} - w_{cr}^{min}$) at stirrup fracture positions were, therefore, plotted in fig. 6.42 against log N_1. The results show considerable scatter, but the curve follows the usual shape of S - N relationships. It is possible that some of the scatter was due to different combinations of the two variables, maximum steel stress and relative slip, in the various beams. The relationships between the maximum repeated load,

V_{max}, expressed as a percentage of $\bar{V}_u$, and the number of cycles to first stirrup fracture, N_1, and the number of cycles to complete beam failure, N_f, are given in a semi - log plot in figs. 6.43 and 6.44 respectively. The curves indicate that the fatigue limit of the beam was about 61% of $\bar{V}_u$

As stated previously, complete collapse did not occur rapidly after fracture of the first stirrup, and most of the beams endured a considerable number of additional load cycles before failure. The number of cycles to first stirrup fracture, N_1, and the number of cycles to complete beam failure, N_f, are given in tables 6.6 & 6.7, together with the values of the ratio N_f/N_1 for the shear spans in which final failure took place. The relationship between the mean values of N_f/N_1 for each maximum load level and $\bar{N}_1$, plotted in fig. 6.45, is virtually linear within the values of $\bar{N}_1$ obtained in the tests. The results show that, in the region just above the fatigue limit, the total life of the beam is far in excess of the number of cycles required to cause fracture of one stirrup.

The test on beam S11 formed an important exception to the general behaviour of the beams under repeated loading. The beam was subjected to 3,088,000 cycles of repeated loading in an uncracked state, and when the beam was subsequently cracked, the diagonal crack pattern was significantly different from the remainder of the beams, as described in section 6.2b. Beam S11 was then subjected to repeated loading with the maximum load = 76.9% of $\bar{V}_u$. In the first cycle of loading, vertical cracks appeared in the top flange in both shear spans, as shown in plate 6.4, and it was immediately obvious that failure was imminent. After 2,800 load cycles, the concrete at the apex of the top flange crack in shear span W crushed, and the beam collapsed. No stirrup fractures had taken place. The high alternating stresses in the concrete at the apex of the top flange crack had obviously caused fatigue failure in compression to take place without the prior stirrup fractures which occurred in all the other beams. The low fatigue life obtained for this beam thus illustrates very clearly the importance of the position and inclination of the diagonal cracks. The result obtained for this beam was excluded from the statistical analysis.

6.4c) STATISTICAL ANALYSIS OF FATIGUE TEST DATA

For the reasons discussed in section 4.8d, statistical analysis of fatigue test data is essential in all investigations if any significance is to be placed on the results. The considerable scatter which exists in all experimental fatigue data results in the fact that the mean S - N curve is an inadequate representation of the fatigue properties of the specimen and it is thus necessary to introduce the additional parameter of probability, PR. It is, therefore, assumed that the test results at each maximum stress level form a representative sample, taken from an infinite population of values which are distributed about a certain mean value. In the analysis which follows, it has been assumed that the logarithm of the fatigue life is normally distributed, which leads to the fact that the probability, PR, is given by the cumulative normal distribution function as detailed in section 4.8d and section 5.5 (equation 5.28). Table 6.8 gives summarised details of the test data, mean values, standard deviations, and coefficients of variation. In determining the values of the mean fatigue life at the maximum load level of 62.9% of $\overline{V}_u$, the run - out values were included in the analysis since this leads to a more accurate (although still a lowerbound) estimate of the mean fatigue life than if they were excluded. However, since only one value was obtained for N_f at this load level, no reasonable estimate of the standard deviation was possible and a value of 0.35 was, therefore, assumed for continuity of the curves in the figure - it must be emphasised that this was merely an estimate from the trends of the standard deviation - log N curves given in fig.4.46. It is significant to note that these relationships did not follow the same form as those obtained for steel strand, since the standard deviation increased at low values of N in the beam tests of series S. A possible reason for this was that at this high load level, the true value of the maximum load (as a proportion of the actual static ultimate strength) varied significantly from the value of $\overline{V}_u$ used in the calculations. The full S - N - PR curves have been plotted in figs. 4.47 and 4.48 for both N_1 and N_f for probabilities of failure, PR, ranging from 0.05 to 0.95.

TABLE 6.1

PRESTRESSING AND STATIC DIAGONAL TENSION CRACKING DETAILS

Beam No.	Final Prestressing force, P_e	Shear span W		Shear span E	
		Principal tensile stress at diagonal cracking, f_{crws}	$\frac{f_{crws}}{\overline{f}_{crws}}$	Principal tensile stress at diagonal cracking, f_{crws}	$\frac{f_{crws}}{\overline{f}_{crws}}$
	lbs	lbs/in^2		lbs/in^2	
S1	41,920	327	0.875	402	1.076
S2	41,440	314	0.840	387	1.035
S3	41,530	321	0.859	319	0.853
S4	41,990	386	1.033	328	0.876
S5	42,050	357	0.955	357	0.855
S6	42,270	373	0.998	379	1.014
S7	41,910	327	0.875	440	1.177
S8	41,800	390	1.043	395	1.057
S9	41,610	382	1.022	342	0.915
S10*	40,290	-	-	353	0.944
S11*	39,670	374	1.000	434	1.161
S12	41,820	381	1.019	387	1.035
S13	40,680	393	1.051	393	1.051
S14	41,850	358	0.958	375	1.003
S15	40,730	375	1.003	375	1.003
S16	41,150	402	1.076	402	1.076
S17	40,300	442	1.183	364	0.974

* Beams had a previous load history.

Mean diagonal tension cracking strength, $\overline{f}_{crws} = 373.8$ lbs/in^2.

TABLE 6.2.

CONCRETE PROPERTIES - SERIES S

Beam No.	6" Cube strength f_{cu}		Modulus of rupture strength f_r		Cylinder splitting strength f_t	
	lbs/in^2	N/mm^2	lbs/in^2	N/mm^2	lbs/in^2	N/mm^2
S1	7548	52.0	587	4.04	423	2.92
S2	9039	62.3	983	6.78	578	3.98
S3	8288	57.1	820	5.65	573	3.95
S4	8439	58.2	880	6.07	571	3.94
S5	9130	62.9	842	5.81	569	3.92
S6	8645	59.6	860	5.93	634	4.37
S7	8946	61.7	858	5.92	585	4.03
S8	8605	59.3	660	4.55	470	3.24
S9	7326	50.5	647	4.46	506	3.49
S10	6855	47.3	620	4.27	422	2.91
S11	7874	54.3	620	4.27	446	3.08
S12	6662	45.9	573	3.95	490	3.38
S13	7867	54.2	775	5.34	534	3.68
S14	6994	48.2	687	4.74	495	3.41
S15	8217	56.6	663	4.57	511	3.52
S16	7444	51.3	670	4.62	487	3.36
S17	7724	53.2	560	3.86	435	3.00

TABLE 6.3.

RESULTS OF STATIC TESTS TO FAILURE

Beam No.	Shear force at Diagonal tension cracking, V_{crws}		Prior load history in cracked state		Shear force at top flange cracking	Static Ultimate shear strength, V_u
	Shear span W	Shear span E	$\frac{V^{max}}{\overline{V}_u}$	No. of cycles endured		
	Tons	Tons	%		Tons	Tons
S1	4.60	5.25	-	-	6.95	7.21
S5	4.75	4.75	-	-	7.31	7.55
S8	5.02	5.07	-	-	6.98	7.20
S17	5.40	4.74	-	-	6.65	6.65
S10	-	4.65	62.9	3,871,000	7.01	7.17
S12	4.95	5.00	62.9	4,962,000	4.50	6.40
S13	5.00	5.00	62.9	3,932,000	6.96	7.15

Mean static ultimate shear strength, $\overline{V}_u$, = 7.153 Tons

TABLE 6.4

SHEAR FORCES CORRESPONDING TO LOAD STAGE NUMBERS ON PLATES

Beam S5			Beam S8			Beam S10			Beam S12			Beam S17		
Load Stage No	Shear force, V	$\frac{V}{V_u}$	Load Stage No.	Shear force, V	$\frac{V}{V_u}$	Load Stage No.	Shear force, V	$\frac{V}{V_u}$	Load Stage No.	Shear force, V	$\frac{V}{V_u}$	Load Stage No.	Shear force, V	$\frac{V}{V_u}$
	Tons	%		Tons	%		Tons	%		Tons	%		Tons	%
1	1.00	14.0	1	1.00	14.0	1	2.80	39.1	1	1.80	25.2	1	1.00	14.0
2	2.01	28.1	2	2.00	28.0	2	3.80	53.1	2	2.80	39.1	2	2.00	28.0
3	3.00	41.9	3	3.00	41.9	3	4.50	62.9	3	3.80	53.1	3	3.01	42.1
4	4.00	55.9	4	4.00	55.9	4	5.20	72.7	4	4.50	62.9	4	4.00	55.9
5	4.78	66.8	5	5.02	70.9	5	5.70	79.7	5	5.00	69.9	5	5.00	69.9
6	5.31	74.2	6	5.07	70.9	6	6.10	85.3	6	5.42	75.8	6	5.50	76.9
7	5.72	79.9	7	5.57	77.8	7	6.41	89.6	7	5.65	79.0	7	5.90	82.5
8	6.10	85.3	8	6.02	84.1	8	6.70	93.6	8	5.85	81.8	8	6.35	88.7
9	6.45	90.1	9	6.40	89.4	9	7.01	98.0	9	6.05	84.6	9	6.65	93.0
10	6.73	94.1	10	6.67	93.2	10	7.17	100.2	10	6.26	87.5	-	-	-
11	6.98	97.6	11	6.98	97.6	-	-	-	11	6.40	89.4	-	-	-
12	7.15	99.9	12	7.20	100.6	-	-	-	-	-	-	-	-	-
13	7.31	102.2	-	-	-	-	-	-	-	-	-	-	-	-

TABLE 6.5

LOAD HISTORY OF STIRRUPS

Beam No.	Stirrup No.	Previous Maximum load level, $\frac{V^{max}}{\overline{V}_u}$ %	Number of cycles endured
S3	E4	62.9	2,700,000
S4	W4	69.9	828,000
S7	W4	76.9	137,000

TABLE 6.6

RESULTS OF FATIGUE TESTS ON BEAMS WITH DIAGONAL TENSION CRACKS

Beam No.	Maximum load level, $\frac{V^{max}}{\bar{V}_u}$	Number of cycles to first stirrup fracture, N_1		Number of cycles to complete beam collapse, N_f	Shear span in which complete collapse occurred
		Shear span W	Shear span E		
	%				
S3	62.9	1,007,000	-	2,700,000	W
S10	62.9	3,871,000 →	3,871,000 →	3,871,000 →	-
S12	62.9	808,500	2,815,000	4,962,000 →	-
S13	62.9	3,932,000 →	3,932,000 →	3,932,000 →	-
S4	69.9	-	463,000	828,000	E
S6	69.9	304,000	285,000	350,000	E
S9	69.9	240,000	631,000	734,000	W
S15	69.9	320,200	503,400	1,010,000	W
S2	76.9	-	159,000	226,000	E
S7	76.9	83,000	130,000	137,000	E
S14'	76.9	34,000	-	48,600	W
S16	76.9	79,300	56,100	82,000	E
S11	76.9	-	-	2,800	W

$$\frac{V^{min}}{\bar{V}_u} = 25.2\%$$

$\bar{V}_u$ = 7.153 Tons = 16,020 lbs (71.26 KN)

TABLE 6.7

DETAILS OF STIRRUP FATIGUE FRACTURES

Beam No.	Ratio, $\frac{N_f}{N_1}$, for shear spans in which complete collapse occurred	Mean value of ratio, $\frac{N_f}{N_1}$, for each load level	Number of stirrup fractures at end of test.		Shear span in which complete collapse occurred
			Shear span W	Shear span E	
S3	2.68	4.41	4 (W2,W3,W4 & W5)	-	W
S10	-		-	-	-
S12	6.14*		3 (W2,W3 & W4)	2 (E3 & E4)	-
S13	-		-	-	-
S4	1.79	2.31	-	4 (E2,E3,E4 & E5)	E
S6	1.23		1 (W3)	4 (E2,E3,E4 7 E5)	E
S9	3.06		4 (W2,W3,W4 & W5)	1 (E4)	W
S15	3.16		4 (W2,W3,W4 & W5)	2 (E3 & E4)	W
S2	1.42	1.34	-	2 (E3 & E4)	E
S7	1.05		1 (W3)	2 (E3 & E4)	E
S14	1.43		2 (W3 & W4)	-	W
S16	1.47		1 (W3)	2 (E3 & E4)	E

*Lowerbound value

TABLE 6.8

SUMMARY OF FATIGUE TEST DATA

	Maximum load level, $\frac{V^{max}}{\bar{V}_u}$	Sample size, n	Mean fatigue life, $\bar{N}$	Standard deviation of N, S	Coefficient of variation of N, C_v	Mean of Log N, $= \overline{\log N}$	$\log^{-1}(\overline{\log N})$	Standard deviation of log N, s
	%				%			
First stirrup fracture, N_1	62.9	5	2,486,700*	1,132,000	45.5	6.3085*	2,034,000*	0.2892
	69.9	7	392,400	142,600	36.3	5.5701	371,600	0.1530
	76.9	6	90,200	46,500	51.6	4.9024	79,900	0.2431
Complete beam collapse, N_f	62.9	4	3,886,000*	-	-	6.5774*	3,779,000*	-
	69.9	4	730,500	278,300	38.1	5.8330	680,800	0.2008
	76.9	4	123,500	77,400	62.7	5.0233	105,500	0.2871

*Lowerbound values.

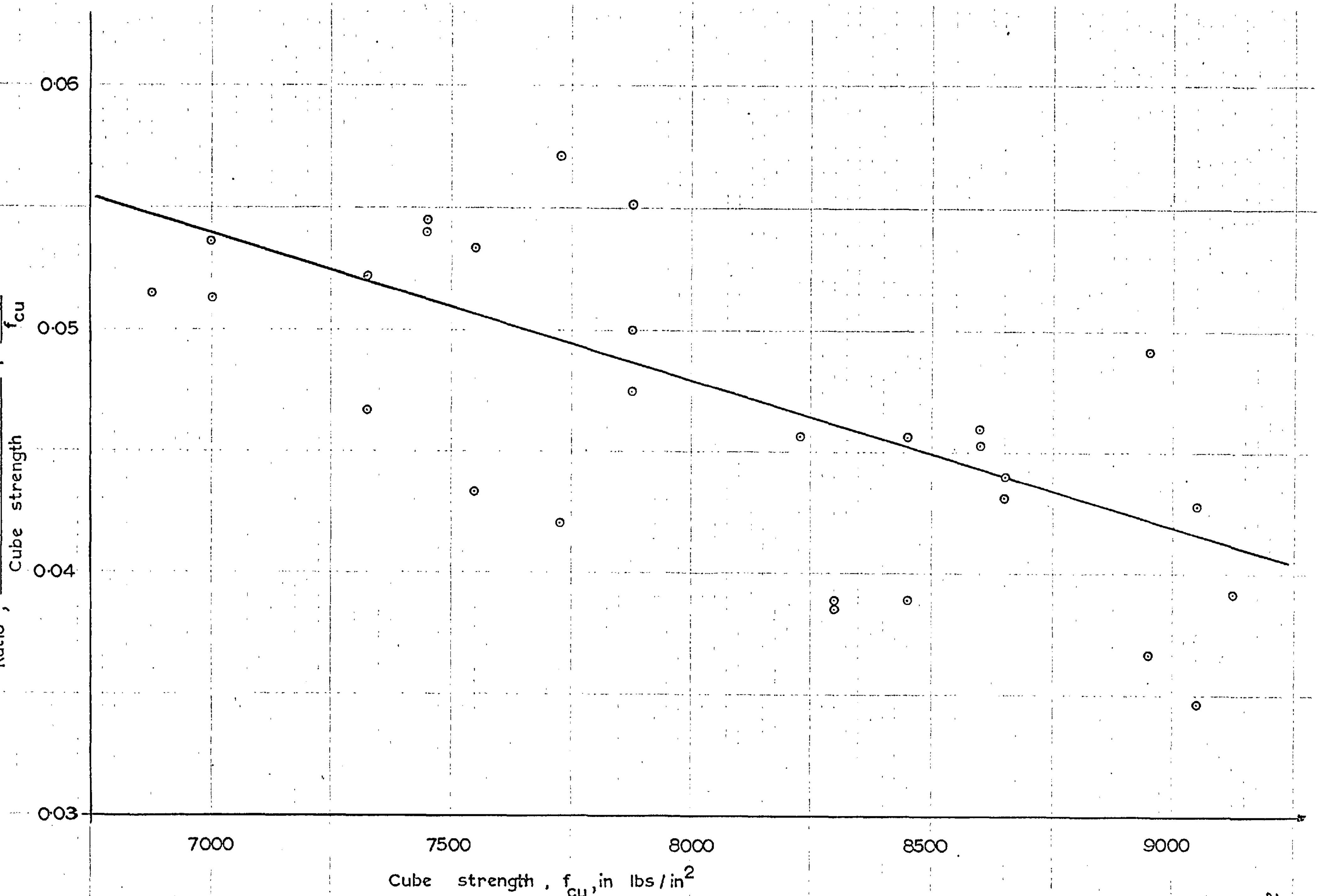
0·06
0·05
0·04
0·03
Ratio , $\frac{\text{Principal tensile stress}}{\text{Cube strength}}$, $\frac{\sigma_{cg}}{f_{cu}}$
7000
7500
8000
8500
9000
Cube strength , f_{cu}, in lbs / in^2

Fig. 6.1

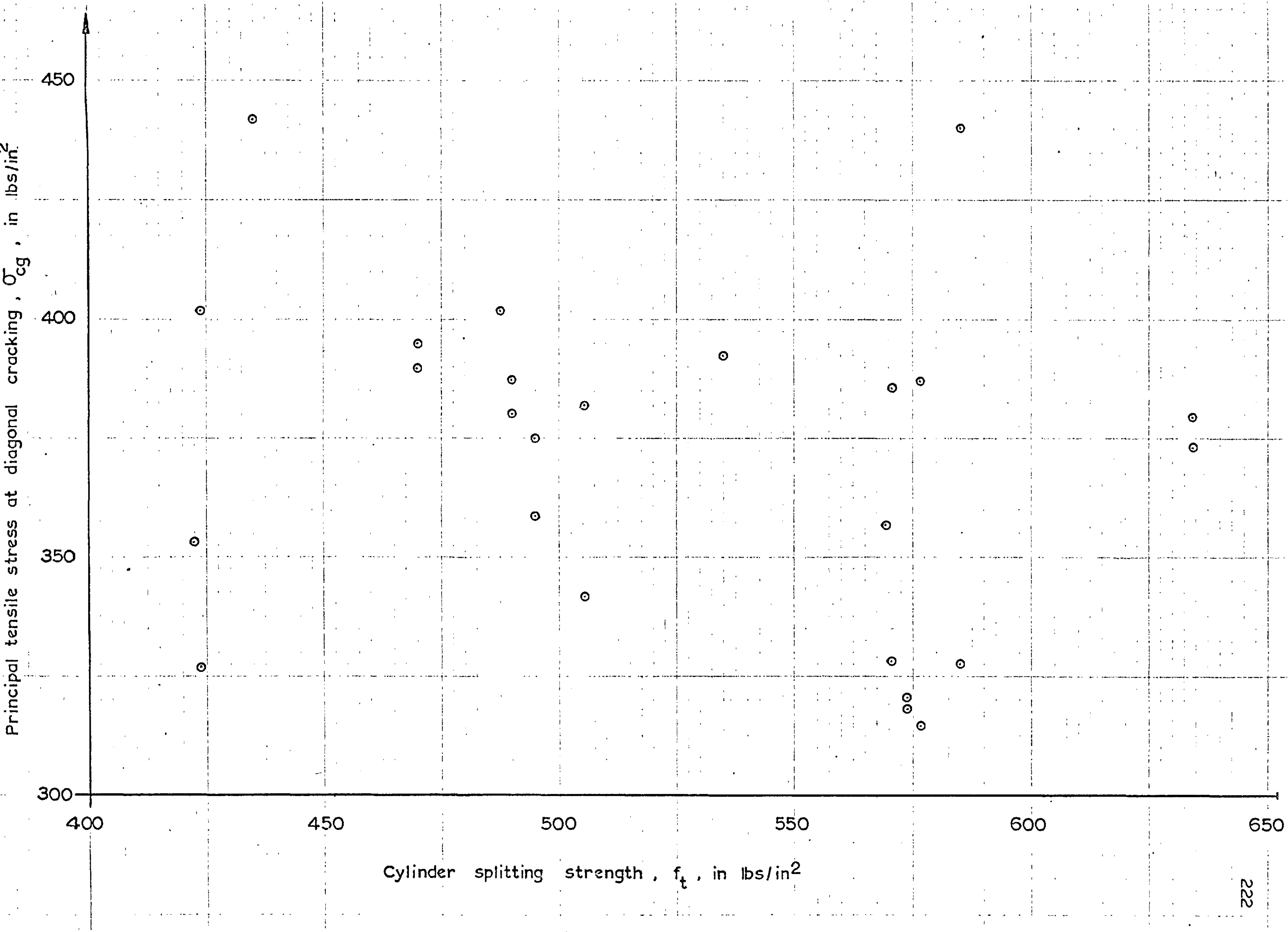

Principal tensile stress at diagonal cracking , σ_{cg} , in lbs/in^2
450
400
350
300
400
450
500
550
600
650
Cylinder splitting strength , f_t , in lbs/in^2

Fig. 6.2

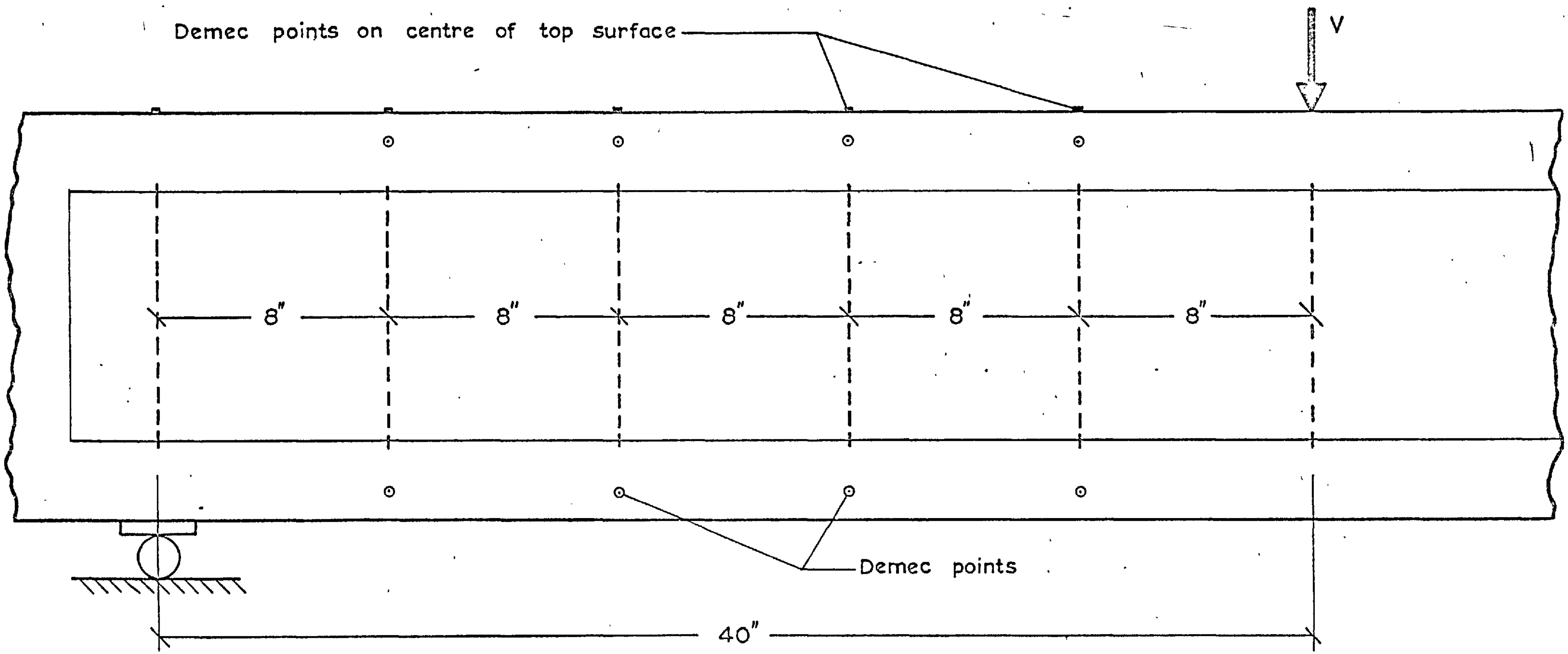

LAYOUT OF DEMEC POINTS — SERIES S.

(Dotted lines indicate stirrups)

Fig. 6.3

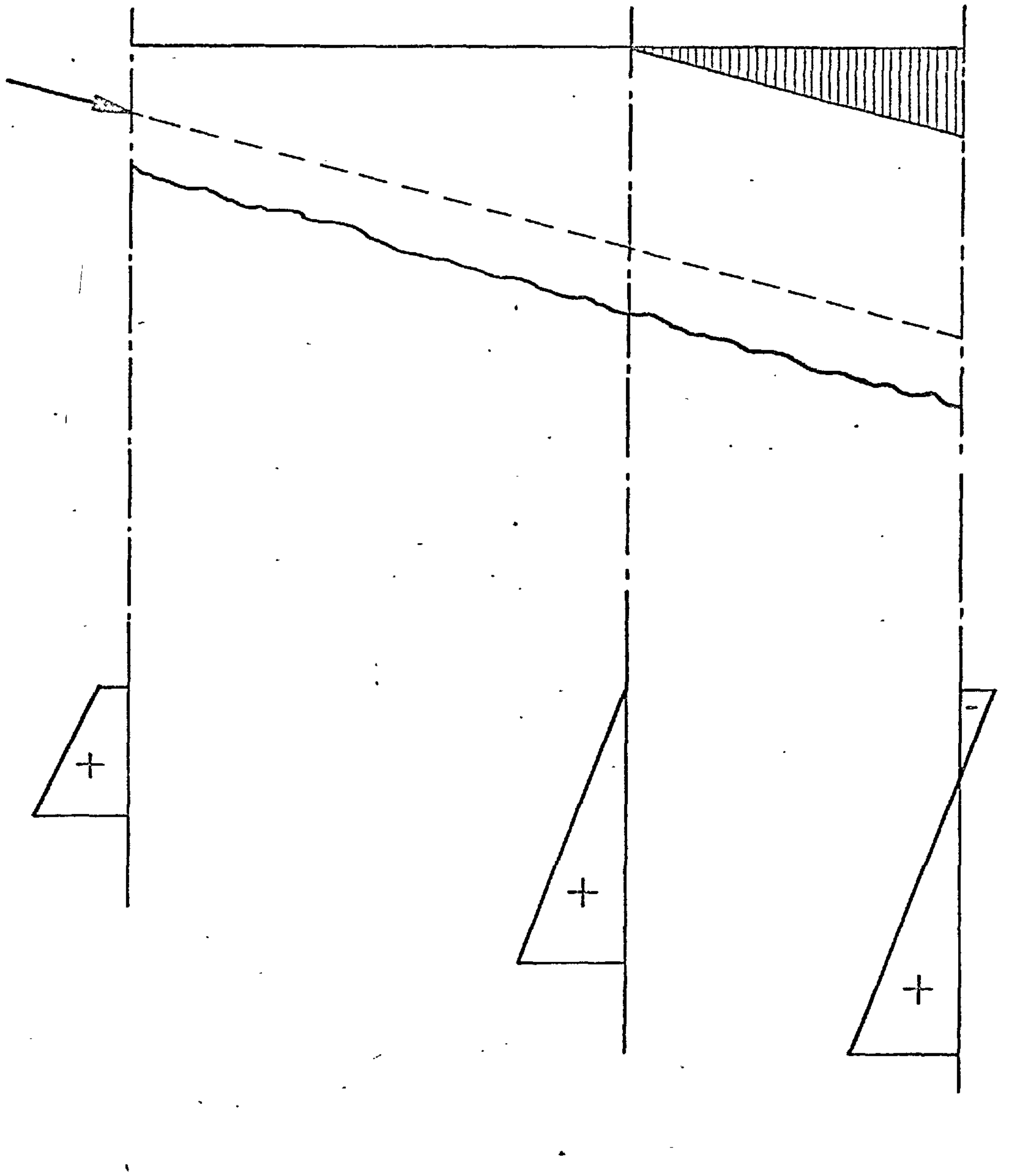

CONCRETE STRESS DISTRIBUTIONS ABOVE DIAGONAL CRACKS

(Shaded area represents concrete in tension)

Fig. 6.4

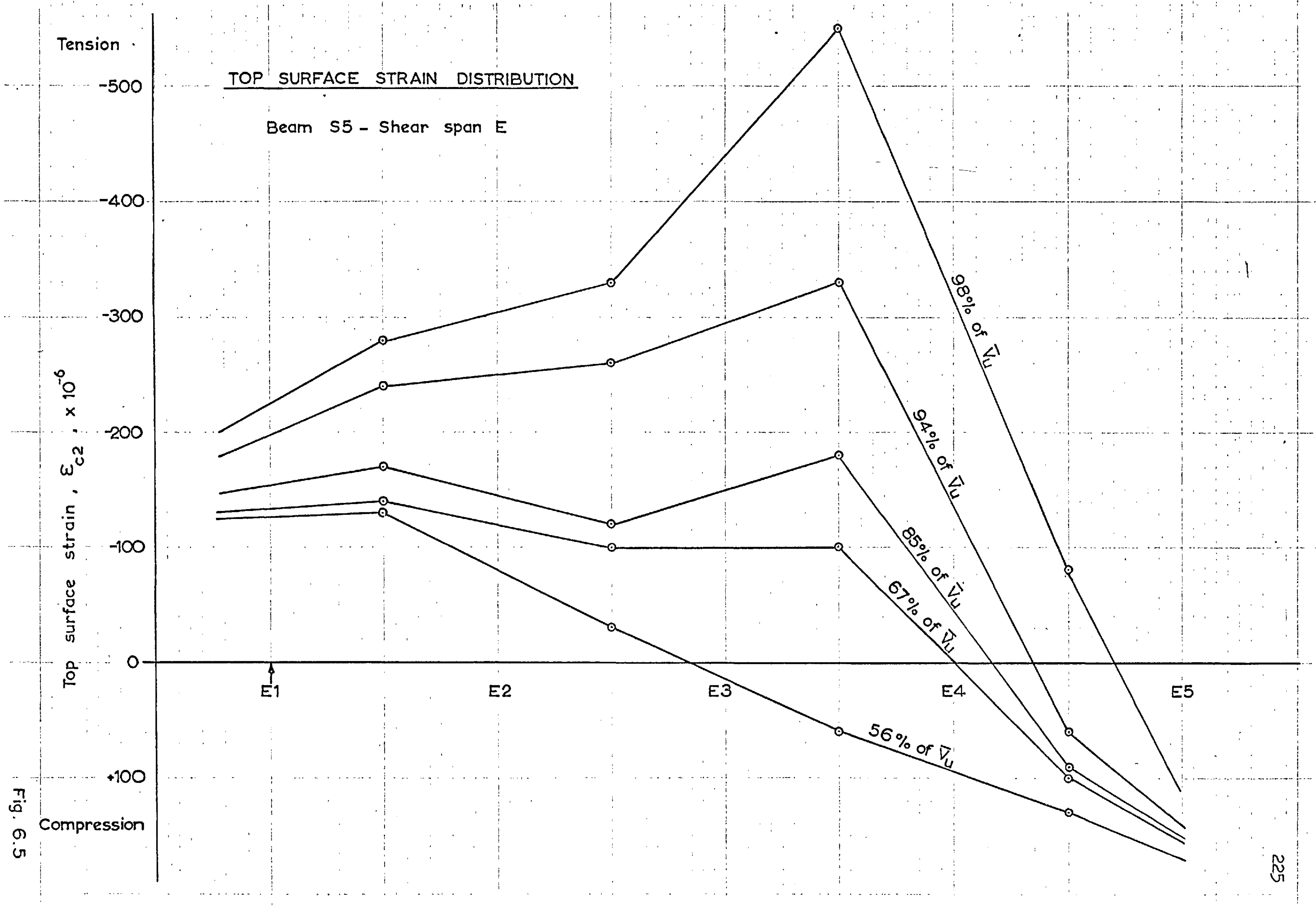

TOP SURFACE STRAIN DISTRIBUTION
Beam S5 - Shear span E
Tension
Compression
Top surface strain , ε_{c2} , x 10^{-6}
-500
-400
-300
-200
-100
0
+100
E1
E2
E3
E4
E5
98% of $\bar{V}_u$
94% of $\bar{V}_u$
85% of $\bar{V}_u$
67% of $\bar{V}_u$
56 % of $\bar{V}_u$

Fig. 6.5

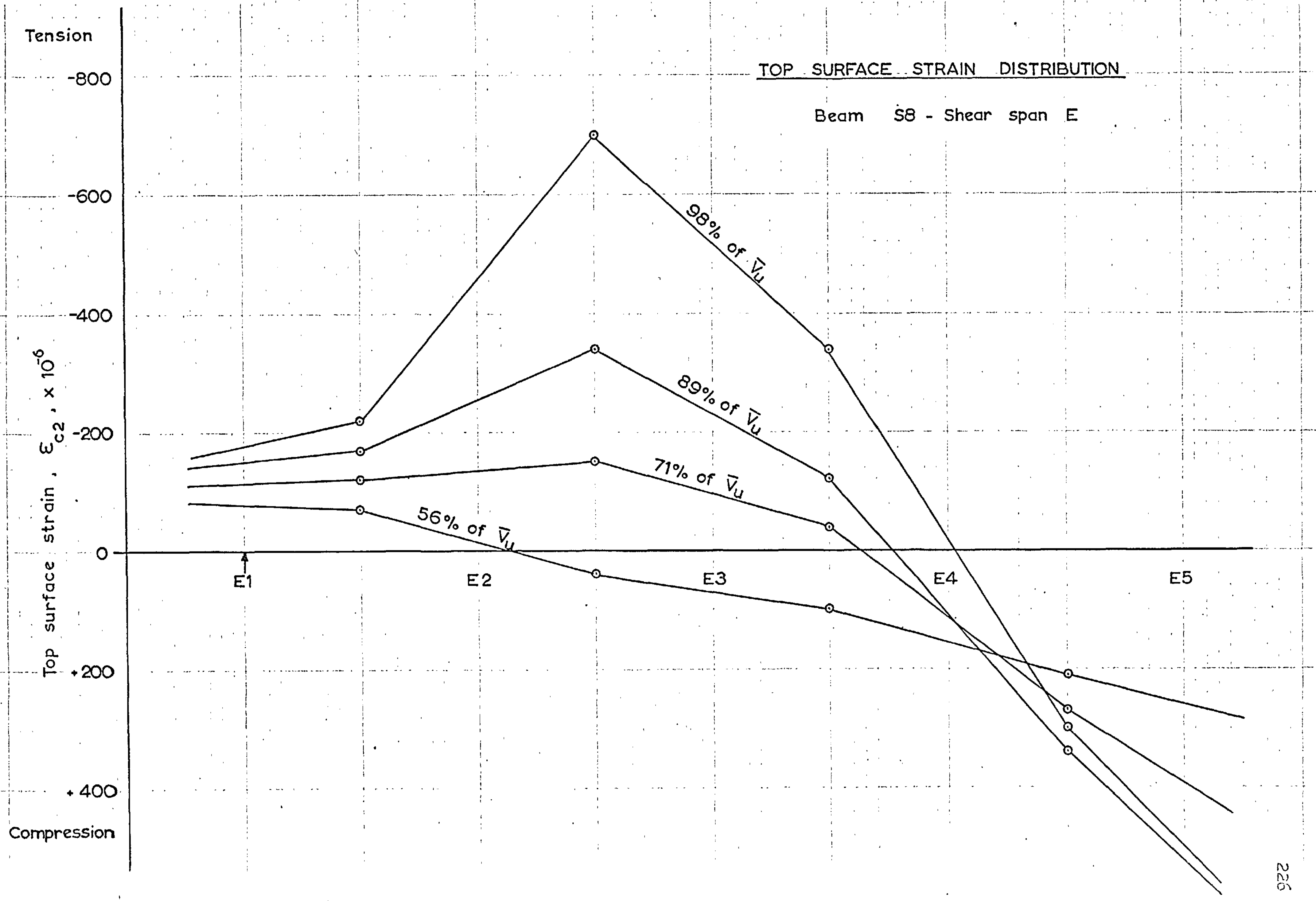
TOP SURFACE STRAIN DISTRIBUTION
Beam S8 - Shear span E
Tension
Compression
Top surface strain , ε_{c2} , $\times 10^{-6}$
-800
-600
-400
-200
0
+200
+400
E1
E2
E3
E4
E5
98% of $\bar{V}_u$
89% of $\bar{V}_u$
71% of $\bar{V}_u$
56% of $\bar{V}_u$

Fig. 6.6

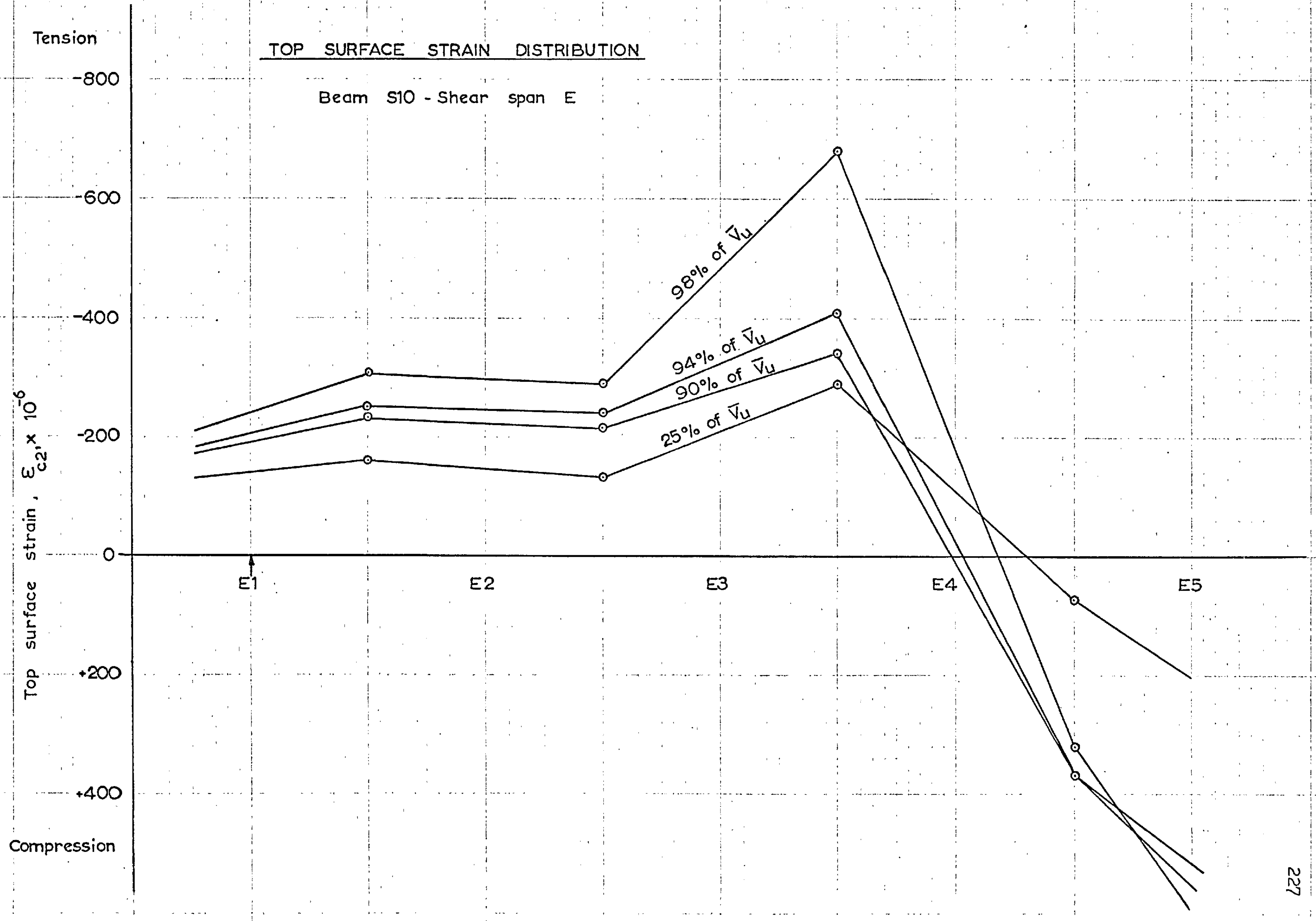

TOP SURFACE STRAIN DISTRIBUTION
Beam S10 - Shear span E
Tension
Compression
Top surface strain, ε_{c2}, x 10^{-6}
-800
-600
-400
-200
0
+200
+400
E1
E2
E3
E4
E5
98% of $\overline{V}_u$
94% of $\overline{V}_u$
90% of $\overline{V}_u$
25% of $\overline{V}_u$

Fig. 6.7

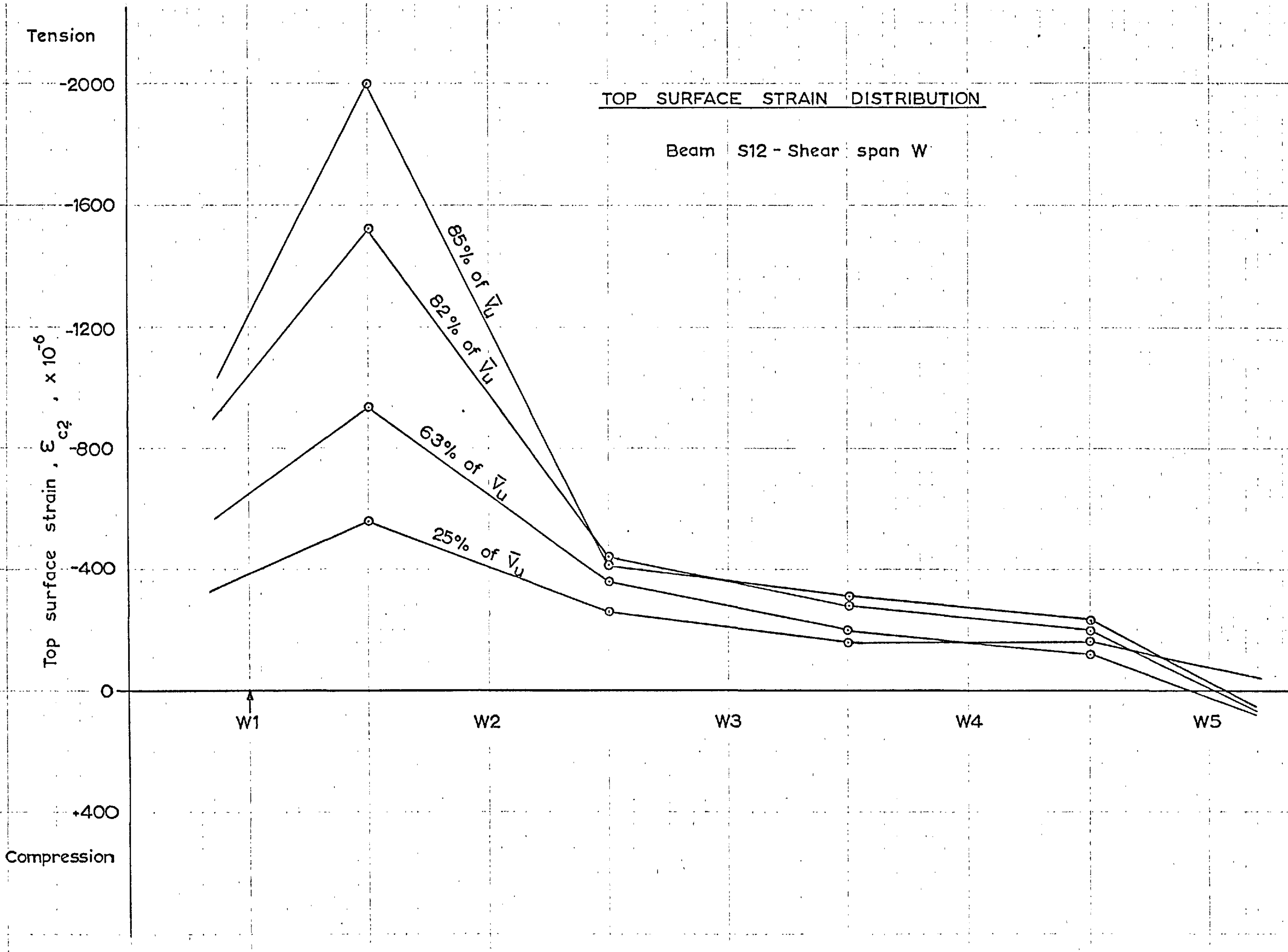

TOP SURFACE STRAIN DISTRIBUTION
Beam S12 - Shear span W
Tension
Compression
Top surface strain , ε_{c2} , $\times 10^{-6}$
-2000
-1600
-1200
-800
-400
0
+400
W1
W2
W3
W4
W5
85% of $\bar{V}_u$
82% of $\bar{V}_u$
63% of $\bar{V}_u$
25% of $\bar{V}_u$

Fig. 6.8

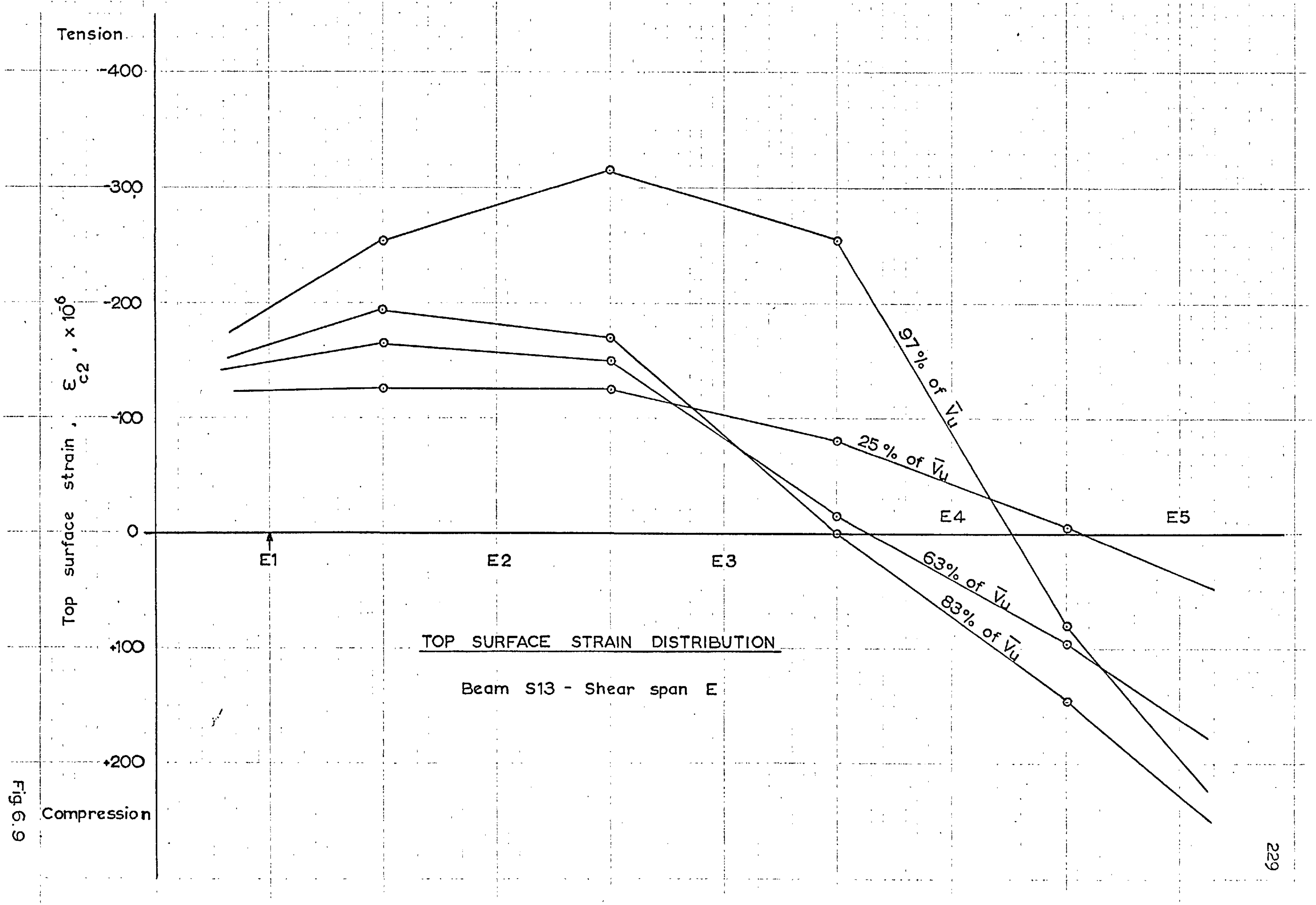
Tension
-400
-300
-200
-100
0
+100
+200
Compression
Top surface strain, ε_{c2}, $\times 10^{-6}$
E1
E2
E3
E4
E5
97% of $\bar{V}_u$
25% of $\bar{V}_u$
63% of $\bar{V}_u$
83% of $\bar{V}_u$
TOP SURFACE STRAIN DISTRIBUTION
Beam S13 - Shear span E

Fig. 6.9

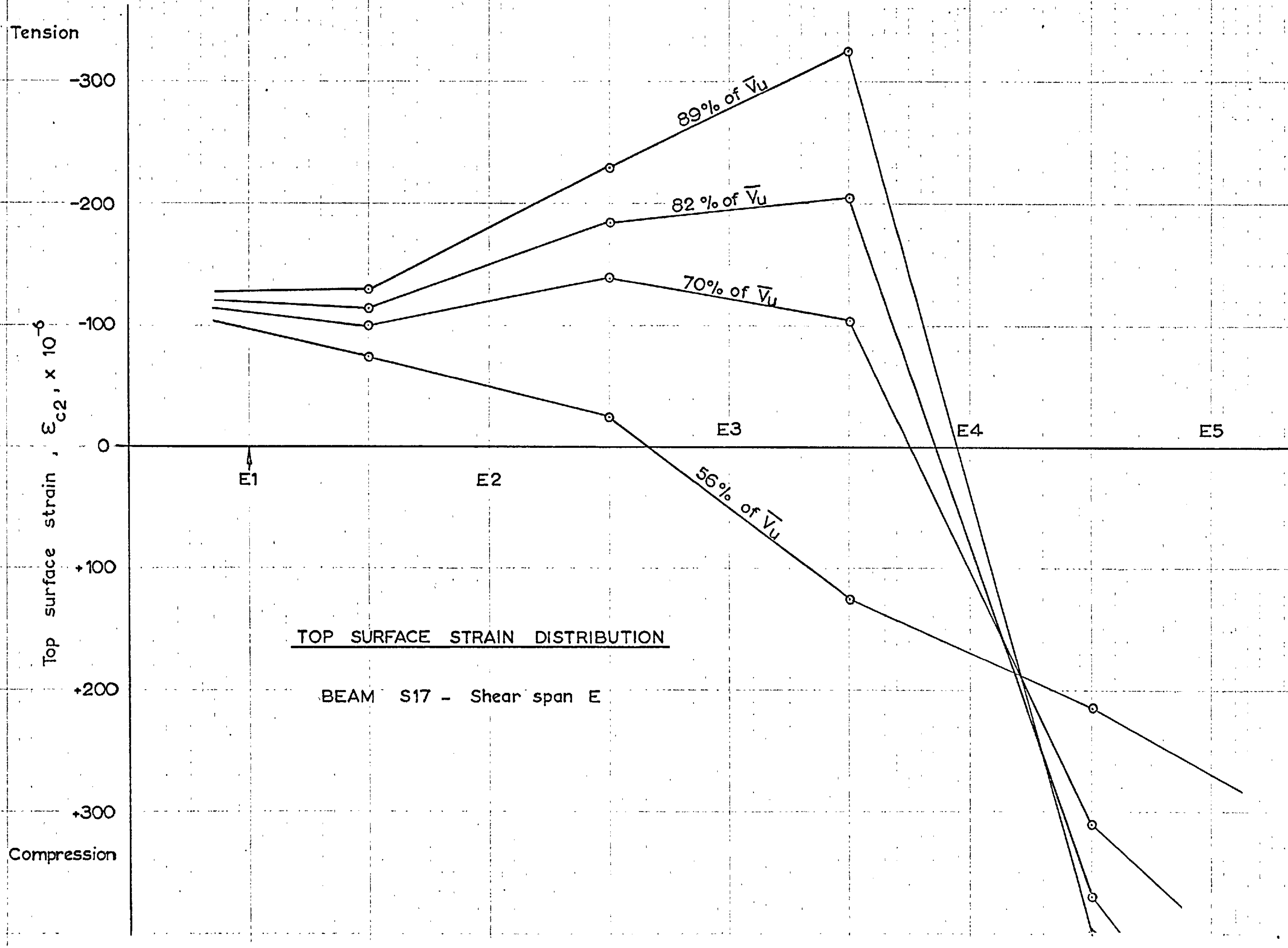

Tension
-300
-200
-100
0
+100
+200
+300
Compression
Top surface strain, ε_{c2}, x 10^{-6}
89% of $\overline{V}_u$
82 % of $\overline{V}_u$
70% of $\overline{V}_u$
56% of $\overline{V}_u$
E1
E2
E3
E4
E5
TOP SURFACE STRAIN DISTRIBUTION
BEAM S17 - Shear span E

Fig. 6.10

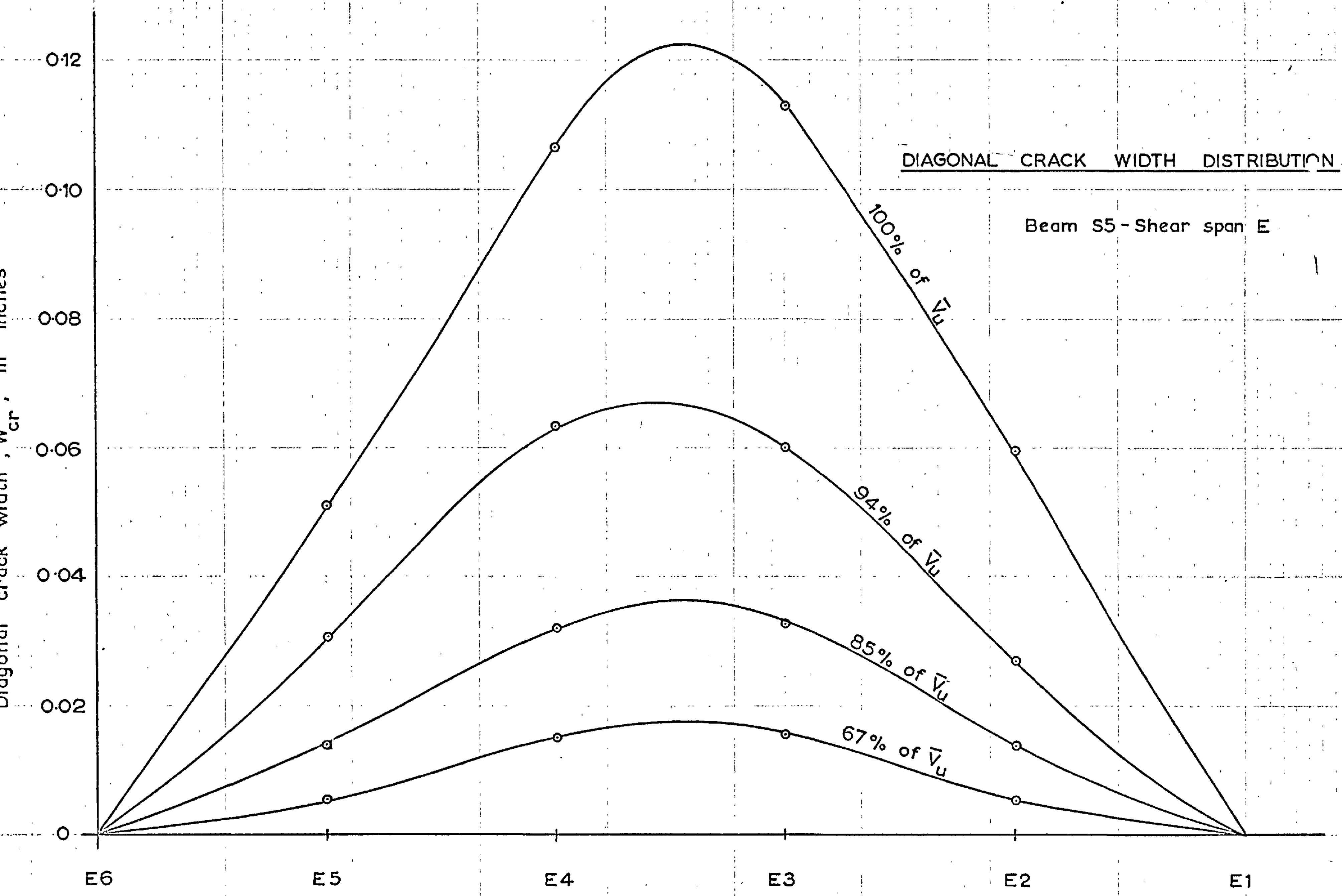
DIAGONAL CRACK WIDTH DISTRIBUTION
Beam S5 - Shear span E
Diagonal crack width, W_{cr}, in inches
0.12
0.10
0.08
0.06
0.04
0.02
0
E6
E5
E4
E3
E2
E1
100% of $\bar{V}_u$
94% of $\bar{V}_u$
85% of $\bar{V}_u$
67% of $\bar{V}_u$

Fig. 6.11

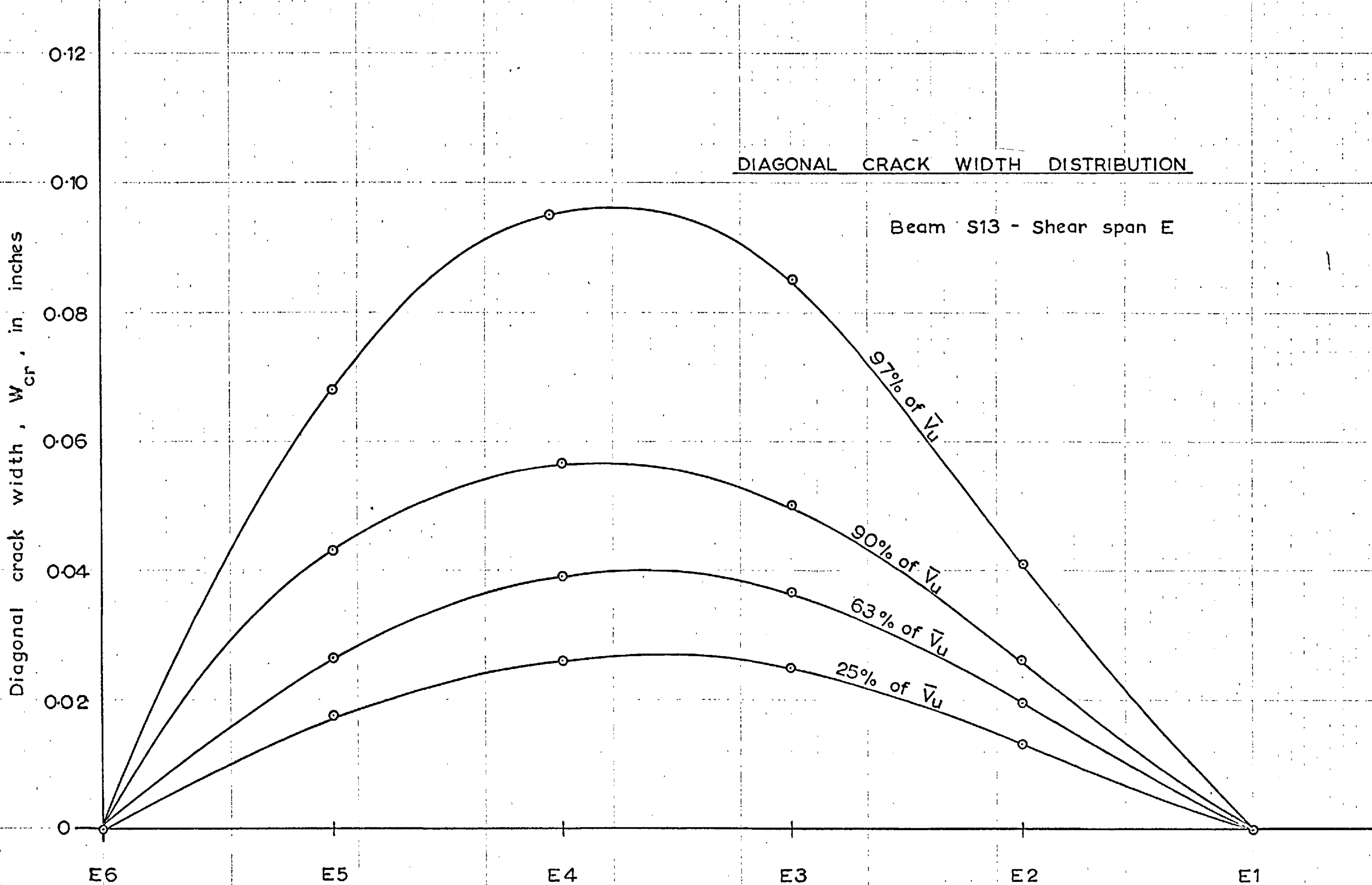
DIAGONAL CRACK WIDTH DISTRIBUTION
Beam S13 - Shear span E
Diagonal crack width, W_{cr}, in inches
0·12
0·10
0·08
0·06
0·04
0·02
0
97% of $\bar{V}_u$
90% of $\bar{V}_u$
63% of $\bar{V}_u$
25% of $\bar{V}_u$
E6
E5
E4
E3
E2
E1

Fig. 6.12

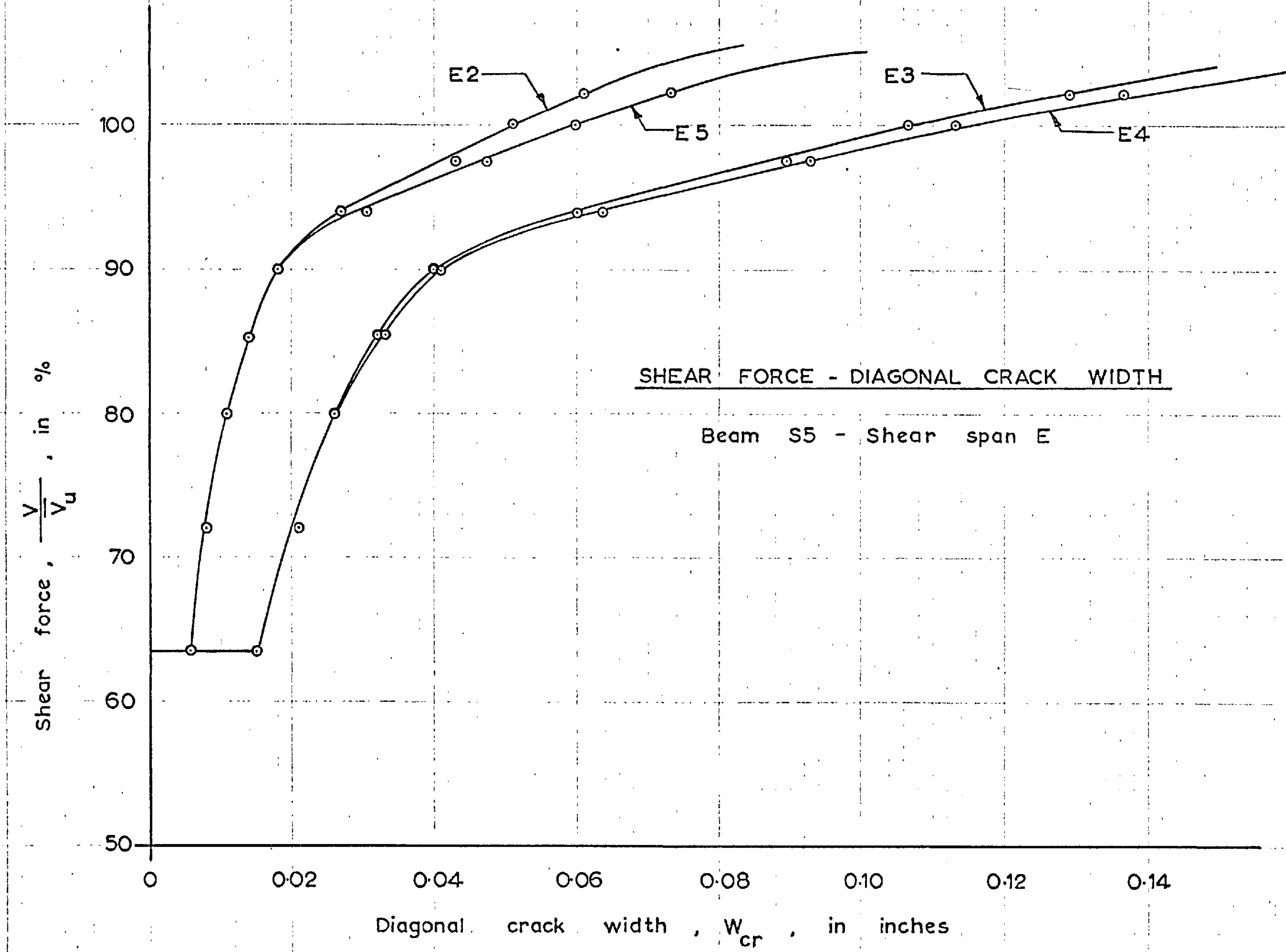
SHEAR FORCE - DIAGONAL CRACK WIDTH
Beam S5 - Shear span E
E2
E3
E4
E5
Shear force, $\frac{V}{V_u}$, in %
Diagonal crack width, W_{cr}, in inches
50
60
70
80
90
100
0
0·02
0·04
0·06
0·08
0·10
0·12
0·14

Fig. 6.13

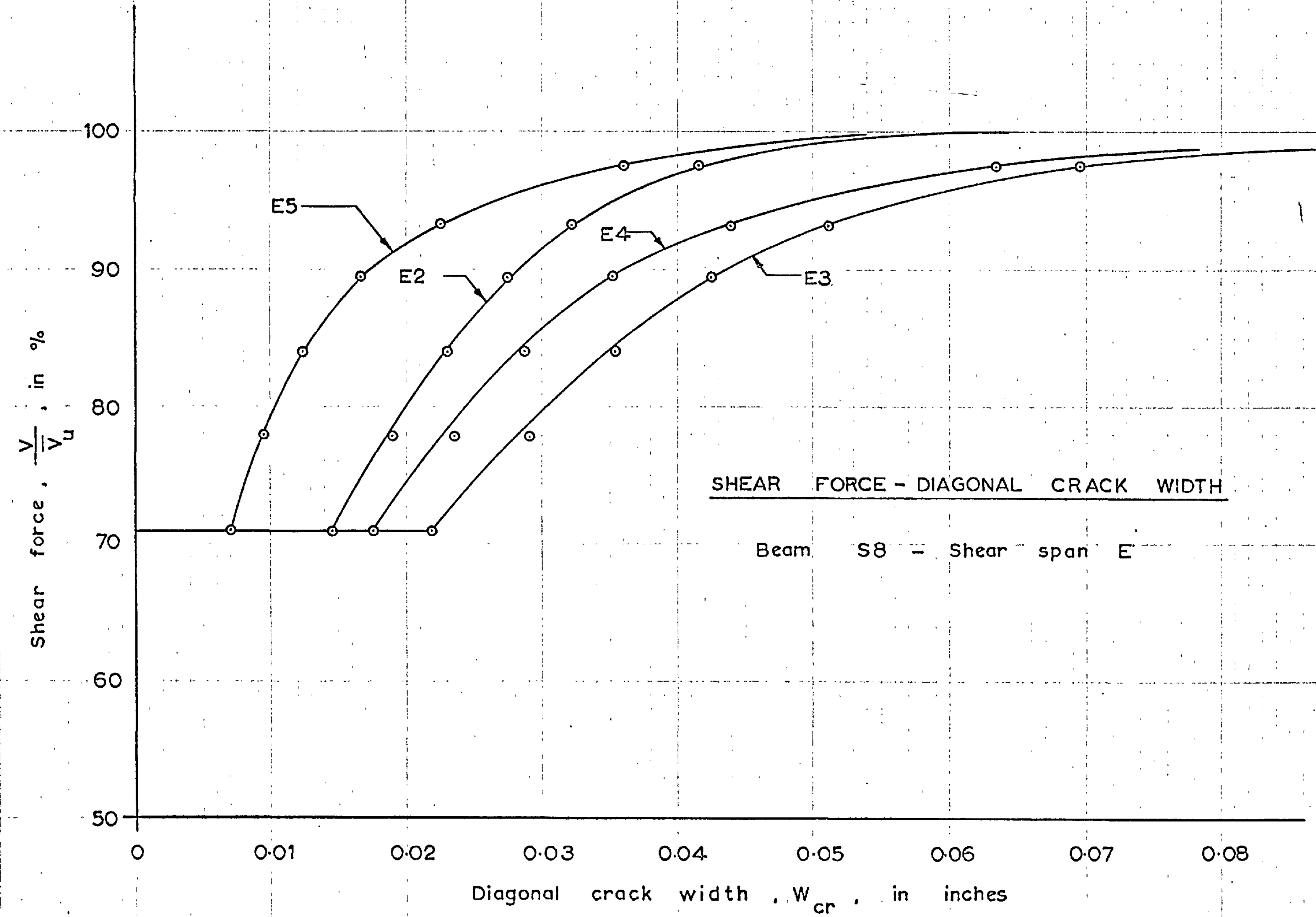
SHEAR FORCE - DIAGONAL CRACK WIDTH
Beam S8 - Shear span E
E5
E2
E4
E3
100
90
80
70
60
50
0
0·01
0·02
0·03
0·04
0·05
0·06
0·07
0·08
Shear force, $\frac{V}{V_u}$, in %
Diagonal crack width, W_{cr}, in inches

Fig. 6.14

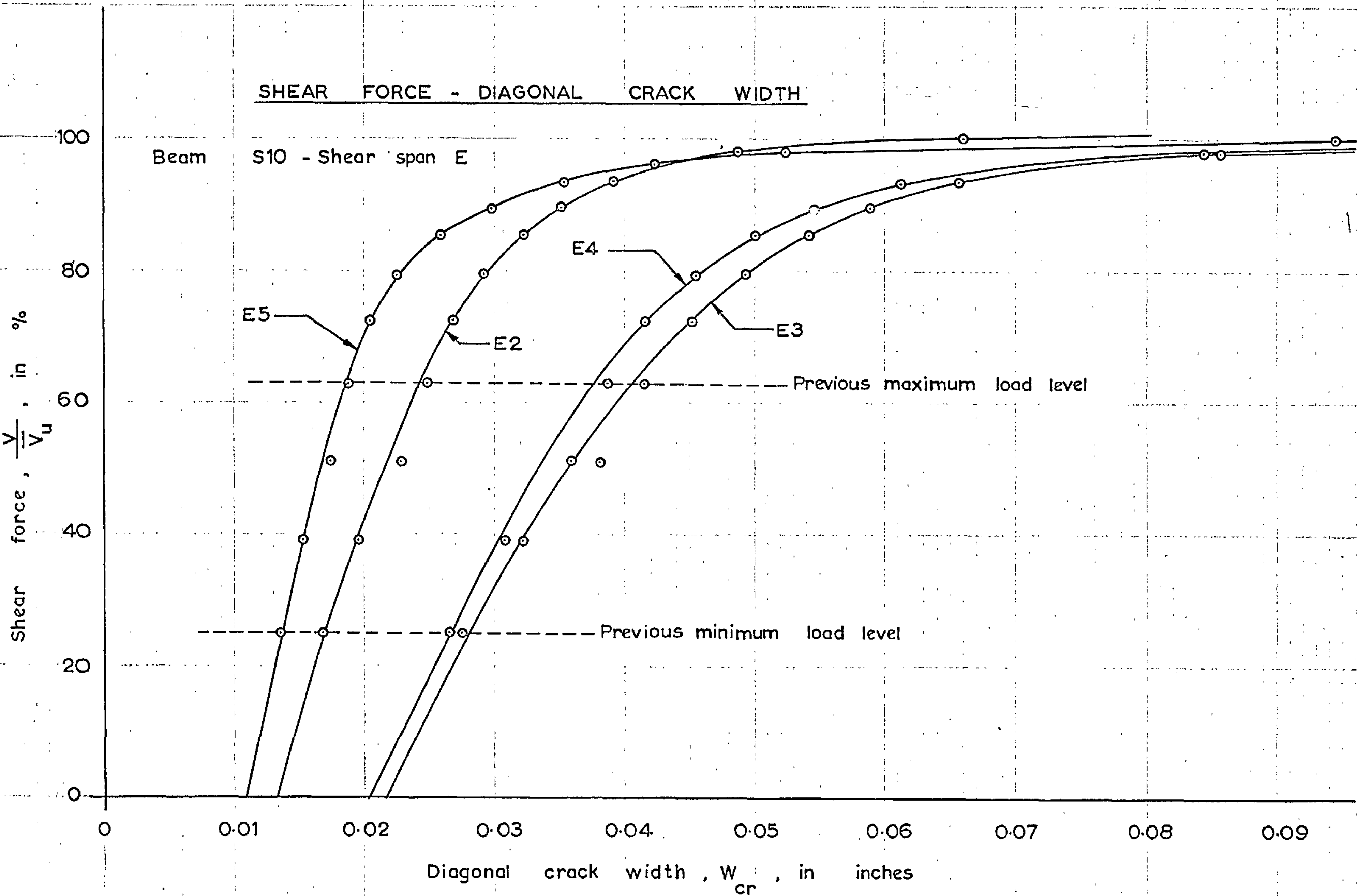
SHEAR FORCE - DIAGONAL CRACK WIDTH
Beam S10 - Shear span E
E5
E2
E4
E3
Previous maximum load level
Previous minimum load level
Shear force, $\frac{V}{V_u}$, in %
0
20
40
60
80
100
0
0·01
0·02
0·03
0·04
0·05
0·06
0·07
0·08
0·09
Diagonal crack width, W_{cr}, in inches

Fig. 6.15

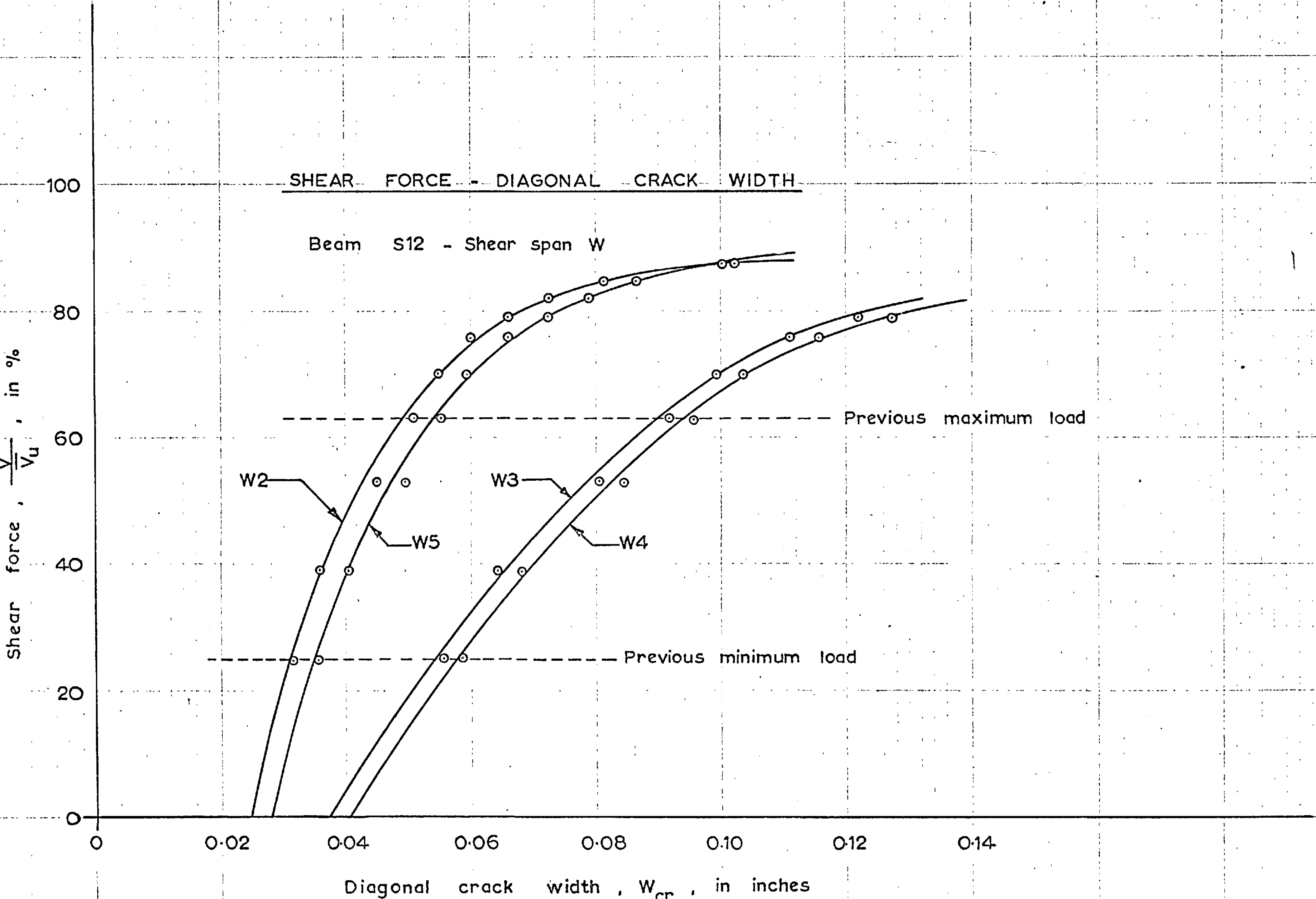
SHEAR FORCE - DIAGONAL CRACK WIDTH
Beam S12 - Shear span W
Previous maximum load
Previous minimum load
W2
W5
W3
W4
Shear force , $\frac{V}{V_u}$, in %
100
80
60
40
20
0
0
0·02
0·04
0·06
0·08
0·10
0·12
0·14
Diagonal crack width , W_{cr} , in inches

Fig. 6.16

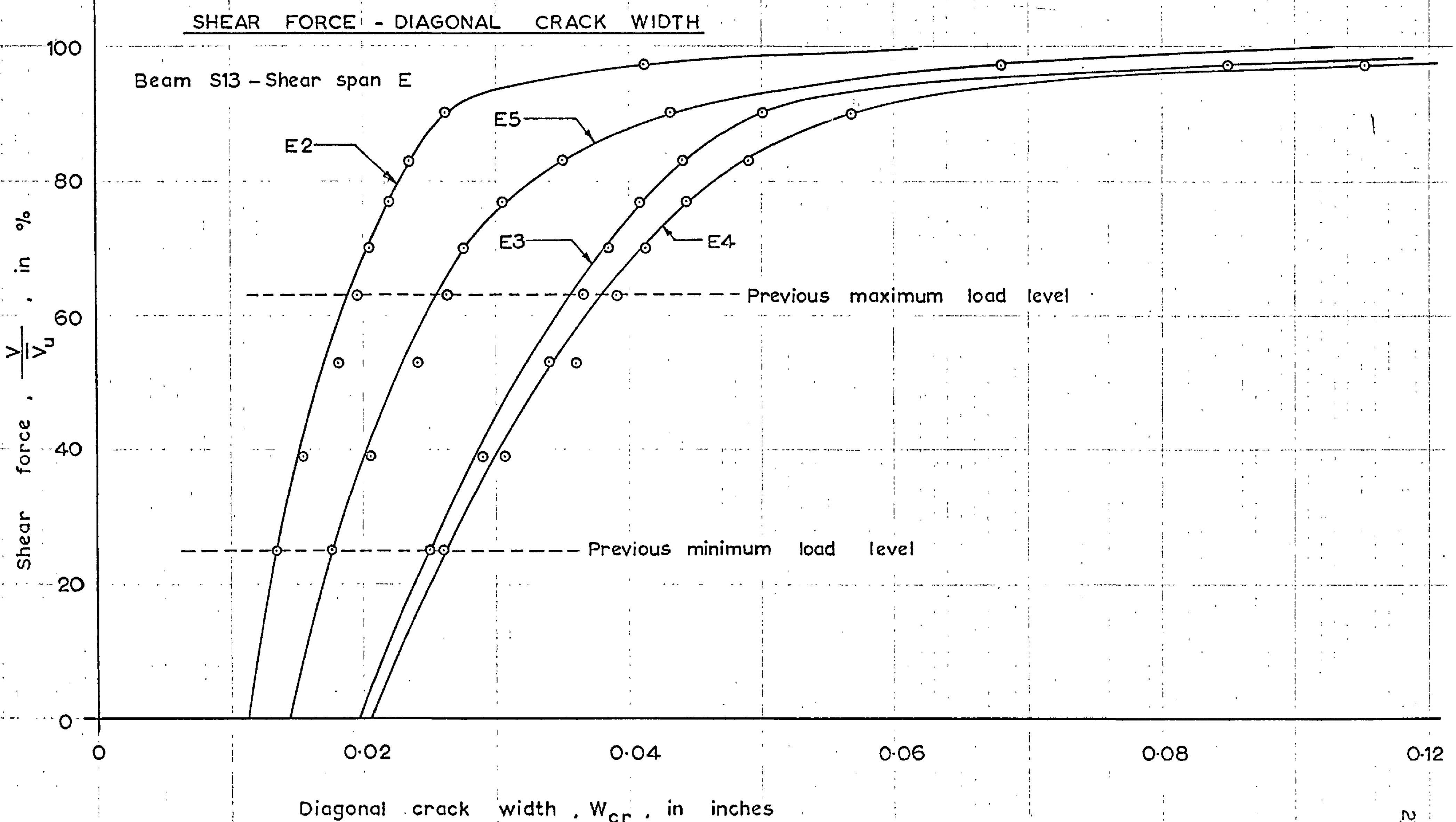

SHEAR FORCE - DIAGONAL CRACK WIDTH
Beam S13 - Shear span E
E2
E3
E4
E5
Previous maximum load level
Previous minimum load level
Shear force , $\frac{V}{V_u}$, in %
100
80
60
40
20
0
0
0·02
0·04
0·06
0·08
0·12
Diagonal crack width , W_{cr} , in inches

Fig. 6.17

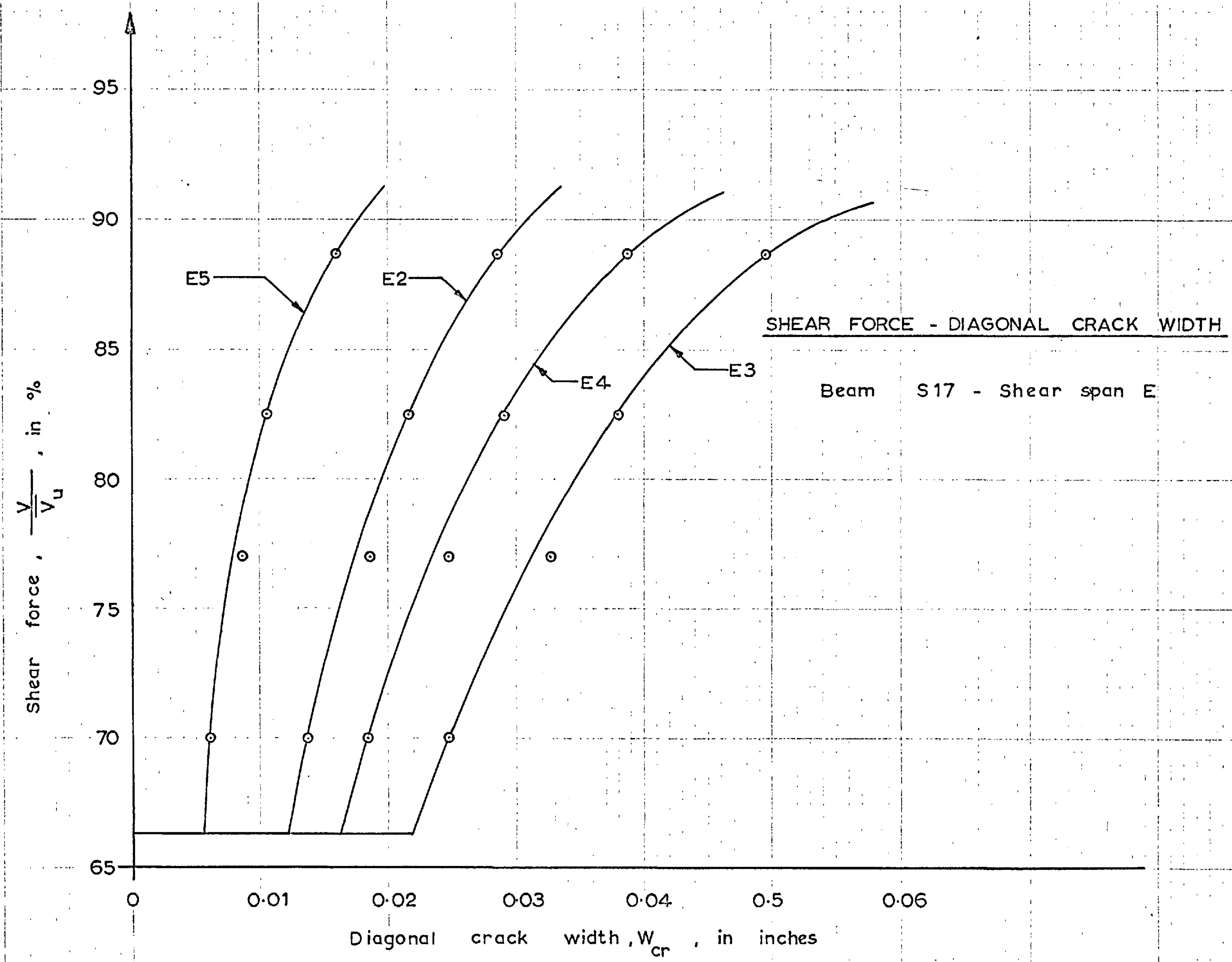
SHEAR FORCE - DIAGONAL CRACK WIDTH
Beam S17 - Shear span E
E5
E2
E4
E3
95
90
85
80
75
70
65
0
0·01
0·02
0·03
0·04
0·5
0·06
Shear force , $\frac{V}{V_u}$, in %
Diagonal crack width , W_{cr} , in inches

Fig. 6.18

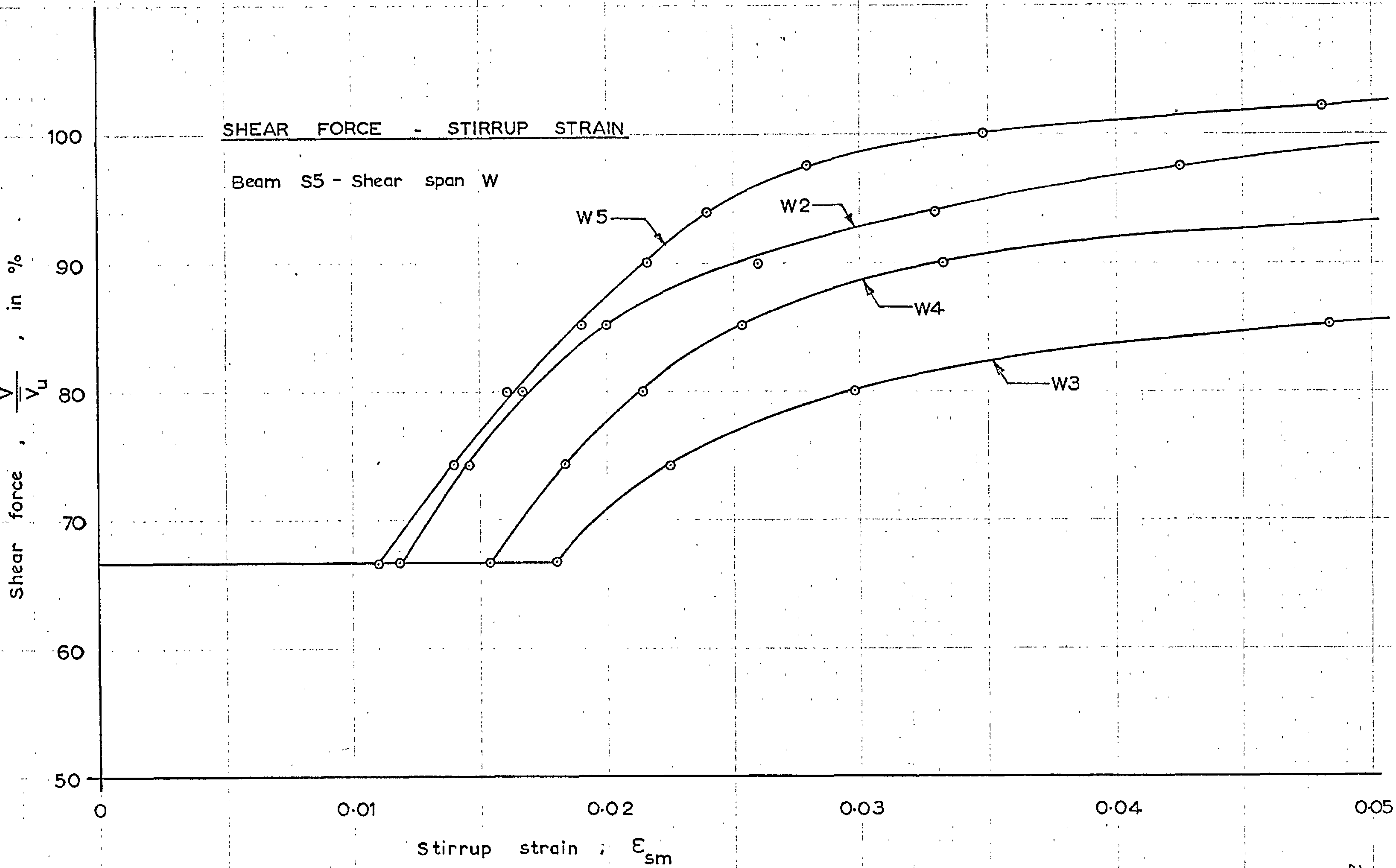
SHEAR FORCE - STIRRUP STRAIN
Beam S5 - Shear span W
W5
W2
W4
W3
Shear force , $\frac{V}{V_u}$, in %
100
90
80
70
60
50
0
0·01
0·02
0·03
0·04
0·05
Stirrup strain ; ε_{sm}

Fig. 6.19

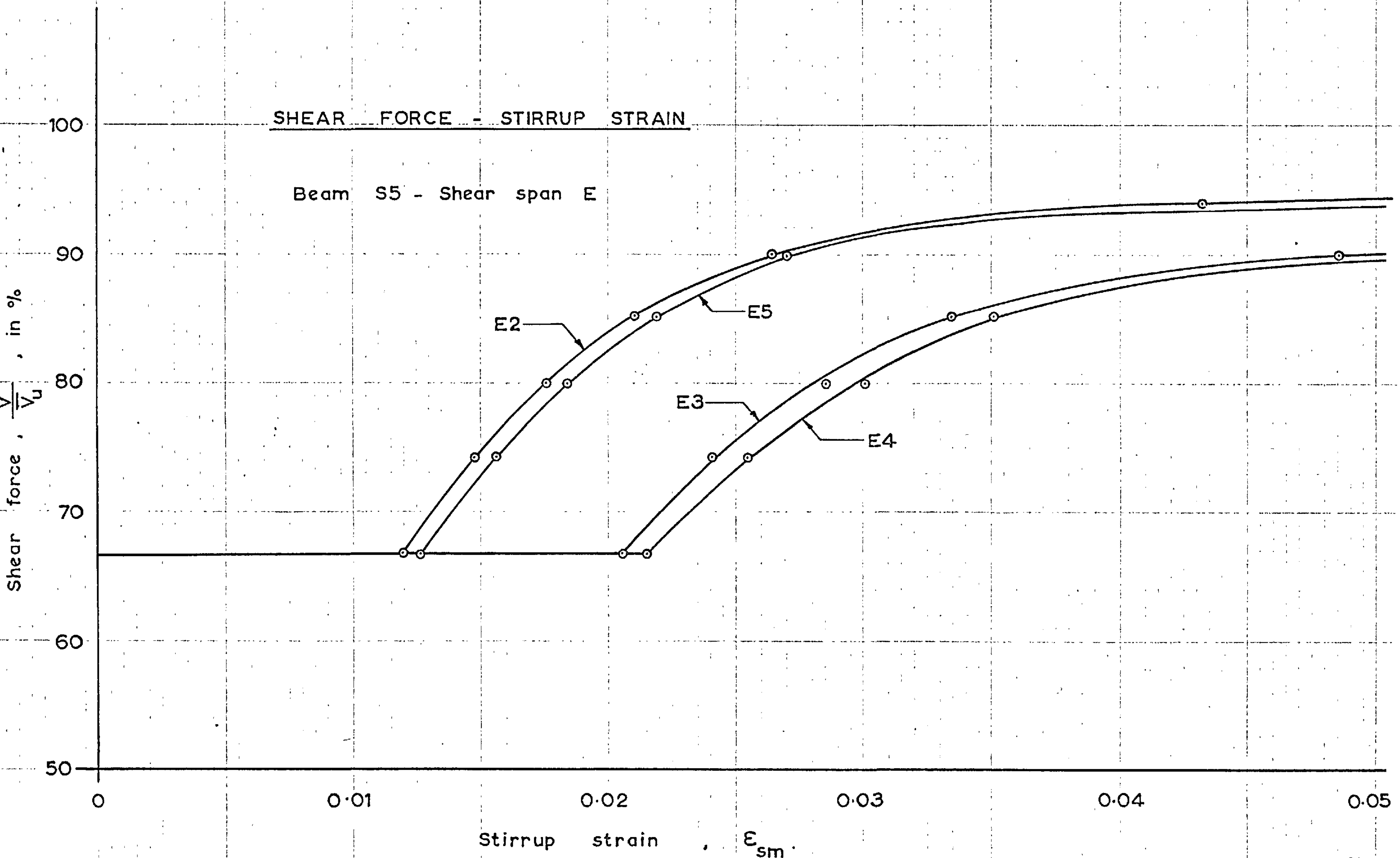
SHEAR FORCE - STIRRUP STRAIN
Beam S5 - Shear span E
Shear force, $\frac{V}{V_u}$, in %
100
90
80
70
60
50
0
0·01
0·02
0·03
0·04
0·05
Stirrup strain, ε_{sm}.
E2
E5
E3
E4

Fig. 6.20

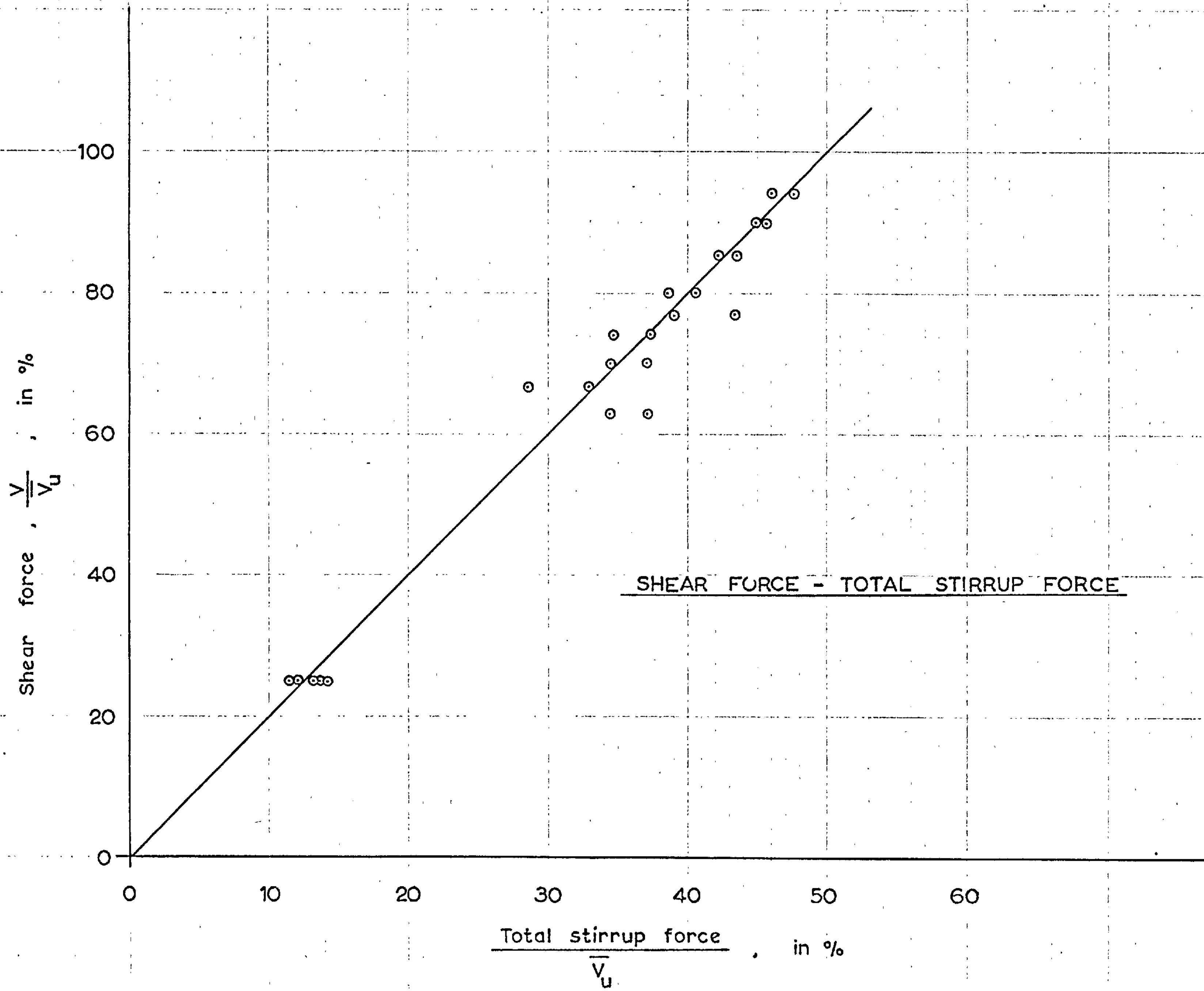
SHEAR FORCE - TOTAL STIRRUP FORCE
Shear force, $\frac{V}{V_u}$, in %
Total stirrup force / $\overline{V}_u$, in %
0
20
40
60
80
100
0
10
20
30
40
50
60

Fig. 6.21

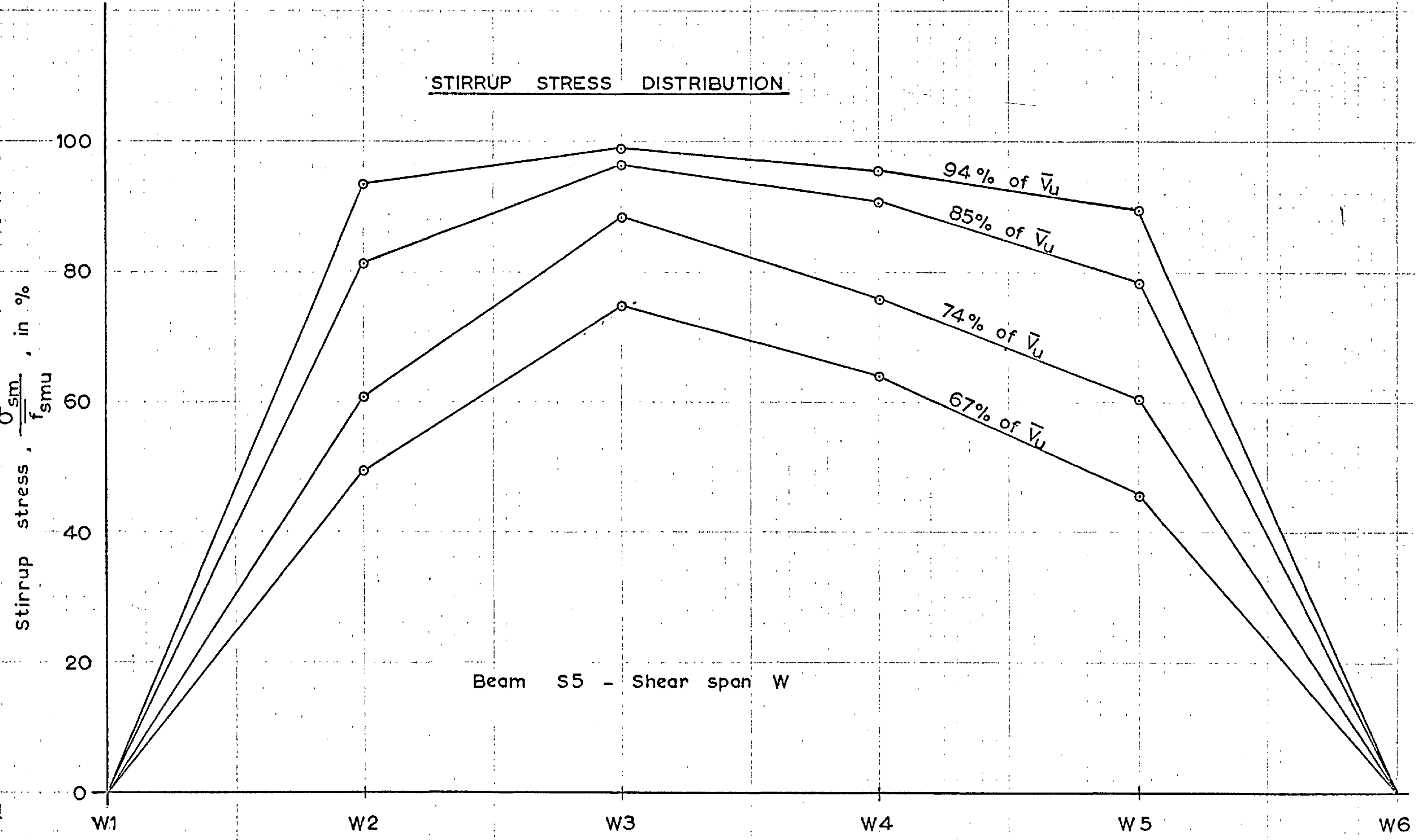
STIRRUP STRESS DISTRIBUTION
Stirrup stress , $\frac{\sigma_{sm}}{f_{smu}}$, in %
0
20
40
60
80
100
94 % of $\bar{V}_u$
85% of $\bar{V}_u$
74% of $\bar{V}_u$
67% of $\bar{V}_u$
Beam S5 - Shear span W
W1
W2
W3
W4
W5
W6

Fig. 6.22

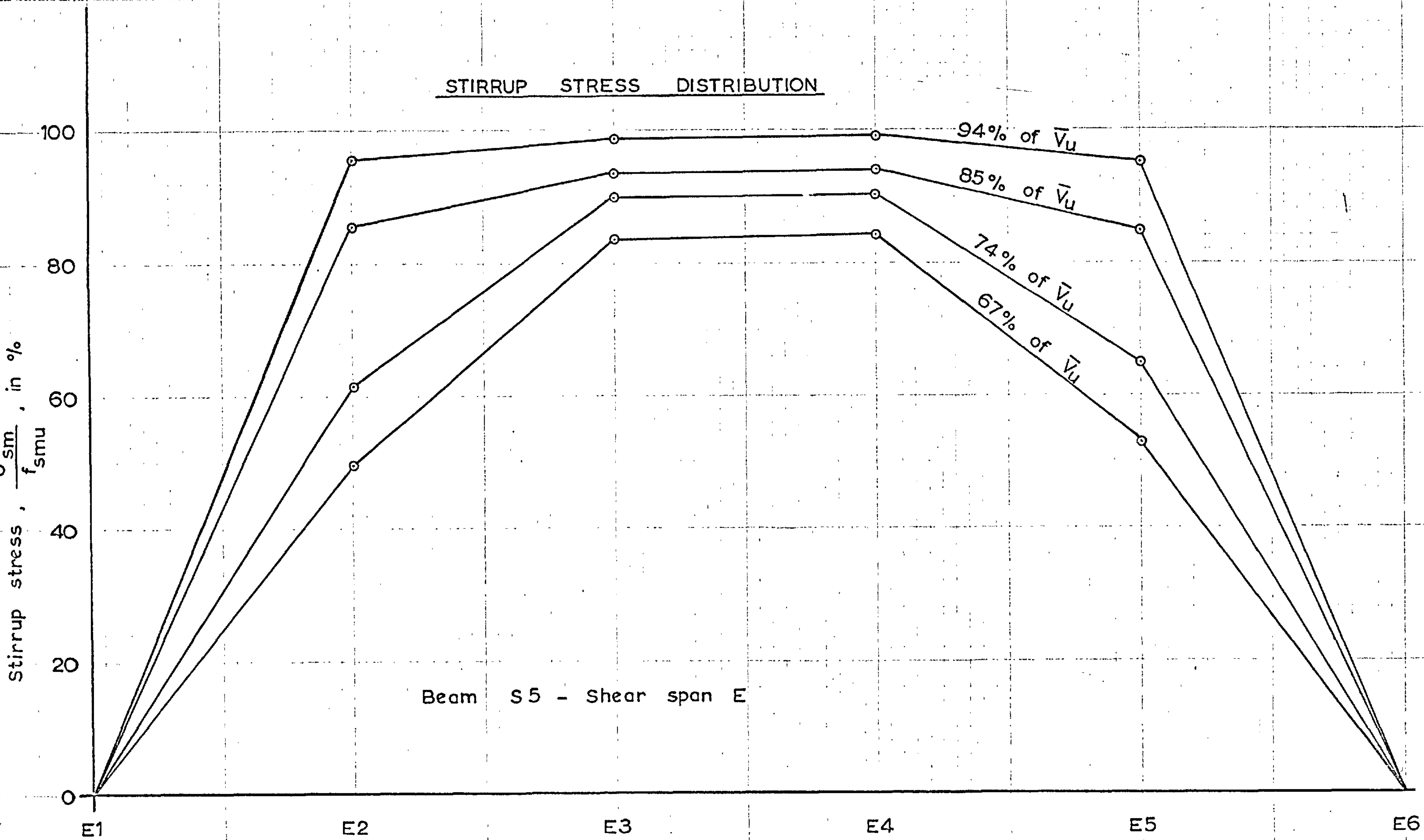

STIRRUP STRESS DISTRIBUTION
94% of $\bar{V}_u$
85% of $\bar{V}_u$
74% of $\bar{V}_u$
67% of $\bar{V}_u$
Stirrup stress, $\frac{\sigma_{sm}}{f_{smu}}$, in %
100
80
60
40
20
0
Beam S5 - Shear span E
E1
E2
E3
E4
E5
E6

Fig. 6.23

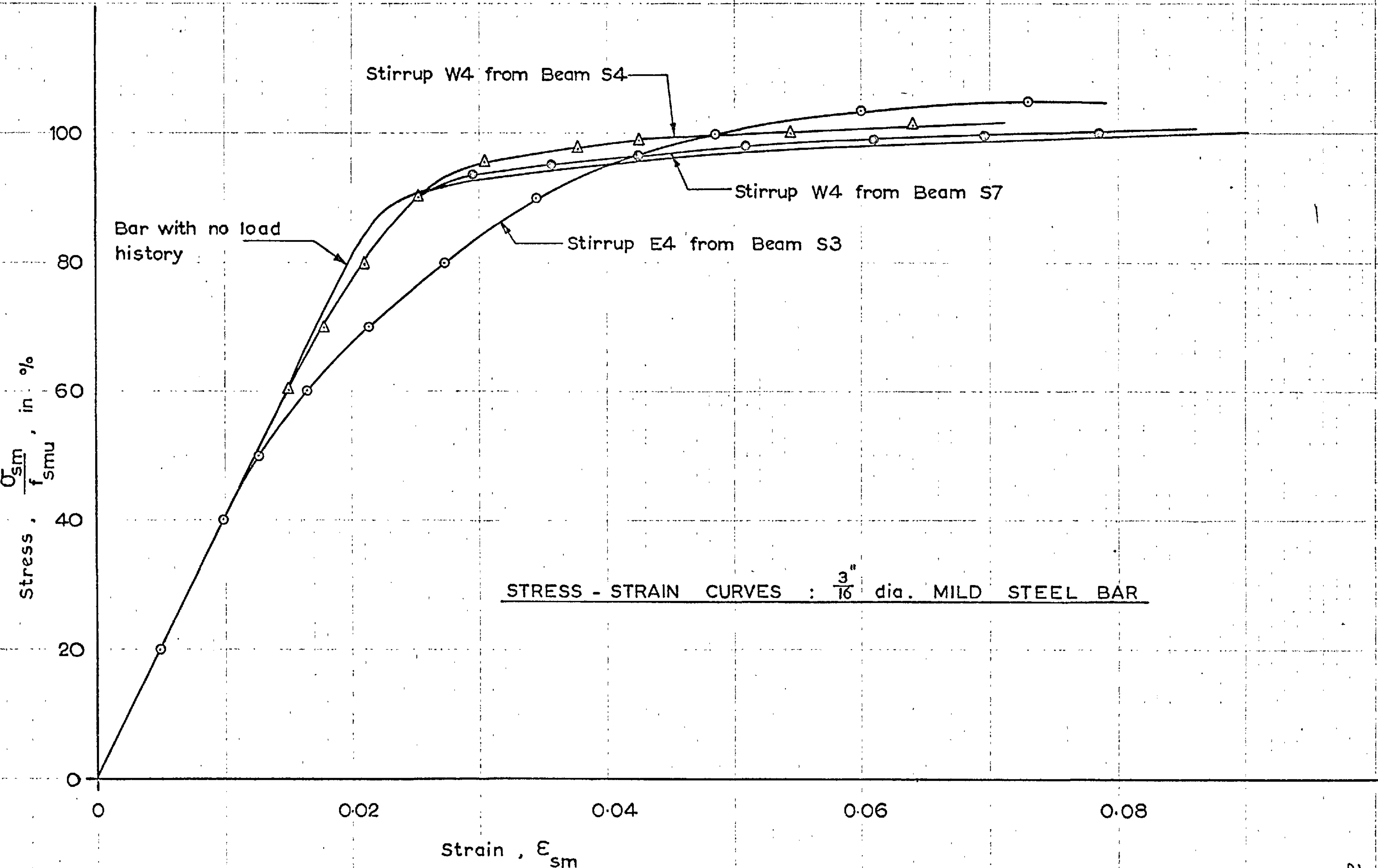
STRESS - STRAIN CURVES : 3/16" dia. MILD STEEL BAR
Stirrup W4 from Beam S4
Stirrup W4 from Beam S7
Stirrup E4 from Beam S3
Bar with no load history
Stress , $\frac{\sigma_{sm}}{f_{smu}}$, in %
Strain , ε_{sm}
0
20
40
60
80
100
0.02
0.04
0.06
0.08

Fig. 6.24

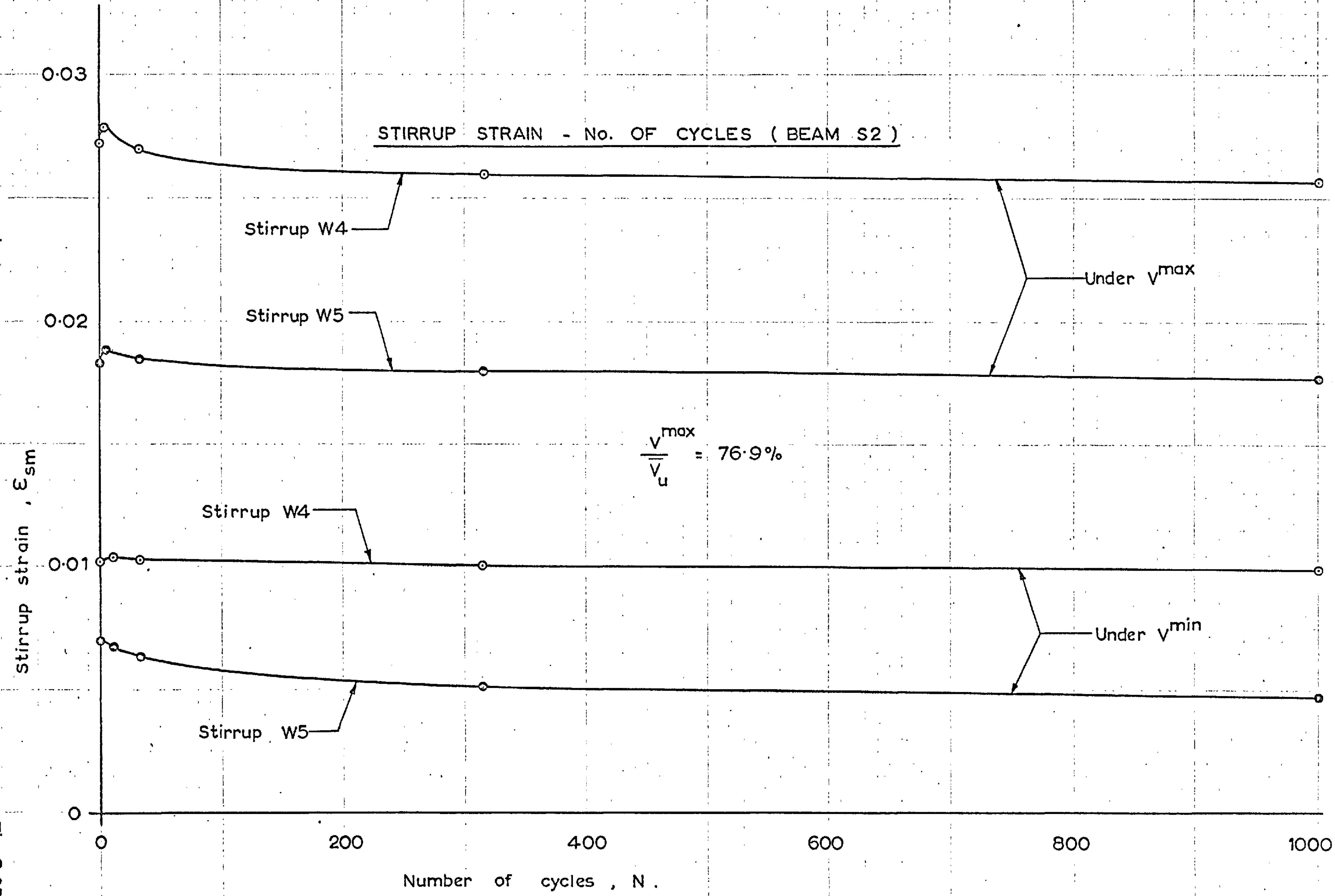
STIRRUP STRAIN - No. OF CYCLES (BEAM S2)
0·03
0·02
0·01
0
Stirrup W4
Stirrup W5
Stirrup W4
Stirrup W5
Under V^{max}
Under V^{min}
$\frac{V^{max}}{\overline{\overline{V}}_u}$ = 76·9%
Stirrup strain , ε_{sm}
0
200
400
600
800
1000
Number of cycles , N .

Fig. 6.25

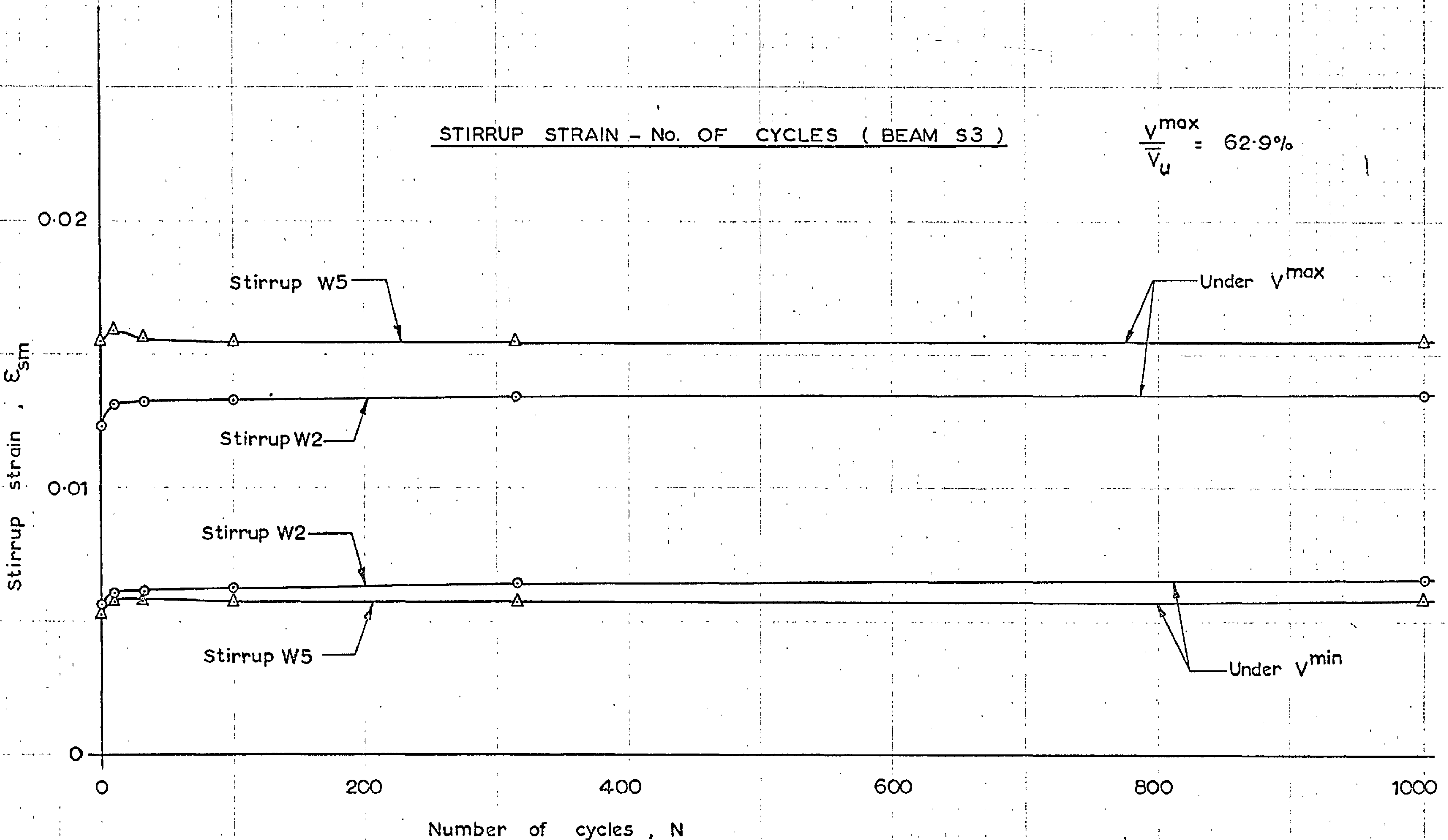
STIRRUP STRAIN – No. OF CYCLES (BEAM S3)
$\frac{V^{max}}{V_u}$ = 62·9%
Stirrup W5
Under V^{max}
Stirrup W2
Stirrup W2
Stirrup W5
Under V^{min}
Stirrup strain , ε_{sm}
0·02
0·01
0
0
200
400
600
800
1000
Number of cycles , N

Fig. 6.26

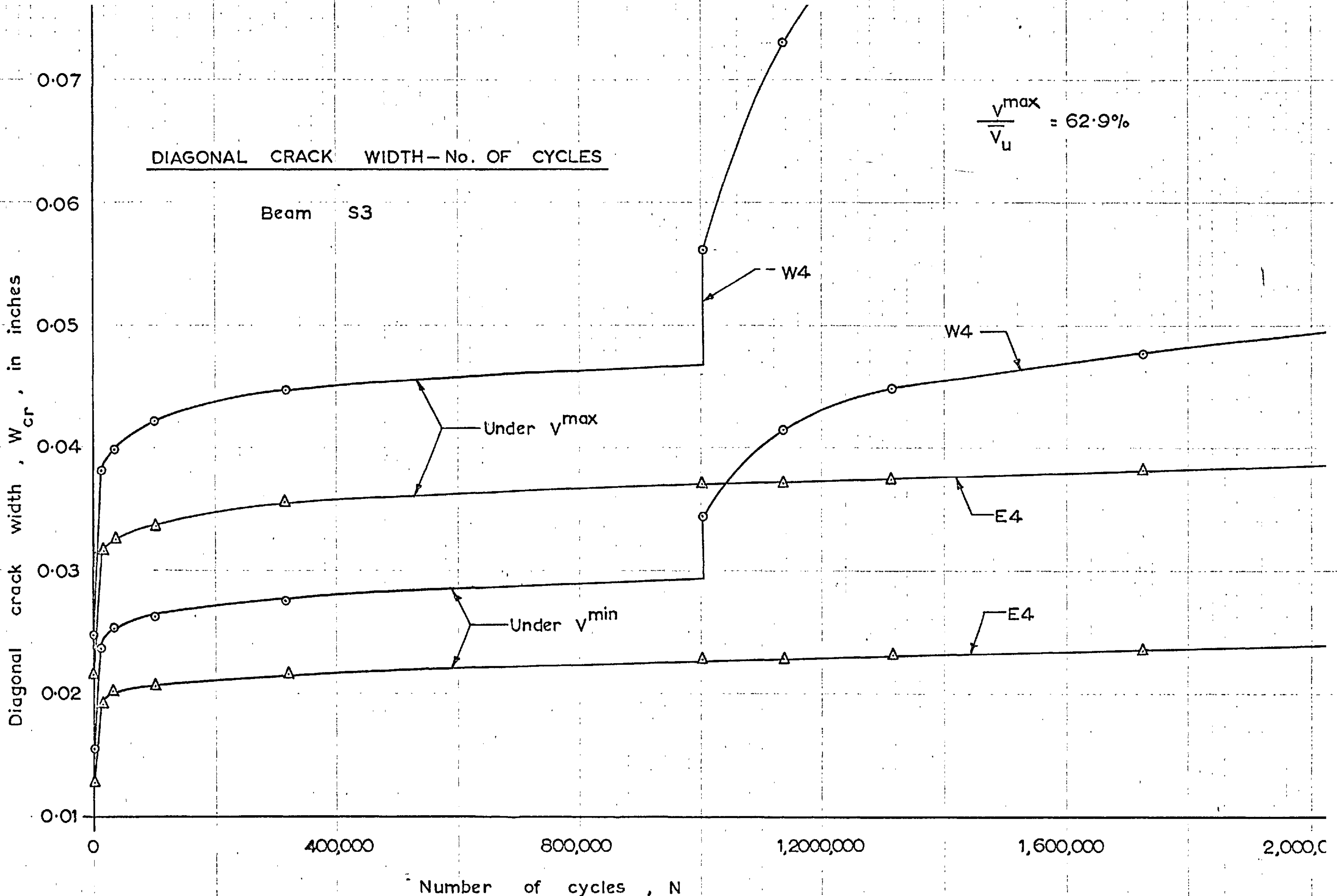
DIAGONAL CRACK WIDTH – No. OF CYCLES
Beam S3
$\frac{V^{max}}{V_u}$ = 62·9%
W4
W4
E4
E4
Under V^{max}
Under V^{min}
Diagonal crack width, W_{cr}, in inches
0·01
0·02
0·03
0·04
0·05
0·06
0·07
0
400,000
800,000
1,2000,000
1,600,000
2,000,0
Number of cycles, N

Fig. 6.27

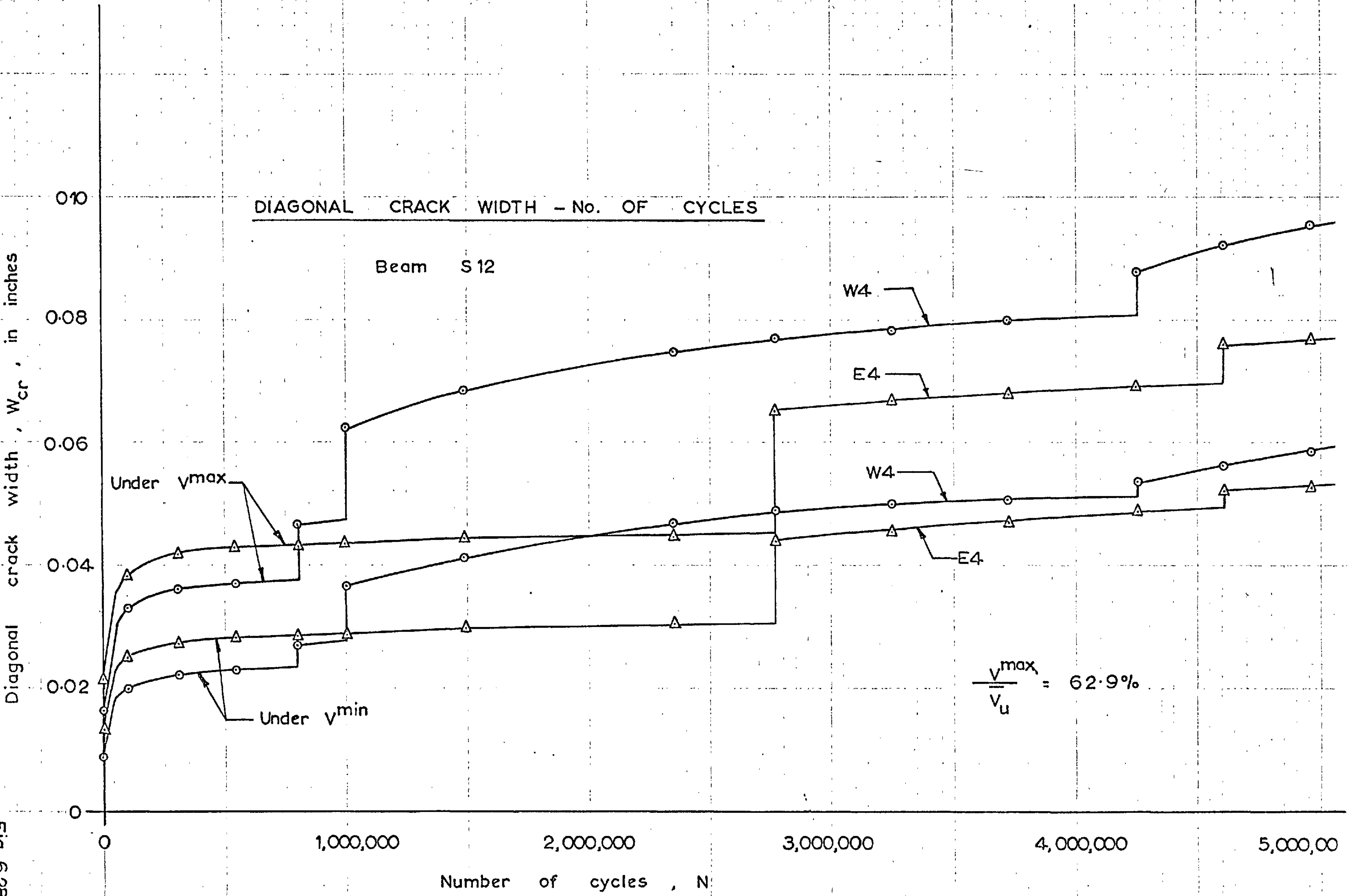
DIAGONAL CRACK WIDTH – No. OF CYCLES
Beam S 12
Diagonal crack width, W_{cr}, in inches
0·10
0·08
0·06
0·04
0·02
0
W4
E4
W4
E4
Under V^{max}
Under V^{min}
$\frac{V^{max}}{V_u}$ = 62·9%
0
1,000,000
2,000,000
3,000,000
4,000,000
5,000,00
Number of cycles, N

Fig. 6.28

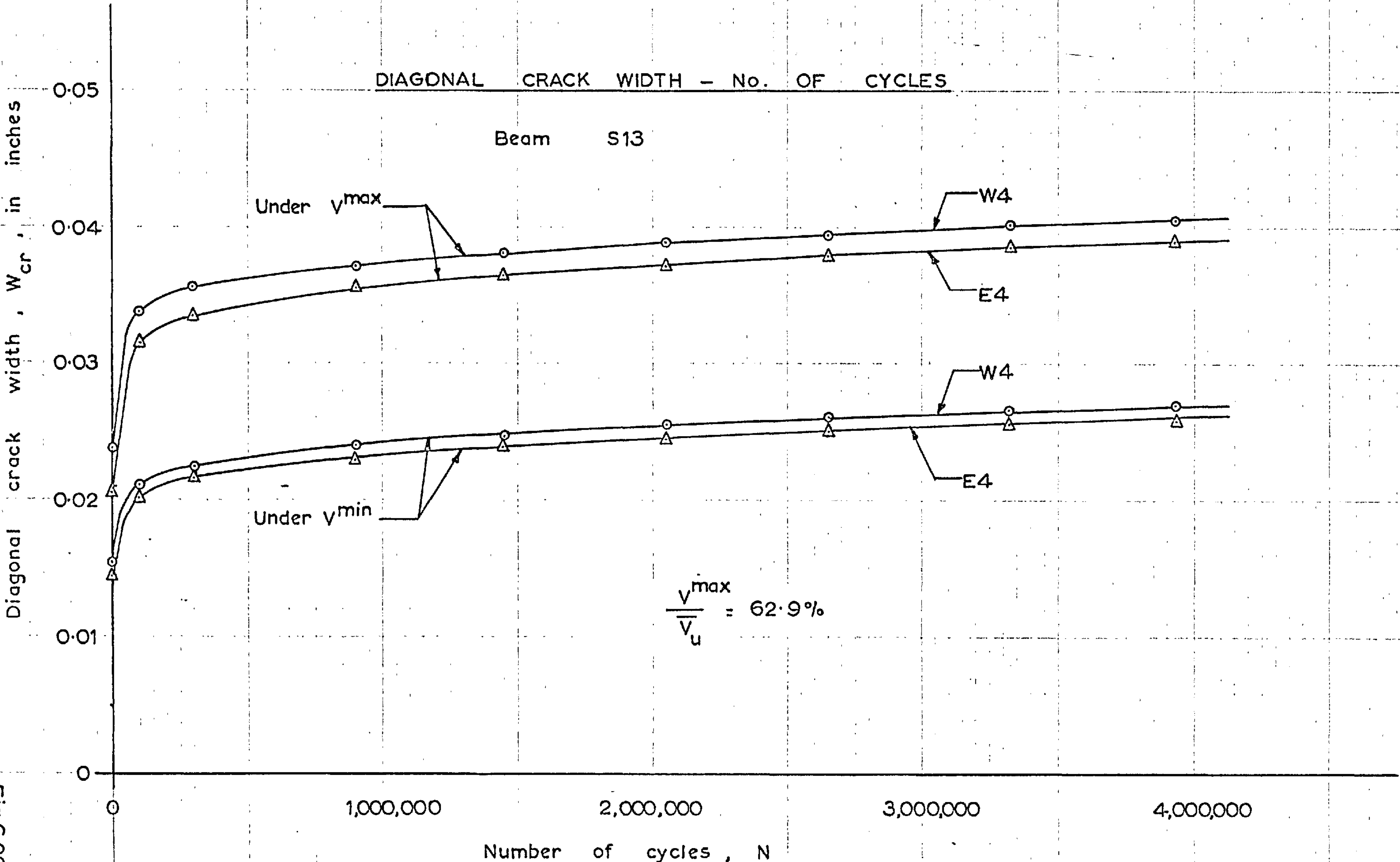

DIAGONAL CRACK WIDTH – No. OF CYCLES
Beam S13
Under V^{max}
Under V^{min}
W4
E4
W4
E4
$\frac{V^{max}}{\overline{V_u}}$ = 62·9%
Diagonal crack width, W_{cr}, in inches
0·05
0·04
0·03
0·02
0·01
0
0
1,000,000
2,000,000
3,000,000
4,000,000
Number of cycles, N

Fig.6.29

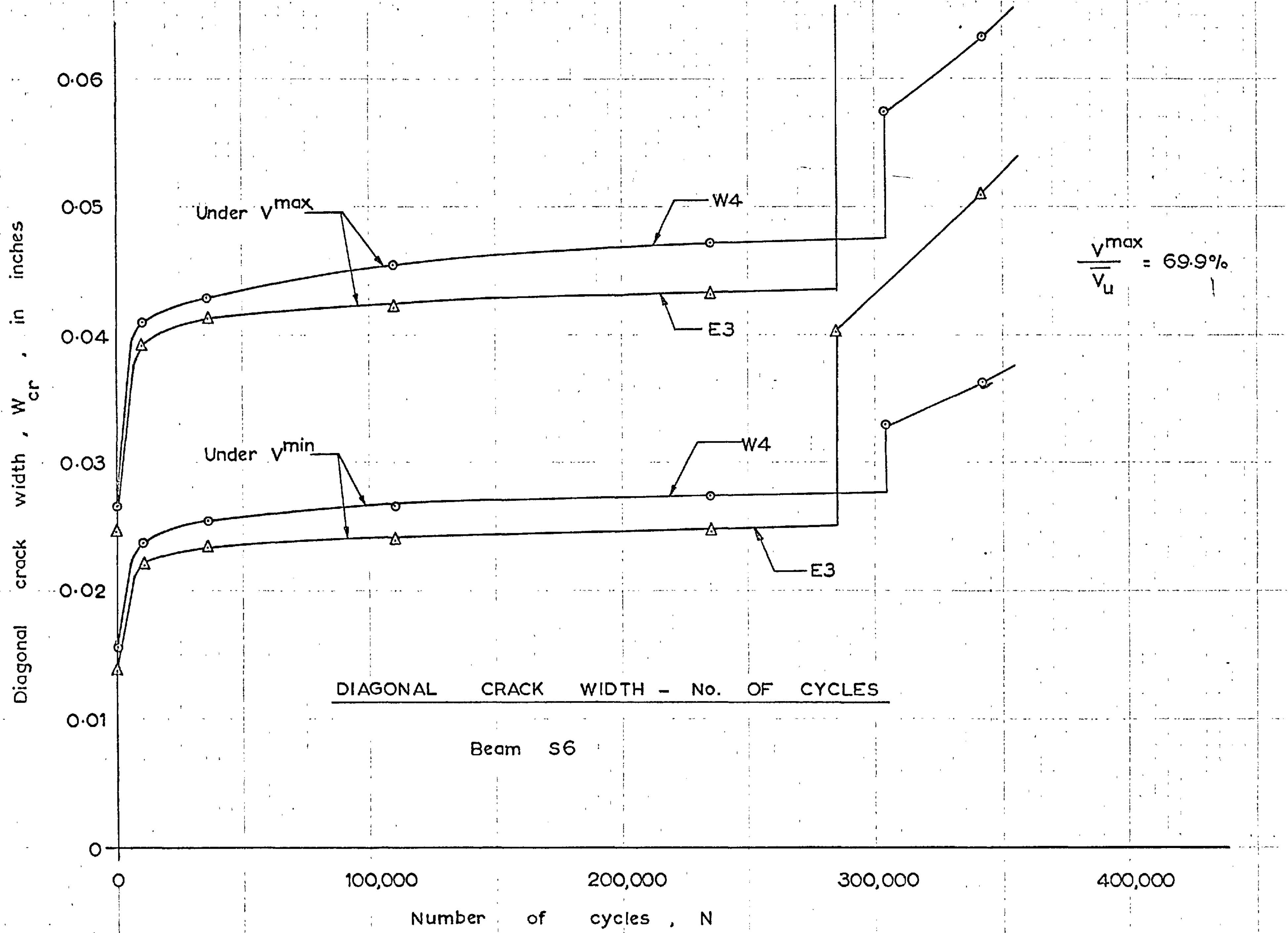
0·06
0·05
0·04
0·03
0·02
0·01
0
Diagonal crack width , W_{cr} , in inches
Under V^{max}
W4
E3
Under V^{min}
W4
E3
$\frac{V^{max}}{V_u}$ = 69·9%
DIAGONAL CRACK WIDTH – No. OF CYCLES
Beam S6
0
100,000
200,000
300,000
400,000
Number of cycles , N

Fig. 6.30

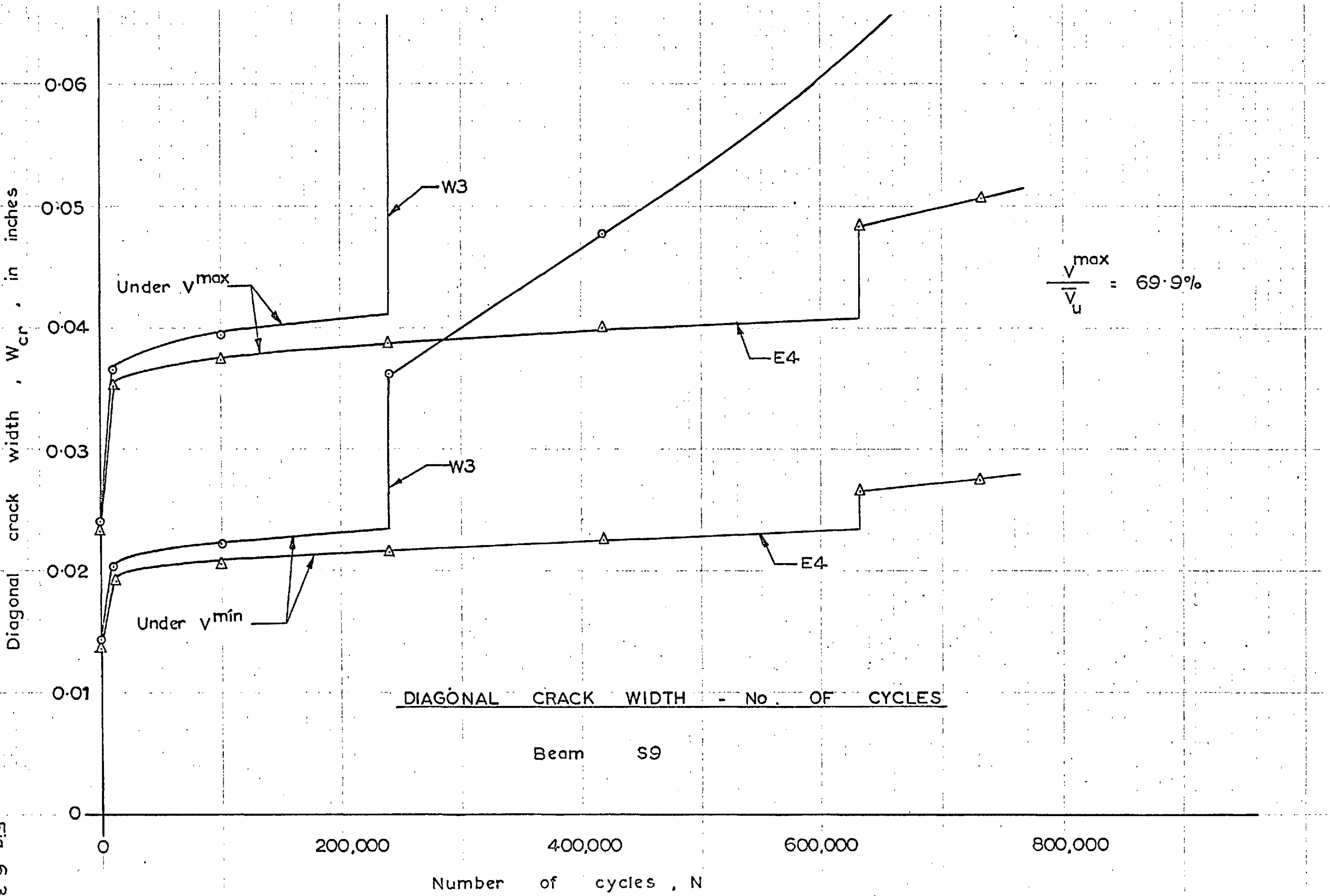

Diagonal crack width, W_{cr}, in inches
0·06
0·05
0·04
0·03
0·02
0·01
0
W3
W3
E4
E4
Under V^{max}
Under V^{min}
$\frac{V^{max}}{\bar{V}_u}$ = 69·9%
DIAGONAL CRACK WIDTH - No. OF CYCLES
Beam S9
0
200,000
400,000
600,000
800,000
Number of cycles, N

Fig. 6.31

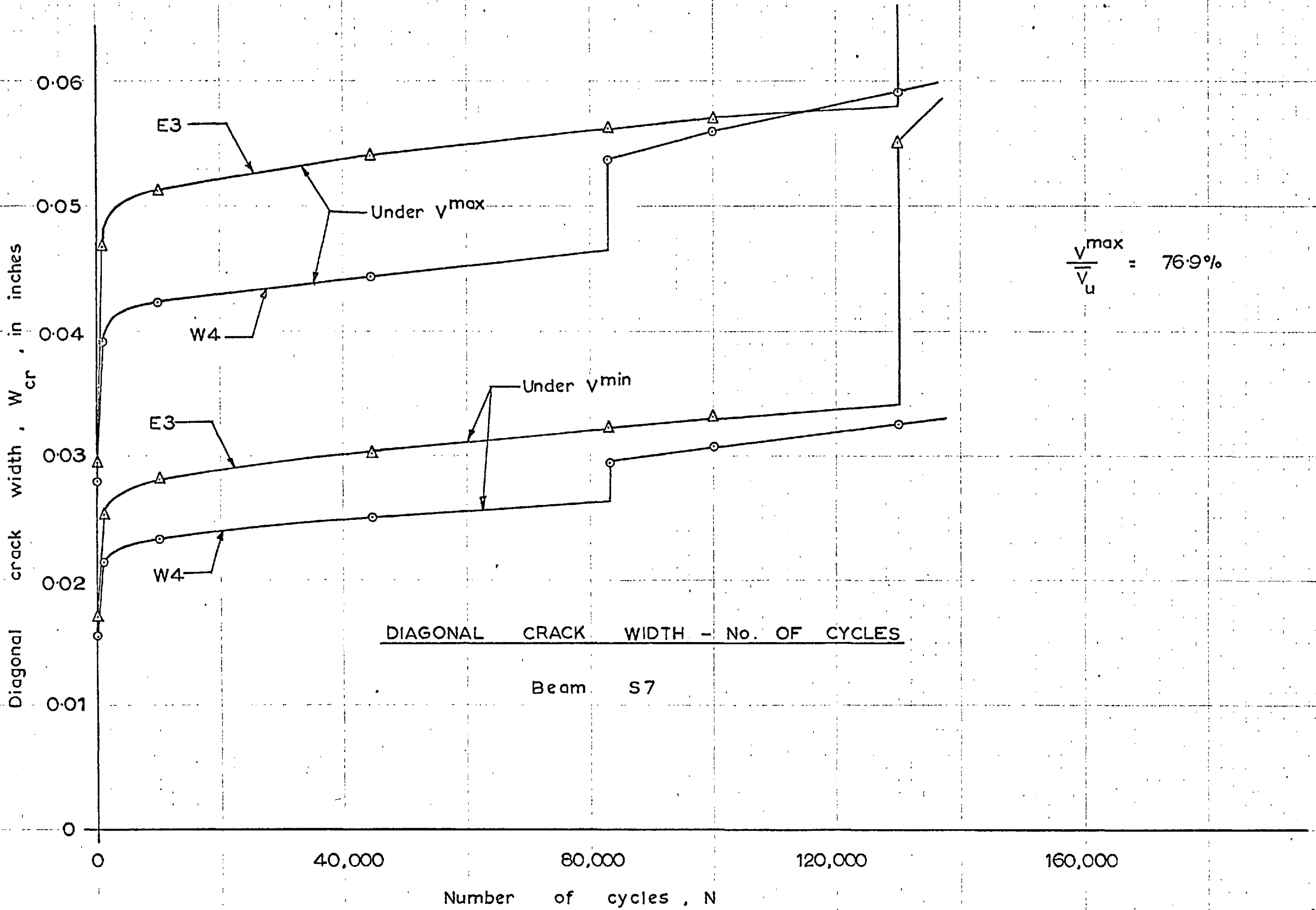

DIAGONAL CRACK WIDTH - No. OF CYCLES
Beam S7
$\frac{V^{max}}{V_u}$ = 76·9%
Under V^{max}
Under V^{min}
E3
W4
E3
W4
Diagonal crack width, W_{cr}, in inches
0·06
0·05
0·04
0·03
0·02
0·01
0
0
40,000
80,000
120,000
160,000
Number of cycles, N

Fig. 6.32

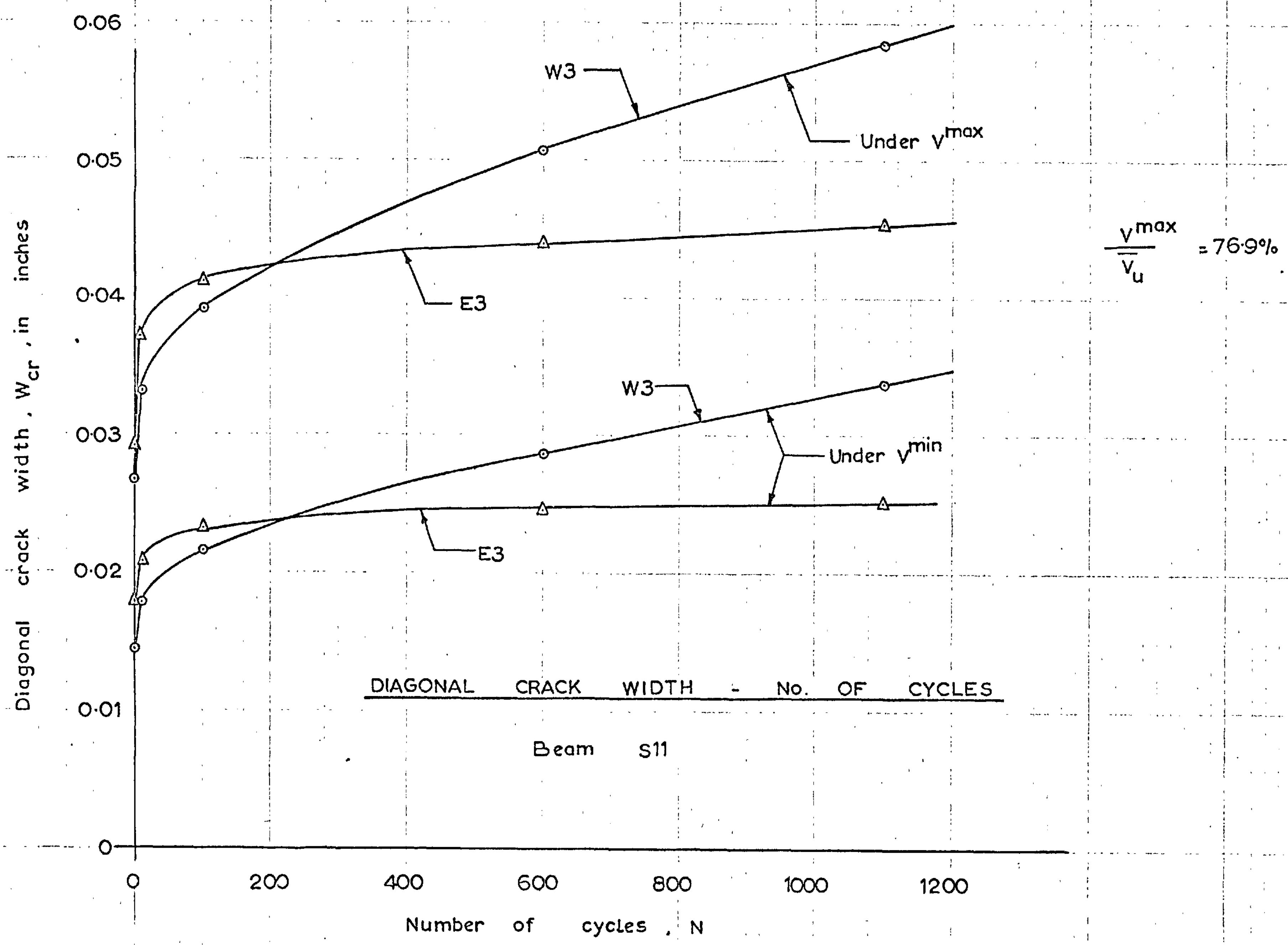

0.06
0.05
0.04
0.03
0.02
0.01
0
Diagonal crack width, W_{cr}, in inches
0
200
400
600
800
1000
1200
Number of cycles, N
W3
E3
Under V^{max}
W3
E3
Under V^{min}
$\frac{V^{max}}{V_u}$ = 76.9%
DIAGONAL CRACK WIDTH - No. OF CYCLES
Beam S11

Fig. 6.33

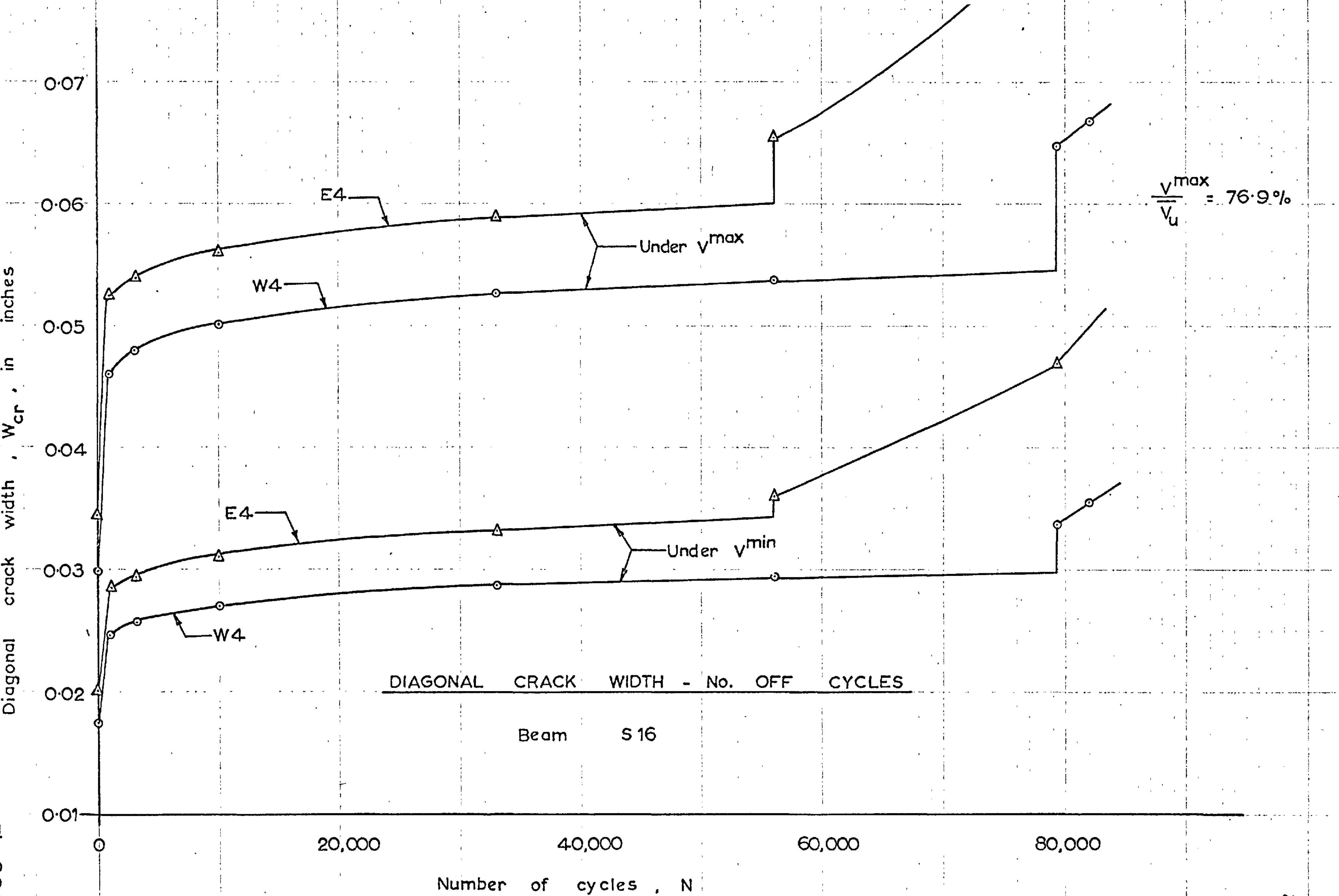
DIAGONAL CRACK WIDTH - No. OFF CYCLES
Beam S 16
$\frac{V^{max}}{V_u} = 76 \cdot 9\%$
E4
W4
Under V^{max}
E4
W4
Under V^{min}
Diagonal crack width, W_{cr}, in inches
0·07
0·06
0·05
0·04
0·03
0·02
0·01
0
20,000
40,000
60,000
80,000
Number of cycles, N

Fig. 6.34

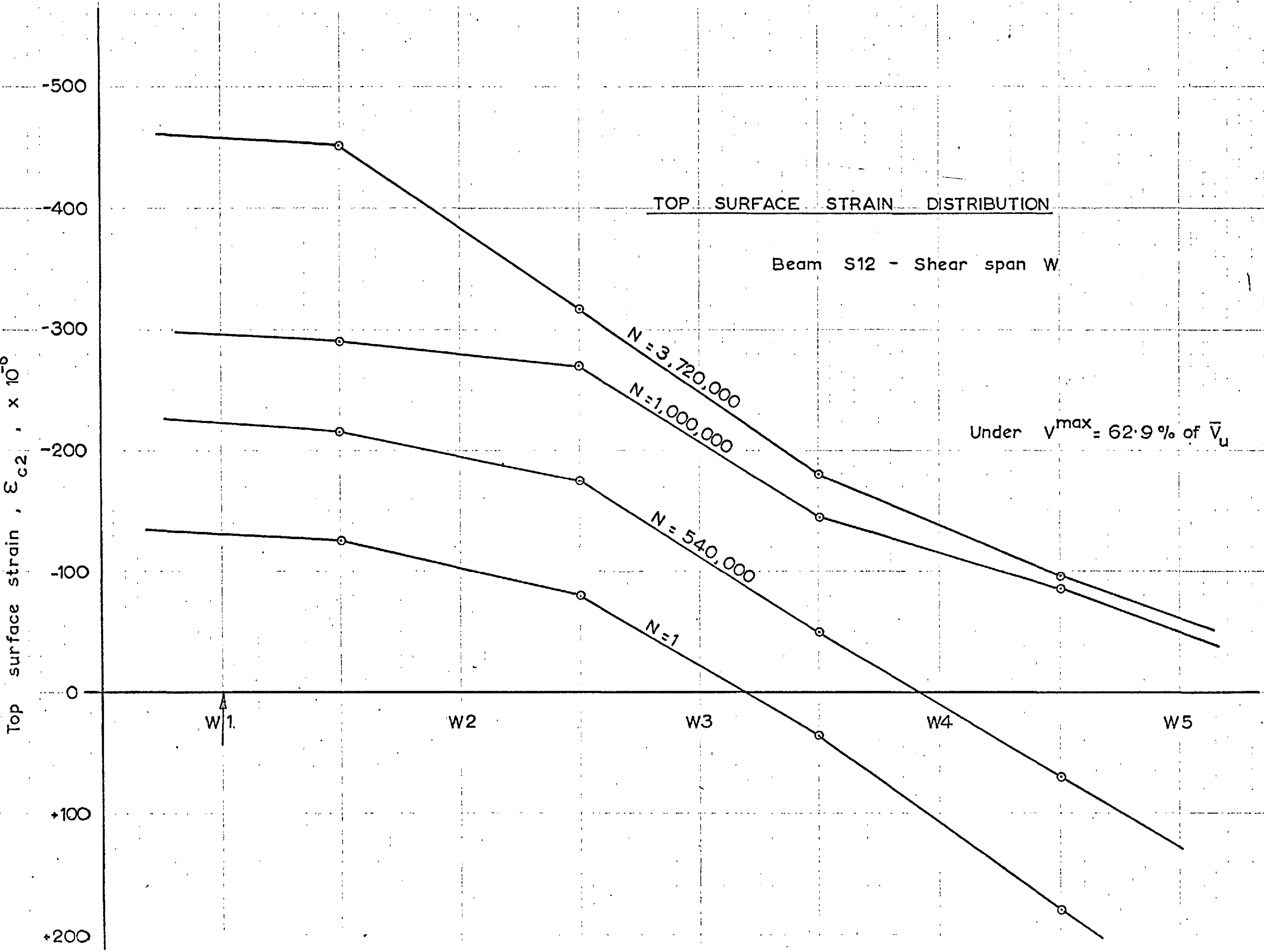
TOP SURFACE STRAIN DISTRIBUTION
Beam S12 - Shear span W
Under $V^{max} = 62{\cdot}9\%$ of $\bar{V}_u$
N = 3,720,000
N = 1,000,000
N = 540,000
N = 1
Top surface strain, ε_{c2}, $\times 10^{-6}$
-500
-400
-300
-200
-100
0
+100
+200
W1
W2
W3
W4
W5

Fig. 6.35

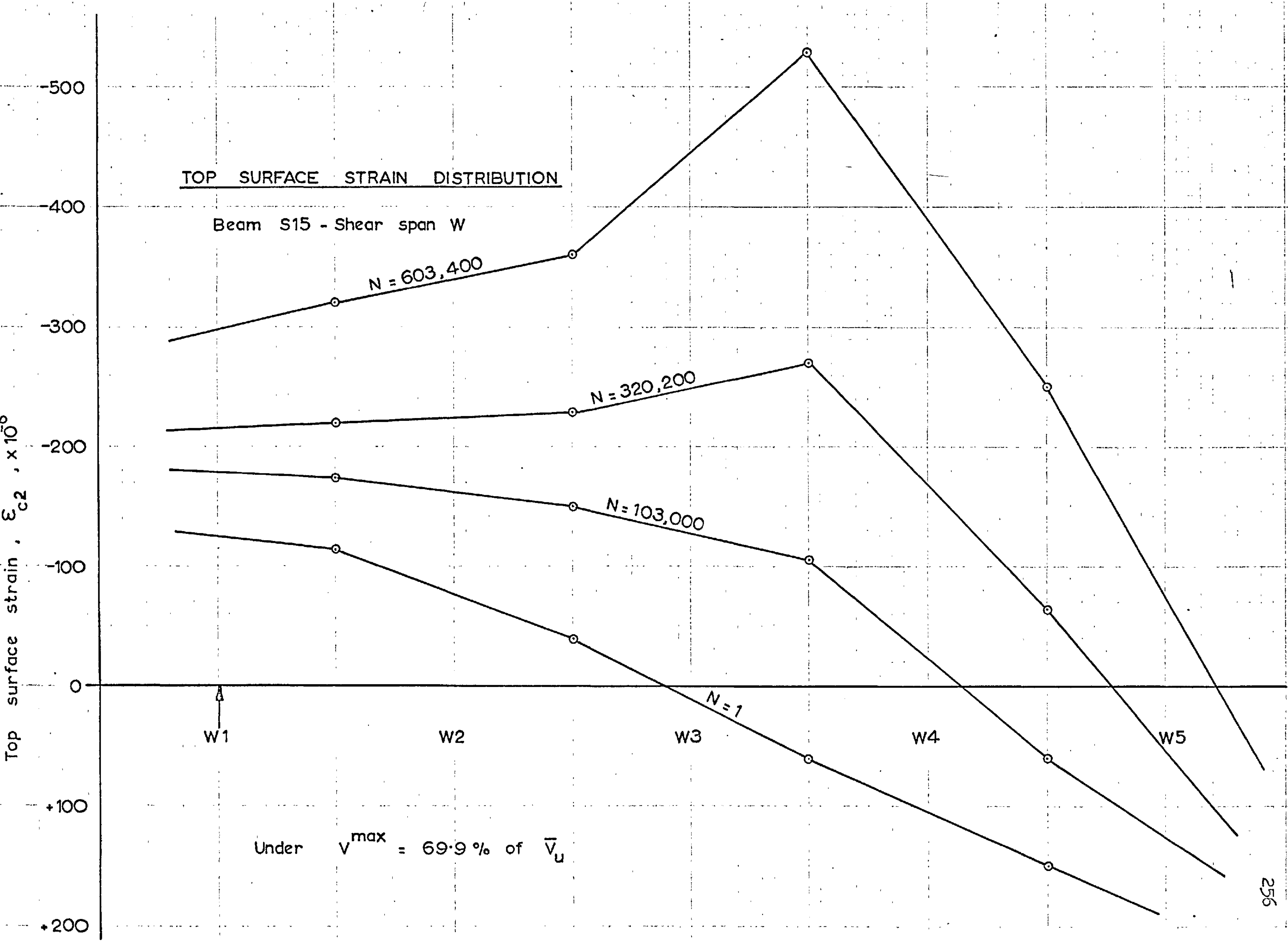
TOP SURFACE STRAIN DISTRIBUTION
Beam S15 - Shear span W
N = 603,400
N = 320,200
N = 103,000
N = 1
-500
-400
-300
-200
-100
0
+100
+200
W1
W2
W3
W4
W5
Top surface strain , ε_{c2} , $\times 10^{-6}$
Under V^{max} = 69·9 % of $\overline{V}_u$

Fig.6.36

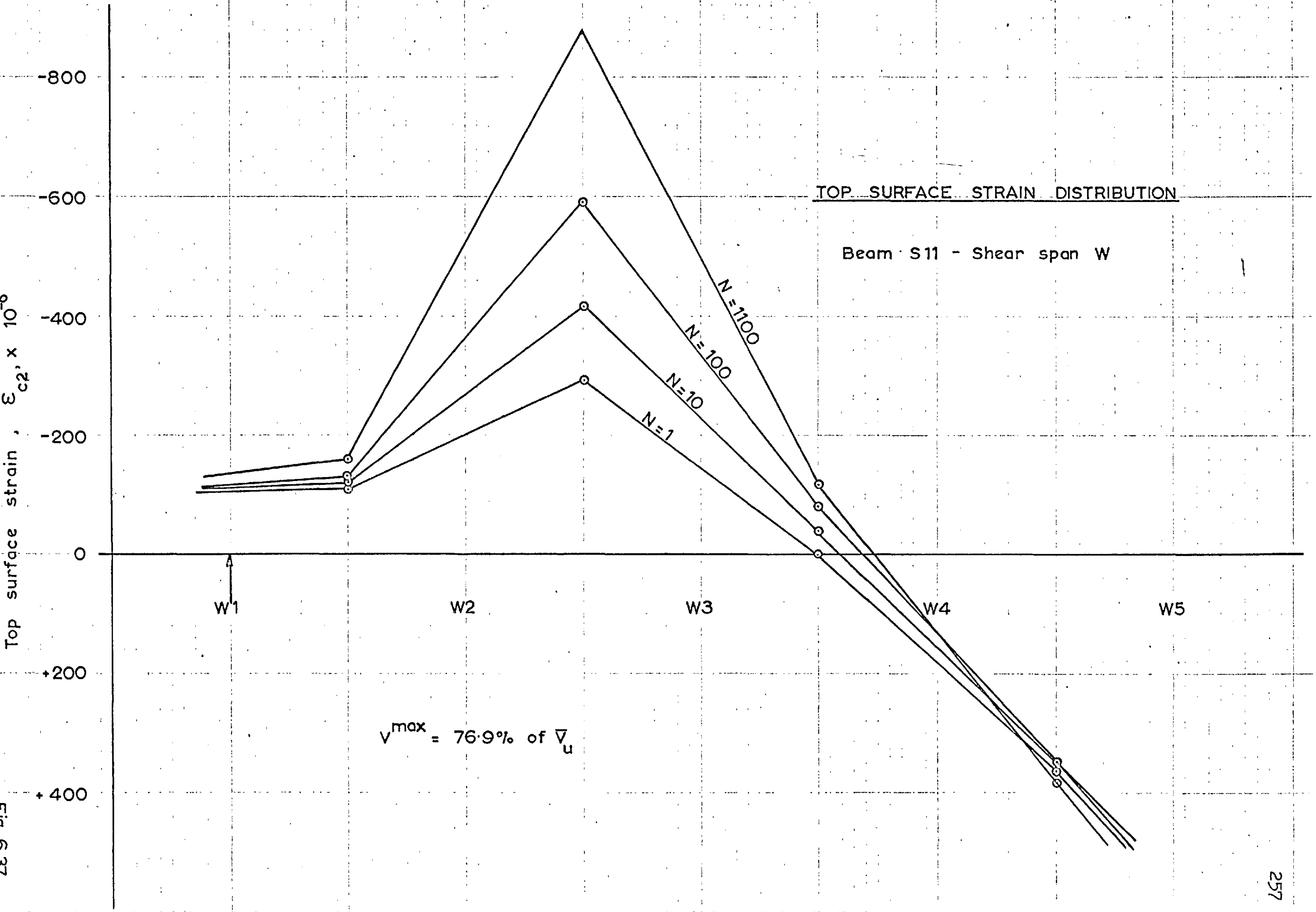
TOP SURFACE STRAIN DISTRIBUTION
Beam S11 - Shear span W
Top surface strain, ε_{c2}, x 10^{-6}
-800
-600
-400
-200
0
+200
+400
W1
W2
W3
W4
W5
N = 1100
N = 100
N = 10
N = 1
V^{max} = 76·9% of $\overline{V}_u$

Fig. 6.37

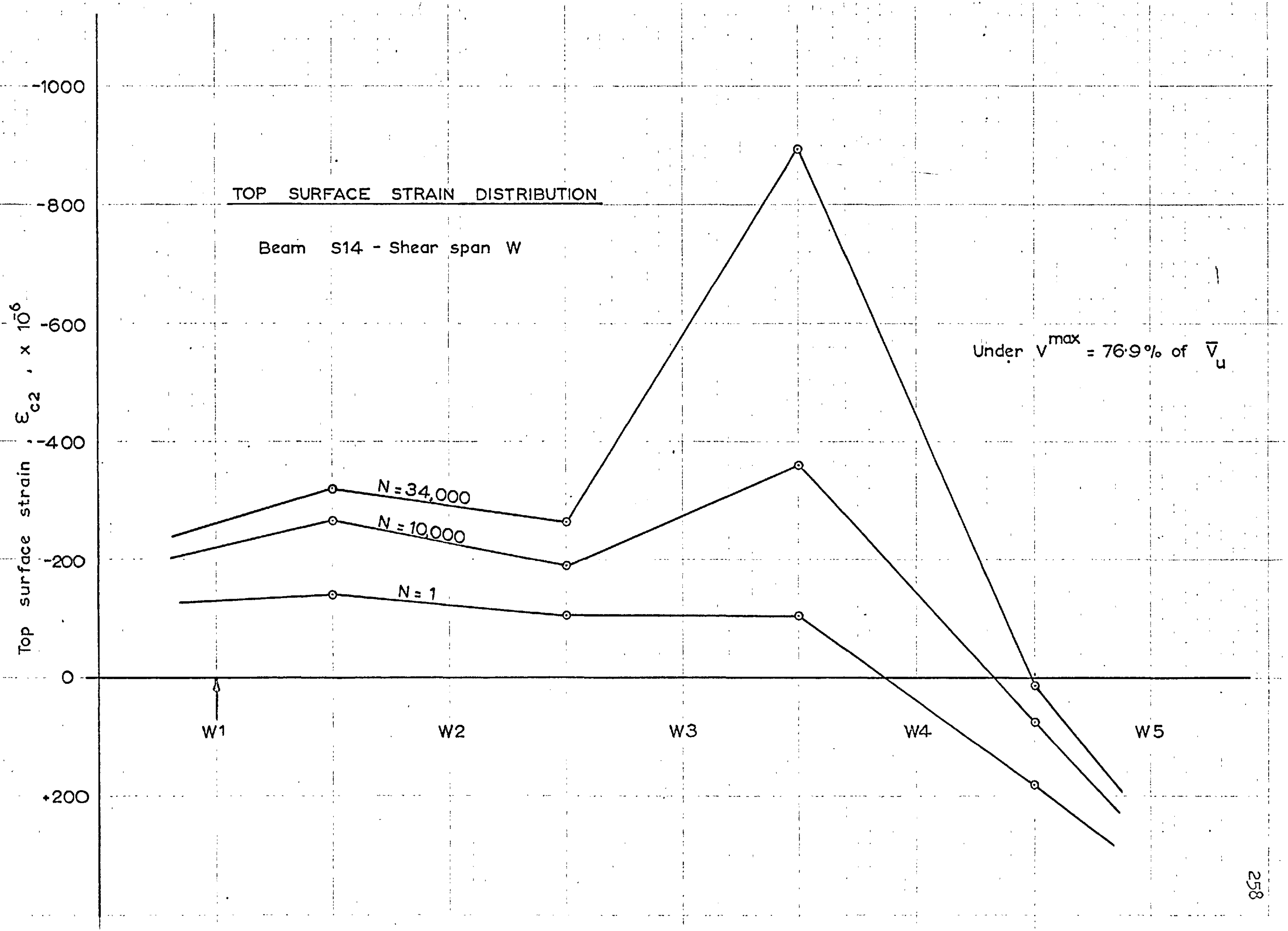
TOP SURFACE STRAIN DISTRIBUTION
Beam S14 - Shear span W
Under V^{max} = 76·9% of $\overline{V}_u$
Top surface strain ε_{c2}, $\times 10^{-6}$
-1000
-800
-600
-400
-200
0
+200
N = 34,000
N = 10,000
N = 1
W1
W2
W3
W4
W5

Fig. 6.38

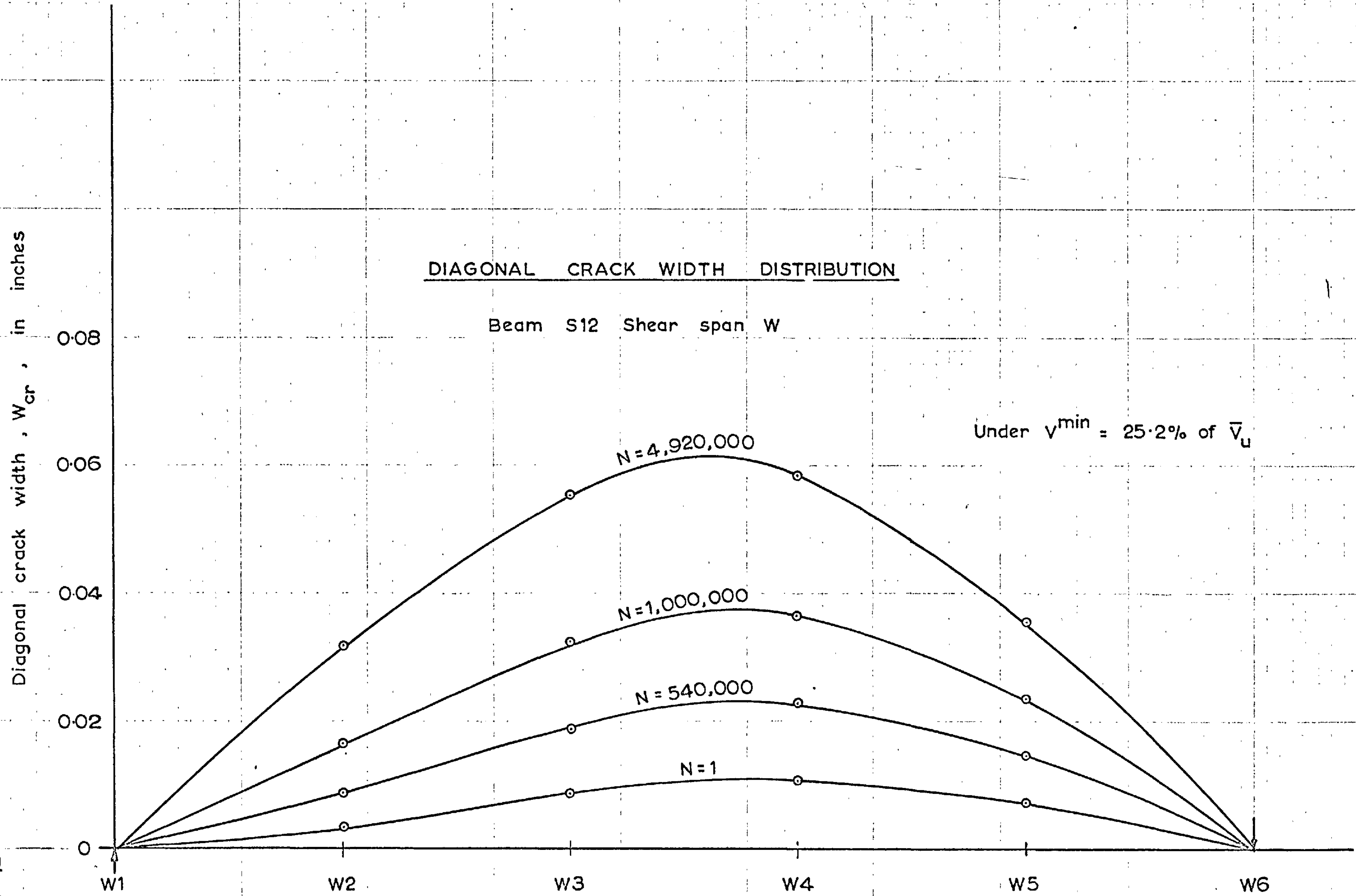

DIAGONAL CRACK WIDTH DISTRIBUTION
Beam S12 Shear span W
Under V^{min} = 25·2% of $\overline{V}_u$
Diagonal crack width , W_{cr} , in inches
0·08
0·06
0·04
0·02
0
N = 4,920,000
N = 1,000,000
N = 540,000
N = 1
W1
W2
W3
W4
W5
W6

Fig. 6.39

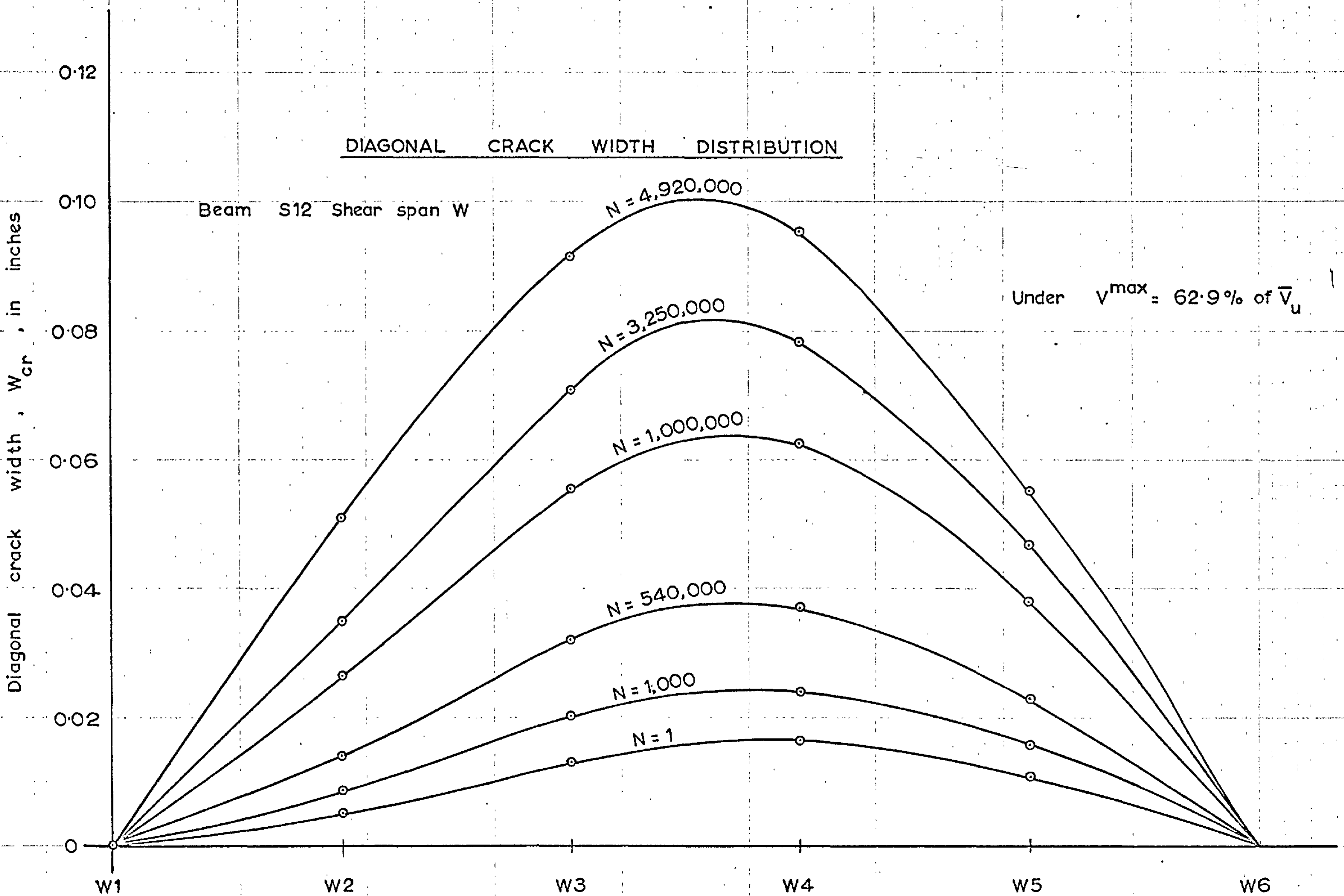

DIAGONAL CRACK WIDTH DISTRIBUTION
Beam S12 Shear span W
Under V^{max} = 62·9 % of $\overline{V}_u$
Diagonal crack width, W_{cr}, in inches
0·12
0·10
0·08
0·06
0·04
0·02
0
N = 4,920,000
N = 3,250,000
N = 1,000,000
N = 540,000
N = 1,000
N = 1
W1
W2
W3
W4
W5
W6

Fig. 6.40

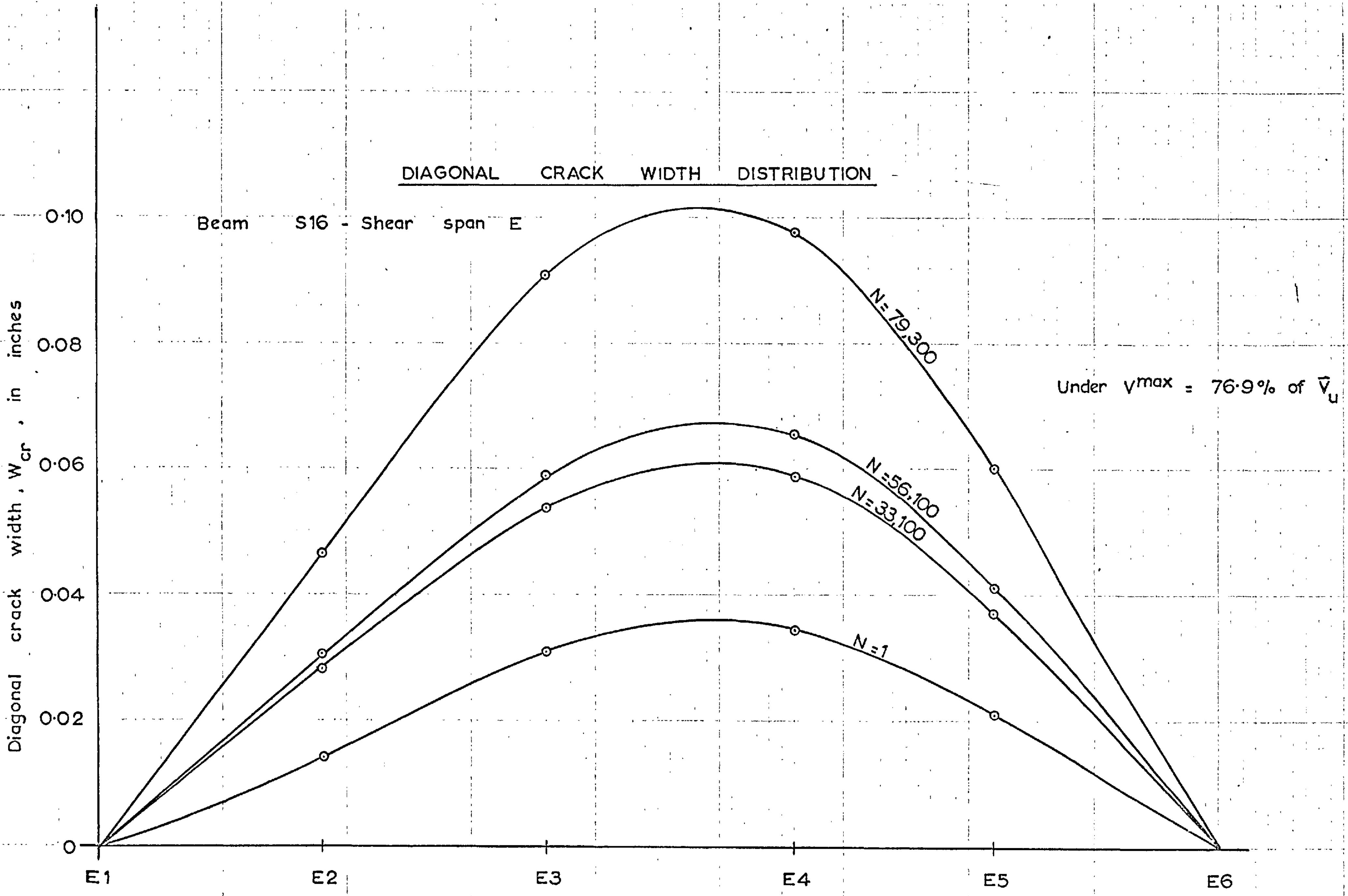
DIAGONAL CRACK WIDTH DISTRIBUTION
Beam S16 - Shear span E
Under V^{max} = 76·9% of $\bar{V}_u$
Diagonal crack width, W_{cr}, in inches
0·10
0·08
0·06
0·04
0·02
0
E1
E2
E3
E4
E5
E6
N=79,300
N=56,100
N=33,100
N=1

Fig.6.41

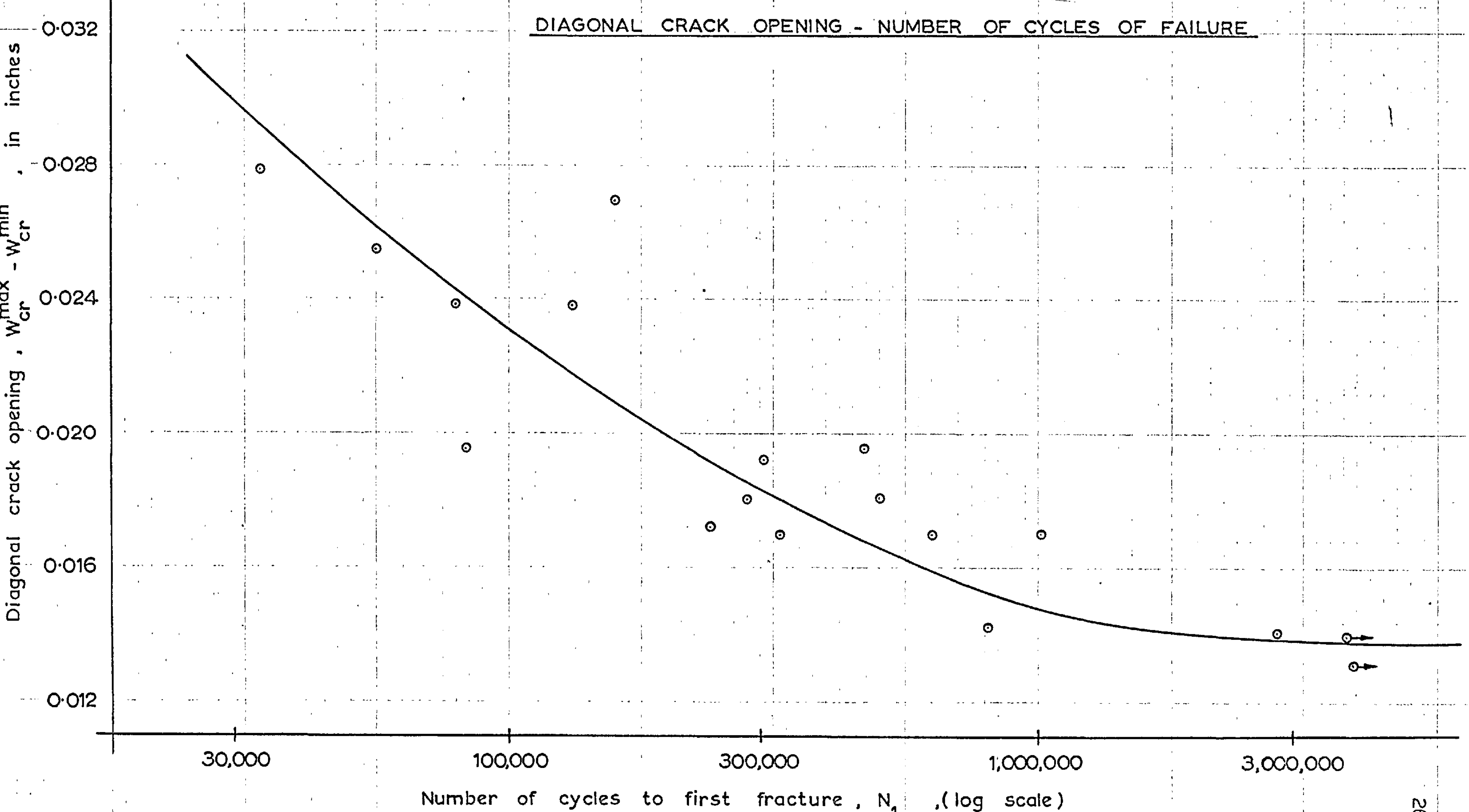
DIAGONAL CRACK OPENING - NUMBER OF CYCLES OF FAILURE
Diagonal crack opening , $W_{cr}^{max} - W_{cr}^{min}$, in inches
0·032
0·028
0·024
0·020
0·016
0·012
30,000
100,000
300,000
1,000,000
3,000,000
Number of cycles to first fracture , N_1 ,(log scale)

Fig. 6.42

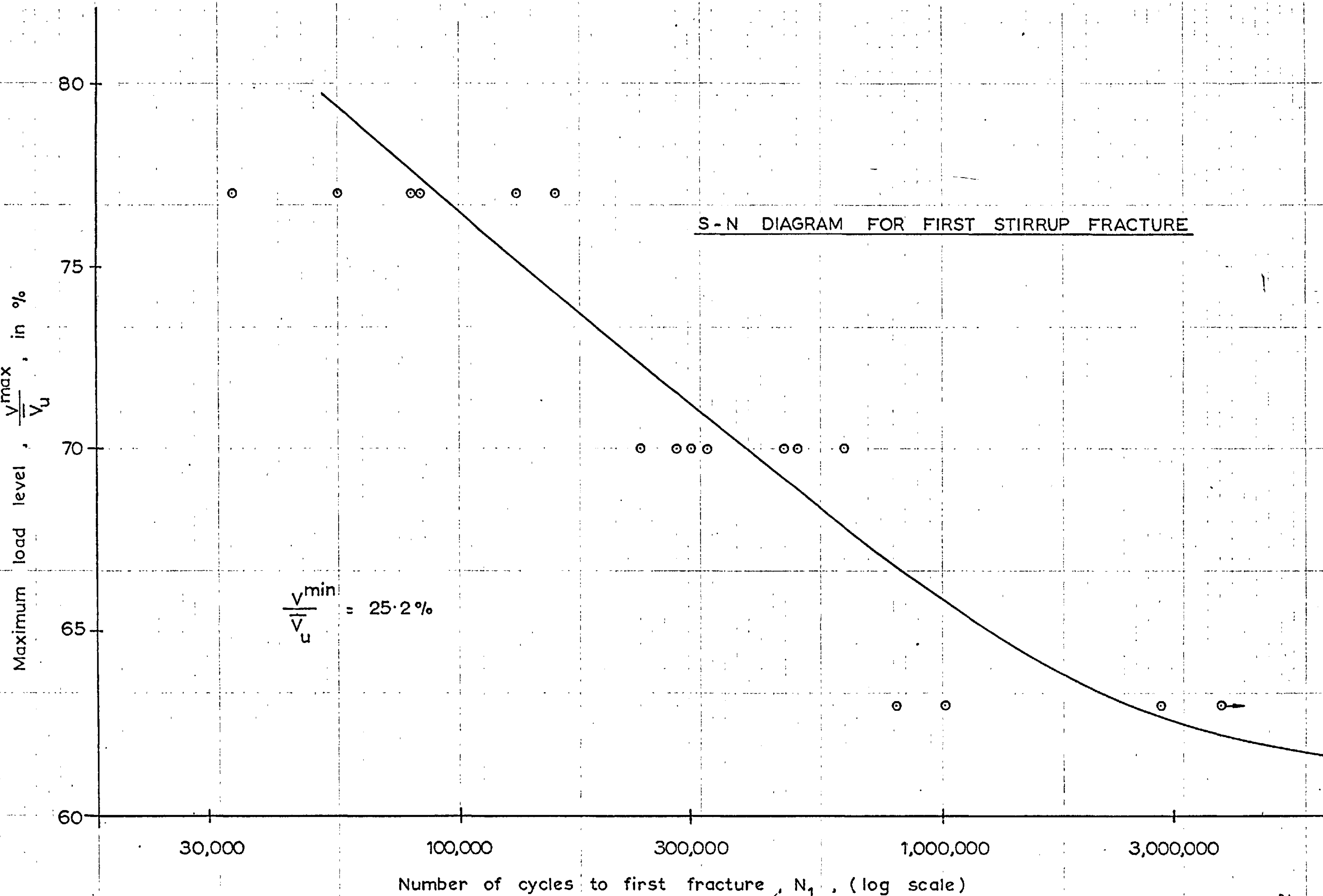
S - N DIAGRAM FOR FIRST STIRRUP FRACTURE
80
75
70
65
60
Maximum load level, $\frac{V^{max}}{V_u}$, in %
$\frac{V^{min}}{V_u} = 25 \cdot 2\ \%$
30,000
100,000
300,000
1,000,000
3,000,000
Number of cycles to first fracture, N_1, (log scale)

Fig. 6.43

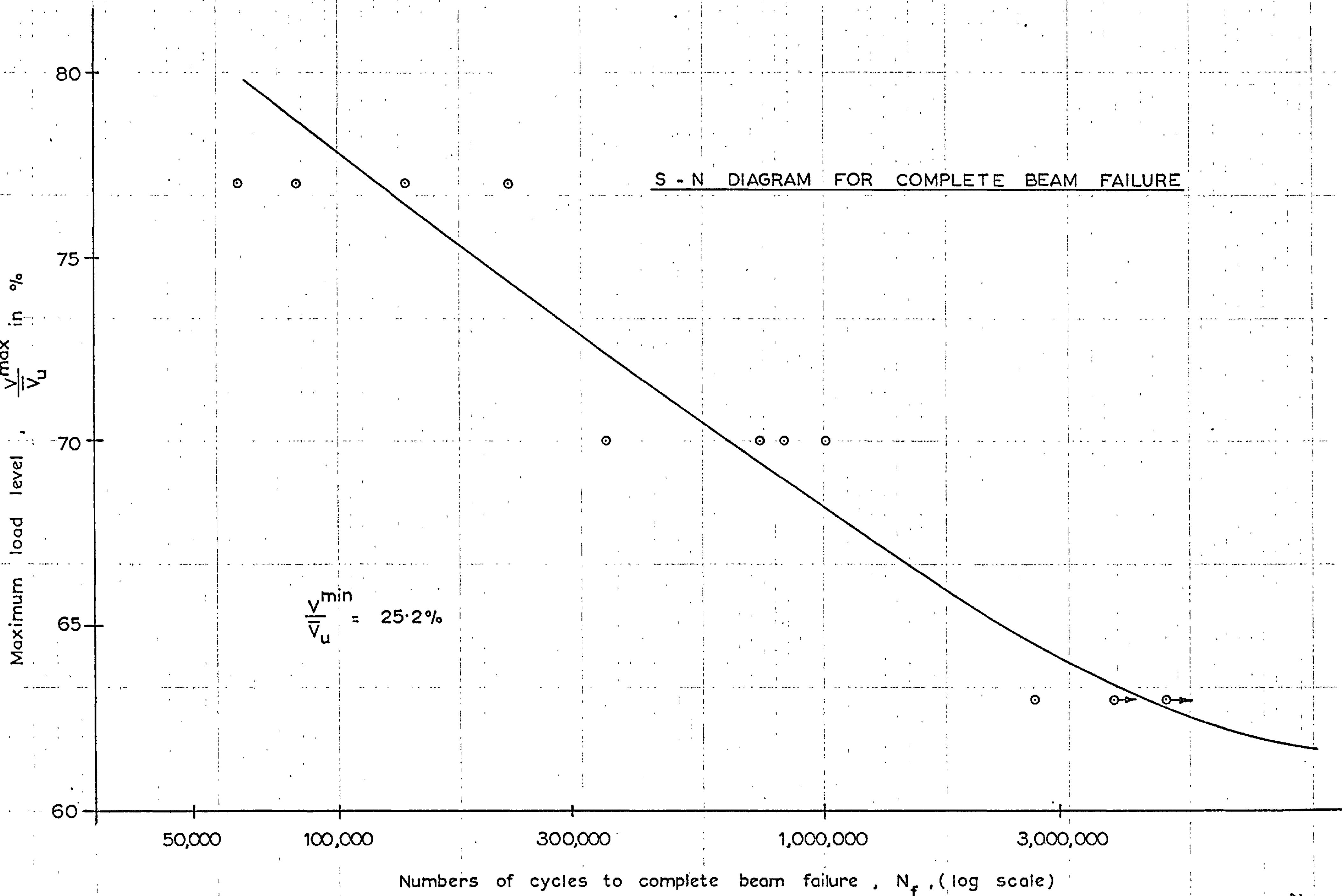
S - N DIAGRAM FOR COMPLETE BEAM FAILURE
Maximum load level , $\frac{V^{max}}{\bar{V}_u}$ in %
80
75
70
65
60
$\frac{V^{min}}{\bar{V}_u}$ = 25·2%
50,000
100,000
300,000
1,000,000
3,000,000
Numbers of cycles to complete beam failure , N_f ,(log scale)

Fig. 6.44

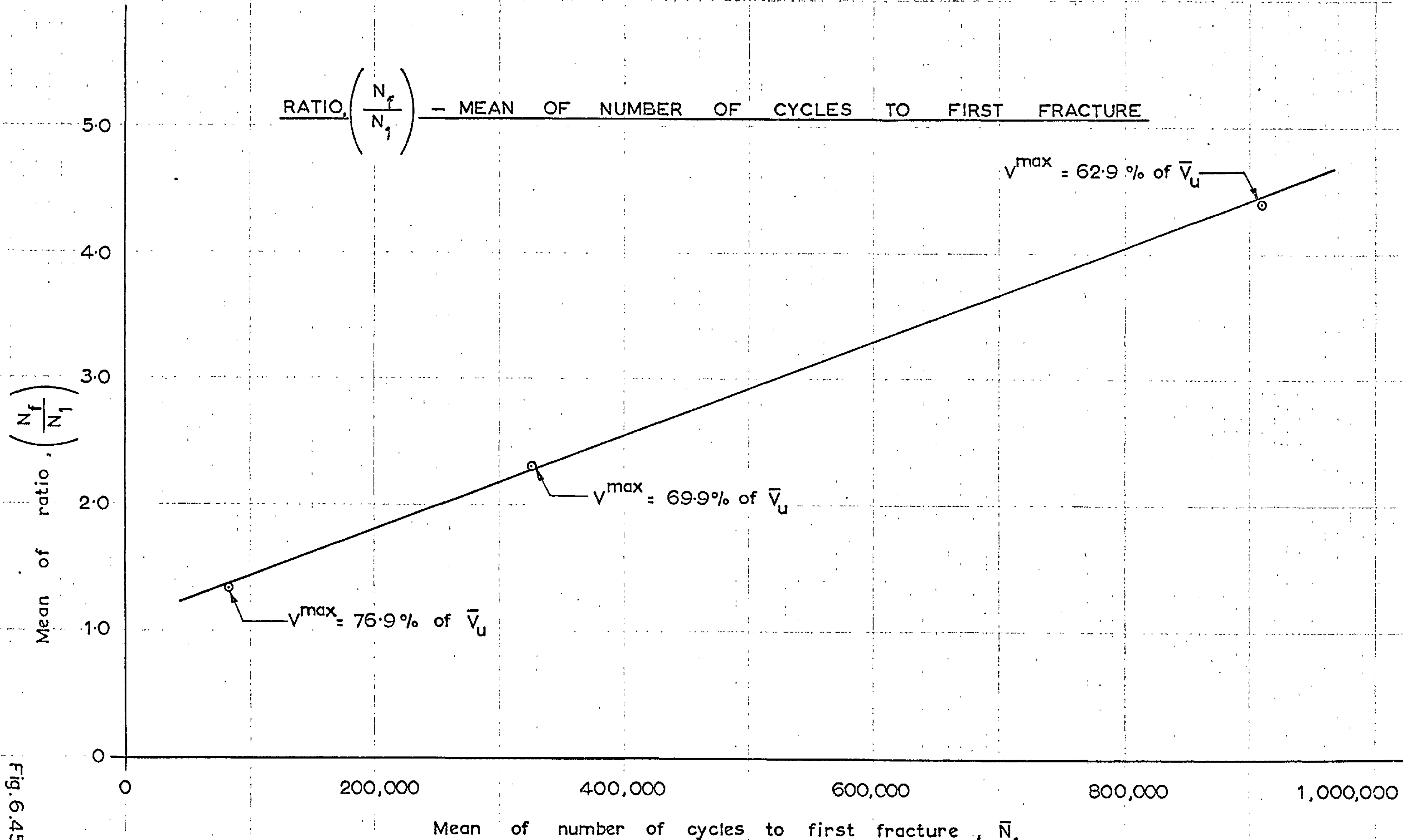

RATIO, $\left(\frac{N_f}{N_1}\right)$ – MEAN OF NUMBER OF CYCLES TO FIRST FRACTURE
V^{max} = 62·9 % of $\bar{V}_u$
V^{max} = 69·9% of $\bar{V}_u$
V^{max} = 76·9 % of $\bar{V}_u$
5·0
4·0
3·0
2·0
1·0
0
0
200,000
400,000
600,000
800,000
1,000,000
Mean of ratio, $\left(\frac{N_f}{N_1}\right)$
Mean of number of cycles to first fracture, $\bar{N}_1$

Fig. 6.45

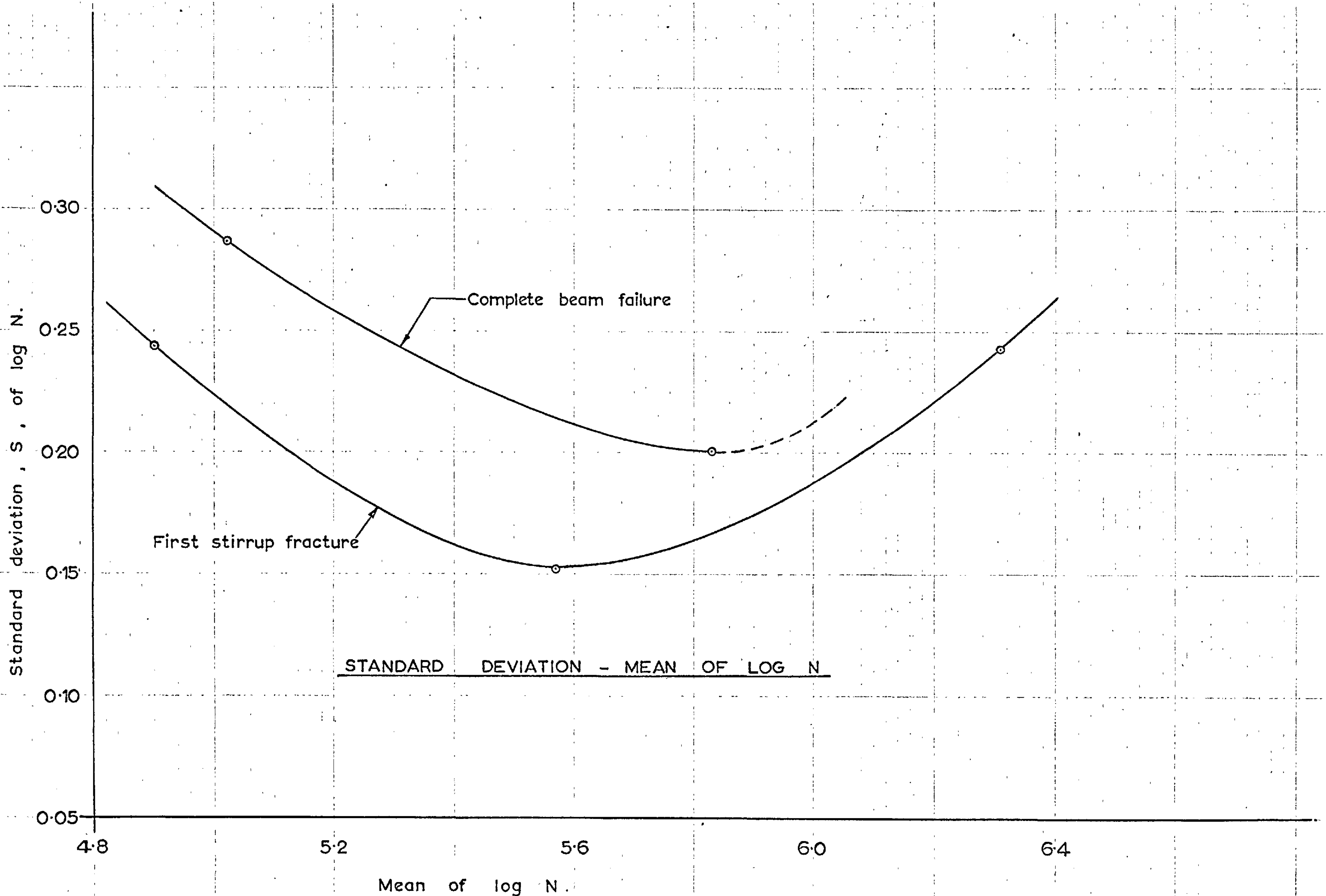
STANDARD DEVIATION - MEAN OF LOG N
Complete beam failure
First stirrup fracture
Standard deviation, S, of log N.
0·30
0·25
0·20
0·15
0·10
0·05
4·8
5·2
5·6
6·0
6·4
Mean of log N.

Fig. 6.46

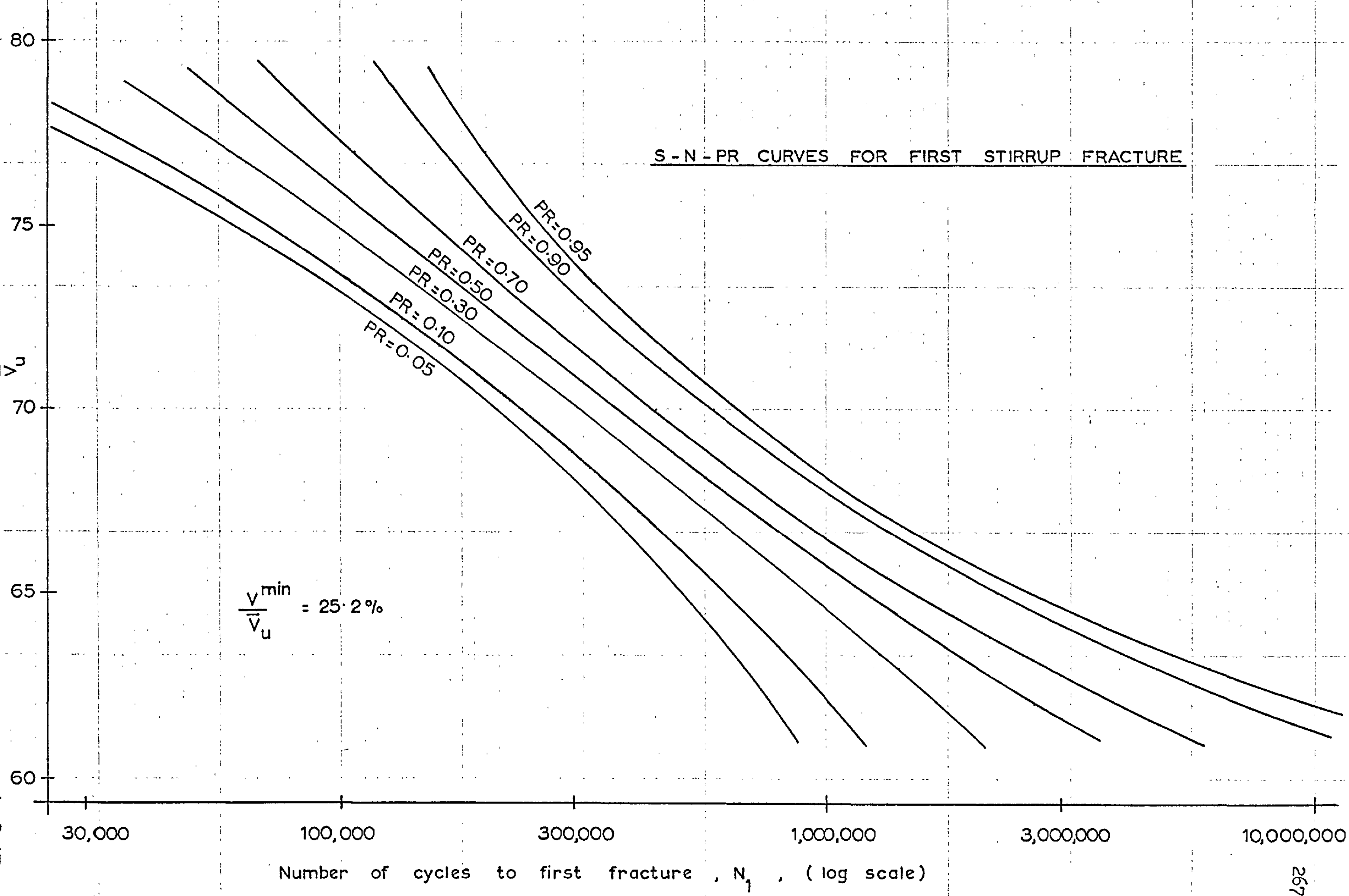
S - N - PR CURVES FOR FIRST STIRRUP FRACTURE
PR = 0.95
PR = 0.90
PR = 0.70
PR = 0.50
PR = 0.30
PR = 0.10
PR = 0.05
$\frac{V^{min}}{\bar{V}_u} = 25 \cdot 2\%$
Maximum load level , $\frac{V^{max}}{\bar{V}_u}$, in %
80
75
70
65
60
30,000
100,000
300,000
1,000,000
3,000,000
10,000,000
Number of cycles to first fracture , N_1 , (log scale)

Fig. 6.47

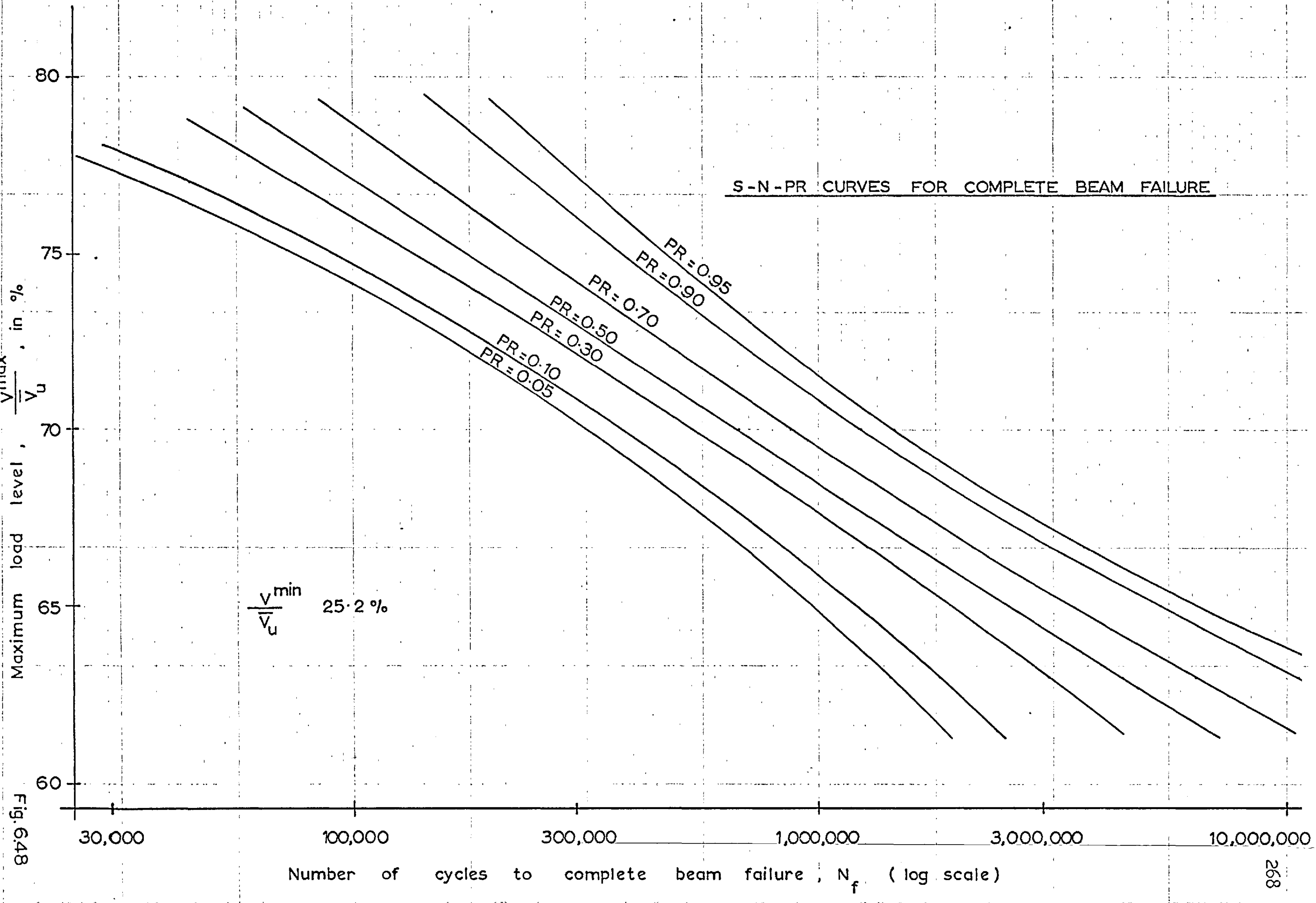
S-N-PR CURVES FOR COMPLETE BEAM FAILURE
PR = 0·95
PR = 0·90
PR = 0·70
PR = 0·50
PR = 0·30
PR = 0·10
PR = 0·05
$\frac{V^{min}}{\bar{V}_u}$ 25·2 %
Maximum load level, $\frac{V^{max}}{\bar{V}_u}$, in %
80
75
70
65
60
30,000
100,000
300,000
1,000,000
3,000,000
10,000,000
Number of cycles to complete beam failure, N_f (log scale)

Fig. 648

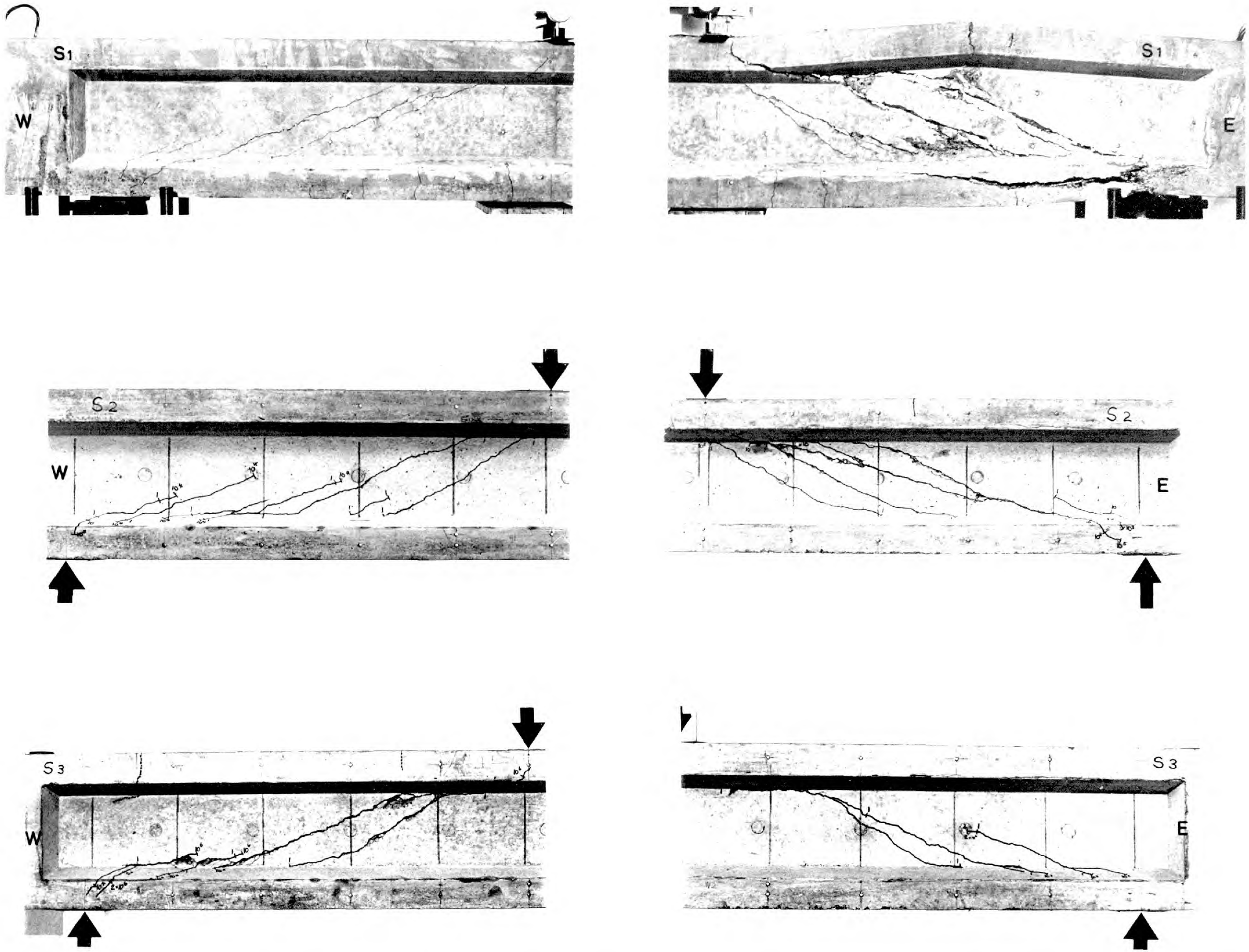

PLATE 6.1

PLATE 6.2

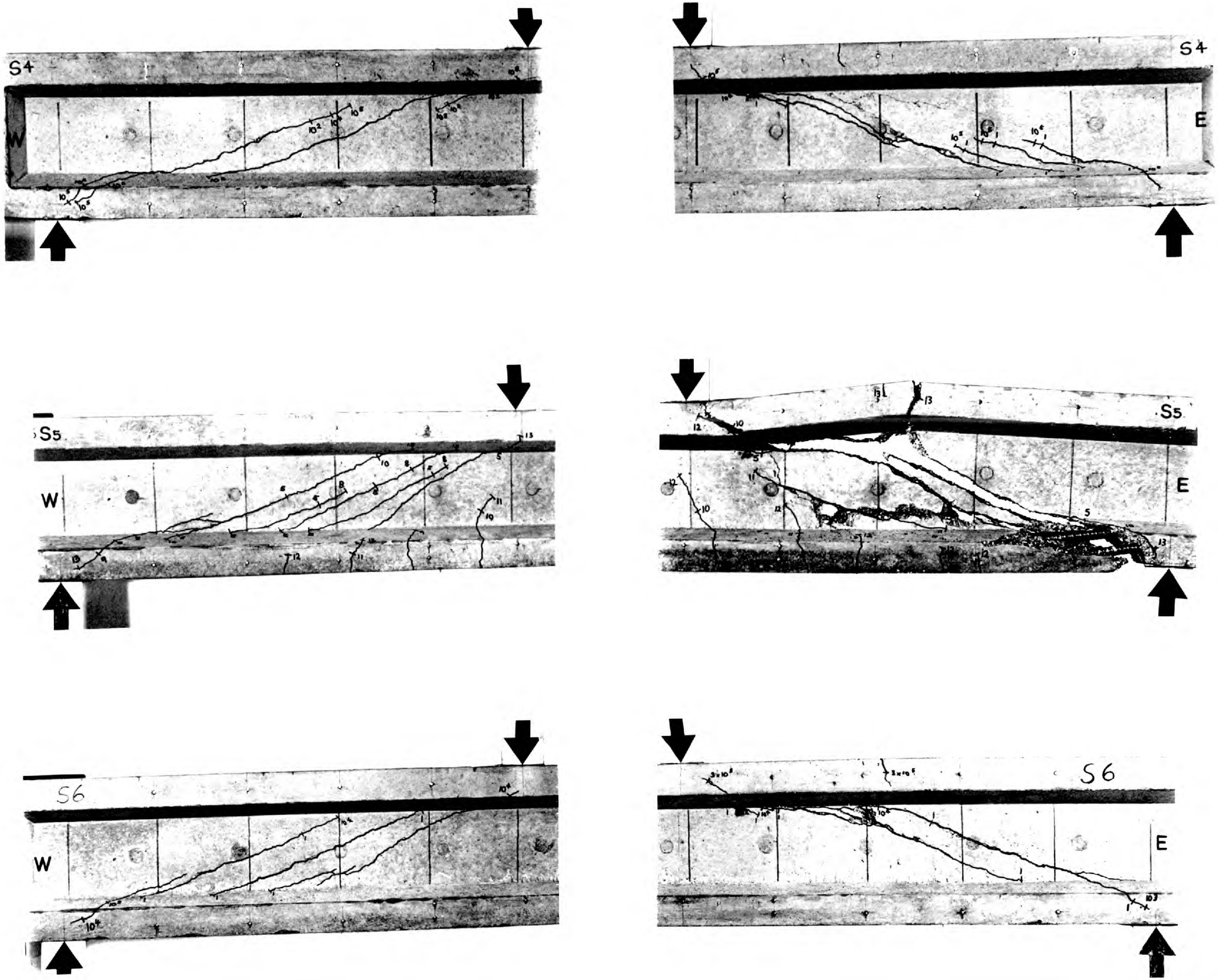

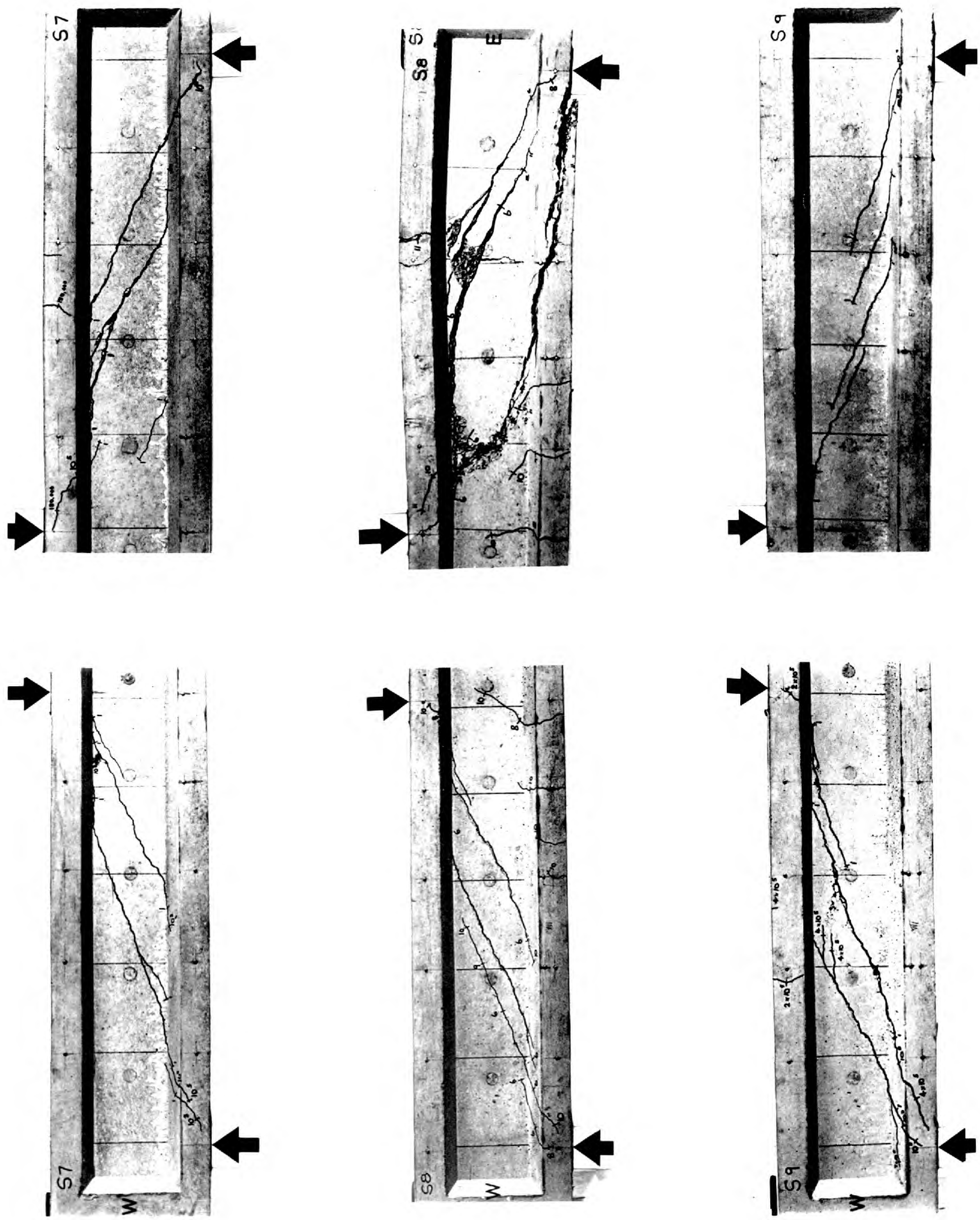

PLATE 6.3

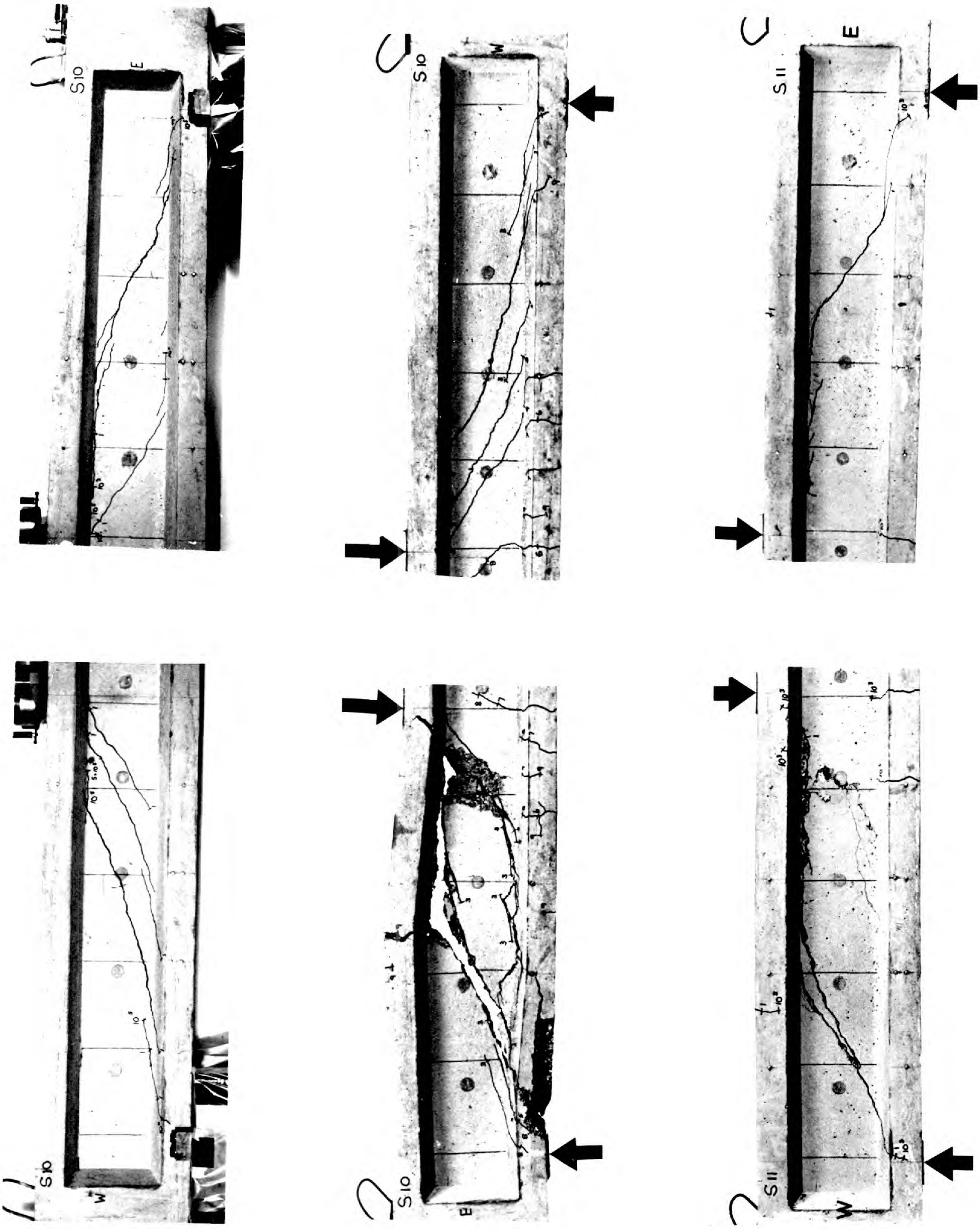

PLATE 6.4

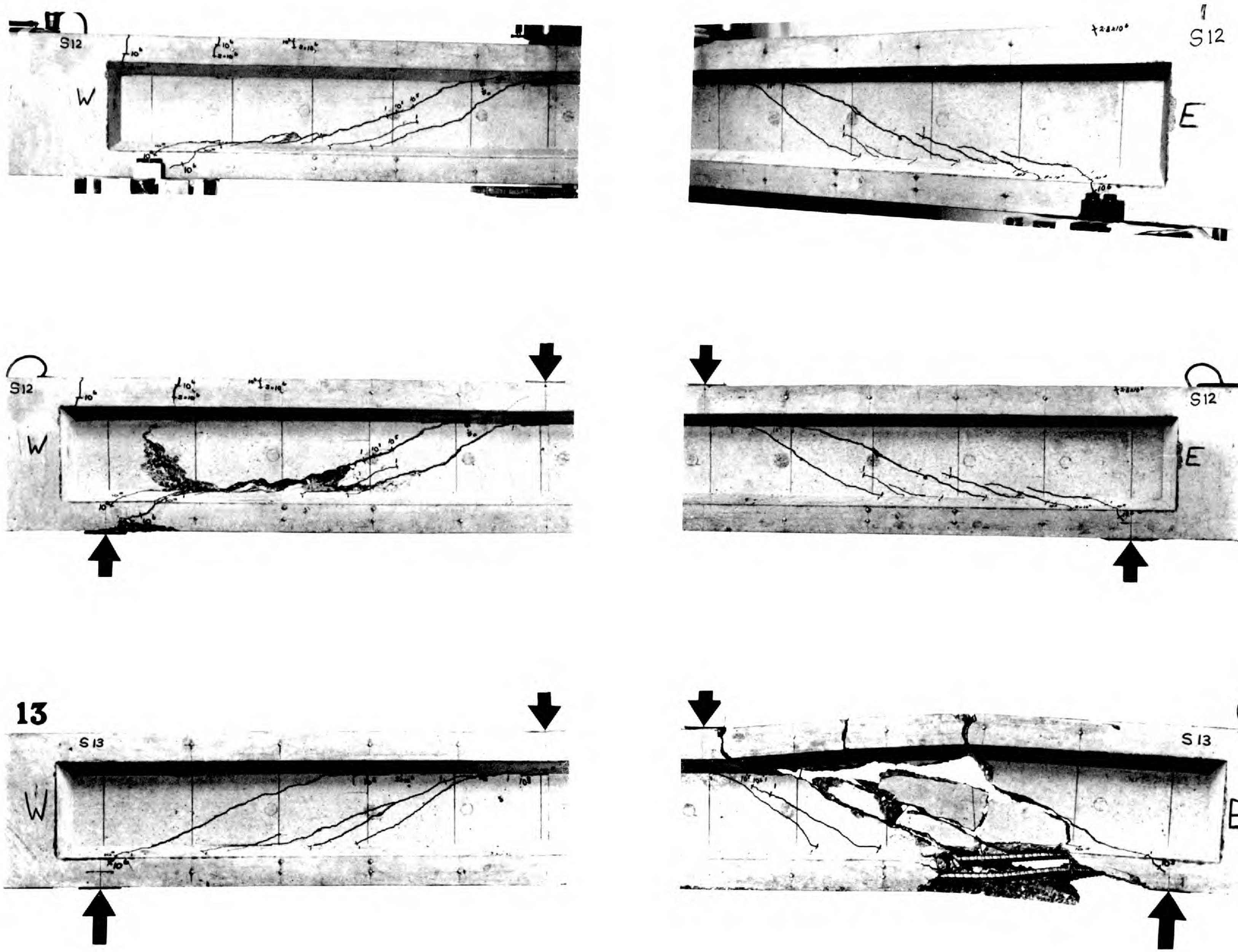

PLATE 6.5

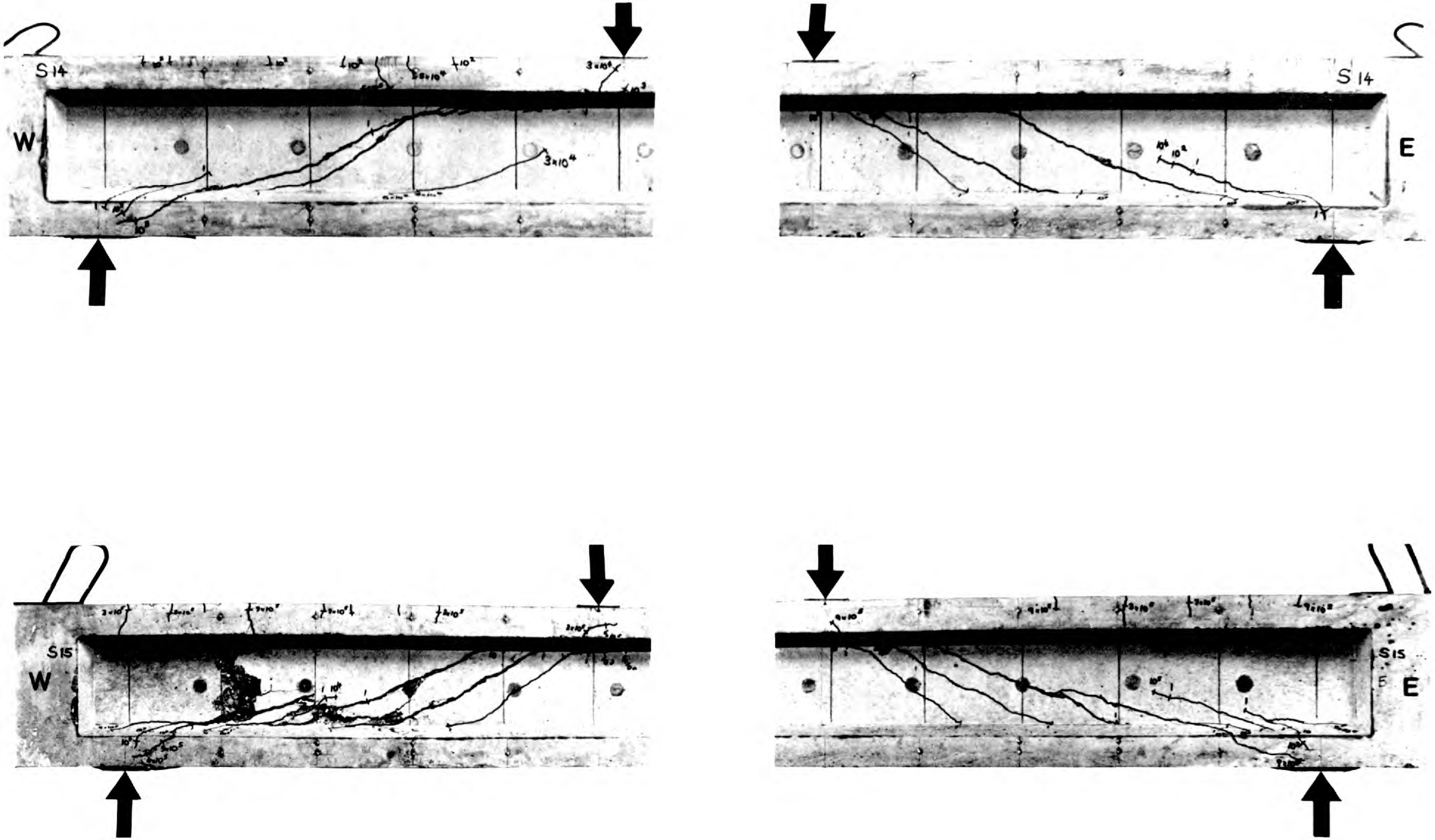

PLATE 6.6

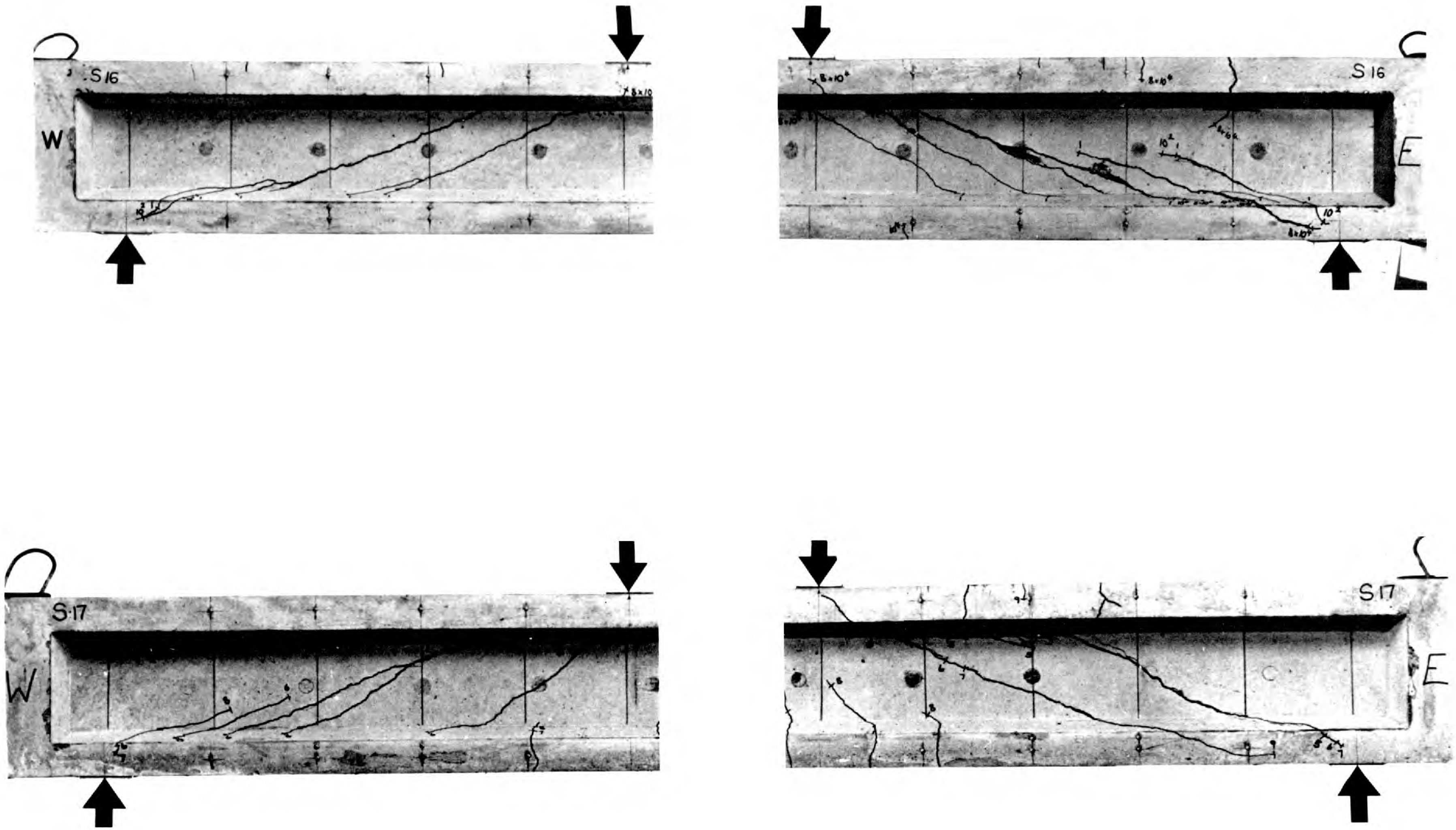

PLATE 6.7

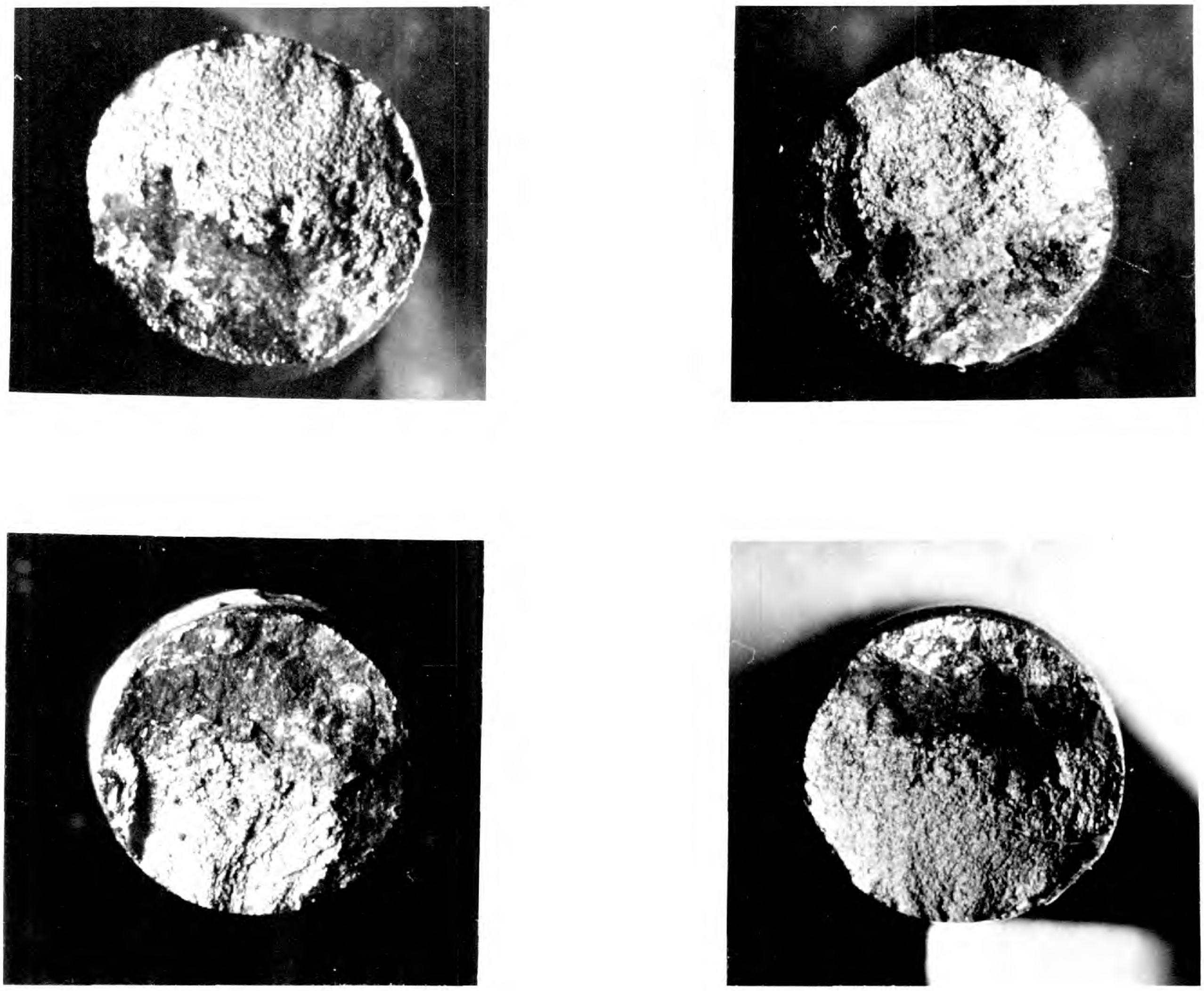

EXAMPLES OF STIRRUP FATIGUE FRACTURES

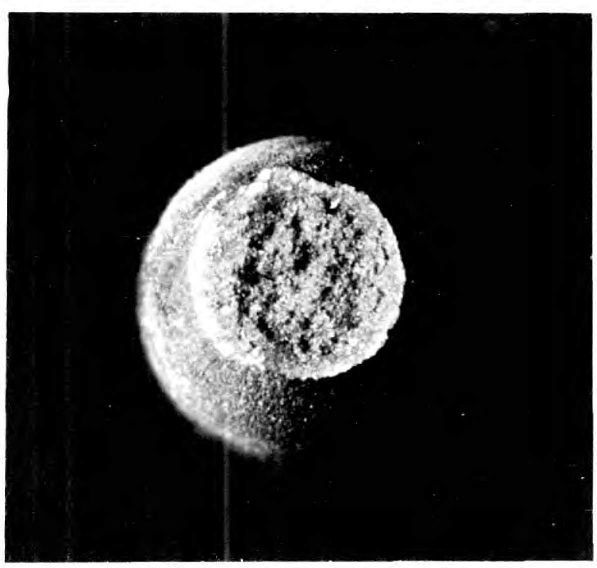

EXAMPLE OF STATIC DUCTILE FRACTURE

PLATE 6.8

EXAMPLE OF STIRRUP FRACTURE SHOWING FRETTING CORROSION

PLATE 6.9

CHAPTER 7

CONCLUSIONS AND SUGGESTIONS FOR FUTURE RESEARCH.

7.1) MAIN CONCLUSIONS

The results of the present investigation, together with some previously accepted facts, lead to the following conclusions about the fatigue behaviour of prestressed concrete structures :-

7.1a) IN FLEXURE

(1) Flexural cracking is possible in prestressed concrete sections under repeated loads of lesser magnitude than the static flexural cracking load. The flexural cracking life may be satisfactorily predicted by means of normal elastic stress analysis, and the use of an experimentally obtained S - N relationship.

(2) Fatigue failures will not occur in uncracked sections. However, in a poorly - proportioned section, fatigue failures may occur at repeated load levels below the static flexural cracking load, if the section is cracked by a previous overload.

(3) The response of cracked sections to load is significantly affected by repeated loading of magnitude sufficient to cause flexural cracks to open. This is brought about by progressive breakdown of the bond between the prestressing steel and the concrete, and changes in the stress - strain relationship of concrete. These changes occur rapidly in the early load cycles, but reach virtually stable values after about 30,000 cycles.

(4) Fatigue failure of normal under - reinforced sections generally occurs by fracture of the prestressed reinforcement. When the reinforcement consists of a small number of steel elements, complete collapse will soon occur after the first fracture. However, if the section contains a number of steel elements, many more load cycles will be resisted before structural collapse, and the failure will be more gradual, although progressive.

(5) ....

(5) Concrete fatigue failures (in compression) are also possible at high load levels in under - reinforced sections, and at lower load levels in over - reinforced beams.

(6) In sections with poor bond, a considerable reduction in the fatigue strength of steel (from its strength in air) is likely to occur due to the action of fretting. In structures with deflected cables and saddle - points, the reductions may be even greater than those found to date.

(7) A comprehensive theory is presented for prediction of the fatigue life in flexure of prestressed concrete sections, the criterion of failure being steel fatigue fracture. The theory includes statistical analysis and makes allowance for a reduction in the fatigue strength of prestressing steel when embedded in concrete.

(8) Statistical analysis is essential in all fatigue investigations.

(9) A prior history of repeated loading has no significant effect on the static ultimate flexural strength of sections in subsequent tests to failure.

7.1b) IN SHEAR

(1) Diagonal tension cracking is possible in prestressed concrete sections under repeated loads of lesser magnitude than the static diagonal tension cracking load. The fatigue strength of concrete in tension in the web of prestressed I - beams may be considerably higher than that of control specimens subjected to repeated tensile stresses.

(2) A prior history of repeated loading on a beam in an uncracked state, has no significant effect on the static diagonal cracking strength, but it does significantly affect the propagation of diagonal cracks, which may, in its turn, have a detrimental effect on the subsequent fatigue strength.

(3) ....

(3) The width of diagonal cracks increases considerably under the action of repeated loading. This is brought about by progressive bond breakdown between the web reinforcement and adjacent concrete. Once formed, diagonal cracks in the web of I - beams will not close completely on unloading.

(4) The stresses in web reinforcement are negligible before the occurrence of diagonal cracking.

(5) Shear failures in fatigue may occur in prestressed concrete beams with diagonal cracks by fatigue fracture of the web reinforcement. However, even with a small number of effective stirrups crossing the diagonal cracks, there will be a very considerable difference between the number of cycles to first fracture of a stirrup, and the number of cycles to complete collapse, when the repeated loading is in the region of the fatigue limit.

(6) A prior history of repeated loading has no significant effect on the static ultimate shear strength of beams in subsequent tests to failure.

7.2) SUGGESTIONS FOR FUTURE RESEARCH

7.2a) IN FLEXURE

(1) The amount of useful information pertaining to flexural cracking under repeated load is extremely limited, and since it is a phenomenon which is subject to considerable scatter, it is desirable that further tests be carried out to verify the results obtained in this investigation.

(2) It is imperative that the effects of fretting between steel and concrete be illucidated by further research on the subject. The author's results have shown that considerable reductions in the fatigue strength of steel may occur as a result of fretting, and since even the basic mechanism of fretting between steel and concrete is unknown, it is essential that the effect of the important parameters be investigated.

(3) Further well - instrumented beam tests are essential once the action of fretting has been better established. These tests should incorporate different bond conditions, and must have a statistical basis.

7.2b) IN SHEAR

(1) A greater number of beam tests are required to investigate the effect of repeated loading on diagonal cracking in prestressed I - beams. The author's results are based on two tests only, and cannot, therefore, be stated to be conclusive.

(2) The effect of repeated loading on beams which fail statically in shear - compression, web - crushing, and other less common modes of shear failure, should be determined.

(3) Investigations should be carried out to compare the fatigue behaviour of mild steel in air with its behaviour when used as web reinforcement.

R E F E R E N C E S

1) GENE M. NORDBY. "Fatigue of Concrete - A Review of research." A.C.I. Journal, Vol. 55. August, 1958.

2) J.W. MURDOCK. "A critical review of research on fatigue on plain concrete." University of Illinois Experimental Station Bulletin No. 475. February, 1965.

3) J.L. VAN ORNUM. "Fatigue of concrete." A.S.C.E. Transactions. Vol. 58, pp. 294 - 320. 1907.

4) E. PROBST. "The influence of rapidly alternating loading on concrete and reinforced concrete." "The Structural Engineer." Vol. 9. October and December, 1931.

5) J. deC. ANTRIM & J.F. McLAUGHLIN. "Fatigue study of air-entrained concrete." Journal A.C.I. Vol. 30, No. 11. May 1959.

6) E.W. BENNETT & S.E. St.J. MUIR. "Some fatigue tests of high-strength concrete in axial compression." Magazine of concrete research. Vol. 19, No. 59. June, 1967.

7) F.S. OPLE & C.L. HULSBOS. "Probable fatigue life of plain concrete with stress gradient." A.C.I. Journal. Vol. 63, No. 1. January, 1966.

8) F.S. OPLE & C.L. HULSBOS. "Probable life of Prestressed beams as limited by concrete failure." Report No. 223.26A, Fritz Engineering Laboratory, Lehigh University. October, 1963.

9) J.A. NEAL. "Mechanism of fatigue failure for plain concrete." A.S.M.E. - Materials Technology - Interamerican approach. May 20 - 24. pp. 215 - 221. 1968

10) C.E. KESLER. "Statistical relation between cylinder, modified cube and beam strength of plain concrete." Proceedings A.S.T.M. Vol. 54. 1954. pp. 1178 - 1187.

11) B.M. ASSIMACOPOULOUS & R.F. WARNER & C.E. EKBERG. "High speed fatigue tests on small specimens of plain concrete." Journal. Prestressed Concrete Institute. Vol. 4. No. 2. September, 1959.

12) B.P. SINHA, K.H. GERSTLE & L.G. TULIN. "Stress - strain relations for concrete under cyclic loading." A.C.I. Journal Proceedings. Vol. 61, No. 2. February, 1964.

13) H.F. CLEMMER. "Fatigue of concrete." Proceedings A.S.T.M. Vol. 22 II (1922).

14) R.B. CREPPS. "Fatigue of mortar." Proceedings A.S.T.M. Vol. 23 II (1923).

15) W.K. HATT. "Fatigue of concrete." Proceedings, 4th Annual Meeting, Highway Research Board, National Research Council. December, 1924.

16) H.A. WILLIAMS. "Fatigue tests of lightweight aggregate concrete beams." Proceedings A.C.I. Vol. 39. 1943.

17) C.E. KESLER. "Effect of speed of testing on the flexural fatigue strength of plain concrete." Highway Research Board. Proceedings, 32nd Annual Meeting. 1953.

18) J.W. MURDOCK & C.E. KESLER. "Effect of Range of Stress on fatigue strength of plain concrete beams." A.C.I. Journal Proceedings, Vol. 55 No. 2. August, 1958.

19) JOHN T. McCALL. "Probability of fatigue failure of plain concrete." A.C.I. Journal. Vol. 55. No. 2. August, 1958.

20) H. HILSDORF & C.E. KESLER. "The Behaviour of concrete in flexure under varying repeated loads."
T. and A.M. Report No. 172. University of Illinois, 1960.

21) A.C.I. COMMITTEE 215. "Fatigue of Concrete."
A.C.I. Bibliography No. 3. A.C.I. Detroit, 1960.

22) G.B. WELCH. "Fatigue of plain concrete beams subjected to repeated dynamic loading."
Institution of Engineers - Australia. Civil Engineering Transactions, Vol. C E 9, No. 2. October, 1967.

23) A.M. FREUDENTHAL. "Planning and interpretation of fatigue tests."
Symposium on statistical aspects of fatigue, S.T.P. No. 121, A.S.T.M., Philadelphia. June, 1951.

24) F.B. STULEN. "On the Statistical nature of Fatigue."
Symposium on statistical aspects of fatigue, S.T.P. No. 121, A.S.T.M., Philadelphia. June, 1951.

25) A.M. FREUDENTHAL & E.J. GUMBEL. "On the statistical interpretation of fatigue tests."
Proceedings, Royal Society, London. Vol. 216. Series A, February, 1953.

26) A.M. FREUDENTHAL & E.J. GUMBEL. "Minimum life in Fatigue."
Journal, American Statistical Association, Vol. 49. 1954.

27) AMERICAN SOCIETY FOR TESTING MATERIALS. "Manual on Fatigue Testing."
A.S.T.M. Special Technical Publication No. 91 (1949).

28) AMERICAN SOCIETY FOR TESTING MATERIALS. "A guide for fatigue testing and the statistical analysis of fatigue data."
A.S.T.M. Special Technical Publication No. 91 - A. (1963).

29) R.B. HEYWOOD. "Designing against Fatigue."
Chapman and Hall Limited, London. 1962.

30) A.S. TETELMAN & A.J. McEVILY. "Fracture of Structural Materials." John Wiley. 1967.

31) Z.D. JASTRZEBSKI. "Nature and properties of engineering materials." John Wiley. 1966.

32) F. LEONHARDT. "Prestressed Concrete - Design and Construction." Wilhelm Ernst and Soln. Berlin - Munich. 1964.

33) A. HALD. "Statistical tables and formulas" John Wiley & Sons, New York. 1952.

34) E.W. BENNETT & R.K. BOGA. "Some fatigue tests of large diameter deformed hard drawn wire used for prestressed concrete." Civil Engineering, Vol. 62, No. 726. January, 1967.

35) F.M. GORODNITSKY & W.P. KONEVSKY. "Investigations of the Fatigue Properties of steel reinforcement." F.I.P. Symposium on Steel for Prestressing. Madrid, 1968.

36) R. BAUS & A. BRENNEISEN. "The Fatigue strength of Prestressing Steel." F.I.P. Symposium on Steel for Prestressing. Madrid, 1968.

37) R.F. WARNER & C.L. HULSBOS. "Fatigue properties of Prestressing strand." P.C.I. Journal, Vol. 11, No. 1. February, 1966.

38) R.F. WARNER & C.L. HULSBOS. "Probable fatigue life of Prestressed Concrete Flexural members." Report No. 223.24A. Fritz Engineering Laboratory. Lehigh University. July, 1962.

39) H. WASCHEIDT. "Zur frage der Dauerschwingfestigkeit von Betonstaehlen im embetonierten Zustand." Technische Mitteilungun Krupp (Forchungsberichte) Vol. 24, No. 4. November, 1966. pp. 173 - 93.

40) W.J. HARRIS. "Influence of fretting on fatigue."
A.G.A.R.D. - Advisory report 8. April, 1967.

41) A.J. FENNER & J.E. FIELD. "Fatigue damage due to fretting."
N.E. Coast Institution Engineers Shipbuilders, Report 76. 1960.

42) S. SORET. "Fatigue behaviour of high - yield steel reinforcement."
Concrete and Constructional Engineering. Vol. 60, No. 7.
July, 1965. pp. 272 - 80.

43) F.C. LEA. "Repeated stresses on reinforced concrete."
Structural Engineer. Vol. 18, No. 2. 1940.

44) B. LeCAMUS. "Recherches sur le comportement du Beton et du Beton arme soumis a des efforts repetes."
Compte rendu des recherches effectuees en 1945/1946. Laboratoires du Batiment et des Travaux Publics, Paris 1946.

45) B. BRESLER & V. BERTERO. "Behaviour of R.C. under repeated load."
A.S.C.E. - Proceedings, Vol. 94. (Structural Division) No. ST.6.
June, 1968.

46) C.W. MUHLENBRUCH. "The effect of repeated loading on the Bond strength of Concrete."
Part I, Proceedings A.S.T.M. Vol. 45 1945. pp. 814 - 845.
Part II, Proceedings A.S.T.M. Vol. 48 1948. pp. 977 - 985.

47) N.W. HANSON. Discussion of a paper by Jack R. Janney, "Nature of bond in pre - tensioned prestressed concrete."
A.C.I. Journal Vol. 50. May, 1954.

48) R.F. WARNER & C.L. HULSBOS. "Probable fatigue life of Prestressed Concrete beams."
Journal of Prestressed Concrete Institute. April, 1966.
Vol. 11, No. 2.

49) R.E. ROWE. "An appreciation of the work carried out on fatigue in Prestressed Concrete Structures."
Magazine of Concrete Research Vol. 9, No. 25. March, 1957.

50) N.M. HAWKINS. "An evaluation of work on the fatigue strength of prestressed concrete beams."
Institution of Engineers, Australia, Transactions. March, 1964.

51) E. FREYSSINET. "A revolution in the technique of utilization of concrete."
Structural Engineer. Vol. 14, No. 5. May, 1936.

52) P. LEBELLE. "Coefficients de securite des pieces fleches en beton precontraint."
Institut Technique du Batiment. Circulaire Serie J. No. 5. February, 1945.

53) P.W. ABELES. "Fatigue tests on partially prestressed concrete members."
4th Congress, International Association for Bridge and Structural Engineering, 1952.

54) P.W. ABELES. "Static and fatigue tests on Partially Prestressed concrete construction."
A.C.I. Journal Proceedings Vol. 51. December, 1954.

55) F. CAMPUS. "Le beton precontraint."
Annales des Travaux Publics de Belgique. Vol. 103, No. 2. April, 1950.

56) G. MAGNEL. "Essai de fatigue d'une poutre en beton precontraint."
Proceedings of the International Congress of Prestressed concrete, Ghent, 1951. Communication No. B.51.

57) P. XERCAVINS "Recherche de la valeur optimum de la tension des armatures de precontrainte."
2nd Concress of the F.I.P., Amsterdam, 1955. Session Ib. Paper No. 5.

58) A.M. OZELL & E. ARDAMAN. "Fatigue tests of Pretensioned prestressed Beams."
A.C.I. Journal Proceedings, Vol. 53, No. 4. October, 1956.

59) A.M. OZELL & J.F. DINIZ. "Fatigue tests of prestressed concrete beams pretensioned with $\frac{1}{2}$" strands."
P.C.I. Journal, Vol. 3. No. 1. June, 1958.

60) S.C.C. BATE. "The relative merits of plain and deformed wires in prestressed beams under static and repeated loading."
I.C.E. Proceedings, Vol. 10, August, 1958.

61) S.C.C. BATE. "A comparison between prestressed and reinforced concrete beams under repeated loading."
I.C.E. Proceedings. Vol. 24. pp. 331 - 358. March, 1963.

62) S.C.C. BATE. "An experimental study of strand in prestressed concrete beams under static and repeated loading."
Proceedings I.C.E., Vol. 23. 1962. pp. 625 - 638.

63) W.J. VENUTI. "A Statistical approach to the analysis of fatigue failure of Prestressed Concrete Beams."
A.C.I. Journal Vol. 62. No. 11. November, 1965.

64) W.J. VENUTI. "Probability of fatigue failure of bonded type prestressed concrete beams."
Technical report No. 20. Stanford University, 1963.

65) F. SAWKO & G.P. SAHA. "Fatigue of concrete and its effect upon prestressed concrete beams.
Magazine of Concrete Research, Vol. 20. No. 62. March, 1968.

66) C.E. EKBERG, R.E. WALTHER & R.G. SLUTTER. "Fatigue resistance of Prestressed concrete beams in bending."
Proceedings A.S.C.E., Vol. 83. No. ST.4. July, 1957. Paper 1304.

67) T.Y. LIN. "Design of Prestressed Concrete Structures."
John Wiley, 2nd Edition (1963)

68) A.M. OZELL. "Fatigue tests of prestressed concrete I - beams with depressed strands."
4th Congress of the F.I.P, Rome, 1962. Theme 1.

69) K.E. KNUDSEN & W.J. ENEY. "Endurance of a full scale pre-tensioned concrete beam."
Lehigh University Progress Report No. 5. April, 1953.

70) SIMSLOVA, ROESLI, BROWN & ENEY. "Endurance of a full - scale pre - tensioned concrete beam."
Lehigh University Progress Report No. 6. May, 1954.

71) T.E. STELSON & J.N. CERNICA. "Fatigue properties of concrete beams"
A.C.I. Journal Vol. 55. No. 2. August, 1958.

72) T.S. CHANG & C.E. KESLER. "Fatigue behaviour of Reinforced Concrete Beams."
A.C.I. Journal Vol. 55, No. 2. August, 1958.

73) R.G. SLUTTER & C.E. EKBERG. "Static and Fatigue tests on Prestressed Concrete railway slabs."
Bulletin American Railway Engineering Association. Vol. 60. No. 544. June - July, 1958.

74) T.Y. LIN. "Strength of Continuous Prestressed Concrete beams under static and repeated loads."
A.C.I. Journal Proceedings, Vol. 51, No. 10. June, 1955.

75) W. EASTWOOD & R.M. RAO. "Fatigue tests on Lee - McCall Prestressed Concrete Beams."
Civil Engineering and Public Works Review. Vol. 52. No. 613. July, 1957.

76) G.M. NORDBY & W.J. VENUTI. "Fatigue and Static tests of steel strand prestressed Beams of expanded shale concrete and conventional concrete."
A.C.I. Journal Proceedings, Vol. 54, No. 2. August, 1957.

77) T.S. CHANG & C.E. KESLER. "Static and fatigue strength in shear of beams with tensile reinforcement."
A.C.I. Journal Proceedings Vol. 54, No. 12. June, 1958.

78) B.P. SINHA, K.H. GERSTLE & L.G. TULIN. "The Response of singly reinforced concrete beams to Cyclic loading."
A.C.I. Journal Proceedings, Vol. 61, No. 8. August, 1964.

79) G.L. AGRAWAL, L.G. TULIN & K.H. GERSTLE. "Response of doubly reinforced concrete beams to cyclic loading."
A.C.I. Journal Proceedings Vol. 62, No. 7. July, 1965.

80) R. TAYLOR. "Some fatigue tests on reinforced concrete beams."
Magazine of Concrete Research. Vol. 16, No. 46. March, 1964.

81) P.W. ABELES. "Studies of crack widths and deformations under sustained and fatigue loading."
P.C.I. Journal, Vol. 10, No. 6. December, 1965.

82) R. TAYLOR. Discussion to "A comparison between prestressed concrete and reinforced concrete beams under repeated loading," by S.C.C. Bate.
Proceedings I.C.E. Vol. 26, September, 1963.

83) P.W. ABELES. "Prestressed reinforced concrete sleepers tested as simply supported beams."
Concrete and Constructional Engineering, Vol. 42, Nos. 4 & 5. April - May, 1947.

84) J.M. HANSON & C.L. HULSBOS. "Fatigue tests of two prestressed concrete I - beams with inclined cracks."
Highway Research Record. Number 103. January, 1965.

85) SOZEN, ZWOYER & SIESS. "Strength in shear of beams without web reinforcement."
University of Illinois Experimental Station Bulletin No. 452.

86) J.M. HANSON & C.L. HULSBOS. "Overload behaviour of pretensioned prestressed concrete I - beams with web reinforcement."
Highway Research Record No. 76. January, 1964.

87) F.M. McCLARNON, M. WAKABAYASHI & C.E. EKBERG.
'Further investigation into the shear strength of prestressed concrete beams without web reinforcement."
Fritz Engineering Laboratory Report No. 223.22. Lehigh University. January, 1962.

88) J.M. HANSON & C.L. HULSBOS. "Overload behaviour of prestressed concrete beams with web reinforcement."
Lehigh University. Fritz Engineering Laboratory Report No.223.25 February, 1963.

89) G. HANANDEZ. "Prestressed Concrete Beams with web reinforcement."
University of Illinois. Ph.D. Thesis. May, 1958.

90) J.G. MacGREGOR, M.A. SOZEN & C.P. SIESS. "Strength and Behaviour of prestressed concrete beams with web reinforcement."
University of Illinois. Structural Research Series No. 201. August, 1960.

91) J.G. MacGREGOR, M.A. SOZEN & C.P. SIESS. "Strength of Prestressed Concrete Beams with Web reinforcement."
A.C.I. Journal Proceedings Vol. 62, No. 12. December, 1965.

92) J.M. HANSON & C.L. HULSBOS. "Ultimate shear tests of prestressed concrete I - beams under concentrated and uniform loadings."
Prestressed Concrete Institute Journal, Vol. 9, No. 3. June, 1964.

93) C.L. HULSBOS & D.A. Van HORN "Strength in shear of prestressed concrete I - beams."
Iowa State University, Engineering experiment station, Progress Report. April, 1960.

94) R.N. BRUCE. "The action of vertical, inclined, and prestressed stirrups in prestressed concrete beams."
P.C.I. Journal. February, 1964.

95) A.C.I. - A.S.C.E. COMMITTEE 326. "Shear and Diagonal Tension."
A.C.I.Journal Proceedings, Vol.59. January, February & March 1962.

96) R. WALTHER. "Calculation of the Shear strength of Reinforced and Prestressed concrete beams by the shear failure theory."
C. & C.A. Library. Translation No. 110 (1964).

97) R. WALTHER. "The Shear strength of Prestressed Concrete Beams."
Proceedings, 3rd Congress of the International Federation of Prestressing. Berlin, 1958.

98) M.A. SOZEN. "Strength in shear of Prestressed Concrete beams without web reinforcement."
University of Illinois. Structural Research Series No. 139.
August, 1957.

99) R.E. WALTHER & R.F. WARNER. "Ultimate strength tests of Prestressed and conventionally reinforced concrete beams in combined bending and shear."
Fritz Engineering Laboratory. Lehigh University, Institute of Research. September, 1958.

100) R.H. EVANS & A.H.H. HOSNY. "The shear strength of post-tensioned prestressed concrete beams."
3rd Congress of the F.I.P., Berlin 1958 Papers. Paper No. 11.

101) R. WALTHER. "The Ultimate strength of Prestressed and conventionally reinforced concrete under the combined action of moment and shear."
Lehigh University, Fritz Engineering Laboratory. Report No. 223.17.
October, 1957.

102) C.L. HULSBOS & F.G.E. IRWIN. "Shear strength of prestressed concrete I - beams without web reinforcement." January, 1957.
Iowa State College Engineering Experiment Station Progress Report.

103) R.N. BRUCE. "An experimental study of the action of web reinforcement in prestressed concrete beams."
University of Illinois. Ph.D. Thesis. September, 1962.

104) N.F. SOMES. "Moment - rotation characteristics of Prestressed Concrete members. Stage 1 : Rectangular sections."
C. & C.A. Technical Report TRA/398. September, 1966.

105) H. RUSCH. "Researches toward a general flexural theory in structural concrete." A.C.I. Journal Proceedings, Vol. 57, No. 1. July, 1960. pp. 1 - 27.

106) E. HOGNESTAD, N.W. HANSON & D. McHENRY. "Concrete stress distribution in ultimate strength design." A.C.I. Journal, Vol. 27, No. 4. December, 1955.(Proceedings, Vol. 52. pp. 455 - 79).

107) J.D. GEDDES & I. SOROKA. "Cement grouts and the grouting of post - tensioned prestressed concrete." University of Newcastle-on-Tyne. Department of Civil Engineering Bulletin No. 26. June, 1966.

108) J. WARWARUK, M.A. SOZEN & C.P. SIESS. "Strength and behaviour in flexure of Prestressed Concrete Beams." University of Illinois Engineering Experiment Station, Bulletin No. 464. August, 1962.

APPENDIX

METHODS OF ANALYSIS OF DATA FROM BEAMS IN SERIES F

In the beam tests, the strain profiles on both sides of the beam at five adjacent sections in the constant moment zone were determined by demec gauge readings at four levels in the compression flange - the layout of the demec points was as shown in fig. 4.1.

The purpose of the analysis detailed here was to determine the minimum steel stresses and strains, σ_s^{min} and ε_s^{min}, peak and mean curvatures, ϕ^{max} and $\overline{\phi^{max}}$, the neutral axis depth, d_n, the extreme compression fibre strain, ε_{c2}, the factor k_2, the internal lever arm, l_a, the maximum steel stresses and strains σ_s^{max} and ε_s^{max}, the apparent tensile strain in the concrete at the level of the steel, ε_{cs}^{m}, and the bond strain compatibility factor, F. The steel stresses and strains under minimum load were calculated by hand, but all other computations were carried out with the use of an IBM 7094 digital computer. The programmes were written in Fortran IV language. The theory of analysis followed that given in chapter 5.

The effective prestressing force on the section (unloaded) at the time of test, P_e, was known accurately since creep and shrinkage losses were measured directly from the time of stressing (see section 3.5). The elastic strain in the concrete at the level of the steel due to prestress, ε_{cspo}, was also measured at the time of stressing.

Therefore, at the time of test, the elastic strain in the concrete at the steel level was reduced to :-

$$\varepsilon_{csp} = \varepsilon_{cspo} \frac{P_e}{P_o} \qquad \text{... (A1)}$$

The mean strain at each level in the five adjacent sections in the compression zone was determined by taking the average of the strains measured on each side of the beam. The method of least squares was then used to fit the best linear relationship to the strains at each section. The strain values used were the absolute strains, the zero readings being taken before prestressing. From this linear relationship, the curvature,

ϕ^{max} and neutral axis depth, d_n, was obtained directly for each section. The average curvature, $\bar{\phi}^{max}$ was given by the mean of the curvatures at the five adjacent sections. For the purpose of analysis, the peak extreme compression fibre strain, ε_{c2}^{max}, and the peak apparent tensile strain in the concrete at the level of the steel, ε_{c2}^{max}, were also obtained directly from the least - squares fit.

Since the value of ε_{c2}^{max} was known, it was, therefore, possible to determine the value of the factor k_2 directly from equation (5.19), once the relation between stress and strain in the concrete was known for each fibre as detailed in section 5.4b. Due to the lack of complete qualitative information, it was assumed that the relation followed closely the static stress - strain curve although corrections were made at higher stress levels. Only one relationship, pertaining to the stable state condition, was used, since it was assumed in calculations of the fatigue strength, that the stable state stress conditions existed throughout the life of the beams. In almost all cases, the maximum stresses in the concrete were less than 60% of the static ultimate strength and, therefore, the errors in k_2 were assumed to be negligible.

The assumed relationship between stress and strain in concrete stressed to varying levels under repeated loading was :

$$\frac{\sigma_c}{f'_c} = 3\,\frac{\varepsilon_c}{\varepsilon_{co}} - 3\left[\frac{\varepsilon_c}{\varepsilon_{co}}\right]^2 + \left[\frac{\varepsilon_c}{\varepsilon_{co}}\right]^3 \qquad \ldots \text{(A2)}$$

This relationship is compared with an experimental static stress - strain curve in fig. A.1., for the values of $f'_c = 5{,}000$ lbs/in^2, and $\varepsilon_{co} = 0.0035$.

In the calculations for the static tests to failure, the stress - strain relationship was assumed to be parabolic - rectangular, with :-

$$\frac{\sigma_c}{f'_c} = 1.7\,\frac{\varepsilon_c}{\varepsilon_{co}} - 0.4\left[\frac{\varepsilon_c}{\varepsilon_{co}}\right]^2 - 0.3\left[\frac{\varepsilon_c}{\varepsilon_{co}}\right]^2 \qquad \ldots \text{(A3)}$$

$$\text{for } \varepsilon_c \leqslant \varepsilon_{co}$$

From these relations, the actual steel strain ε_s^{max}, could be calculated and thus the bond strain compatibility factor, F, was evaluated:-

$$F = \frac{\varepsilon_s^{max} - \varepsilon_{sp} - \varepsilon_{csp}}{\varepsilon_{cs}^{max}}$$

The value of the steel stress, σ_s^{min}, under M^{min}, was calculated directly from equation (5.15).

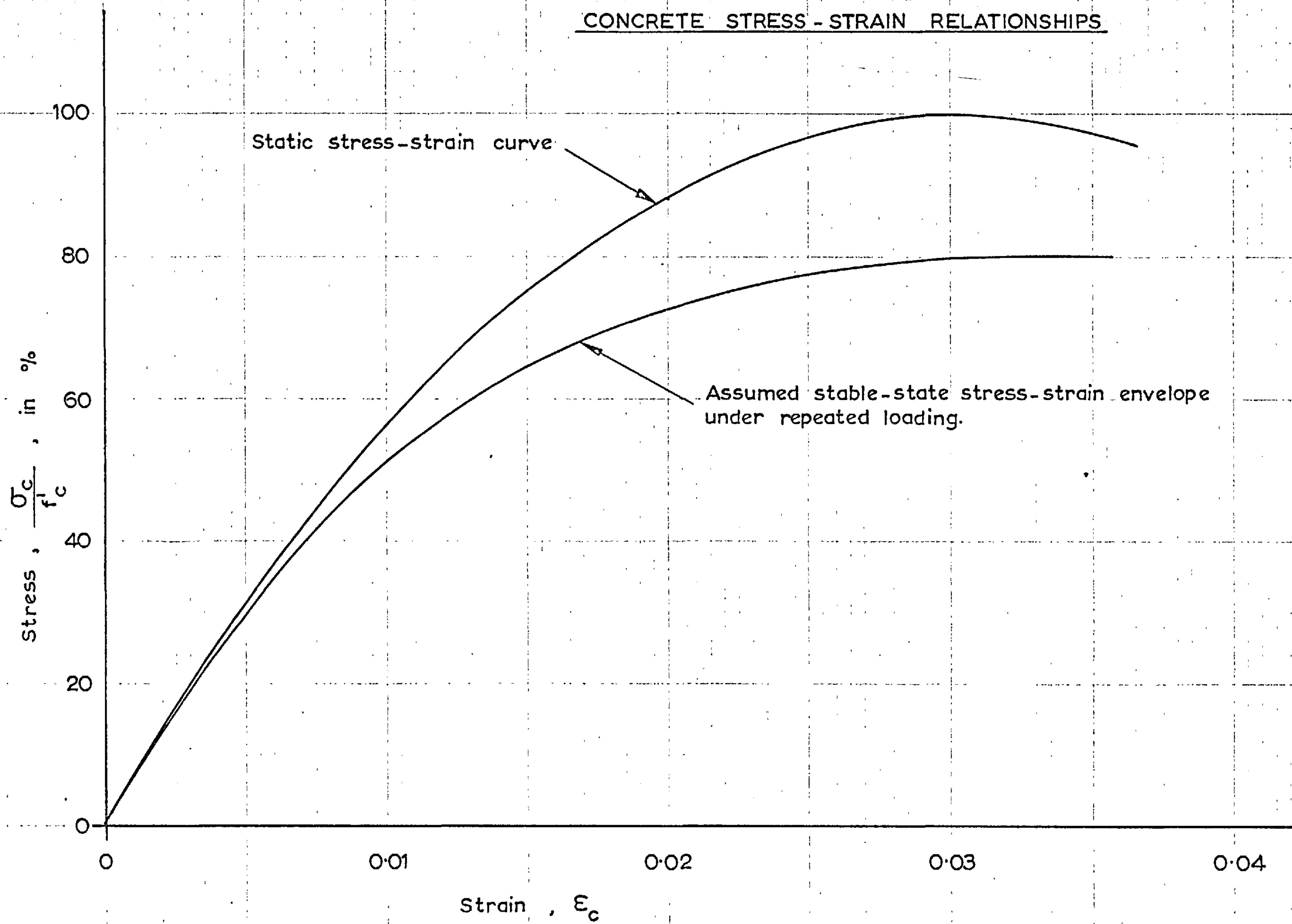
CONCRETE STRESS - STRAIN RELATIONSHIPS
Static stress-strain curve
Assumed stable-state stress-strain envelope under repeated loading.
Stress , $\frac{\sigma_c}{f'_c}$, in %
0
20
40
60
80
100
0
0·01
0·02
0·03
0·04
Strain , ε_c

Fig. A.1